

UNCLASSIFIED

AD NUMBER
AD477715
NEW LIMITATION CHANGE
TO Approved for public release, distribution unlimited
FROM Distribution authorized to U.S. Gov't. agencies and their contractors; Administrative/Operational Use; NOV 1965. Other requests shall be referred to Air Force Cambridge Research Laboratory, Office of Aerospace Research, Attn: CRJ, Hanscom AFB, MA.
AUTHORITY
afcr1 ltr 5 aug 1966 [67-1]

THIS PAGE IS UNCLASSIFIED

AFCRL-65-848
NOVEMBER 1965
SPECIAL REPORTS, NO. 38

TERRESTRIAL SCIENCES LABORATORY PROJECT 8523

AIR FORCE CAMBRIDGE RESEARCH LABORATORIES

L. G. HANSCOM FIELD, BEDFORD, MASSACHUSETTS

**US-IGY Drifting Station Alpha Arctic
Ocean 1957-1958**

G. H. CABANISS

K. L. HUNKINS*

N. UNTERSTEINER†

Compilers

* Lamont Geological Observatory, Columbia University

† University of Washington

**OFFICE OF AEROSPACE RESEARCH
United States Air Force**



AD 477 715

Abstract

During the International Geophysical Year a drifting ice floe, ALPHA, served as a platform for scientific studies of the Arctic Ocean environment from June 1957 to November 1958. Disciplines represented were meteorology, ice physics, oceanography, geophysics, geology, and marine biology. The scientific papers that presented the results of the various investigations are reproduced in this volume.

Preface

Station Alpha in the Arctic Ocean was the first floe-station established and maintained by the United States in the IGY. Its scientific program was thoroughly planned, and it lived fully up to expectations, providing much new information on arctic meteorology, geophysics, and biology. The cost, however, was considerable: Robert Johns, U. S. Weather Bureau technician, and AlC M. Fendley, U. S. Air Force, lost their lives while performing their duties at the station.

The success of the Station Alpha project was a direct result of the efforts and cooperation given by the officers and men at the station as well as at Alaskan Air Command Headquarters.

Although the papers contained in this volume were previously published in professional journals, they are presented here because it is felt that there is a need for a collection of all the results from Station Alpha under one cover. The compilers of this collection are grateful to the authors and publishers of these papers for permission to reproduce them, and they hope that it will be helpful to anyone planning similar research in the future.

K. L. Hunkins
Lamont Geological Observatory
Columbia University

N. Untersteiner
Department of Atmospheric Sciences
University of Washington

G. H. Cabaniss
Air Force Cambridge Research Laboratories

Contents

Introduction	1
Compilers' Note	6
Meteorology	
The Equilibrium Drift of Ice Station Alpha, Reed and Campbell	7
The Roughness Parameters of Sea Ice, Untersteiner and Badgley	27
On the Mass and Heat Budget of Arctic Sea Ice, Untersteiner	35
Heat Balance at the Surface of the Arctic Ocean, Badgley	69
Remarks on the Cooling Power in Polar Regions, Untersteiner	81
Ice Physics	
Seismic Studies of Sea Ice, Hunkins	87
Pack-Ice Studies in the Arctic Ocean, Schwarzscher	103
The Deuterium Content in Arctic Sea Ice, Friedman, Schoen, and Harris	117
Oceanography	
Waves on the Arctic Ocean, Hunkins	123
Geophysics and Geology	
Seismic Studies of the Arctic Ocean Floor, Hunkins	139
Some Features of Arctic Deep-Sea Sedimentation, Hunkins	163

Contents

Dredged Gravels from the Central Arctic Ocean, Schwarzacher and Hunkins	171
Biological and Geological Observations on the First Photographs of the Arctic Ocean Deep-Sea Floor, Hunkins, Ewing, Heezen, and Menzies	185
Marine Biology	
Some Biological Oceanographic Observations in the Central North Polar Sea, Drift Station Alpha, 1957-1958, English	195
Some Remarks on Arctic Ocean Plankton, English	233
Arctic Archibenthal and Abyssal Mollusks from Drifting Station Alpha, Clarke	249
Zooplankton Collections from the High Polar Basin with Special Reference to the Copepoda, Johnson	271
Preliminary Reports, Abstracts, and General Information	
Ice Drift in the Arctic Ocean, Browne	287
Preliminary Results of Thermal Budget Studies on Arctic Pack Ice During Summer and Autumn, Untersteiner and Badgley	295
The Trachymedusa, Botrynum Ellinorae, an Indicator Plankton of Arctic Water, Mohr and English	305
Primary Production in the Central North Polar Sea; Drifting Station Alpha, 1957-1958, English	309
The Ice Floes of Station Alpha, Hansen	313

Introduction

ORGANIZATION

Drifting Station Alpha was one of two scientific stations on the floating ice of the Arctic Ocean. They were established and supported by the U. S. Air Force under Project ICE SKATE as a major contribution to the Arctic Ocean Study Program formulated by the U. S. National Committee for the International Geophysical Year (1957-1958). The scientific programs conducted on these stations were largely an outgrowth and expansion of investigations conducted by the Air Force Cambridge Research Laboratories (formerly Air Force Cambridge Research Center) on Fletcher's Ice Island T-3 (IGY Drifting Station Bravo) in 1952-1954 and 1955.

At Station Alpha, the following organizations conducted research programs under the direction and contractual sponsorship of the Air Force Cambridge Research Laboratories: (1) the Lamont Geological Observatory (Columbia University) undertook investigations in marine geology and geophysics, aurora and airglow, geomagnetics, ice drift and ocean currents, and seismic properties of sea ice; (2) the Woods Hole Oceanographic Institution (with partial IGY support) initiated the physical oceanography program; (3) the Arctic Institute of North America conducted studies in marine biology and continued the oceanographic

(Received for publication 1 September 1965)

observations; and (4) the U. S. Geological Survey measured and interpreted fluctuations in the deuterium content of sea ice. In addition, the University of Wisconsin made several gravity ties from land bases to the station floe as an adjunct to the AFCRL-supported development of a world gravity network.

The University of Washington, with financial support from the U. S. National Committee for the IGY for the field operations and from the U. S. Navy Office of Naval Research for the data reduction and interpretation phases, also carried out a comprehensive program on Alpha. The transfer of mass and energy across the sea-ice-air interfaces was investigated and, following the IGY, an extensive study of the theory of ice drift was made and tested against the observed drift of Station Alpha.

Other agencies participating in the Station Alpha scientific operations were the U. S. Weather Bureau (synoptic surface and upper-air observations), the U. S. Air Force Arctic Aeromedical Laboratory (partial support of the oceanographic and meteorological programs), the U. S. Army Signal Corps (partial support of the meteorological program), the U. S. Army Cold Regions Research and Engineering Laboratory, formerly the Snow, Ice, and Permafrost Research Establishment (mechanical and elastic properties of sea ice), and the U. S. Navy Underwater Sound Laboratory (Arctic Ocean acoustics).

The logistical support, consisting of camp construction, maintenance, and supply, was performed by the Alaskan Air Command of the U. S. Air Force. The support flights were staged from Ladd Air Force Base, Fairbanks, Alaska.

HISTORY

In March 1957, several flights were made to find a suitable floe for the station. After one was located, the first ski-equipped C-47 aircraft landed on 4 April 1957, and left a party consisting of Col. J. Fletcher, Major R. Freeman, Rev. T. Cunningham, S. J., and M. Swiertz on the ice floe. Their primary mission was to install a radio beacon and begin construction of a runway, using the heavy equipment that was dropped by parachute. A crew of six expert construction workers, headed by Fritz Awe, arrived on 15 April. By the end of May, a 1500-m-long runway had been completed, and most of the camp's 26 Jamesway huts had been erected, wired, and modified for their respective purpose.

The camp was equipped with a continuous electrical power supply, oil heating, weasels, caterpillars, and a grader for transport and runway maintenance, electric washer, dryer, and shower facilities, and an excellent radio station for both official and amateur frequencies. The gross weight of the camp was approximately 500 tons. The major portion of this weight consisted of fuel that was flown in primarily by C-124 Globemaster aircraft.

For routine resupply flights, C-54 and C-47 aircraft were used. From June to August, melt-water holes and channels on the runway made it unusable, and all resupply was by parachute drop. The frequency of aircraft landings and paradrops is shown in Figure 1.

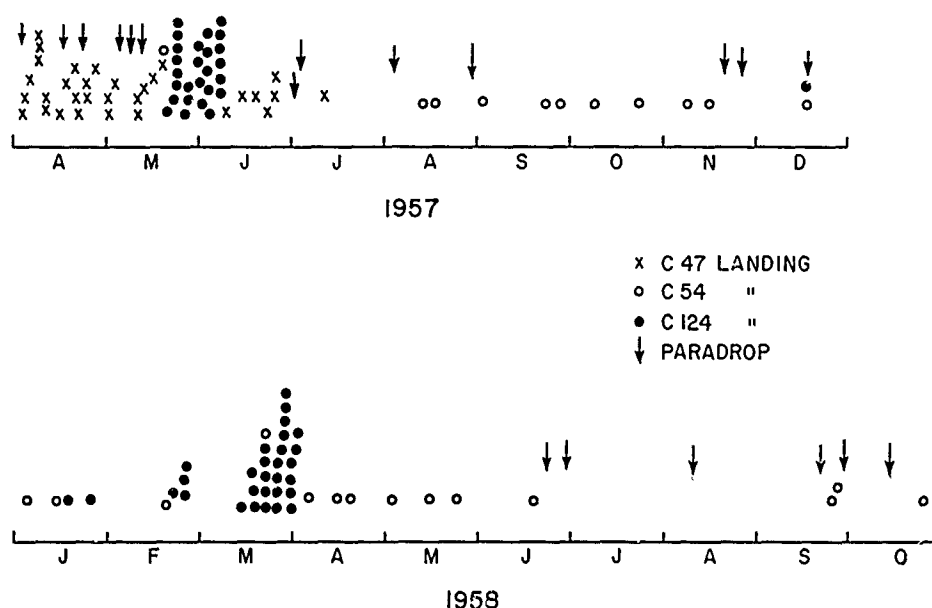


Figure 1. Air Support of Drifting Station "A"

Scientific observations began according to schedule with the commencement of the IGY on 1 June 1957. The choice of floe proved to be a fortunate one as no fractures occurred for almost exactly one year. On 3 April 1958, the first crack formed near the camp. Ridging along this crack and subsequent cracks made the camp position untenable. A possible new location was found about 2 km away; however, the difficulties and hazards of moving the entire camp that distance were so great that for a time abandonment of the camp was considered. But, due to the special requests of the camp commander and scientific leader, permission was obtained to continue operations with a skeleton crew which, if necessary, could be evacuated by one C-47. After the situation had been assessed and the decision made by Alaskan Air Command to provide the additional support necessary for moving to the new floe, the personnel were returned with additional help. With the outstanding efforts of all concerned, the move was completed by 5 May 1958. Careful planning resulted in a minimum loss of scientific data, and the new camp benefited from lessons learned in the construction and use of the first.

Operations continued without disturbance throughout the summer of 1958. In September and October cracking and ridging in the vicinity of the camp went on almost continuously, and gradually began to interfere with scientific activities. By mid-October serious fracturing occurred inside the camp area and on the runway and forced final abandonment on 7 November 1958. Personnel were evacuated to Thule Air Base, Greenland, by the Strategic Air Command.

STATION PERSONNEL

The number of people at Station Alpha usually varied between 25 and 30, about half being U. S. Air Force personnel and half civilian scientific investigators. The Air Force personnel supported and maintained the station. Included among the specialized servicemen were cooks, radio operators, mechanics, heavy-equipment operators, medical corpsmen, and electricians. All the Air Force men volunteered for duty at the station on the basis of a 6-month tour. The camp commander, an Air Force officer, was in overall charge of the station. He was responsible for camp operations, logistics, and safety.

The civilian investigators came from various universities and research institutions. The length of their tour at the station depended on the nature of their project and varied from a few days to over a year. A scientific leader was appointed by the U. S. National Committee for the International Geophysical Year; his role was to represent the investigators to the Air Force in matters of common interest such as research and personnel requirements. He reported on activities at the station to the U. S. National Committee.

Scientific Leaders were:

- F. Badgley, University of Washington
- G. Cvijanovich, Lamont Geological Observatory
(Columbia University)
- M. Davidson, Lamont Geological Observatory
(Columbia University)
- N. Untersteiner, University of Washington
- F. van der Hoeven, Lamont Geological Observatory
(Columbia University)

Scientific Investigators were:

- A. Assur, CRREL (SIPRE)
- R. Edwards, Woods Hole Oceanographic Institution
- T. English, Arctic Institute of North America
- J. Farlow, Woods Hole Oceanographic Institution
- G. Frankenstein, CRREL (SIPRE)
- A. Hanson, University of Washington
- K. Hunkins, Lamont Geological Observatory
(Columbia University)

B. Isaacs, Lamont Geological Observatory
(Columbia University)
E. Kelly, U. S. Navy Underwater Sound Laboratory
E. Langdon, U. S. Weather Bureau
G. Latham, Lamont Geological Observatory
(Columbia University)
R. Neuffer, Arctic Institute of North America
J. Scholten, Argentine Antarctic Institute
W. Schwarzacher, University of Washington
W. Senior, U. S. Navy Oceanographic (Hydrographic) Office
K. Staack, U. S. Weather Bureau
T. Stetson, Woods Hole Oceanographic Institution
O. Wattenbarger, U. S. Weather Bureau

Short-term investigators were:

J. Buckley, University of Alaska
R. Carpenter, U. S. Weather Bureau
H. Fleming, Columbia University
E. Herrin, Southern Methodist University,
Seismological Observatory
R. Iverson, University of Wisconsin
T. Laudon, University of Wisconsin
T. MacDonald, U. S. Weather Bureau
L. Rowinski, University of Alaska

COMPILERS' NOTE

The following ALPHA papers were omitted from this compilation in order to keep it a reasonable length:

Cabaniss, G. H. (editor) (1962) Geophysical Data From U. S. Arctic Ocean Drift Stations, 1957-1960, AFCRL Research Notes, AFCRL-62-83, 234 pp. (Publication may be obtained from AFCRL, Bedford, Mass.)

English, T. S. (1961) Some Biological Oceanographic Observations in the Central North Polar Sea - Drift Station Alpha, 1957-1958, Contract AF19(604)-3073, Sci. Rep. 15, AFCRL-652, Arctic Institute of North America. (Only Part II, Oceanographic Data, June-October 1958, omitted; however, it appears in Cabaniss, 1962.)

Farlow, J. A., III (1959) Project Ice Skate Oceanographic Data, Woods Hole Oceanographic Institution, Ref. 58-28. (Published in Cabaniss, 1962.)

Reed, R. and Campbell, W. (1960) Theory and Observations of the Drift of Ice Station Alpha, ONR Task No. NR 307-250 Final Report, Univ. of Washington, 255 pp.

The Equilibrium Drift of Ice Station Alpha

R. I. Reed

W.J. Campbell

Reprinted from the
JOURNAL OF GEOPHYSICAL RESEARCH,
Vol. 67, No. 1, pp. 281-297, January 1962

The Equilibrium Drift of Ice Station Alpha¹

RICHARD J. REED AND WILLIAM J. CAMPBELL

*Department of Meteorology and Climatology
University of Washington, Seattle*

Abstract. The problem of the equilibrium (unaccelerated) drift of an ice floe (no internal resistance) is solved by a treatment similar to Shuleikin's. Curves of drift angle, drift speed, and wind factor as functions of wind speed are computed for two different sets of parameters and compared with Shuleikin's curves for one of the sets. As a test of the theory, drift angles, drift speeds, and wind factors were plotted against wind speed for 107 periods between July 1, 1957, and August 31, 1958, in which the drift of station Alpha was essentially unaccelerated. The data exhibited considerable scatter, and it was necessary to compute mean drifts in various wind categories in order to bring out the empirical relationships. The observed drift angles were smaller than the theoretical in all wind categories, though the departures were not as great for our curves as for Shuleikin's curve. The graphs of drift speed and wind factors also exhibited systematic deviations from the theoretical curves, the ice drifting faster than the theoretical speed in light winds and slower in strong winds.

In explaining the deviations between observation and theory six sources of error are considered: navigation errors, errors due to residual accelerations, errors due to use of averaged data, errors due to variations in parameters, errors caused by gradient currents, and errors attributable to internal stresses. Although part of the scatter is found to be the result of the navigation errors, it is concluded that gradient currents and internal stresses are probably the main causes of drift anomalies. Evidence from the present study and from other sources suggests that a permanent current of about 3 cm sec^{-1} exists in the region of the drift of Alpha. This would account for the above-normal drift in light winds. The below-normal drift in strong winds is believed to be the result of internal resistance, though tests failed to show this conclusively.

Introduction. Drifting station Alpha was established on the arctic pack ice as part of the IGY effort in April 1957 and was maintained until November 1958, when it had to be abandoned because of breakup of the ice floe. The path of the station during this interval is shown in Figure 1. Throughout the period of drift, daily navigational fixes were taken whenever possible—by star shots during periods of complete or partial darkness and by sun shots during the perpetual daylight of late spring and summer.

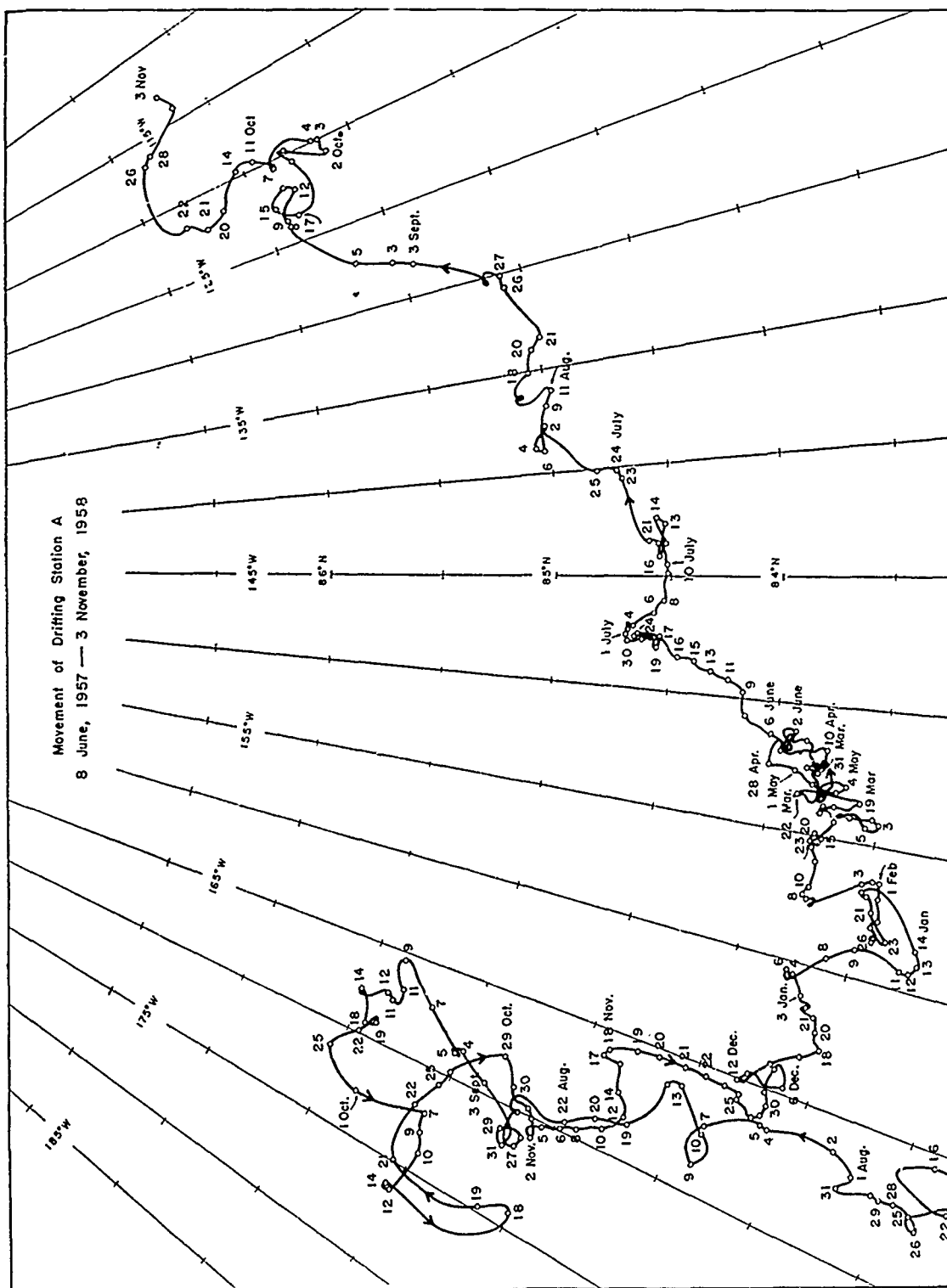
A complete summary of the drift data and corresponding wind data for the period July 1, 1957, to September 1, 1958, has been presented elsewhere [Reed and Campbell, 1960]. The present paper is concerned only with what we shall refer to as the 'equilibrium drift data.' A period of equilibrium drift is defined as a period

between successive positions in which the motion of the ice is relatively unaccelerated. The motion was regarded as relatively constant when the speed and curvature accelerations were less than 10 per cent of the Coriolis acceleration.

The purpose of the present paper is to extend Shuleikin's [1938] theory of the drift of ice fields under balanced forces and to test the extended theory by use of the equilibrium drift data for station Alpha. Considerable attention is given to the causes of discrepancies between the observed and theoretical drift behavior in order to assess possible weaknesses and omissions of the theoretical treatment.

Theory of ice drift under balanced forces. The theory of ice drift developed here follows closely that of Shuleikin [1938]. Stresses within the pack ice are neglected, and a boundary layer is assumed to exist beneath the ice, as was first hypothesized by Rossby and Montgomery [1935]. Because the motion is assumed to occur under balanced forces, the equation of motion takes the form

¹ Contribution 61, Department of Meteorology and Climatology, University of Washington, Seattle.



DRIFT OF ICE STATION ALPHA

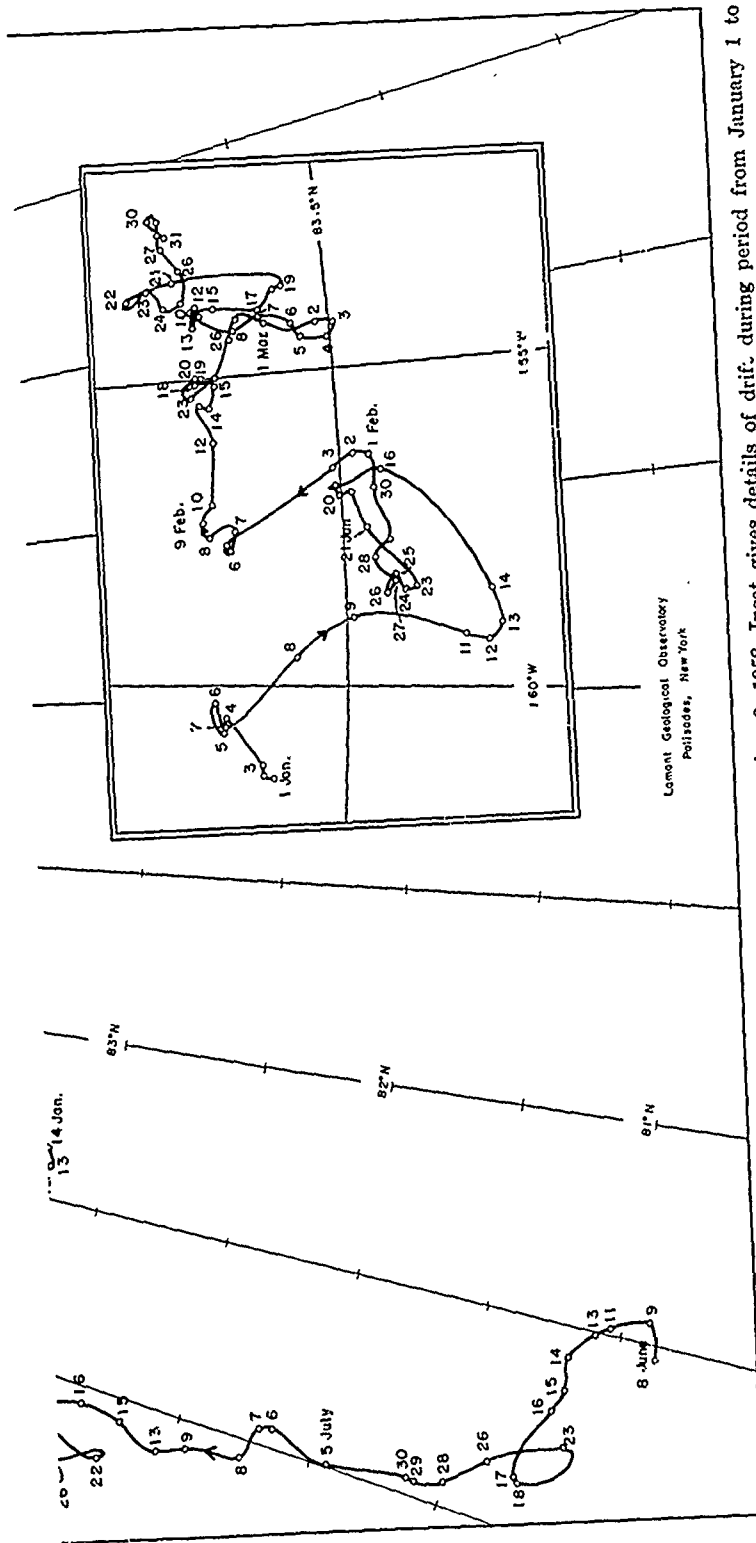


Fig. 1. Drift of Station Alpha during period from June 8, 1957, to November 3, 1958. Inset gives details of drift during period from January 1 to March 31, 1958. (Adapted from map supplied by Lamont Geological Observatory.)

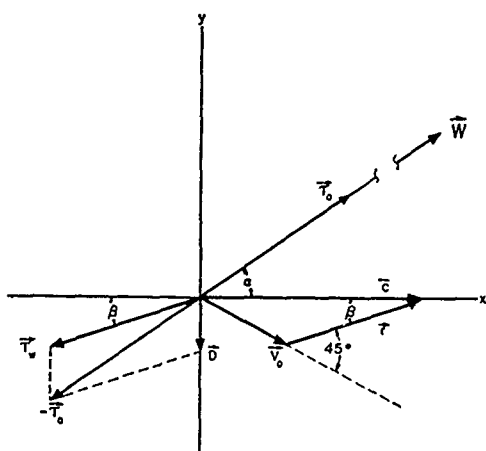


Fig. 2. Balance of forces in equilibrium drift. See text for explanation of symbols.

$$\tau_a + \tau_w + D = 0 \quad (1)$$

where τ_a is the wind stress, τ_w the water drag, and D the Coriolis force.

The arrangements of the velocities and forces are illustrated in Figure 2. The x axis has been chosen in the direction of the drift so that $c_y = 0$, $c_x = c$. The velocity V_0 shown in the diagram is the current velocity at the interface between the boundary layer and the deeper layer in which the Ekman spiral is assumed to prevail. In accordance with Ekman's well-known result, this vector forms a 45° angle with the stress at the top of the spiral layer and hence with the relative motion vector r .

Resolving the forces into x and y components gives

$$\tau_w \cos \beta = \tau_a \cos \alpha \quad (2)$$

$$\tau_w \sin \beta + mfc = \tau_a \sin \alpha \quad (3)$$

where m is the mass of ice per unit horizontal area and $f = 2\omega \sin \varphi$, the Coriolis parameter; and resolving the velocities gives

$$r \cos \beta + V_0 \cos (\pi/4 - \beta) = c \quad (4)$$

$$r \sin \beta - V_0 \sin (\pi/4 - \beta) = 0 \quad (5)$$

where α and β are the angles between wind and drift and between the drift and relative drift, respectively, and r is the velocity of ice relative to water.

Further relationships between the variables

are obtained from the usual expression for water drag under neutral stability:

$$\tau_w = Ar^2 \quad (6)$$

where

$$A = \rho_w k_0^2 \left[\ln \frac{h + z_0}{z_0} \right]^{-2}$$

ρ_w being the water density, k_0 the von Karman constant, h the thickness of the boundary layer, and z_0 the roughness of the underside of the ice; and, from the familiar equation first derived by Ekman,

$$\tau_w = \rho_w H f V_0 / \sqrt{2\pi} \quad (7)$$

where H denotes the so-called depth of frictional resistance.

Our object is to express the drift angle α , drift speed c , and the wind factor c/W as functions of the wind stress τ_a (hence of the wind itself) for chosen values of the Coriolis param-

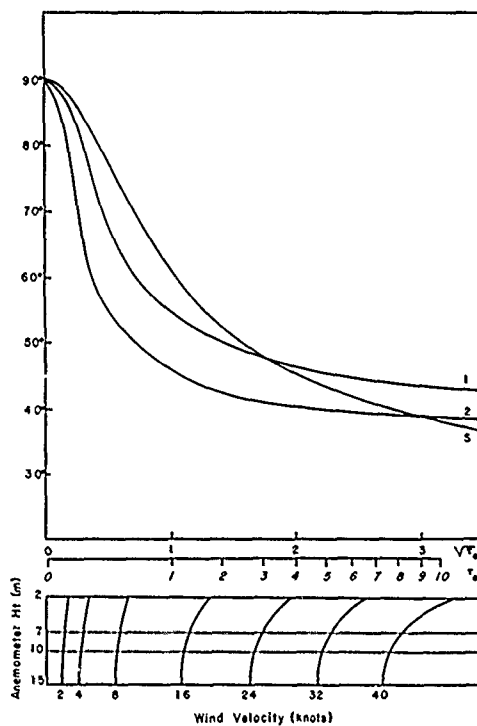


Fig. 3. Drift angle α as function of wind stress τ_a and wind speed W for cases 1 and 2 and Shuleikin's case (S). Wind scale at bottom is for roughness parameter of 0.2 mm.

DRIFT OF ICE STATION ALPHA

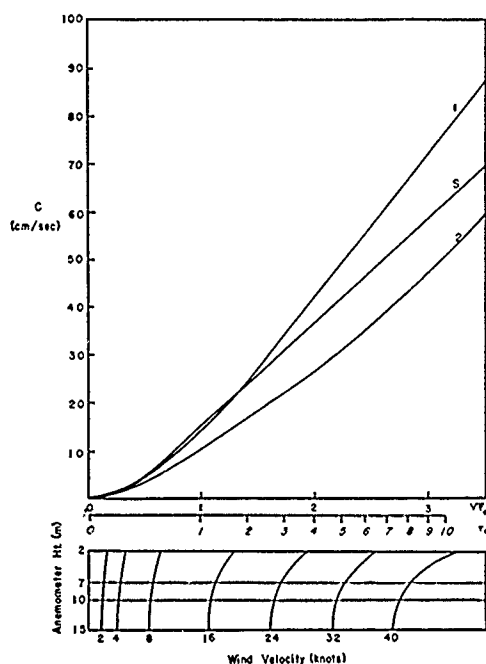


Fig. 4. Drift speed c as function of wind stress τ_a and wind speed W for cases 1 and 2 and Shuleikin's case (S). Wind scale at bottom is for roughness parameter of 0.2 mm.

eter, ice thickness, and the roughness of the top and bottom surfaces.

It, Shuleikin's solution of the problem the quantities α , β , c , r , V_0 , τ_w , and H are treated as unknowns; hence an additional equation is needed to form a complete set of seven equations in seven unknowns. As his additional relationship Shuleikin takes the empirical expression, derived by Ekman from observations of Mohn and Nansen,

$$V_0/W = 0.0127/\sin \varphi \quad (8)$$

Since this relationship was derived for the open ocean where the turbulent regime may be quite different from that under the ice, there is some question concerning its validity in the present problem.

In view of the empirical nature of (8), it is desirable to seek an alternative method of solution. We retain (2) to (7) as before, but from the requirement of continuity of mixing length and eddy viscosity at the interface between the boundary and the spiral layers we arrive at an additional theoretical relationship,

$$V_0 = Br^{3/2} \quad (9)$$

where

$$B = k_0 \left[\ln \frac{h + z_0}{z_0} \right]^{-3/2} [f(h + z_0)]^{-1/2} \quad (10)$$

The derivation of this equation is given in the Appendix along with further details of the solution of the new set of equations, (2) to (7), and (9).

It is convenient first to determine c and $\sin \beta$ for various assumed values of r , using the equations

$$c^2 = r^2 + \sqrt{2Br^{5/2}} + B^2r^3 \quad (11)$$

and

$$\sin \beta = \left[\frac{B^2r}{2(B^2r + \sqrt{2B^2r + 1})} \right]^{1/2} = \frac{Br^{3/2}}{\sqrt{2c}} \quad (12)$$

It will be noted that, unlike Shuleikin's treatment which gives a constant value for β and a fixed ratio of r to c , the present solutions permit a varying angle and ratio.

Next, for assumed values of r and corresponding values of c and $\sin \beta$, τ_a is determined from the expression

$$\tau_a^2 = A^2r^4 + 2mfA \sin \beta c r^2 + m^2f^2c^2 \quad (13)$$

Finally, α is determined as a function of τ_a .

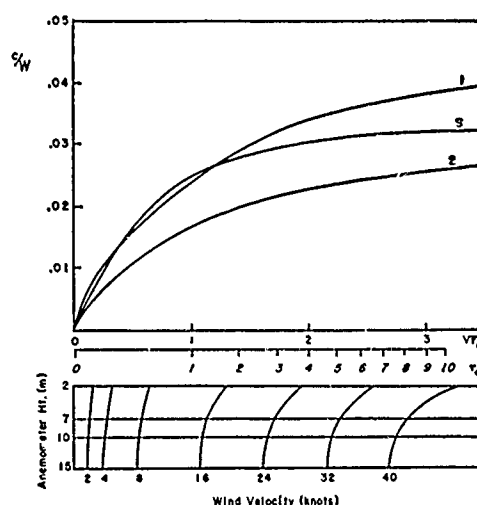


Fig. 5. Wind factor c/W as function of wind stress τ_a and wind speed W for cases 1 and 2 and Shuleikin's case (S). Wind scale at bottom is for roughness parameter of 0.2 mm.

REED AND CAMPBELL

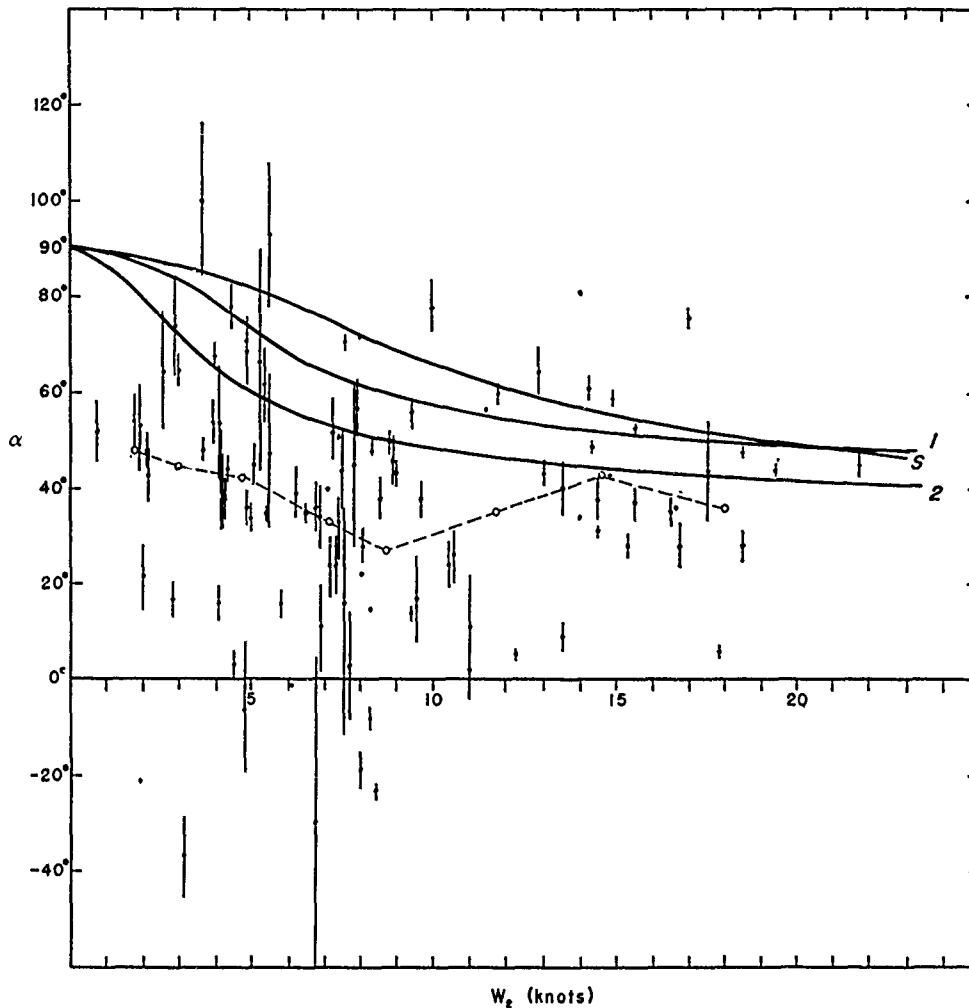


Fig. 6. Observed drift angle α , with maximum likely error, versus wind speed at 2 meters, W_2 , for cases of equilibrium drift. Also shown are theoretical curves 1 and 2 and Shuleikin's curve (S). Dashed lines join mean values of α in different wind categories.

from the relationship

$$\tan \alpha = \tan \beta$$

$$+ \frac{\sqrt{2Bmf}}{\sin 2\beta} \left[\frac{\cos \beta}{A^3 \cos \alpha \tau_a} \right]^{1/4} \quad (14)$$

By following the above procedure, we have prepared Figures 3, 4, and 5 for the following choice of parameters: (1) $m = 300$ grams, $\varphi = 83.5^\circ$, $\rho_a k_a = 20 \times 10^{-7} \text{ g cm}^{-2}$, $z_0 = 2.65$ cm, and $h = 2$ meters; (2) m , φ , and $\rho_a k_a$ as before, but $z_0 = 24$ cm and $h = 4$ meters. The alternative choices correspond to values for A

of 0.008 and 0.02, respectively. The symbols ρ_a and k_a refer to the density and drag coefficient of air, respectively.

The chosen value of m is believed to represent a reasonable estimate of the mean mass of a unit vertical section of the floe on which station Alpha was located, taking into account proportionately the typical thickness and the added thickness in regions of pressure ridges. The latitude figure is the approximate mean during the period of drift.

An important advantage of the present solution is that α and c have been determined as

DRIFT OF ICE STATION ALPHA

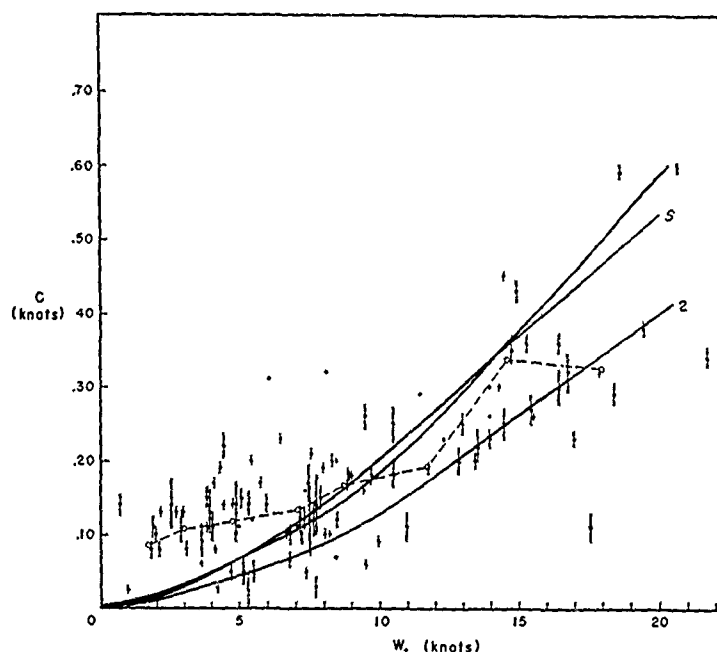


Fig. 7. Observed drift speed c , with maximum likely error, versus wind speed at 2 meters, W_2 , for cases of equilibrium drift. Also shown are theoretical curves 1 and 2 and Shuleikin's curve (S). Dashed lines join mean values of c in different wind categories.

functions of τ_0 , the wind stress, rather than of the wind itself. This means that the curves in Figures 3 and 4 represent the true functional relationships between these quantities and the stress—subject, of course, to the many assumptions that have been made.

However, in plotting the curves of wind factor in Figure 5, it is necessary to attach a velocity scale to the various graphs. The conversion from wind to stress has been made assuming a roughness parameter of 0.2 mm. This figure was provided by F. I. Badgley (personal communication) and is based on the results of wind-profile measurements at Alpha. It yields a drag coefficient of 1.5×10^{-3} as compared with Rossby and Montgomery's estimate of 2.5×10^{-3} and a highly questionable value given by Sverdrup [1957] of 6.9×10^{-4} . These figures are for the 7-meter level, appropriate to the wind measurements on the *Maud*. Since winds from levels between 2 and 15 meters have been used by various authors, we have presented a variable wind scale along the bottom of the diagrams. Note that the abscissa is the square root of τ_0 , and therefore the velocity scales are linear.

The choices of h and z_0 are little more than educated guesses. We hoped that, by assuming two pairs of values for h and z_0 which gave widely different values of the drag coefficient, the correct value would be bracketed somewhere between. In line with remarks of Shuleikin [1950], we selected boundary layers of depths of the order of meters. For the underside roughness we chose one small value of the size estimated by Rossby and Montgomery [1935] and a second larger value which may be more realistic if their method of estimating the underside roughness is valid. They make their estimation by assuming that the ridges below the ice are the same size as those above (about 1 meter) and multiplying this by Nikuradze's factor of 1/30. However, isostatic equilibrium requires the underside ridges to be several times as large as those above, and the experience of one of the authors in diving below the pack ice suggests that this is the case. The larger figure for the roughness may therefore be more accurate, if the ridges are the predominant roughness elements.

In any case, the differing assumptions give drag coefficients of 0.008 and 0.02, the first

REED AND CAMPBELL

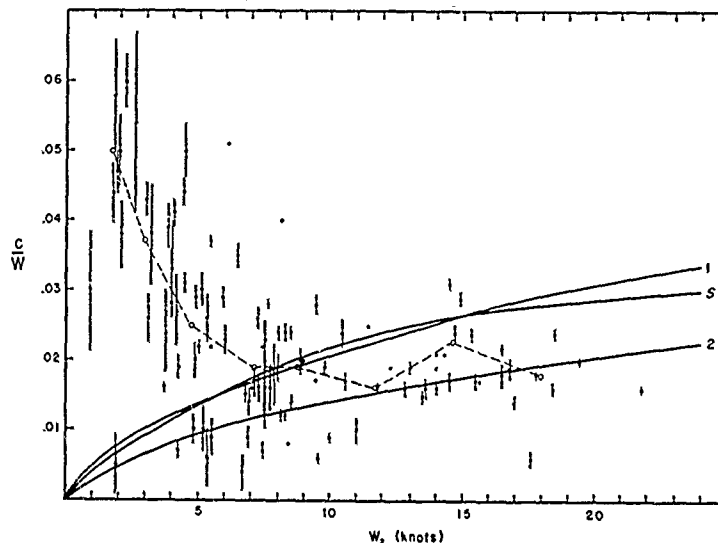


Fig. 8. Observed wind factor c/W , with maximum likely error, versus wind speed at 2 meters, W_2 , for cases of equilibrium drift. Also shown are theoretical curves 1 and 2 and Shuleikin's curve (S). Dashed lines join mean values of c/W in different wind categories.

being very close to Shuleikin's and Rossby and Montgomery's figures and the second being considerably higher than previous estimates but not very much beyond the figure of *Browne and Crary* [1958]. At least in terms of present thinking on the matter, we have bracketed the true value.

Before discussing the various curves, we must mention that in order to arrive at solutions it has been necessary to assume a constant value for h in any given solution. In reality, the thickness of the boundary layer should increase as the drift increases, but if conditions in the sea are analogous to those in the atmosphere, h will be a slowly varying quantity. Since Shuleikin assumed a constant drag coefficient, his solution implicitly contains this same assumption.

From Figures 4 and 5 it is apparent that our solution 1 and Shuleikin's solution for the same choice of parameters give nearly identical drift speeds and wind factors at light and moderate wind velocities. With strong winds our solution predicts somewhat higher speeds. Solution 2, with the greater value of water drag, naturally gives lesser speeds and wind factors than the other two solutions. However, differences are at most about 40 per cent. Obviously, quite large

variations in choice of parameters lead to relatively small variations in drift speed.

Comparison of curves 1 and 2 in Figure 3 shows that the drift angle is even less sensitive to variation in the drag. At light wind speeds, however, the choice of model makes a considerable difference, as witnessed by the lesser angles in our solutions than in Shuleikin's.

Drift data from station Alpha are not strictly applicable to the isolated floe problem, so it is not possible from the later empirical results to claim superiority for one solution over another. On theoretical grounds it would appear that the best solution should lie somewhere between ours and Shuleikin's.

Observed relationship between wind and drift. In the theory of ice drift developed in the preceding section no account is taken of the existence of stresses within the pack ice, and therefore the theory should be compared with drift data for very loose ice or isolated floes. However, it is instructive to apply this theory to the pack ice, since any discrepancies which appear may provide information on the action of the internal stresses, the presence of other neglected effects, or the weaknesses in the various assumptions contained in the theory.

In applying the theory to the drift data it is

DRIFT OF ICE STATION ALPHA

TABLE 1. Mean Drift Angle α , Drift Speed c , and Wind Factor c/W for Various Wind Categories during Periods of Equilibrium Drift

Wind Category, knots	Average Speed, knots	Drift Angle, degrees	Drift Speed, knots	Wind Factor
0-2.9	1.7	40°26'	0.085	0.050
2.0-3.9	2.9	45°00'	0.109	0.037
4.0-5.9	4.8	43°06'	0.119	0.025
6.0-7.9	7.1	33°20'	0.134	0.019
8.0-9.9	8.7	27°09'	0.167	0.019
10.0-13.9	11.8	35°50'	0.192	0.016
14.0-15.9	14.6	43°08'	0.338	0.023
>16.0	18.0	36°17'	0.324	0.018

necessary first to make sure that accelerations of the ice are negligible, since the theory is based on the condition that the forces are in equilibrium. We have attempted to satisfy this condition by excluding all cases in which the radius of curvature of the trajectory of the station was less than 15 km and in which the drift speed changed by a factor of 100 per cent or more per day.

Of the total of 351 drift intervals during the period July 1, 1957, to August 31, 1958, only 107 qualified as periods of unaccelerated drift according to the foregoing criteria. The drift angles, drift speed, and wind factors for these cases are plotted as functions of wind speed in Figures 6, 7 and 8. The wind in each case is the magnitude of the mean vector wind for the period as determined from summation of hourly mean velocity vectors composed of mean hourly wind speeds, measured at the 2-meter level on the University of Washington micrometeorological mast, and wind directions taken from the nearest standard 3-hourly observation of the U. S. Weather Bureau.

Although the scatter of the individual observations is not so great for these specially selected cases as for all cases, it is nevertheless difficult to fit simple curves to the data. To express objectively the relationship between the variables, we have determined average values of α , c , and c/W for different wind categories and have graphed the results by straight-line segments. The wind categories, number of observations in each category, and the various averages are given in Table 1. Note that two categories are

of odd size owing to a shortage of observations in the ranges 0 to 2 knots and 10 to 14 knots.

The graph of drift angle in Figure 6 reveals that observed angles are smaller than the theoretical ones and that the variation of angle with wind speed is less than is predicted by theory. The minimum near 9 knots and the maximum near 15 knots are most likely due to the limited sample of data and would probably disappear if more observations were available. In any case it is difficult on the basis of qualitative reasoning to account for these irregularities. Also, it would be premature to say that the results in Figure 6 offer convincing evidence that the larger value of drag coefficient used in case 2 is the better value, since other sources of error mentioned previously could cause systematic differences between the observed and theoretical curves.

Equally substantial differences between observation and theory are apparent in Figures 7 and 8, in which are plotted drift speed and wind factor and corresponding theoretical curves. When the wind is nearly calm and the stress is close to zero, there is still, on the average, a residual motion in the ice which must be attributed to other causes, presumably either to gradient currents in the ocean or to internal stresses. At the higher wind speeds, the actual drift is significantly less than the theoretically computed values for curves 1 and S, and it tends to become less for curve 2. Since it is unlikely that the estimate of the drag coefficient between air and ice can be much in error at these speeds, we are forced to conclude either that the water drag is much greater than even our so-called large value or that there is an additional retarding force present at these speeds. Certainly, the results shown here are not inconsistent with the idea expressed later, that the internal stress retards the motion at high wind speeds and accelerates the motion at low speeds.

Because of the behavior of the drift speed, the slope of the curve for the wind factor is opposite to that of the theoretical curves. At higher winds the wind factor is below the theoretical value, and as the wind approaches zero the wind factor approaches infinity rather than zero.

From vector averaging, the over-all averages of the various quantities have been determined.

REED AND CAMPBELL

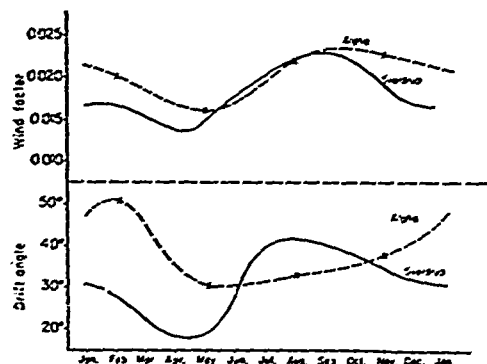


Fig. 9. Seasonal variation of mean drift angle α and wind factor c/W . Solid lines after Sverdrup [1928]; dashed lines, Alpha I data.

The values obtained were: drift angle, $38^{\circ}10'$; drift speed, 8.5 cm sec^{-1} ; wind factor, 0.021. These may be compared with Nansen's values from the drift of the *Fram* (28° for the drift angle and 0.018 for the wind factor) and Sverdrup's values for the *Maud* (33.1° and 0.018).

Sources of deviation between theory and observation. The drift data for station Alpha display wide scatter about the theoretical curves, and this is true whether all periods of drift are considered or only those periods in which the accelerations are so small that the equilibrium theory should apply. Moreover, in periods of small acceleration, in addition to the apparently random scatter about the empirical curves relating wind and drift, the observations display marked systematic deviations from the theoretical relationships, as discussed in the preceding section. Elsewhere the authors [Reed and Campbell, 1960] have examined in considerable detail six possible sources of the random and systematic deviations: (1) errors due to residual accelerations, (2) errors due to the use of averaged rather than instantaneous data, (3) navigation errors, (4) errors caused by variations in parameters such as drag coefficients, (5) errors arising from the effect of gradient currents in the ocean, and (6) errors attributable to internal stresses in the ice. Here we shall summarize the results of the more complete analysis, elaborating only on those aspects of the problem that appear worthy of further investigation.

Because of the criteria used in selecting the

drift data, the first two sources of error are small and can be neglected. The contribution to the random scatter caused by errors in station position can be judged from the error estimates in Figures 6 to 8. It is apparent that navigation errors are a substantial, though not the sole, cause of the scatter.

Since the position errors are independent of wind speed, there will be an apparent drift even when winds are calm, and hence the wind factor will approach infinity, rather than zero as required by theory. This effect is indeed present in the data. However, consideration of typical position errors reveals that they generally will lead to an error of less than 1 cm sec^{-1} , while the data in Figure 7 show that the residual drift is of the order of 2 to 4 cm sec^{-1} . Clearly other factors of importance are involved.

Parameters of the drift equation which undergo variation are latitude, ice thickness, and drag coefficient in air and water. Computations show that variations in latitude and ice thickness were too small to have caused significant deviations from the theoretical curves. Wind profile measurements revealed sizeable changes of surface roughness and hence of the drag coefficient in air.

However, probably of even greater importance in producing differences between the assumed and actual drag were variations in hydrostatic stability. In relating wind to drag we have assumed neutral stability. Actually, stable lapse rates generally prevail near the ice surface, though in late spring and, to a lesser degree, in summer, superadiabatic lapse rates may occur. It is difficult to estimate how much of the data scatter was caused by variations in stability, since turbulence theory does not yet provide any generally accepted method for treating the stable case. Only recently has there been success in handling the unstable case [Ellison, 1957; Panofsky, Blackadar, and McVehil, 1960].

Since there are equally great uncertainties in treating the water drag, it has been necessary to resort to indirect evidence to assess the possible importance of drag variations in drift anomalies. This evidence consists of observations of the seasonal variation in drift behavior, as given by the broken curve in Figure 9. From the figure it is apparent that the drift angle was greatest in winter and least in spring and that

DRIFT OF ICE STATION ALPHA

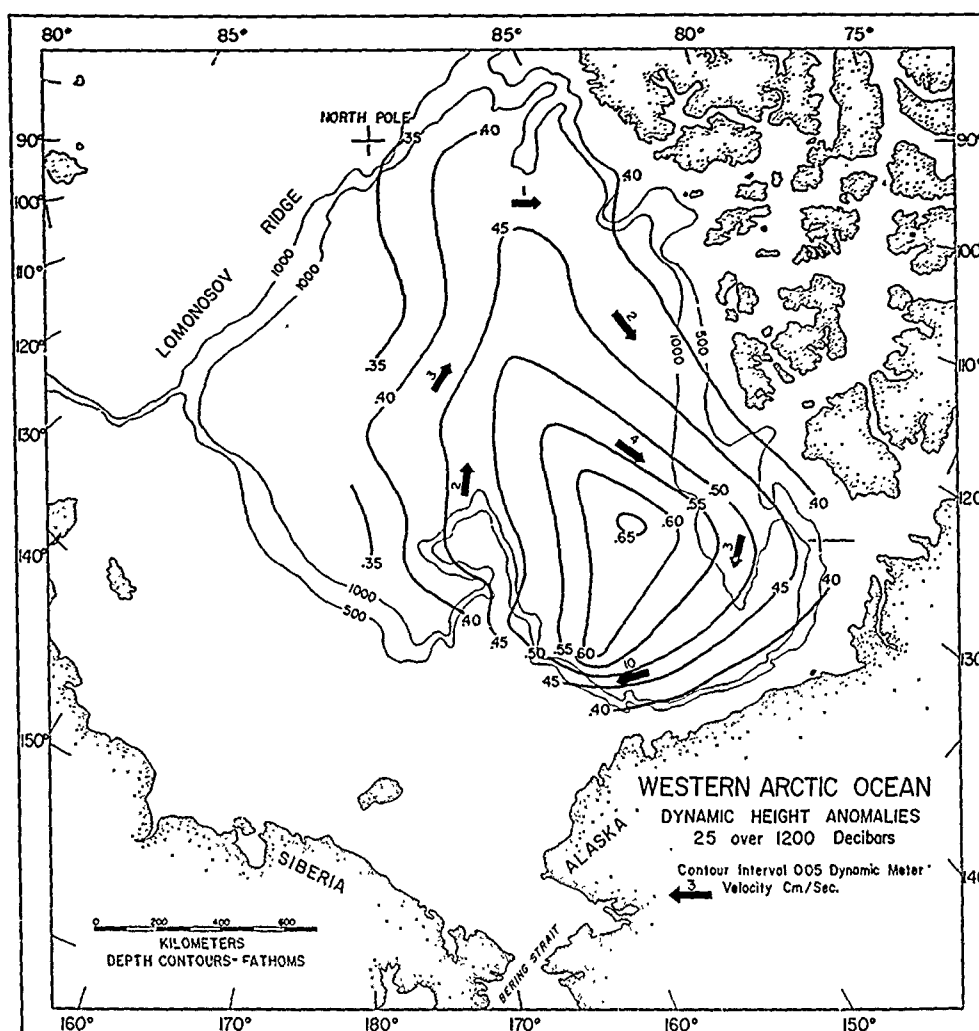


Fig. 10. Average dynamic topography, 25 over 1200 decibars, for the western Arctic Ocean (after Barnes and Coachman).

a rapid decline in angle took place in late March. The wind factor, on the other hand, underwent little seasonal change. When this behavior is compared with the behavior to be expected from the inferred seasonal variations in air and water drag, only partial agreement is obtained, suggesting that variations in parameters affecting the drags do not exert a strong systematic effect on drift behavior. However, in view of the many uncertainties involved, this cannot be regarded as a firm conclusion.

Gradient currents are a further likely source

of deviations between theory and observation. The ice drift is the vector sum of the gradient current and the wind drift in the absence of a current. This may be seen from the fact that the additional Coriolis force due to the gradient current exactly balances the force of gravity along the sloping ice surface.

The average dynamic height anomalies and corresponding gradient currents for the Beaufort Sea and the adjoining portion of the Arctic Ocean are shown in Figure 10. From the figure, it is apparent that the average current in the region of the drift of station Alpha is about 3

REED AND CAMPBELL

cm sec⁻¹. In individual cases it seems plausible that gradient currents could exceed this figure by a considerable amount. Gradient currents must be regarded, therefore, as a likely major cause of the data scatter, and they could almost, in themselves, account for a primary difference between the observed and theoretical drift—the tendency for the drift speed to remain greater than zero and for the wind factor to approach infinity as the wind approaches zero. As was mentioned previously, the residual drift appears to lie somewhere between 2 and 4 cm sec⁻¹ (see Fig. 7).

Nansen [1902] and *Sverdrup* [1928] proposed methods of detecting the presence of gradient currents from the wind and drift data. In *Sverdrup*'s method, which we shall follow here, resultant drifts for winds blowing from each of the four quadrants are determined and the drift vectors are plotted from a common origin. In the absence of a gradient current it would be expected that the heads of the vectors would lie on a circle centered at the origin. The effect of a uniform current would be to displace the circle from the origin, since the ice drift would be greater than normal in a certain direction and less in the opposite direction. The vector from the origin to the center of the circle gives the gradient current. Using this method, *Sverdrup* could find no evidence of a significant permanent current on the north Siberian shelf.

To determine whether the drift currents shown in Figure 10 were detectable in the drift data for station Alpha we have divided the data according to season and wind-speed categories and have applied *Sverdrup*'s method to all speed categories in which several winds were observed in at least three different quadrants. During the five seasons studied it was possible to construct thirteen circles. By and large, the currents derived from these circles were consistent within each season, and the season-to-season change in current direction showed a rotation in the clockwise or anticyclonic sense. Current speeds ranged from 6.5 cm sec⁻¹, during the period July to September, 1957, when the atmospheric circulation reinforced the normal direction of ice drift, to 1.0 cm sec⁻¹, during the period October to December, 1957, when the atmospheric circulation counteracted it.

The shape of the anticyclonic gyral, as indi-

cated by the drift data, was different from the long-term mean in Figure 10. However, it is known from the work of *Gudkovich* [1959] and others that the gyral is not steady but undergoes pulsations and long-period fluctuations in response to variations in the atmospheric circulation.

The presence of the gyral may also account for the observed drift angles being smaller than the theoretical ones. As was shown by *Gordienko* [1958], the flow about the gyral parallels the isobars on mean surface pressure charts. Thus in the typical case, in which the daily pressure pattern resembles the longer-term mean, there is an additional drift component at an angle of about 30° to the wind (the average angle between wind and isobars in the Arctic). The angle between the resultant drift and wind will lie somewhere between 30° and the angle given by theory, and since the theoretical angle is always greater than 30° (see Fig. 3) the usual effect of the gradient current is to cause the observed drift angle to appear to be less than the angle given by theory.

If this explanation is correct, the angle between wind and drift should be greatest in winter and early spring, when the air is very stable and the angle between wind and isobars is especially large, and least in late spring, when the air is often unstable and the angle between wind and isobars is relatively small. Such a seasonal change in drift angle was noted.

From the foregoing remarks it appears likely that the residual drift in light winds is mainly the result of gradient currents and that many of the larger deviations between observed and theoretical drifts are also attributable to this cause.

The importance of the final source of error—the neglect of internal stresses—can only be inferred from differences between observed and theoretical drifts which cannot be attributed to other causes. Since the theoretical curves and the 'other causes' are both subject to considerable uncertainty, it would be premature at this time to equate the internal stress in a specific case with the estimated residual force. But it is perhaps not too early to see whether the internal stress can be formulated in such a manner that it can qualitatively account for the observed differences.

Sverdrup [1928] and *Browne and Crary*

DRIFT OF ICE STATION ALPHA

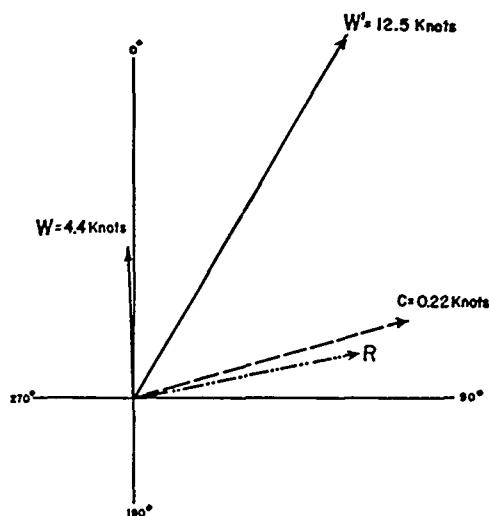


Fig. 11. Plot of drift vector c , wind speed W , theoretical wind corresponding to c , W' , and the internal ice resistance R , January 29-30, 1958. Scales are given on diagram except for R which is arbitrary.

[1958] have suggested alternative approaches to the problem of internal stress. Sverdrup postulated a resistance proportional to the ice velocity and directed opposite to it and, in support of his formulation, noted that the seasonal variations in drift characteristics given by his data (Fig. 9) were in accordance with the seasonal variations in ice compactness. Browne and Crary hypothesized that the effect of transmission of stress from a distance is to cause the ice to drift with the mean wind over some sizeable area rather than with the local wind. In support of their view they presented evidence that the drift of ice island T-3 (Bravo) was better correlated with the winds over an area of approximately 20,000 km² than with the wind observed at the island itself.

In the present work a somewhat different hypothesis regarding the form of the internal stress is put forth. If one tries to visualize time lapse photographs of the pack ice as viewed, say, from a satellite, keeping in mind the more or less close relationship that exists between drift velocity and wind velocity, one forms a mental image of a fluidlike flow in which the ice responds sluggishly to the air circulation. The ice pack does not move as a single gigantic plate under the integrated wind stress over the entire polar basin; instead it breaks up into

small pieces, or floes, which respond to the local wind and which, because of the spatial variation of wind, must react one with another. Faster moving floes must transmit momentum to regions of slight movement, thereby undergoing a retarding force, while the slow-moving floes are accelerated by contact with their surroundings.

Thus it would not appear unreasonable to treat the ice as a highly viscous fluid, the ice floes constituting, so to speak, fluid molecules which rub and bump against one another and thereby diffuse momentum. By analogy, then, with the viscous term in the Navier-Stokes equations, we shall assume that the resistance per unit mass is of the form

$$R = K \nabla^2 c \quad (15)$$

where K is the kinematic 'viscosity' of the ice and ∇ is the two-dimensional gradient operator.² In component form, (15) becomes

$$R_x = K \nabla^2 c_x \quad (16)$$

$$R_y = K \nabla^2 c_y \quad (17)$$

Because of well-known properties of the Laplacian, these equations state that regions of deficient x or y momentum will experience an accelerating force and areas of excessive x or y momentum will undergo a deceleration. Although this concept must be roughly true, it should be mentioned that the derivation of (15) requires that various stress coefficients be equal, and this may not be correct, since the transfer of momentum in shear and in compression may not be physically similar.

Equations 16 and 17 may be put in suitable form for making qualitative estimates of the internal stress from synoptic weather charts by assuming that the motion of the ice is non-divergent and that it obeys Zubov's rule [Zubov and Somov, 1940; Gordienko, 1958]. In this rule it is stated that, to a first approximation, the ice moves in the direction of the iso-

² After the present research was completed, the authors' attention was directed to a recent paper by M. I. Ruzin, 'The Wind Drift of Ice in a Heterogeneous Pressure Field' (translated for Geophysics Research Directorate, AF Cambridge Research Center, by the American Meteorological Society, contract AF19 (604)-6113), in which an identical formulation of the internal stress is made.

REED AND CAMPBELL

bars at a speed inversely proportional to their spacing. It follows that

$$R_x = -\kappa \partial \zeta_g / \partial y \quad (18)$$

$$R_y = \kappa \partial \zeta_g / \partial x \quad (19)$$

where ζ_g is the vorticity of the geostrophic wind and κ is a constant of proportionality. The success of this formulation in accounting for the differences between theory and observation was tested as follows.

From synoptic charts analyzed for the period January to March, 1958, ζ_g was determined each day at grid points spaced 250 km apart. By means of finite differences, smoothed over a square with sides of twice the grid distance, $\partial \zeta_g / \partial x$ and $\partial \zeta_g / \partial y$ were measured and their mean values over the drift intervals were computed by graphical integration. Next, the direction of the assumed internal stress for periods of equilibrium drift was plotted in arbitrary units on a polar diagram from the vector sum of $\partial \zeta_g / \partial x$ and $-\partial \zeta_g / \partial y$.

An example of such a diagram is shown in Figure 11. Also plotted on the diagram is W , the observed wind; c , the ice drift; and W' , the wind required by theory (curves 1) to account for the drift. In this instance the drift was too far to the right of the observed wind and too fast. From an examination of the forces it is apparent that these discrepancies can be explained by the presence of an additional force acting in the direction from W to W' , which is very nearly the direction of R . On the other hand, a gradient current toward the east would equally well account for the deviations, so the agreement could be fortuitous.

Altogether, 20 periods of equilibrium drift occurred during the 3-month interval, and each case has been analyzed in the same manner as the example. For each of these it has been determined whether the assumed internal resistance vector is in the proper direction to account for the anomaly in the drift speed and drift angle. The analysis showed that in 13 out of 20 cases the internal resistance was properly oriented to account for the sign of anomalies in speed and angle. This result would seem to indicate either that the internal resistance is not a predominant factor in the drift anomalies or that the present formulation and measurement of this force are too crude to reveal its

true effects. It is our belief that the latter is more likely the case and that the matter deserves further study.

Summary and conclusions. When only those cases are considered in which the ice movement is essentially unaccelerated, there still remain significant systematic differences between the observed drift and the drift predicted by equilibrium theory. These differences consist of speeds greater than are predicted for drift in light winds and less than are predicted for drift in strong winds and of drift angles smaller than the predicted values at all wind speeds.

In an attempt to determine the cause or causes of the deviations between observed and theoretical drifts, six possible types of error have been examined. Unless estimated position errors are much greater than we believe them to be, *navigation errors*, though occasionally large, cannot account for the bulk of data scatter. Because of the manner in which the data were selected, *errors due to residual accelerations* and *errors due to use of averaged data* are insignificant.

Errors due to variations in the parameters of the theory are unimportant as regards variations in latitude and ice thickness but are conceivably significant as regards variations in drag parameters, though the seasonal variations in drift behavior failed to support this belief.

Gradient currents and internal stresses are believed to be the main causes of the differences between theory and observation. Charts of dynamic height anomalies suggest that the mean current in the area of drift is of the order of 3 cm sec⁻¹. Analysis of the drift data indicated the existence of a current of about this strength flowing in nearly the direction of the long-term mean current. This could account for the abnormally large drifts and wind factors at low wind speeds, and it could also be a factor in the reduction of the drift angle below the theoretical values.

Although an analysis of 20 specially selected periods of unaccelerated drifts, for which directions of the internal stress were estimated from synoptic weather charts, failed to show conclusive evidence of the presence of this stress, it is nevertheless believed that the tendency of the pack ice to drift more slowly in moderate to strong winds than is predicted is mainly attributable to the internal resistance.

DRIFT OF ICE STATION ALPHA

Suggestions for future research. The study of the drift of the polar ice is plagued at every turn by uncertainties and difficulties. Throughout this paper reference has been made to problems which require further investigation. Here we shall recall only what appear to be the main obstacles to further progress and shall point out areas that seem ripe for exploitation with tools already at our disposal.

The single most urgently needed study is the study of water drag. Actual measurements are needed to reveal its size and relationship to the ice drift. It is possible that oceanographic data now available or soon to become available from drifting ice stations could shed much light on this problem. We have not had time to investigate the matter fully, but certainly no digested results of drag studies have been brought to our attention. It is conceivable that new instrumentation, such as an inverted mast projecting below the ice with current-, temperature-, and salinity-measuring equipment attached, may be required for an adequate treatment of the problem. Accurate current measurements would, of course, reveal directly the role of gradient currents in explaining drift anomalies.

Direct measurement of the water drag would aid in solving the problem of internal stresses, since these could, in principle at least, be determined as a residual force. Further progress would then depend on the availability of measurements of ice movement from a network of stations in order that the stresses might be related to the differential motions. Since many properties of the ice are known, it is possible that theoretical reasoning alone might lead to advancement. The pack ice is not elastic, plastic, or fluid. How should it be characterized? When this question is answered, a step forward will have been taken. A number of people have given thought to installing strain gages in the ice in order to measure the stresses directly. Although the authors are not qualified to judge the feasibility of such measurements, there can be no doubt about their desirability.

The wind stress, though not so uncertain as other factors, is also deserving of further study. The stress under stable conditions is still not well known and is an important problem, and the means are at hand for making progress in this respect. A sufficiently long series of winds aloft data, gathered either by double-theodolite

observations or from the GMD-1 radiosonde on the 6-second data punchout, would define the wind spiral in the surface layer (and thus the surface stress) under a variety of meteorological conditions. Continued measurements of wind and temperature profiles by micrometeorological masts, such as were carried out on Alpha I, are to be encouraged. Although the aerodynamic method of obtaining the stress is accurate only in the neutral case, approximate results can be obtained in the stable case [Liljequist, 1957].

The accuracy and frequency of the determination of the positions of ice stations are not satisfactory, especially in summer. The value of proposed navigation satellites in improving the quality of drift data should not be overlooked.

The ultimate solution to the drift problem must come from numerical integration of the nonlinear equations by high-speed computer. It is not too early to begin to acquire experience and skill in numerical methods.

APPENDIX

Details of the derivation and solution of the equilibrium drift equations. We consider first the derivation of (9). This equation results from the requirement that the eddy viscosity be continuous at the interface between the boundary and spiral layers.

By definition, the eddy viscosity in the boundary layer may be expressed as

$$\mu = \frac{\tau}{\partial r / \partial z} \quad (\text{A-1})$$

From (6) τ in the boundary layer has the constant value

$$\tau_w = \rho_w k_0^2 r^2 \left[\ln \frac{z + z_0}{z_0} \right]^{-2} \quad (\text{A-2})$$

where z is depth below the undersurface of the ice. From these two equations it can be seen that

$$\mu = \rho_w k_0^2 (z + z_0) r \left[\ln \frac{z + z_0}{z_0} \right]^{-1} \quad (\text{A-3})$$

At the interface between the two layers, the value of the eddy viscosity is

$$\mu_h = \rho_w k_0^2 (h + z_0) r \left[\ln \frac{h + z_0}{z_0} \right]^{-1} \quad (\text{A-4})$$

REED AND CAMPBELL

and this must equal the value of μ in the spiral layer, which in an alternative form of (7) may be written

$$\begin{aligned}\mu_h &= \frac{\tau_w^2}{\rho_w f V_0^2} \\ &= \frac{\rho_w k_0^4}{f} \frac{r^4}{V_0^2} \left[\ln \frac{h+z_0}{z_0} \right]^{-4}\end{aligned}\quad (\text{A-5})$$

Equating (A-4) and (A-5)

$$V_0 = Br^{3/2} \quad (9)$$

where

$$B = k_0 \left[\ln \frac{h+z_0}{z_0} \right]^{-3/2} [f(h+z_0)]^{-1/2} \quad (10)$$

We next consider a procedure for solving (2) to (6) and (9) for α in terms of τ_w and c . Additional dependent variables are β , r , V_0 , and h . However, we here treat h as a parameter of the problem, since we have been unable to find an additional physical relationship involving the thickness of the boundary layer, and since there is some evidence from atmospheric data that it is a slowly varying function of wind speed.

The reduction of variables begins with the division of (3) by (2). Thus

$$\tan \alpha = \tan \beta + mfc/\tau_w \cos \beta \quad (\text{A-6})$$

Substituting for c from (4) and for r from (5), we obtain

$$\tan \alpha = \tan \beta + mfV_0 \frac{\sin\left(\frac{\pi}{4} - \beta\right) \cos \beta + \cos\left(\frac{\pi}{4} - \beta\right) \sin \beta}{\tau_w \sin \beta \cos \beta} \quad (\text{A-7})$$

If we introduce V_0 from (9) and make appropriate trigonometric transformations, (A-7) becomes

$$\tan \alpha = \tan \beta + \frac{\sqrt{2}mfBr^{3/2}}{\tau_w \sin 2\beta} \quad (\text{A-8})$$

Next (6) and (2) are substituted, giving

$$\begin{aligned}\tan \alpha &= \tan \beta \\ &+ \frac{\sqrt{2}Bmf}{\sin 2\beta} \left[\frac{\cos \beta}{A^3 \cos \alpha \tau_w} \right]^{1/4}\end{aligned}\quad (14)$$

This equation now contains only two unknowns, α and β .

A second equation in only two unknowns is obtained by squaring (4) and (5), adding, and making appropriate trigonometric transformations. The result is

$$c^2 = r^2 + \sqrt{2}Br^{5/2} + B^2r^3 \quad (11)$$

A third equation is derived by substitution of (9) into (5).

Thus

$$\sin \beta = \left[\frac{B^2r}{2(B^2r + \sqrt{2}Br^{5/2} + 1)} \right]^{1/2} \quad (12)$$

Finally (6) is substituted into (2) and (3), and these two equations are then squared and added. This yields

$$A^2r^4 + 2mfA \sin \beta r^2 c + m^2 f^2 c^2 = \tau_w^2 \quad (13)$$

The method of solution is to assume values of r and to determine from (11) and (12) corresponding values of c and $\sin \beta$. These values are substituted into (13), giving τ_w . Finally, the values of β and τ_w are substituted into (14), and α is found by trial and error. The final result is to arrive at values of c and α which correspond to selected values of the wind stress.

Acknowledgments. We wish to thank Mrs. Irene Cotell (*nee* Browne) formerly of the Geophysical Research Directorate of the Air Force Cambridge Research Laboratories and Mr. Gary Latham of the Lamont Geological Observatory for supplying the data on station positions; Dr. Clifford A. Barnes and Mr. Lawrence K. Coachman of the Department of Oceanography, University of Washington, for providing their unpublished chart of dynamic topography and gradient currents for the western portion of the Arctic basin and for other advice and assistance; and Dr. Joost A. Businger of the Department of Meteorology and Climatology, University of Washington, for helpful counsel on problems relating to turbulence. This work was supported by the Office of Naval Research under task number NR 307-252.

REFERENCES

- Browne, I. M., and A. P. Crary, The movement of ice in the Arctic Ocean, *Proc. Conf. on Arctic Sea Ice*, Natl. Acad. Sci. Natl. Research Council Publ. 598, 191-209, 1958.
Ellison, T. H., Turbulent transport of heat and

DRIFT OF ICE STATION ALPHA

- momentum from an infinite rough plane, *J. Fluid Mech.*, 2, 456, 1957.
- Gordienko, P., Arctic ice drift, *Proc. Conf. on Arctic Sea Ice, Natl. Acad. Sci. Natl. Research Council Publ.* 598, 210-220, 1958.
- Gudkovich, Z. M., Ice drift in the central arctic basin. Preprints, International Oceanographic Congress, New York, N. Y., 1959.
- Liljequist, G. H., Energy exchange of an antarctic snow-field, 1, Wind structure in the low layer, *Norwegian-British-Swedish Antarctic Expedition, 1949-52, Scientific Results*, vol. II, Norsk Polarinstitut, Oslo, 234 pp., 1957.
- Nansen, F., The oceanography of the north polar basin, *The Norwegian North Polar Expedition 1893-1896, Scientific Results*, vol. 3, 357-386, 1902.
- Panofsky, H. A., A. K. Blackadar, and G. E. McVehil, The diabatic wind profile, *Quart. J. Roy. Meteorol. Soc.*, 86, 390-398, 1960.
- Reed, R. J., and W. J. Campbell, Theory and observations of the drift of ice station Alpha, *Final Rept., task number NR 307-250*, University of Washington, Seattle, 255 pp., 1960.
- Rossby, C. G., and R. B. Montgomery, The layer of frictional influence in wind and water currents, *Papers Phys. Oceanog. Meteorol. Mass. Inst. Technol. and Woods Hole Oceanog. Inst.*, 3, 1-100, 1935.
- Shuleikin, V. V., The drift of ice-fields, *Compt. rend. (Doklady) acad. sci. USSR*, 19, 589-594, 1938.
- Shuleikin, V. V., The present status of the theory of ice field drift, in *Pamiat' Iulia Mikhailovicha Shokal' Skogo*, vol. II, 63-82, *Izvest. Moscow Akad. Nauk SSSR*, 1950. Translated for Air Force Cambridge Research Center, Bedford, Mass., 1954.
- Sverdrup, H. U., The wind-drift of the ice on the north Siberian shelf, *The Norwegian North Polar Expedition with the "Maud" 1918-1925, Scientific Results*, vol. 4, 1-46, 1928.
- Sverdrup, H. U., The stress of the wind on the ice of the polar sea, *Skifter No. 111, Norsk Polarinstitut*, 11 pp., 1957.
- Zubov, N. N., and M. M. Somov, The ice drift of the central part of the Arctic basin, *Problemy Arktiki*, 2, 51-68, 1940. Translated for Air Force Cambridge Research Center, Bedford, Mass., by the American Meteorological Society, contract AF 19 (604)-1936.

(Manuscript received April 8, 1961; revised October 26, 1961.)

The Roughness Parameters of Sea Ice

N. Untersteiner

F.I. Badgley

Reprinted from the
JOURNAL OF GEOPHYSICAL RESEARCH,
Vol. 70, No. 18, pp. 4573-4577, September 1965

The Roughness Parameters of Sea Ice¹

N. UNTERSTEINER AND F. I. BADGLEY

*Department of Atmospheric Sciences
University of Washington, Seattle*

Abstract. The influence of the roughness length on calculated fluxes of momentum and matter in the boundary layer is discussed. From observations of the velocity profiles of wind and water current, the roughness length of arctic sea ice is found to vary greatly around an average of 0.02 cm for the upper and 2 cm for the lower surface.

INTRODUCTION

It is well known that when a fluid flows along a plane, solid surface, equilibrium is attained when the velocity profile is logarithmic or almost logarithmic with distance from the boundary, that is, when

$$u = \frac{1}{k} \left(\frac{\tau_0}{\rho} \right)^{1/2} \ln \frac{z+d}{z_0} \quad (1)$$

where u is the fluid velocity, k a numerical constant (von Kármán's constant) equal to 0.4, τ_0 the tangential stress at the surface, ρ the fluid density, z the distance from the surface, d the so-called displacement distance, and z_0 the roughness parameter, a length generally considered as characterizing the surface. In the following discussion, d will be considered to be zero, which implies that u approaches zero as z approaches z_0 .

In the presence of a density gradient, (1) has to be modified for large z ; but, even then, it is a good approximation near the surface [Lumley and Panofsky, 1964, p. 104].

If observations of u at two or more heights are available, (1) with $d = 0$ may be used to determine τ_0 and z_0 . If z_0 is known, observation of u at only one level will suffice to determine τ_0 .

An alternative expression relating τ_0 and u is

$$\tau_0 = \rho C_D u^2 / 2 \quad (2)$$

where C_D is called the drag coefficient. There is a one-to-one relationship between C_D and z_0 in the logarithmic profile layer:

$$C_D = 2k^2 / [\ln(z/z_0)]^2 \quad (3)$$

This relationship shows that C_D is relatively insensitive to changes in z_0 , especially when z/z_0 is large. At $z = 100$ cm, z_0 can change by an order of magnitude, from 0.001 to 0.01 cm, with a concomitant increase in C_D by a factor only 1.5. For the same z (100 cm), an increase of z_0 from 2.0 to 20.0 cm increases C_D by a factor of 4.8.

C_D or z_0 can also be related to the coefficient of eddy diffusivity for momentum, K_m , and thereby to the eddy diffusivities for heat and matter, K_h and K_s , which are usually taken to be equal to K_m or differ from it by a constant factor. It can be shown that

$$K_m = kzu \left(\frac{C_D}{2} \right)^{1/2} = \frac{k^2 zu}{\ln(z/z_0)} \quad (4)$$

Using this relationship one can show, for instance, that a change in z_0 from 0.001 to 0.01 cm (as above) would change the computed flux of water vapor for a given humidity profile by 23%.

It is our intent to report observed values of z_0 for both the upper and the lower surface of floating sea ice. This should allow the reader to assess the accuracy and expected variation in stresses computed from (1) or (2). These values were obtained by extrapolating observed wind and water current profiles to the level where $u = 0$, which is, by definition, $z = z_0$. According to a rule of thumb, z_0 is equal to about 1/30 of the height of the dominant actual roughness elements of the surface, but in practice these elements are difficult or impossible to identify.

¹ Contribution 100, Department of Atmospheric Sciences, University of Washington, Seattle.

UNTERSTEINER AND BADGLEY

RESULTS

Upper surface. The data were obtained at United States Drifting Station Alpha during the International Geophysical Year. One observation site was utilized from July 1957 to April 1958, another from May to September, 1958. The two sites were on floes (2 to 4 m thick) about 2 km apart. The surface was generally uniform, and its shallow snowdrifts, ripples, or meltwater ponds were typical of old pack ice of undisturbed growth. The nearest open leads or prominent pressure ridges were more than 500 m away. The wind velocity was measured at 20, 40, 80, and 160 cm above the surface by means of light-weight 3-cup anemometers (manufactured by Thornthwaite Associates). From a total of several hundred 10-minute runs, the 186 showing logarithmic or nearly logarithmic profile were selected and used to determine z_0 by graphical extrapolation as described above. All cases with blowing snow were excluded. The deviation of the observed wind velocities from a logarithmic profile was, at an average over all levels and velocities, 0.18% of the wind speed. The greatest deviation of a single measurement in the data used was 1.0%.

The values of z_0 scatter over roughly three orders of magnitude, the logarithmic average being 0.02 cm. The values were plotted versus time (Figure 1) in the anticipation that some of the scatter might be related to the varying state of the surface: dry snow in winter, slush during spring melt, and bare ice with puddles during summer. If any such trend exists, it is so small as to be obscured by the scatter.

Figure 2 shows the same observations plotted versus wind speed at 160 cm. There seems to be little systematic dependence. If anything, there is a slight decrease of z_0 with increasing wind, as found by Liljequist [1957, p. 196] for the same range of speed.

Lower surface. The flow velocity under the ice was measured at the edge of ice island Arlis II in the Greenland Sea in February and March, 1965, at approximately 75°N, 14°W. The Savonius rotor current meter (manufactured by Hydro Products, Inc.) with a rotor height of 20 cm and a starting speed of 1 cm/sec was lowered through a hole of about 1-m² cross section in ice of 5 m thickness. Successive readings were taken at levels of 50, 100, 200, and

400 cm below the bottom of the ice near the upstream edge of the hole during periods when the current was generally toward the edge of the island. Under these conditions, the current profile could be presumed to be representative of the field of pack ice adjacent to the island. The nearest open water was several kilometers away. Since the ice was no longer growing, it can be assumed that the effect of free convection (by the release of heavy brine under rapidly growing ice) was negligible.

The current normally undergoes fluctuations of up to 20 minutes duration which make it necessary to average the individual profiles. After some trials, it was found that consistent results could be obtained by reading the meter after it had been at a given level for 30 seconds and averaging the profiles in groups of ten. A total of 18 such groups was obtained; 16 of them showed a logarithmic or nearly logarithmic profile, the average and maximum deviations from the logarithmic profile (as above) being 1.6% and 5.2%. The resulting values for z_0 have been entered in Figure 2. As in the case for air, the scatter is considerable, and a dependence on the flow velocity is absent or small. The average is about 2 cm.

DISCUSSION

A possible explanation of the wide variation in z_0 (or C_D) is suggested by observations made in pipes [Schlichting, 1955, p. 426]. Rib-like corrugations formed by deposits in a water duct were found to be 25 to 50 times as effective in retarding the flow as random roughness elements in the same sized pipe. The snow surface is characteristically corrugated, and it may be that only a slight change in the angle between the wind and the corrugations could change the effective roughness by a similarly large factor. Additional scatter could be due to instrumental errors, to nonstationarity of the flow, and to varying density stratification. Whether the observed variance can be explained by one or all of these factors cannot be ascertained from the present data. A more elaborate treatment, such as described by Robinson [1962], would be meaningful only if the data were of high accuracy and if simultaneous, compatible density (temperature, salinity) measurements were available.

The two curves shown in Figure 2 indicate the

ROUGHNESS PARAMETERS OF SEA ICE

31

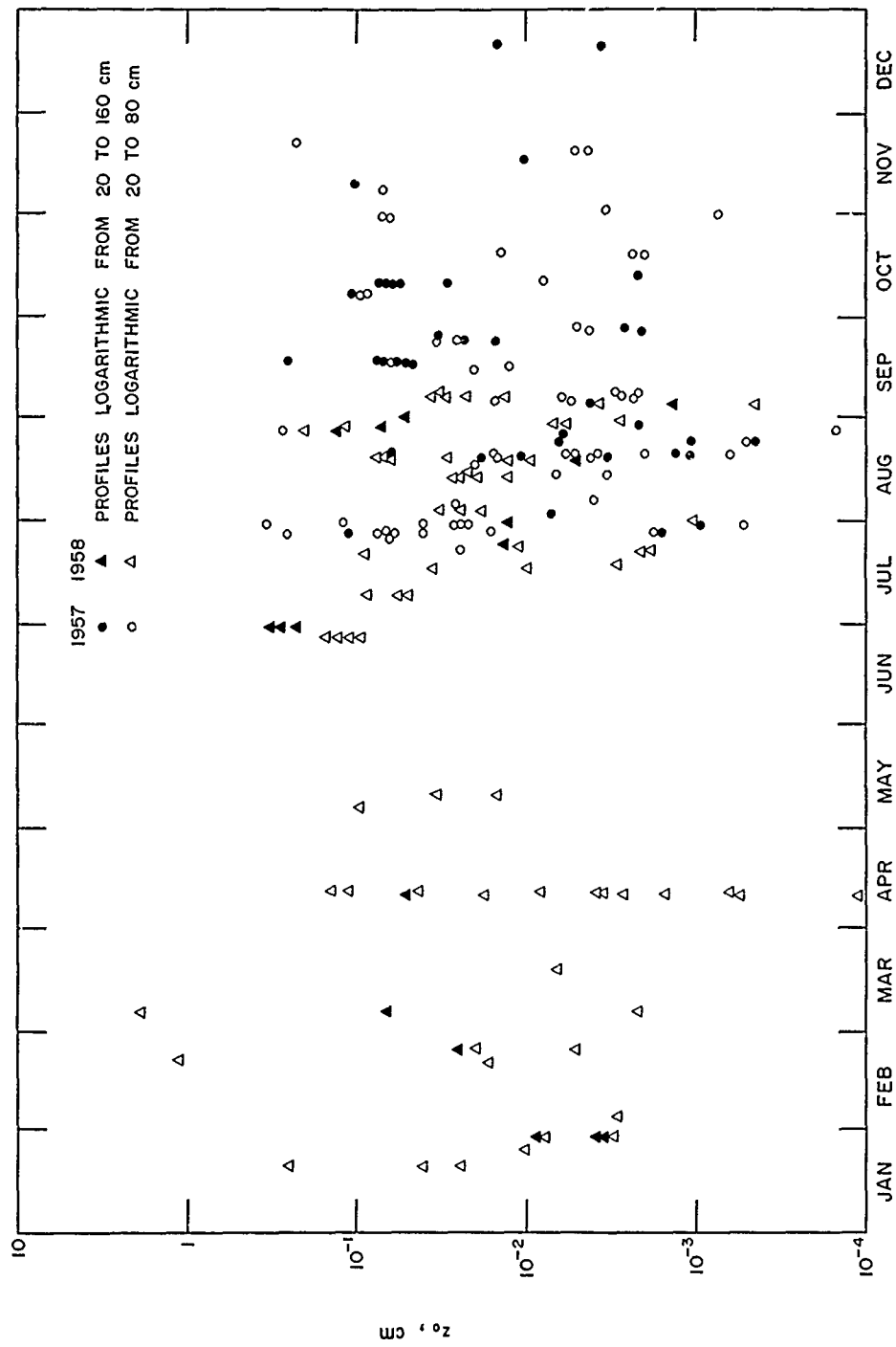


Fig. 1. Observed values of the roughness parameter (upper surface) of sea ice at U. S. Drifting Station Alpha.

UNTERSTEINER AND BADGLEY

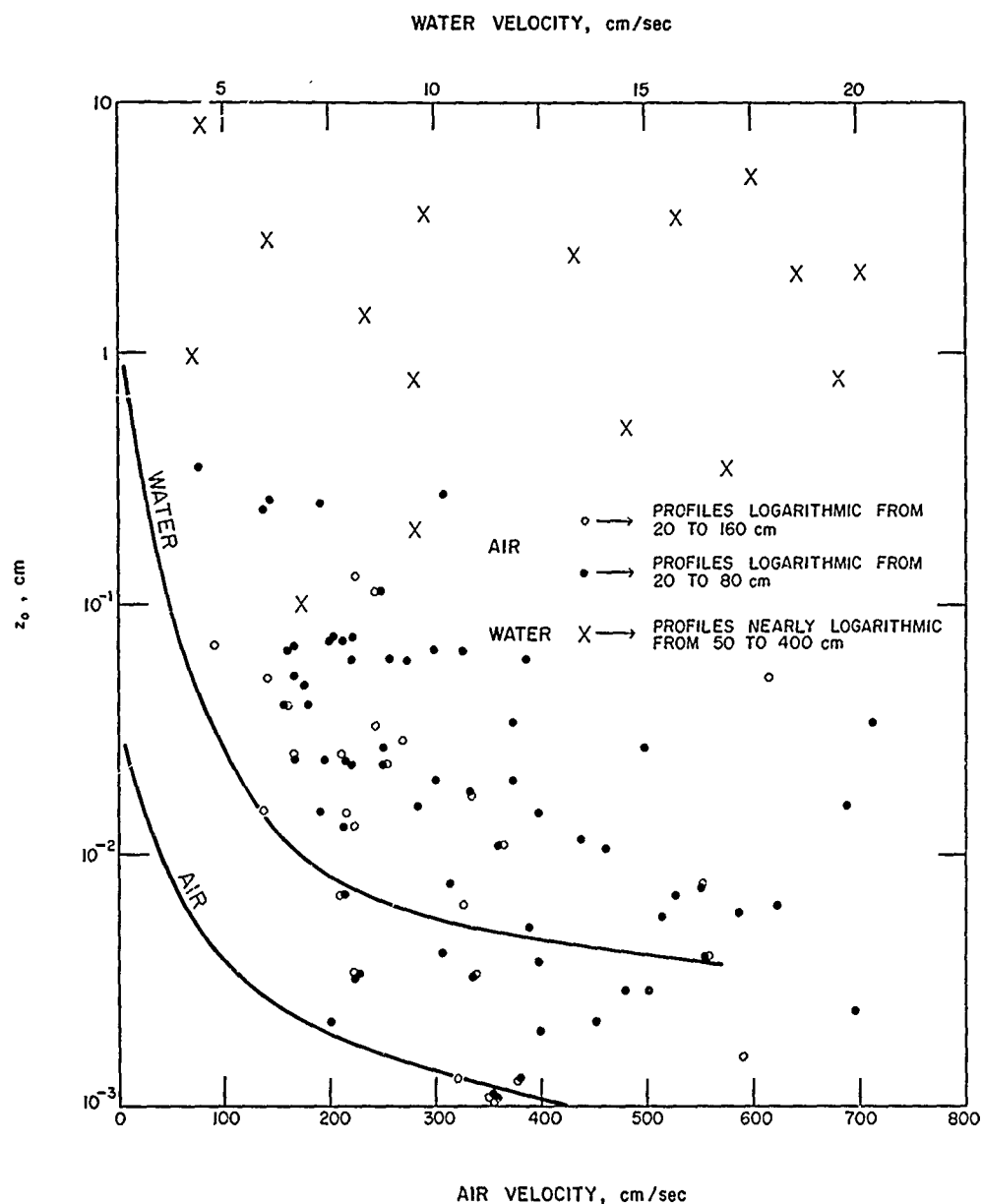


Fig. 2. Observed roughness parameters of sea ice plotted versus flow velocity (lower scale for air velocity at 160 cm height, upper scale for water velocity at 400 cm depth). The two curves represent the limiting values of z_0 for hydrodynamically smooth flow.

limiting values of z_0 for hydrodynamically smooth flow (see acknowledgments). In these cases, the intercept of the logarithmic profile for $u = 0$ is $9\nu/u_* \equiv 9\nu/(\tau_0/\rho)^{1/2}$ [see Schlichting, 1955, p. 407], where u_* is the friction velocity and ν the kinematic viscosity. Once this

limiting value has been reached, the intercept is independent of the roughness. The few values near 10^{-4} in Figure 1 have been omitted in Figure 2. Obviously, the bulk of the data represents fully rough flow.

In a recent study, Campbell [1965] has com-

ROUGHNESS PARAMETERS OF SEA ICE

puted the annual average field of sea ice movement in the Arctic Ocean under the action of wind and water stresses. He introduced various combinations of roughness parameters into his numerical model and compared results with the observed flow pattern. The best resemblance was obtained with $z_0 = 0.02$ cm for the upper surface and $z_0 = 2.6$ cm for the lower surface. The former was taken from our wind data, which were available to him, whereas the latter was, at the time, a guess which is corroborated by the present results.

Acknowledgments. We are indebted to Professor R. O. Reid for pointing out the limiting values of z_0 for hydrodynamically smooth flow as shown in Figure 2.

This research was supported by the National Science Foundation, grant Y/21.14/337, and by

the Office of Naval Research, NR 307-252, contract Nonr 477(24).

REFERENCES

- Campbell, W. J., The wind-driven circulation of ice and water in a polar ocean, *J. Geophys. Res.*, 70(14), 3279-3301, 1965.
- Liljequist, G. H., Energy exchange of an antarctic snow-field; wind structure in the low layer, *Norwegian-British-Swedish Antarctic Expedition, 1949-52, Scientific Results*, vol. 2, part 1, 1957.
- Lumley, J. L., and H. A. Panofsky, *The Structure of Atmospheric Turbulence*, Interscience Publishers, New York, London, Sydney, 1964.
- Robinson, S. M., Computing wind profile parameters, *J. Atmospheric Sci.*, 19, 189-190, 1962.
- Schlichting, H., *Boundary Layer Theory*, Pergamon Press, New York, London, Paris, 1955.

(Manuscript received May 10, 1965;
revised June 4, 1965.)

On the Mass and Heat Budget of Arctic Sea Ice

N. Untersteiner

Reprinted from the
ARCHIV FUR METEOROLOGIE, GEOPHYSIC UND BIOKLIMATOLOGIE,
Vol. 12, No. 2, pp. 151-182, 1961

Nicht im Handel

Reprint from

Archiv für Meteorologie, Geophysik und Bioklimatologie

Serie A: Meteorologie und Geophysik, Band 12, 2. Heft, 1961

Herausgegeben von

Doz. Dr. W. Mörikofer, Davos, und Prof. Dr. F. Steinhauser, Wien
Springer-Verlag in Wien

551.311.181:551.511.33

On the Mass and Heat Budget of Arctic Sea Ice¹

By

N. Untersteiner, Wien²

With 12 Figures

Summary. Measurements during the drift of "US Drifting Station A" show an annual mass increase of old ice consisting of 12.5 g/cm² snow and 52 g/cm² bottom accretion. During the summer seasons 1957 and 1958 an amount of 19.2 and 41.4 g/cm² respectively, was lost by surface ablation. The ratio of ablation on elevated "dry" surface and in meltwater ponds is 1:2.5. The average pond area was about 30%. Bottom ablation by heat transfer from the ocean was found to be 22 cm (July to Aug./Sept.).

Methods of measuring mass changes are described. In view of their importance as a means of checking the computed heat budget their accuracy is discussed in detail.

The heat budget is computed for a selected period during the height of the melt season. The average daily totals are, in cal/cm²: + 142 from net short wave radiation, — 8 from net long wave radiation, + 9 from turbulent heat transfer, and — 11 from evaporation. The mean daily surface ablation is 0.8 cm. About 90% of it is due to the absorption of short wave radiation.

Only 62% of the total heat supply are transformed at the surface. 38% are transmitted into the ice and mainly used to increase the brine volume. The vertical distribution of this energy was used to compute the extinction coefficient for short wave radiation. From 40 to 150 cm depth it is 0.015 cm⁻¹, somewhat smaller than that of glacier ice.

The heat used during the summer to increase the brine volume in the ice acts as a reserve of latent heat during the cooling season. By the time an ice sheet of 300 cm thickness reaches its minimum temperature in March, 3000 cal/cm² have been removed to freeze the brine in the interior of the ice and the meltwater ponds, and 1700 cal/cm² to lower the ice temperature. Based upon the observed mass and temperature changes the total heat exchange at the upper and lower boundary is estimated. During the period

¹ Contribution No. 51, Department of Meteorology and Climatology, University of Washington.

² The field work was carried out while on leave from the Zentralanstalt für Meteorologie und Geodynamik, Wien.

N. UNTERSTEINER:

May–August the upper boundary received 8.3 kcal/cm^2 , while during the period September–April 12.8 kcal/cm^2 were given off to the atmosphere. The results are compared with those of YAKOVLEV, and considerable disagreement is found with respect to the amounts of heat involved in evaporation and in changes of ice temperature ("heat reserve").

Zusammenfassung. Beobachtungen während der Drift von "US Drifting Station A" zeigen an altem Eis einen jährlichen Massenzuwachs von $12,5 \text{ g/cm}^2$ Schnee und 52 g/cm^2 Eis an der Unterseite. Während der Schmelzperioden 1957 und 1958 betrug der Massenverlust an der Oberseite $19,2$ bzw. $41,4 \text{ g/cm}^2$. Das Verhältnis der Ablation auf „trockenen“ Eisflächen zu der in Wassertümpeln beträgt etwa $1:2,5$. Etwa 30% der Gesamtfläche werden im Sommer von den Wassertümpeln eingenommen. Die Ablation an der Unterseite durch Wärmezufuhr vom Meer betrug etwa 22 cm (Juli bis August/September).

Die Methoden der Messung des Massenhaushalts werden beschrieben. In Anbetracht ihrer Bedeutung als Kontrolle des berechneten Wärmehaushalts wird ihre Genauigkeit näher untersucht.

Die Wärmebilanz der Eisoberfläche wird für einen ausgewählten Zeitraum während des Maximums der Ablationsperiode berechnet. Es ergeben sich folgende mittlere Tagessummen in cal/cm^2 : $+142$ kurzwellige Strahlungsbilanz, -8 langwellige Strahlungsbilanz, $+9$ Konvektionswärmestrom, -11 Verdunstung. Die mittlere tägliche Oberflächen-Ablation betrug in dieser Zeit $0,8 \text{ cm}$. Etwa 90% davon werden durch Absorption kurzwelliger Strahlung verursacht.

Nur 62% des gesamten Wärmeangebotes werden an der Oberfläche umgesetzt. 38% gelangen in tiefere Schichten und werden dort hauptsächlich zur Vergrößerung des Volumens der Salzlösung verwendet. Die vertikale Verteilung dieser Energie wird zur Berechnung des Extinktionskoeffizienten für kurzwellige Strahlung herangezogen. In einer Tiefe von 40 bis 150 cm ergibt sich ein Wert von $0,015 \text{ cm}^{-1}$, etwas weniger als in Gletschereis.

Die Wärmemenge, welche im Sommer zur Erhöhung der Eistemperatur und der damit verbundenen Vergrößerung des Volumens der Salzlösung aufgewendet wurde, dient während der Abkühlungsperiode als Wärmereserve. Von ihrem Beginn bis zur Erreichung minimaler Eistemperaturen in März werden einer 3 m dicken Eisdecke 3000 cal/cm^2 an latenter Wärme (Verkleinerung des Volumens der Salzlösung und Gefrieren der Schmelzwassertümpel) und 1700 cal/cm^2 mit der reinen Temperaturerniedrigung entzogen. Auf Grund der beobachteten Massen- und Temperaturänderungen der Eisdecke wird der gesamte Wärmeumsatz an ihren Grenzflächen abgeschätzt. Während der Periode Mai bis August erhält die Oberfläche des Eises $8,3 \text{ kcal/cm}^2$ während in der Periode September bis April $12,8 \text{ kcal/cm}^2$ an die Atmosphäre abgegeben werden. Die Resultate werden mit denen von YAKOVLEV verglichen, wobei sich beträchtliche Unterschiede in den Beträgen der Verdunstung und der Wärmereserve der Eisdecke ergeben. Im Zusammenhang mit den unterschiedlichen Beträgen der Wärmereserve wird die spezifische Wärme des Meereises näher diskutiert.

Résumé. Les observations faites lors de la dérive du "US drifting station A" font apparaître un accroissement annuel de masse de la banquise de $12,5 \text{ g/cm}^2$ sous forme de neige et de 52 g/cm^2 par congélation à la base. Pendant les périodes de fonte de 1957 et de 1958, la perte de

On the Mass and Heat Budget of Arctic Sea Ice

masse à la surface fut de 19,2 et 41,4 g/cm² respectivement. Le rapport de l'ablation sur la glace "sèche" à celle des flaques est de 1:2,5. Les flaques occupent en été env. 30% de la surface totale. L'ablation à la face inférieure de la banquise par la chaleur de l'eau fut d'environ 22 cm (Juillet à août/septembre).

On décrit les méthodes de mesure du bilan de masse et leur précision. On calcule ce bilan de chaleur à la surface au moment du maximum d'ablation et on en donne les composantes suivantes pour les sommes journalières moyennes en cal/cm²: bilan radiatif de courte longueur d'onde + 142, bilan radiatif de grande longueur d'onde — 8, flux de convection + 9, évaporation — 11. L'ablation superficielle moyenne est de 0,8 cm par jour dont 90% résulte de l'absorption du rayonnement à courte longueur d'onde.

Le 62% seulement de l'apport de chaleur est transformé à la surface de la glace; le 38% pénètre en profondeur et sert surtout à accroître le volume du mélange salin. A une profondeur de 40 à 150 cm le coefficient d'extinction pour le rayonnement court est de 0,015 cm⁻¹, plus faible que dans le glacier terrestre.

La quantité de chaleur accumulée en été sert de réserve pendant la période froide pour élever la température de la glace et pour augmenter le volume de la solution saline. Du début de celle-ci jusqu'au minimum des températures en mars, une couche de 3 m d'épaisseur perd 3000 cal/cm² en chaleur latente et 1700 cal/cm² par chute de température. Il est possible d'estimer le bilan total de chaleur des surfaces de la glace à l'aide des variations observées de masse et de température. Pendant la période de mai à août, la surface de la glace reçoit 8,3 kcal/cm², tandis qu'elle cède à l'air 12,8 kcal/cm² de septembre à avril. Les résultats obtenus diffèrent de ceux de YAKOVLEV dans les quantités de l'évaporation et de la réserve calorifique de la glace. Discussion au sujet de la chaleur spécifique de la glace de banquise.

Introduction

By far the greatest ice-covered area on the northern hemisphere is the Arctic pack ice. Compared to the Greenland ice cap, its mass is small, however, its great influence on the heat exchange between earth and atmosphere and its high sensitivity to climatic fluctuations make it an important factor in the distribution of heat over the hemisphere. The conditions necessary for the formation and preservation of sea ice are of equal interest to meteorology and oceanography.

The present report contains part of the results of heat and mass budget studies of sea ice carried out on "US Drifting Station A" during the International Geophysical Year 1957/58. A brief description of the expedition is given in [34]. Remarks on the methods of investigation as well as some preliminary results have been published in [33].

The camp built on a large ice floe in April, 1957, was damaged by ice cracks and pressure ridges in May, 1958, and had to be transported to another floe where the observations were continued until the camp had to be finally abandoned on 6 November, 1958. In the following, the two periods are called "Station 1" and "Station 2."

N. UNTERSTEINER:

1. Mass Budget

The total mass of ice present on the Arctic Ocean is in general controlled by two processes: a) by large-scale horizontal drift, and b) by local melting and freezing. In some parts of the Arctic Ocean the horizontal drift is rapid (e. g. SSSR NP-I, May, 1937: 90° N, February, 1938: 70° N), and the ice may be transported to climatologically different regions within one year. Ablation and accretion of the ice take place at two surfaces. Considerations of the horizontal transport are complicated by the fact that frequently the condition of continuity is not valid. For example, in the case a flow divergence, large amounts of new ice may be formed where the ocean surface becomes exposed to the atmosphere by the parting of a continuous ice cover.

The general pattern of ice drift in the Arctic ocean is known primarily by the drifts of the ships "Fram," "Maud," and "Sedov," as well as by the Soviet and American drifting Stations (see [9, 15]). The tangential forces exerted on the ice by air and water are also basically known [9, 15]. The physical relationships found between air and ice movement represent average values with good accuracy but large deviations are observed in individual cases.

Their cause may be largely the fact that the pack ice cover can accumulate tensions so that the movement at one place is not only a function of the locally applied forces but influenced by forces transmitted over longer distances. The irregular distribution of such forces due to the irregular shape of the ice floes make the mechanical properties of large sheets of sea ice different from those of small samples. Investigations of the deformation of large fields of sea ice in relation to wind fields are highly desirable for an understanding of the ice budget in the Arctic ocean.

The following considerations of the mass budget refer to an individual ice floe. A simplified plot of its drift during the existence of "Station A" is given in Fig. 1. The total distance covered from May, 1957, to November, 1958, was 3200 km.

1.1. Methods of Observation

Ablation and accumulation on ice surface are commonly observed by means of stakes. The upper surface of sea ice is in most cases irregular (hummocks, pressure ridges, meltwater ponds, snow-drifts, sastrugi), and the mass changes by ablation and accumulation are comparatively small. Therefore, accurate measurements can only be obtained when a sufficiently great number of stakes is used. At Station A, 15 stakes were used from July to September, 1957, 20 stakes from October, 1957, to May, 1958, and 30 stakes from May to October, 1958. During the two latter periods they were placed in two perpendicular lines, at equal distances.

When observing the mass changes of sea ice it is to be noted that not all the meltwater formed at the surface runs off. A certain part

On the Mass and Heat Budget of Arctic Sea Ice

remains on the ice in ponds and re-freezes in the fall. During summer, ablation takes place both at the upper and lower surface.

After some experiments, the measuring arrangement shown in Fig. 2 was finally used. In addition to the stakes ($Z_1 - Z_3$), a water level recorder (tide gauge) was installed. It permits the observation of the hydrostatic equilibrium of the ice floe. The recordings of this instrument are particularly valuable since they are representative of a relatively large area. The support carrying the recording drum is anchored at a level L which remains fixed relative to the main body of the ice. The

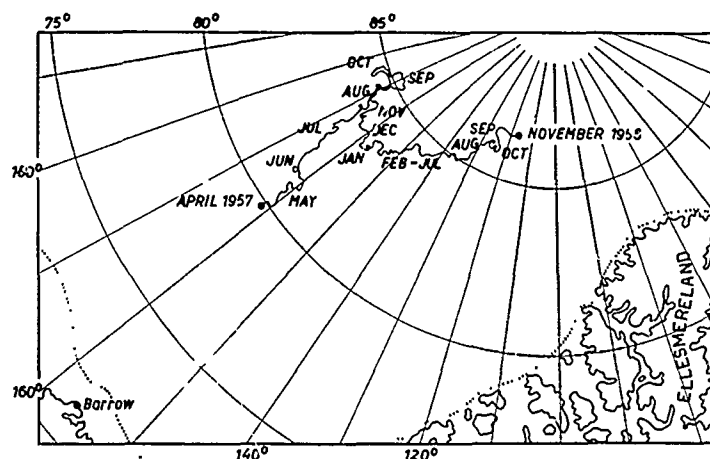


Fig. 1. Drifting Station A during the International Geophysical Year 1957/58

vertical movements of an ice plate (density ρ_i) floating in water (density ρ_w) are recorded as changes of l . Ablation or accretion at the upper or lower surface correspond to changes of l_1 and l_2 . Assuming constant density, the state of equilibrium is given by

$$\rho_i (l_1 + l_2) = \rho_w (l_2 + l).$$

In the case of ice and sea water, mass changes at the upper and lower surface are recorded with a sensitivity ratio of about 7 : 1,

$$\Delta l = \frac{\rho_i}{\rho_w} \Delta l_1 - \frac{\rho_i}{\rho_w} \Delta l_2. \quad (1)$$

In the recordings of Δl , the contributions of Δl_1 and Δl_2 cannot be distinguished. Therefore, separate measurements of bottom ablation and accretion are necessary. In order to avoid the tedious and inaccurate procedure of measuring ice thickness through bore holes another device has been used (see Fig. 2). The "measuring wire" which is normally frozen into the ice, is released by electrical heating and pulled up so that the cross bar at its lower end rests against the ice bottom. The upper

N. UNTERSTEINER:

end of the wire is read against a fixed scale. Since the lower ice surface of old ice floes is comparatively smooth, a number of 3 to 4 of such measuring points was considered sufficient within the accuracy of all other observations.

In the water level recordings, two sources of error should be noted:

a) *Ice density.* Old sea ice has an average salinity of about 2‰ . The size of the brine pockets is variable with temperature and leads to changes of the average density. Between -1 and -10°C the latter is of the order of 1% . According to eq. (1), the corresponding variation of l is of the same magnitude. In order to keep its absolute magnitude small it is advisable,

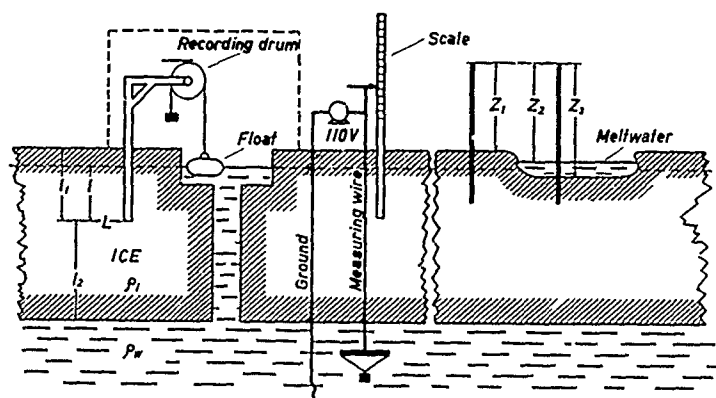


Fig. 2. Means of measuring mass changes of the ice cover

to make l also small, i. e. to anchor the support just deep enough to avoid difficulties with surface melting. Strictly speaking, it would be necessary to allow for the vertical distribution of salinity as well. Furthermore, the air content near the surface may not be constant during the ablation season. Pertinent observations are not available. However, for the present purpose it seems permissible to neglect changes of ice density.

The average ice density as measured by weighing cores of known volume was found to be 0.89 g/cm^3 [21]. In April 1958, a crack through the scientific area of Station A afforded a welcome possibility to take a profile of snow height, free-board, and ice thickness. The results are given in Table 1. With the densities of snow ($\rho_s = 0.33\text{ g/cm}^3$) and water ($\rho_w = 1.03\text{ g/cm}^3$) the average density of the ice is found to be 0.91 g/cm^3 . For all further computations, a mean value of 0.90 g/cm^3 has been used.

b) *Fresh water.* Most of the fresh water formed during the melt season runs off over the edges of the floes. If the relative area of open leads is not too great and if mixing by wind not too intensive, the layer of fresh water floating on the denser sea water may become thicker than the floes and expand along the ice bottom. In this case, the ice floats partially or entirely in fresh or low salinity water. With an ice thickness of 300 cm , a maximum hydrostatic adjustment of 9 cm may result. The present data do not allow an evaluation of this effect. Especially during the summer of 1958 there were large areas of open water in the vicinity of the station in which the thickness

On the Mass and Heat Budget of Arctic Sea Ice

of the fresh water layer was only a fraction of the ice thickness [13]. On the other hand, it was necessary for reasons of camp and runway maintenance to drill a large number of drainage holes. The fresh water spreading at the underside of the ice leads to the formation of a sub-layer of fresh ice, as described in [33]. It seems, therefore, not possible to correct the water level recordings for density variations of the water. The estimated maximum

Table 1. Mean Ice Density, April 1958, under the Assumption of $\rho_s = 0.33$ and $\rho_w = 1.03 \text{ g/cm}^3$

Measuring points, distance ~ 5 m	Snow	Ice above water	Ice under water
1	42 cm	22 cm	315 cm
2	41	20	282
3	29	31	288
4	43	27	304
5	30	19	270
6	37	22	274
7	42	25	277
8	53	13	259
9	90	8	270
10	46	18	296
11	29	18	274
12	33	22	291
13	66	17	299
14	19	44	355
15	35	23	303
16	32	25	277
17	31	26	279
18	26	24	315
19	35	17	289
20	79	19	292
21	59	14	296
mean	42.7	22.1	291

$$\bar{\rho}_i = 0.913 \text{ g/cm}^3$$

error is 3 cm. The hydrostatic rise of the ice floe during the ablation season may be too small by this amount. (In maintaining the water level recorder it is particularly important to keep the water in the vertical tube communicating with the ocean either always salty, or always fresh. Here, the error may amount to 9 cm.)

By means of the measuring devices shown in Fig. 2 it is possible to determine the mass budget with reasonable accuracy. If A_T (cm) and A_W (cm) denote the mass losses on the "dry" surface and in ponds, respectively, A_U the loss at the bottom, and F the relative area of ponds, then the total loss of mass, ΔM , (in cm of water) during a certain time interval can be written

$$\Delta M = \rho_i A_T (1 - F) + \rho_i A_W F + \rho_i A_U - F \cdot \Delta u \quad (2)$$

N. UNTERSTEINER:

Table 2. *Examples of Ablation Measurements on Sea and Glacier Ice. By Means of their Standard Deviation and the Graph Shown in Fig. 4 the Number of Observations Necessary to Obtain an Arithmetic Mean of Given Accuracy Can Be Determined*

Station "A", 83°N, 165°W Ablation on elevated surfaces, stakes					Station "A", 83°N, 165°W Ablation in ponds, stakes					Chogo-Lungma-Gl., Karakorum, 4300 m Ice ablation, bore holes				
1958	A	N	p	$\frac{\sigma}{\sqrt{N}}$	%	A	N	p	$\frac{\sigma}{\sqrt{N}}$	%	A	N	p	$\frac{\sigma}{\sqrt{N}}$
July	6/7	3.1	15	1.10	0.28	9	July	6/7	2.9	15	15	7.9	7	2.5
	7/8	0.8	15	0.83	0.21	26	7/8	7/8	2.2	15	1.62	0.31	14	0.95
	8/10	2.4	15	1.02	0.26	11	8/9	2.2	10	1.80	0.57	24	1.4	0.53
	10/11	1.2	15	1.08	0.28	23	9/10	1.4	9	0.72	0.24	17	6.4	1.0
	12/13	1.4	15	0.70	0.18	13	10/11	2.4	13	2.66	0.74	31	7	0.9
	13/14	0.9	15	0.62	0.16	18	11/12	2.0	13	2.52	0.70	35	7	0.34
	14/15	0.2	15	1.00	0.26	130	12/13	2.0	13	1.75	0.48	24	2.0	0.76
	15/17	1.7	15	0.85	0.22	13	13/14	2.3	13	2.11	0.68	25	6.4	1.4
	17/19	1.4	15	0.66	0.17	12	14/15	2.4	13	0.83	0.23	10	1.4	0.44
	22/23	1.0	15	0.63	0.16	16	15/16	2.1	8	0.95	0.34	16	2.6	0.25
	23/24	3.4	15	0.80	0.21	6	16/17	1.9	8	1.48	0.52	27	7.3	0.8
	24/25	0.6	15	0.45	0.12	20	17/18	2.0	9	0.68	0.23	12	10	0.25
	25/26	0.4	15	0.54	0.14	35	18/19	1.8	9	1.20	0.40	22	3.0	0.44
	26/27	1.0	15	0.94	0.24	24	22/23	1.0	13	1.28	0.36	36	7.7	1.8
	27/28	0.4	15	0.86	0.22	55	23/24	3.0	14	2.39	0.64	21	31	0.57
	28/29	2.5	15	0.77	0.20	8	24/25	2.6	14	2.19	0.59	23	1	1.1
	29/30	2.1	15	1.01	0.30	14	25/26	2.0	14	1.99	0.53	26	7.5	0.44
	30/31	1.1	15	1.22	0.32	29	26/27	2.3	14	1.29	0.34	15	2	1.4
Aug.	31/1	0.4	15	1.17	0.30	75	27/28	1.3	14	1.36	0.36	28	1	0.35
	2/3	0.2	15	0.93	0.24	120	28/29	2.7	14	1.51	0.40	15	2	0.44
	3/4	0.1	15	1.02	0.26	260	29/30	2.9	14	2.00	0.54	19	1	0.44
	4/5	0.6	15	1.12	0.29	48	30/31	1.2	14	0.88	0.24	20	1	0.44
	5/6	1.0	15	0.80	0.21	21	31/1	3.4	14	1.64	0.44	13	1	0.44
	6/7	0.2	15	0.87	0.22	110	1/2	2.2	14	1.94	0.52	24	1	0.44

A = Ablation in cm. arith. mean

N = Number of stakes or bore holes

 σ = Standard deviation σ/\sqrt{N} = Mean error of the arith. mean% = $100 \frac{\sigma/\sqrt{N}}{A}$

On the Mass and Heat Budget of Arctic Sea Ice

of the fresh water layer was only a fraction of the ice thickness [13]. On the other hand, it was necessary for reasons of camp and runway maintainance to drill a large number of drainage holes. The fresh water spreading at the underside of the ice leads to the formation of a sub-layer of fresh ice, as described in [33]. It seems, therefore, not possible to correct the water level recordings for density variations of the water. The estimated maximum

Table 1. Mean Ice Density, April 1958, under the Assumption of $\rho_s = 0.33$ and $\rho_w = 1.03 \text{ g/cm}^3$

Measuring points, distance ~5 m	Snow	Ice above water	Ice under water
1	42 cm	22 cm	315 cm
2	41	20	282
3	29	31	288
4	43	27	304
5	30	19	270
6	37	22	274
7	42	25	277
8	53	13	259
9	90	8	270
10	46	18	296
11	29	18	274
12	33	22	291
13	66	17	299
14	19	44	355
15	35	23	303
16	32	25	277
17	31	26	279
18	26	24	315
19	35	17	289
20	79	19	292
21	59	14	296
mean	42.7	22.1	291

$$\bar{\rho}_i = 0.913 \text{ g/cm}^3$$

error is 3 cm. The hydrostatic rise of the ice floe during the ablation season may be too small by this amount. (In maintaining the water level recorder it is particularly important to keep the water in the vertical tube communicating with the ocean either always salty, or always fresh. Here, the error may amount to 9 cm.)

By means of the measuring devices shown in Fig. 2 it is possible to determine the mass budget with reasonable accuracy. If A_T (cm) and A_W (cm) denote the mass losses on the "dry" surface and in ponds, respectively, A_U the loss at the bottom, and F the relative area of ponds, then the total loss of mass, ΔM , (in cm of water) during a certain time interval can be written

$$\Delta M = \rho_i A_T (1 - F) + \rho_i A_W F + \rho_i A_U - F \cdot \Delta d \quad (2)$$

On the Mass and Heat Budget of Arctic Sea Ice

where Δd is the increase of pond depth. This expression holds only for a sufficiently short period in which $\bar{F} = \text{const.}$ Since $A_T, A_W, A_U, \Delta M$, and d are given by the observations (Fig. 2), eq. (2) could be used to determine \bar{F} whose direct measurement is laborious. Experience showed that, during the first part of the ablation season the pond area increased rapidly, and since the necessary observations are not available it is impossible to evaluate eq. (2) under such circumstances.

1.2. Accuracy

The observations of accumulation and ablation are an important and frequently applied means of checking observations of the heat budget. A closer examination of their accuracy seems of interest.

Apart from various experiments with ablatographs (e. g. [12]) and the occasional application of photogrammetry for special purposes [38] stake measurements are most commonly used. On temperate glacier ice, the measurement of the depth of bore holes has some advantages. In both cases the distance from a fixed level to the average ice level is measured. Therefore, the scattering of individual readings should be about equal. A selection of such observations from a subtropical glacier (Chogo-Lungma-glacier [32]) and from sea ice is given in Table 2. It is seen that, on days with little ablation (e. g. Station A, 14/15 July or 2/3 and 3/4 August), the average error of the arithmetic mean can become greater than the mean itself. An observation of such low accuracy is hardly usable to check other observations.

BOCHOW, HÖHNE and RAEUBER [8] have given a handy graph to determine the number of observations necessary to obtain a representative mean. With an additional curve for 90% probability, it is reproduced in Fig. 3. First, the standard deviation of a series of observations, σ , is computed. The arithmetic mean is considered to be representative if it differs, with a predetermined probability P , by not more than x from the true mean. x and P are fixed according to any particular requirements. N is the number of observations. If the point $(x/\sigma, N)$ falls to the right of the chosen P -curve then the arithmetic mean is representative. If it falls to the left, the number of observations necessary for an arithmetic mean of the desired accuracy is established by finding this point of the respective p -curve whose ordinate is x/σ . The abscissa in this point is the required N .

According to Table 2 the standard deviation of ablation measurements on glacier and sea ice is approximately 1.0 cm. It seems reasonable to postulate that the computed mean should be within $\pm 10\%$ of the true mean, with a probability of at least 90%. If the required accuracy of the ablation measurement is ± 0.1 cm, this would require 340 measuring points according to Fig. 3. On the other hand, a given number of observations, $N = 15$, renders an error $x' = 0.45$. According to the requirement stated above, this should be not more than 10% of the true mean. In other words, by using 15 stakes, ablation can only be

N. UNTERSTEINER:

measured with sufficient accuracy if it is not less than 4.5 cm. The daily amounts of ablation at Station A (Table 2) are all much below this magnitude and of a correspondingly little accuracy. When using ablation data to check observations of the heat budget, longer periods with sufficiently great amounts of ablation will have to be considered. On the other hand, the daily amounts of ablation on Chogo-Lungma glacier (Table 2) were large enough to render representative means with only 7 to 10 single values ($\alpha'/\sigma = 0.7$).

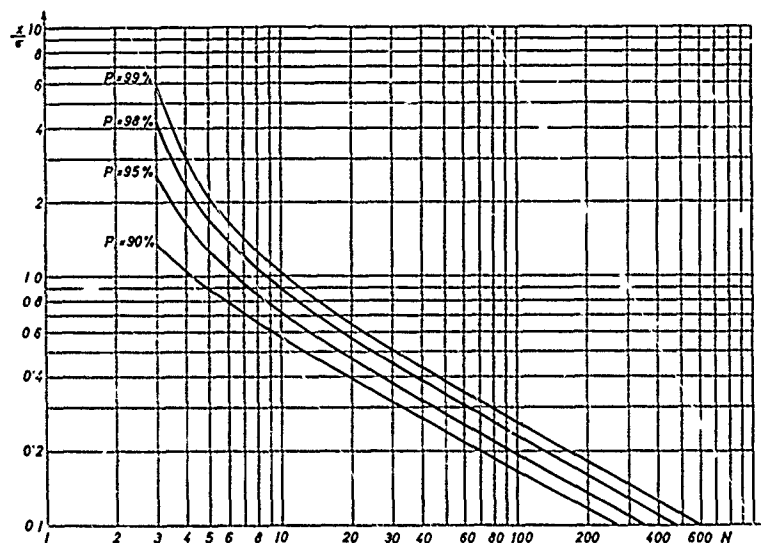


Fig. 3. Graph for the determination of the number of single values (N) necessary to obtain a representative arithmetic mean (after [3])

Much more unfavourable are such considerations for the measurement of accumulation. Due to the surficial irregularities and the transport of snow by wind (formation of sastrugi) the standard deviation becomes very large. For the measurement of accumulation the water level recordings are particularly valuable.

1.3. Results of Observations

Detailed observations of the mass budget began at Station 1, on 10 July, 1957 (Fig. 4). At this date, some ice ablation had already taken place. A few measurements of snow height and density had been made before the onset of melting (early June, first part of curves a and b in Fig. 4). The dashed parts of curves a and b have been extrapolated from our notes on the state of the surface. The data obtained at Station 2 permit a more detailed representation (Fig. 5). While the stake and

On the Mass and Heat Budget of Arctic Sea Ice

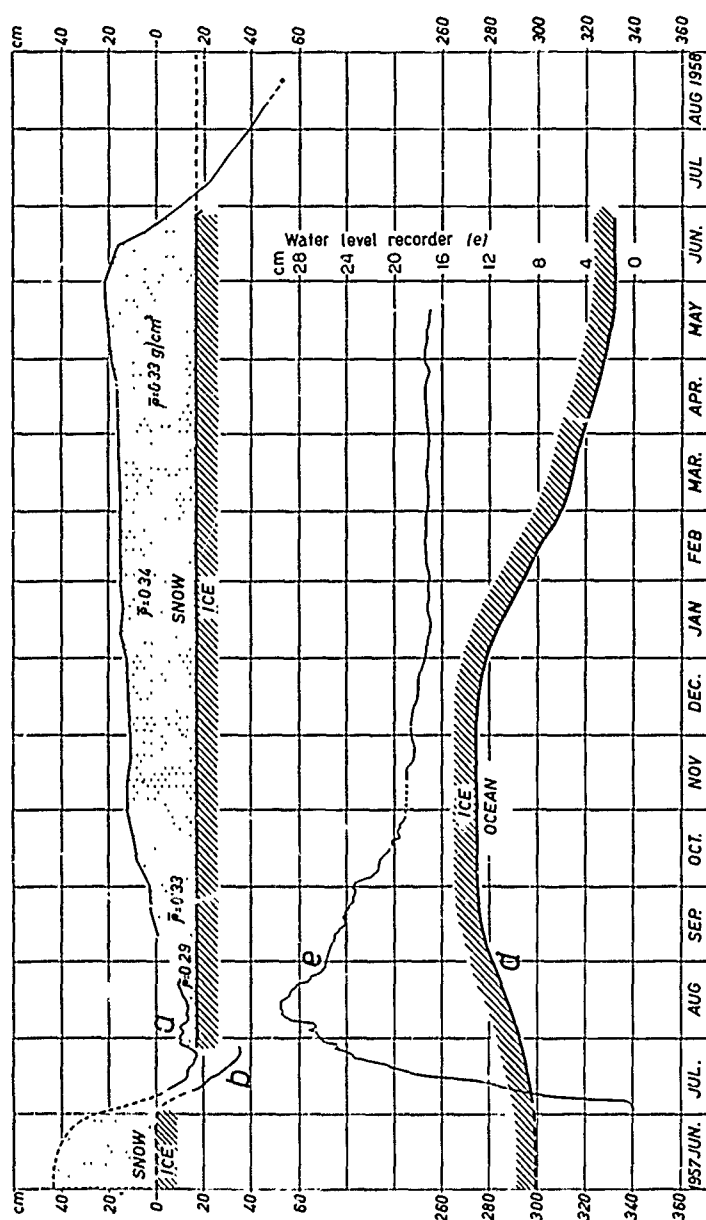


Fig. 4. Mass changes at the upper and lower surface of the ice, station 1. Curve e shows the hydrostatic adjustment of the floe

N. UNTERSTEINER:

thickness readings could be continued for some time after the evacuation on Station 1, the water level recorder was taken down on 19 May and re-installed at Station 2 on 27 May, 1958.

1.3.1. Ablation

By comparison of Fig. 4 and 5 it is seen that the ablation periods 1957 and 1958 began at approximately the same time, however, in 1958

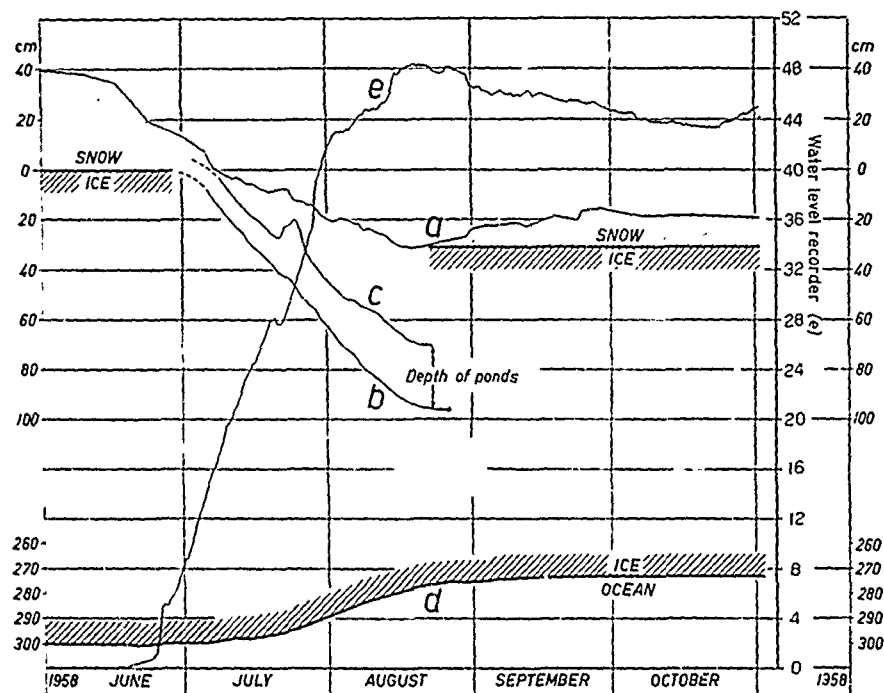


Fig. 5. Mass changes at the upper and lower surface of the ice (see also Fig. 2 and 4)

it lasted about one month longer and led to correspondingly greater ablation. The mean geographical position of the Station in July, 1957, was 82°N , 165°W , and in July, 1958, 84°N , 145°W (distance ~ 300 km.).

Eq. (1) can be used to ascertain the total loss of mass at the surface during the period of ablation. The values of Δl_1 and Δl_2 are taken from curves *e* and *d* in Fig. 4 and 5. For 1957, $\Delta l_1 = 32.2$ cm, and for 1958, $\Delta l_1 = 53.1$ cm (all values in water equivalent). According to the observations of snow height and density, 13.0 and 12.1, respectively, of the above totals come from the melting of snow. The remaining 18.0 and 39.9, respectively, represent the loss of ice at the surface. It is com-

On the Mass and Heat Budget of Arctic Sea Ice

posed of the ablation on "dry" surfaces and in ponds, reduced by the pond volume at the end of the ablation period. The latter is an important factor in the heat budget. The latent heat stored in the pond water retards cooling in the fall. As mentioned earlier, observations of the pond area are not available. The observations of pond depths, too, were only in 1958 sufficiently numerous. In this case, eq. (2) may serve to estimate the pond area F . The values of A_T , A_W , and d are taken from Fig. 5 ($\rho_i = 0.90 \text{ g/cm}^3$). A pond area of $F = 42\%$ is obtained. If the ponded meltwater were spread out it would form a layer of water 10.5 cm thick. The latent heat stored in this layer is 840 cal/cm^2 . If one assumes a similar pond area for 1957, the heat reserve would be 200 cal/cm^2 . Due to the shorter ablation season in 1957, the ponds were not as deep as in 1958. Because of the lower reliability of the 1957 observations too much emphasis should not be placed on the above result.

The amount of solid precipitation during June–August is generally small. A relatively strong snow-fall on 20 July, 1958, is clearly shown by the water level recording (Fig. 5, curve e). A small depression on 21 July is followed by an especially steep rise on 23 July which represents the run-off of the excess melt-water. A large part of the freshly fallen snow was blown into the ponds, as shown by the temporary increase of their depth (curve c).

As it will be explained later, the measurement of ablation of sea ice by means of stakes is of limited value. A large proportion of the total turnover of heat takes place below the surface and does not manifest itself as surficial ablation. The higher the temperature and salinity of the ice, the greater becomes internal melting and the more important it becomes to ascertain the true loss of mass (run-off) by a cumulative method as provided by the water level recorder.

1.3.2. Accumulation

The present observations provide further evidence that the annual amount of precipitation in the central Arctic is small, of the order of 150 mm. It takes only a short time for the freshly deposited snow to attain an approximately constant density of 0.33 g/cm^3 . Similar results were obtained by the Soviet drifting Station NP-II [36]. Some of the average densities observed have been entered in Fig. 4. As mentioned earlier, the water level recordings can be used for the determination of a cumulative snow density. For the time from the beginning depression of the ice floe (Fig. 4, maximum of curve e) until the beginning of ice accretion at the bottom, eq. (1) renders $l_1 = 9.5 \text{ cm}$ of water column or 29 cm of snow with a density of 0.33 g/cm^3 , in excellent agreement with the direct observations (curve a). However, for the time of accretion at the bottom, December–April, eq. (1) renders incorrect values. To a small extent this may be caused by a greater density of the freshly accreted bottom ice but it is easily seen by means of eq. (1) that even an extremely high density of the new ice cannot explain the floe's lack of

N. UNTERSTEINER:

lift. The actual cause is most likely to be sought in the fact that the 80 cm high box covering the water level recorder collected large snow drifts in all directions with a length of up to 20 metres. During clear weather and falling temperatures the surface of recently deposited snow drifts frequently become hardened by sublimation within the uppermost layer so that the drift is not easily removed by wind from another direction. It is, therefore, inevitable that any aerodynamical obstacle collects more or less permanent snow-drifts on all sides which cause an additional depression of the ice. Similar conditions prevailed during the deposition of snow in the fall, 1958 (Fig. 5). At the end of the melting season, when the

Table 3. *Observed Amounts of Mass Loss and Gain at the Upper and Lower Surface of the Ice. The Meltwater Retained in Ponds has been Deducted from the Loss Figures. A_T and A_W are the Amounts of Ablation on Elevated ("Dry") Surfaces and in Ponds, Respectively*

Boundary	Gain	Loss	Ice ablation	
			A_T	A_W
air / ice (cm water)	1956/57 : 13,0	1957 : 32,2	15,5	31,0
		13,0 snow 19,2 ice		
	1957/58 : 12,1		27,6	85,3
	1958 : (5,2) (until Oct.)	1958 : 53,5		
		12,1 snow 41,4 ice		
ice / ocean (cm ice)	1957/58 : 57	1957 : 22		
		1958 : 24		

ponds begin to freeze their level is about 20 to 50 cm below the average "dry" level. Most of the new snow is blown into these depressions and not accurately represented by the stake readings (curve *a*). In this case, the water level recordings are more reliable. The amount of accumulation from the middle of August to the end of October, 1958, is found to be 5.2 cm of water or 16 cm of snow with a density of 0.33 g/cm³. When the ice-cover of the ponds is still thin it is frequently broken by load of the overlying snow. The filling of the ponds with water-saturated snow accelerates the process of freezing. In this manner, atmospheric precipitation which otherwise takes part only indirectly in the mass budget, can contribute a small amount to the formation of ice at the surface.

1.4. Summary

The constituents of the mass budget are summarized in Table 3. Ice accretion during the winter 1957/58 was greater by 16 cm than the ice loss during the previous summer. This was compensated by a relatively great loss during the following summer. Assuming an ice thickness of 300 cm in May, 1957, it was 316 cm in May, 1958, while the September thicknesses decreased from 259 cm in 1957 to 251 cm in 1958. The find-

On the Mass and Heat Budget of Arctic Sea Ice

ings given in Table 3 provide further evidence that the average annual accretion of old ice with a thickness of 3 m is close to 50 cm.

From observations of the thickness of annual layers SCHWARZACHER [29] has derived a numerical relation between September ice thickness and annual accretion (Fig. 6, dotted line). Between thicknesses of 150 and 350 cm it is based on observations but its extrapolation to zero thickness (in September) renders a very high value of 340 cm for accretion

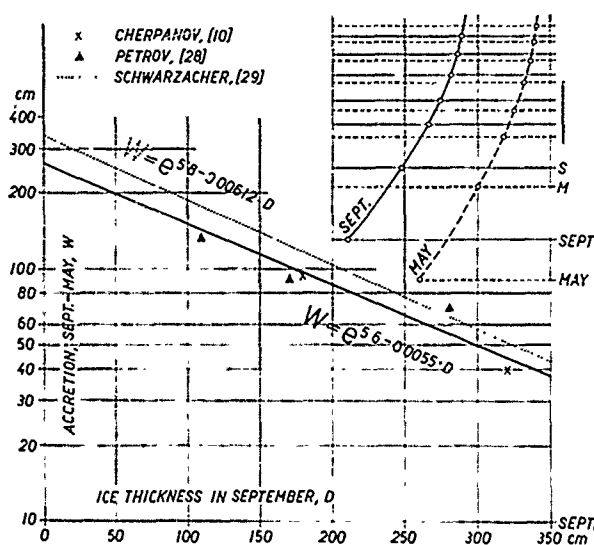


Fig. 6. Relation between ice thickness in September, D , and winter accretion, W (straight lines). Assuming a constant ablation of 50 cm/year and $W = e^{5.6-0.0055D}$, the ice thickness in September and May are indicated by open circles (log time scale on the right). The curved lines connecting them represent the margins of annual variations of thickness

during the first winter. By allowing for the measurements of PETROV [28] and CHERPANOV [10] it seems more favourable to choose somewhat smaller constants (full line). Accretion during the first winter is still 260 m, however, this amount is in better agreement with PETROV's observations of the increase of thickness with time. By using this relation and assuming a constant ablation of 50 cm (which seems justified for ice thicknesses > 200 cm) the increase of thickness in May and September, beginning at $D = 0$, is also shown in Fig. 6.

Under the assumption that the annual layers are identical with winter accretion, SCHWARZACHER [29] uses the above relationship to reconstruct ice thickness and amount of ablation from 1957 back to 1951. The results are interesting and show great variations of ablation which SCHWARZACHER ascribes to a possible variation with ice thickness and

N. UNTERSTEINER:

to the effect of the variable snow cover on accretion. It seems, however, that even greater errors result from neglecting bottom ablation during

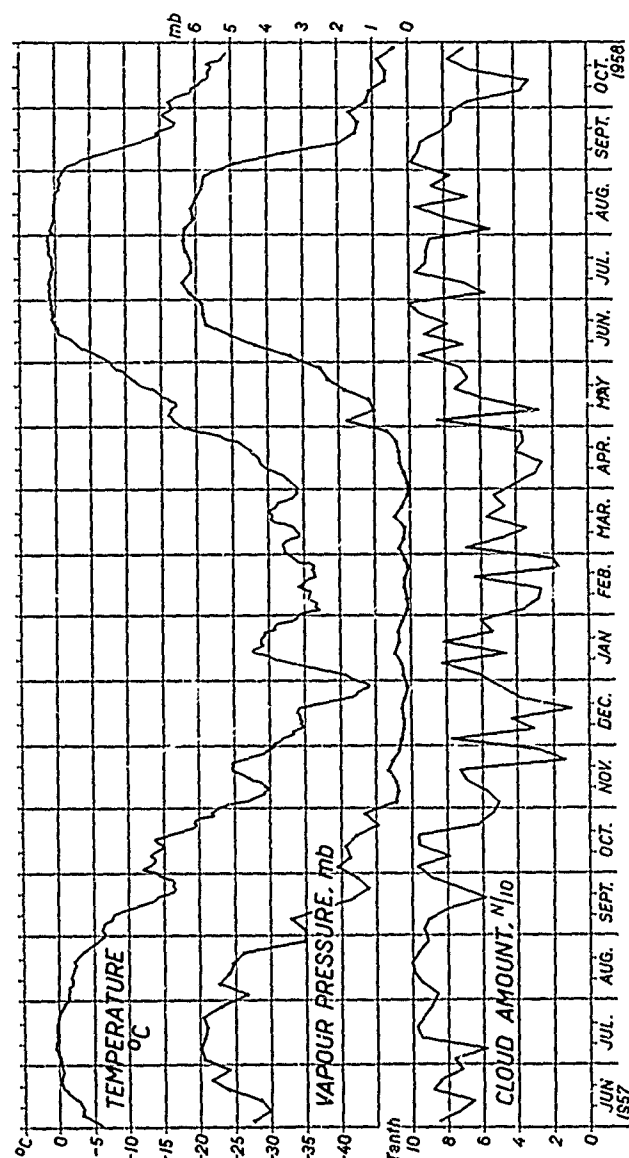


Fig. 7. Temperature (11-day running means), vapour pressure (5-day means), and cloudiness (5-day means) at Drifting Station A, according to observations by the US Weather Bureau

summer. Its amount would have to be added to the annual layers in order to obtain the true amount of winter accretion.

On the Mass and Heat Budget of Arctic Sea Ice

2. Climate

Fig. 7 and Table 4 show the variations of some climatological elements during the time of observation at Drifting Station A. During the melting period the 11-day running means of air temperature remain close to zero (max. 1.2 °C). The lowest temperatures were observed during the last week of December and followed by a relatively warm and cloudy period, as it is typical for the central Arctic [24]. Although the prevalence of low inversions, particularly during the cold season, causes

Table 4. *Monthly Means of Some Climatological Elements at "Drifting Station A"*

	Temperature, °C			Vapour pr. mb	Cloud amt. N/10	Wind, km/h (hourly means)	
	Mean	Daily var.	Interd. var.	Mean	Mean	Mean	Max.
1957 June	— 1.5	1.5	0.9	4.8	7.5	—	—
July	+ 0.1	0.7	0.6	5.8	8.5	14.5	32
Aug.	— 2.8	1.0	1.2	4.4	9.4	17.1	48
Sept.	— 11.6	1.1	2.5	2.2	8.1	10.6	40
Oct.	— 16.0	0.6	3.4	1.6	8.2	18.4	47
Nov.	— 27.7	1.0	2.7	0.5	5.6	10.8	39
Dec.	— 36.7	0.7	3.1	0.2	4.2	6.8	34
1958 Jan.	— 32.1	1.3	3.7	0.3	6.3	13.7	43
Feb.	— 36.1	0.9	3.4	0.1	3.2	10.3	40
Mar.	— 32.0	2.0	2.7	0.2	5.2	10.6	32
Apr.	— 28.4	4.0	1.4	0.3	3.5	6.6	29
May	— 13.4	2.5	2.0	1.8	6.4	10.6	26
June	— 1.8	0.8	0.9	5.0	8.9	11.7	32
July	+ 0.8	0.6	0.5	6.2	8.2	11.1	32
Aug.	0.0	0.7	0.7	6.0	7.7	9.3	29
Sept.	— 11.3	1.0	2.8	2.5	8.7	13.2	34
Oct.	— 22.1	1.5	4.2	0.8	5.8	13.7	42

great non-periodic variations of temperature the mean daily range remains small (Table 4). Daily variations of temperature exist only from March to September, with a maximum amplitude of 4° C in April. During the months without sun no daily period could be detected [18].

Vapour pressure was measured by means of psychrometers, in the instrument shelter about 1.5 m above the ground. The inherent inaccuracy of this method at low temperatures makes the results during the winter months somewhat unreliable. During July and August, vapour pressure reaches its maximum values, close to the saturation point at 0° C.

The amount of clouds also shows a great annual variation. The high degree of cloudiness during the summer months is due to the advection of warm air from the sub-arctic continents. During winter, the frequency distribution of cloudiness (Fig. 8) shows two maxima at 0 and 100% as is common at lower latitudes. The distribution during summer has only one dominating maximum at 100%. (The secondary maximum at

N. UNTERSTEINER:

20-30% in winter would most likely disappear when using a greater number of observations.) A regular daily variation of the cloud amount is not apparent in the available data.

3. Heat Budget of Pond-free Ice

3.1. State of Surface

Since the evaluation of all data from Drifting Station A is not yet completed, the heat budget during a selected period of particular im-

portance is treated in the following. According to Fig. 4 ablation between 10 and 23 July, 1957, was 11.0 cm on „dry” surfaces and 17.8 cm in ponds. A consideration of the heat budget during that time will be preceded by some general remarks.

It was pointed out by HOINKES [19] that when comparing ablation with the heat budget it is necessary to compute the latter for periods with melting and frozen surface separately. Otherwise the heat sums cannot be related to the observed ablation because a loss of mass caused, during a period of positive heat budget, once it has occurred, cannot be restored by a following negative heat budget, that is to say, ablation may have occurred even though the total net heat during both periods may be negative. In the case of sea

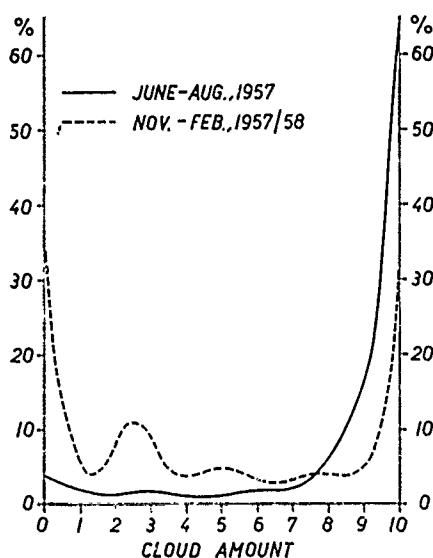


Fig. 8. Frequency of cloud amount, according to 3-hourly observations by the US Weather Bureau

ice this consideration holds only to a limited extent since the meltwater formed is not entirely removed (ponds). For the area covered by ponds the above restriction is not valid. The accurate measurement of the thickness of temporary ice covers of the ponds, as well as the exact determination of the beginning and end of the freezing and thawing processes in general, is difficult. Especially towards the onset and termination of the ablation period the simultaneously existing snow, ice, and water-surfaces with their greatly varying heat absorption (albedo) make the "state of the surface" a poorly defined quality. The state of the various types of surface was noted several times daily. Based upon these observations it can be estimated that during about 7% of the period presently considered the surface was

On the Mass and Heat Budget of Arctic Sea Ice

frozen. It was observed in many instances that, under an overlying frozen crust, melting proceeded at a depth of several centimetres. It seems, therefore, justified to treat the entire period as one with a melting surface.

In connection with this, the particular manner of disintegration of sea ice under the action of solar radiation may be pointed out. When pure glacier ice is exposed to short wave solar radiation an extremely porous surficial layer of a maximum depth of 15 to 20 cm is formed by internal melting. The coherence of the individual grains is not destroyed in this process, and the layer as a whole remains mechanically solid. On the other hand, one frequently finds on glacier tongues spindle-shaped areas of fine-grained ice whose surface appears similar to old firn. These areas represent sections of former crevasses which are filled with frozen water. The grain is columnar and perpendicular to the former walls of the crevasses. In contrast to the metamorphous regular glacier ice this ice disintegrates preferentially into small loose grains. A similar effect is seen on sea ice, although in that case the grain size seems to be greater.

The influence of this "firnification" of ice on the radiation balance is demonstrated by the following experiment. On 3 July, 1958, an area of about 5 m² was scraped with a bulldozer down to the compact ice. The albedo of this surface was 0.38. During the following two days of clear weather with an average insolation of about 20 cal/cm² hr the albedo increased to 0.65 as firnification progressed. The maximum thickness of the "firnified" layer at Station A was 15 cm. Its average density (end of July, 1958) was found to be 0.4 g/cm³. The effect of this firnification is a substantial reduction of ablation rate by an increase of the reflectivity of the ice.

3.2. Net Radiation

3.2.1. Short-Wave

Global radiation was recorded by two solarimeters MOLL-GORCZYNSKI, one pointing upwards and one downwards and a self-balancing potentiometer. The calibration factor given by the manufacturing company was corrected for temperature, according to BENER [7]. The mean cloudiness from 10 to 23 July, 1957, was 94%. In view of such dominating importance of diffuse radiation it is justified to neglect the dependence of the calibration factor on solar elevation [14].

Daily averages of the albedo at the place of radiation measurements varied between 0.56 and 0.68. Further observations of the albedo were made with a portable device consisting of two solarimeters and a potentiometer. It was found that the mean albedo of clean, melting sea ice with a disintegrated surface lies between 0.62 and 0.70. Since the following considerations refer to that type of surface, an albedo of 0.66 has been assumed for calculations of short wave net radiation:

N. UNTERSTEINER:

3.2.2. Long-Wave

Total radiation was recorded by means of a Schulze-radiometer [30] with hemispheres consisting of "Lupolen." This instrument requires separate calibration in the short-wave and long-wave range. Since a suitable standard instrument was not available at Station A, the short-wave calibration was done with the solarimeters. Calibration in the long-wave range by means of a "black body" (without ventilation) rendered unsatisfactory results. The proper method of calibrating the Schulze-radiometer is currently under discussion [20]. Awaiting a final

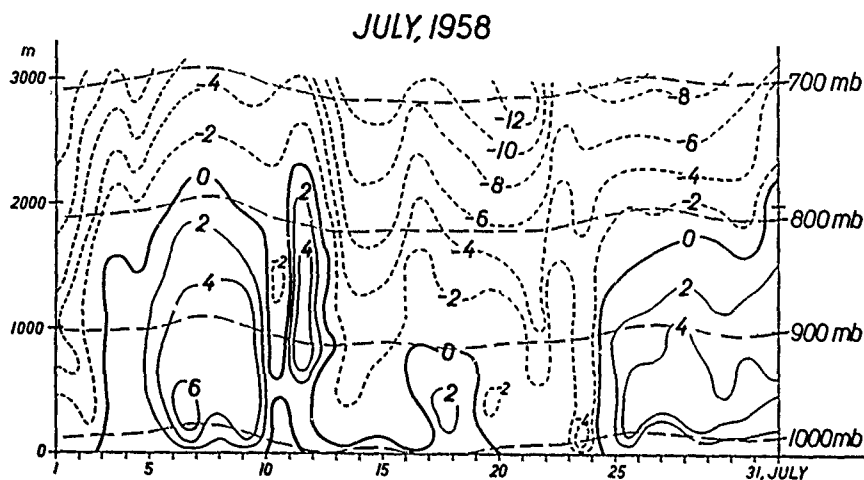


Fig. 9. Temperature in the first 3 km of the atmosphere over Drifting Station A, according to 12-hourly radiosonde observations by the US Weather Bureau

settlement of this question, long-wave radiation has been determined from radiosonde data.

The radiosonde observations of July, 1957, were not available at the time of writing, however, it seems possible to adapt the results of July, 1958, in an appropriate manner. In July, 1958, 8 ascents were made during clear weather (cloudiness $\leq 1/8$). Evaluation of the ELSASSER-diagram (for the use of this diagram in clear and overcast conditions, see [16]) renders intensities of atmospheric radiation between 0.355 and 0.386, with an average of 0.370 cal/cm² min or 533 cal/cm² day. 15 ascents took place during overcast conditions (cloudiness $\geq 7/8$). The corresponding intensities lay between 0.436 and 0.463, with an average of 0.448 cal/cm² min or 645 cal/cm² day. While air temperature near the ground shows extremely small variations, great fluctuations were observed in the free atmosphere as a result of advection and vertical motion of the air (Fig. 9). Frequently, the temperature at cloud base is higher than at the ground, causing a positive net long-wave radiation.

On the Mass and Heat Budget of Arctic Sea Ice

Other means of determining atmospheric radiation are the empirical formulae of ÅNGSTRÖM and ASKLÖF (see [17]):

$$G_0 = \sigma T^4 (0.806 - 0.236 \cdot 10^{-0.052 e}) \text{ and}$$

$$G_w = G_0 + k \cdot w (\sigma T^4 - G_0) \quad [\text{cal/cm}^2 \text{ min}]$$

(G = atmospheric radiation, e = vapour pressure in mb, w = cloudiness in tenths, k = factor depending on type of clouds and regional climatic conditions). By introducing for G_0 and G_{10} the values obtained from the

Table 5. *Daily Means of Cloudiness, Temperature, Vapour Pressure, and Daily Sums of Global Radiation ($S + D$), Atmospheric Radiation (G), Net Short-wave Radiation (NR_S), Net Long-wave Radiation (NR_L), and Net Total Radiation (NR). The Mean Albedo of the Pond-free Ice was 0.66. The Long-wave Radiation of the Melting Ice Surface was Taken to be 0.459 cal/cm². min*

1957 July	10	11	12	13	14	15	16	17	18	19	20	21	22	23	10 th — 23 rd	
$\overline{N}/10$	9.0	7.4	9.7	10.0	9.9	10.0	10.0	9.9	9.4	9.3	10.0	9.8	7.4	9.8	means	9.4
$\overline{T}, ^\circ\text{C}$	-0.4	-0.2	0.8	0.6	0.7	0.8	0.3	0.1	0.0	-0.1	0.5	-0.1	-0.3	0.6		0.24
e , mb	5.7	5.8	6.0	6.1	6.0	5.9	5.9	5.8	5.8	5.8	6.0	5.9	5.7	5.7	totals	5.9
$S + D$ cal/cm ²	522	605	322	302	328	428	399	402	559	400	320	425	532	280		5824
G cal/cm ²	643	633	660	662	660	665	660	641	642	648	662	657	639	660	9132	1983
NR_S	177	206	110	103	112	146	136	137	190	136	109	145	181	95	-108	
NR_e	-17	-27	0	2	0	5	0	-19	-18	-12	2	-3	-21	0	1875	
NR	160	179	110	105	112	151	136	118	172	124	111	142	160	95		

ELSASSER-diagram, the second equation can be used to ascertain the factor k . It is 0.088, somewhat greater than in middle latitudes, due to the prevalence of inversions. Evaluation of the two equations with the actual meteorological data shows that during clear and overcast conditions they render an atmospheric radiation which is low by 17 and 3%, respectively. Under the assumption of a linear variation of this correction, daily sums of atmospheric radiation have been computed with the above formulae for the period from 10 to 23 July, 1957. The results are given in Table 5, together with the daily sums of global radiation ($S + D$), net short-wave radiation (NR_S) as well as mean daily cloud amounts (\bar{N}), air temperature (\bar{T}), and vapour pressure (\bar{e}). In computing the total net radiation the long-wave radiation of the melting ice surface was taken to be 660 cal/cm² day. The sum of net radiation over the entire period (NR) is 1975 cal/cm². This amount of energy is sufficient

N. UNTERSTEINER:

to melt 25.8 cm of pure ice. The actually observed amount of ablation was only 12.3 cm. This apparent discrepancy will be investigated in the following.

3.3. Sensible and Latent Heat

As mentioned in the previous chapter, the mean values of temperature and vapour pressure between 10 and 23 July, 1957, were close to the melting point of ice and to saturation at 0° C, respectively. It can a priori be assumed that the corresponding fluxes of heat and vapour will also be small. For the present purpose, an approximate calculation may suffice.

The mean wind velocity in July, 1957, at a height of 160 cm was 4.0 m/sec. Assuming a roughness parameter of $z_0 = 0.1$ cm and using PRANDTL's relation:

$$\bar{u}_z = 5.75 \cdot u_* \cdot \log \frac{z - z_0}{z_0}$$

the friction velocity u_* becomes 21.7 cm/sec, and the eddy diffusivity $K_{160} = \rho u_* \kappa (z + z_0) = 1.8$ or $K_{100} = 1.0$ g/cm sec. If temperature and vapour pressure follow a logarithmic distribution

$$T_z = T_0 + k_T \ln \frac{z + z_0}{z_0}, \quad e_z = e_0 + k_e \ln \frac{z + z_0}{z_0},$$

the mean vertical fluxes of sensible and latent heat

$$Q_S = 0.24 K \frac{dT}{dz} \cdot t \quad \text{and} \quad Q_L = 600 \cdot K \cdot \frac{0.623}{p} \cdot \frac{de}{dz} \cdot t \quad [\text{cal/cm}^2]$$

attain the following magnitude: $Q_S = 8.6 \text{ cal/cm}^2 \text{ day}$
 $Q_L = -10.8 \text{ cal/cm}^2 \text{ day}.$

This means that the supply of sensible heat by dynamic convection is approximately compensated by the loss of heat by evaporation. Both amounts of heat are smaller by one order of magnitude than net radiation. Although this result represents only a rough estimate it cannot greatly deviate from the true values. If one chooses, instead of $z_0 = 0.1$, other values within the range of experience on glaciers [19, 32] viz. $z_0 = 0.3$ and $z_0 = 0.05$, K_{160} becomes 2.1 and 1.65, respectively. The fluxes of heat become greater by 14% or smaller by 9% which amount to only a few calories per day. The error in the calculation of K introduced by neglecting stability should be even smaller.

In an investigation of the heat budget of arctic pack-ice based upon observations by the Soviet Drifting Station NP-II YAKOVLEV [37] comes to the conclusion that from May to August the very large amount of 5700 cal/cm² was lost by evaporation. The period of melting at NP-II lasted from about 10 July to 20 August, 1950 [36]. During a great part of that period the mean vapour pressure was close to the values observed

On the Mass and Heat Budget of Arctic Sea Ice

at Drifting Station A. In the available condensed version [37] of YAKOVLEV's original publication the methods used in calculating the heat budget are, unfortunately, not communicated. It is, therefore, at present not possible to investigate the cause of the great difference in our findings. A possible explanation is offered in the following chapter.

3.4. Internal Melting, "Heat Reserve"

The ice of glacier tongues is normally contaminated to some degree by debris and cryokonite. In that case, the error committed by allocating the entire absorption of short-wave radiation to the surface is comparatively small. In the case of sea ice the amount of energy penetrating below the surface cannot be neglected.

The mean vertical distribution of the salinity of old sea ice according to SCHWARZACHER [29] is shown in Fig. 10, curve *S*. It is generally assumed that the brine is always in phase equilibrium with the surrounding ice so that the salt concentration in the cavities is a function of temperature alone. The calculation of the conduction of heat is complicated by the fact that thermal conductivity, specific heat, and density are functions of salinity and temperature. Our basic knowledge of the physical constants of sea ice is due to MALMGREN [25]. Important progress has been made by the recent work of WEEKS, ANDERSON, and ASSUR [3, 35, 2, 5].

Of particular importance in the present considerations is the specific heat of sea ice, c_s . It is composed of the specific heat of pure ice increased by the heat required for melting a certain amount of ice to lower the brine concentration. The values of c_s given by MALMGREN can be represented with good approximation by an analytical expression

$$c_s = c + \beta \frac{S}{T^2} \text{ [cal/g } ^\circ\text{C]}, \quad (3)$$

c being the specific heat of pure ice (0.5), S the salinity of the ice in ‰, T the temperature in negative degrees Celsius, and β a constant = 4.1. The heat Q required to raise the temperature of 1 cm³ of ice is

$$dQ = c \cdot \rho \cdot dT. \quad (4)$$

By introducing (3) in (4) and integrating over the temperature interval $T_2 - T_1$ we obtain, under the assumption of constant salinity and density

$$Q = c \cdot \rho (T_2 - T_1) + \rho \cdot \beta \left(\frac{S}{T_1} - \frac{S}{T_2} \right)$$

or in a more practical form

$$Q = \rho \Delta T \left(0.5 + \frac{4.1 S}{T_1 T_2} \right) \quad (5)$$

N. UNTERSTEINER:

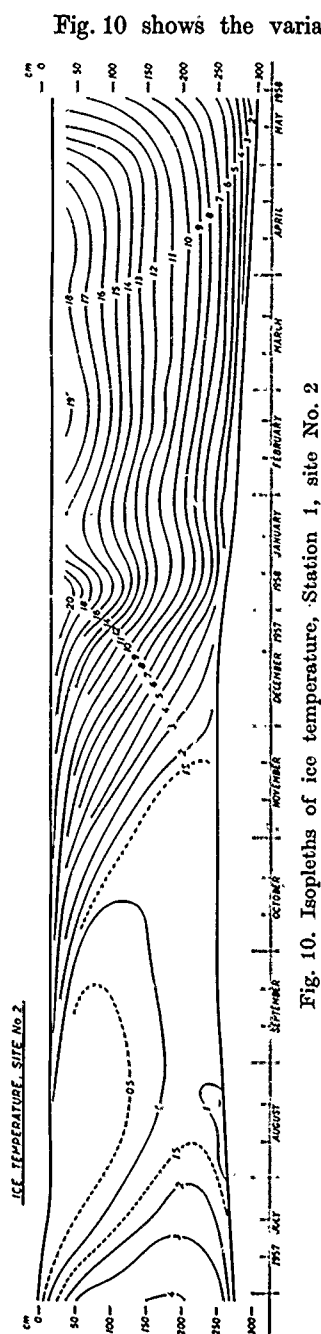


Fig. 10. Isotherms of ice temperature, Station 1, site No. 2.

Fig. 10 shows the variation of ice temperature from July, 1957, to May, 1958, at Station 1. The vertical profiles of temperature at the beginning and end of the period whose heat budget is considered are given as curves T in Fig. 11. Between 10 and 23 July, 1957, the average heating was 0.8°C . At both dates, the level of minimum temperature is about 220 cm below the surface. Conduction from deeper levels does not contribute to the heating of the ice above that level. Curves T and S in Fig. 11 provide the necessary data for an evaluation of eq. (5). The energy required for the observed rise of temperature from 10 to 23 July, 1957, was computed for layers of 10 cm thickness between the surface and a depth of 220 cm. The result is presented as curve E in Fig. 11. Summation of this curve, beginning at the level of minimum temperature upwards to a level 10 cm below the surface renders a total of 700 cal/cm^2 . 12 cm of ice were melted at the surface, and it is likely that a certain amount of brine drained from the porous upper layer. Therefore, the present calculation must be inaccurate at shallow depths. Apart from the energy used for surficial ablation, the energy consumed for internal melting and heating was drawn from the positive radiation balance as observed at the surface.

In this connection it seems of interest to estimate the entire amount of latent heat stored in the ice at the time of maximum temperature. At the end of August the total brine volume in 300 cm thick ice is $32.9\text{ cm}^3/\text{cm}^2$. By the time of minimum temperature in March (Fig. 10) it is reduced to $3.4\text{ cm}^3/\text{cm}^2$, whereby 2400 cal/cm^2 of latent heat are released. Another 600 cal/cm^2 of latent heat are stored in the meltwater ponds, and 1700 cal/cm^2 must be extracted from the ice to lower its temperature from August to March. The heat reserve of an ice sheet of 300 cm thickness in August, with

On the Mass and Heat Budget of Arctic Sea Ice

reference to its temperature in March, is then 4700 cal/cm^2 (Table 7). This amount is about three times as great as the one given by YAKOVLEV [37].

3.4.1. Extinction of Solar Radiation

It is evident that the comparatively large amount of energy of 700 cal/cm^2 which reached the deeper levels between 10 and 23 July could not do so by conduction alone. With a thermal conductivity of the ice of 0.0045 [CGS] the heat flux by conduction becomes of the order of 70 cal/cm^2 in 14 days. It is further seen from curves T in Fig. 11

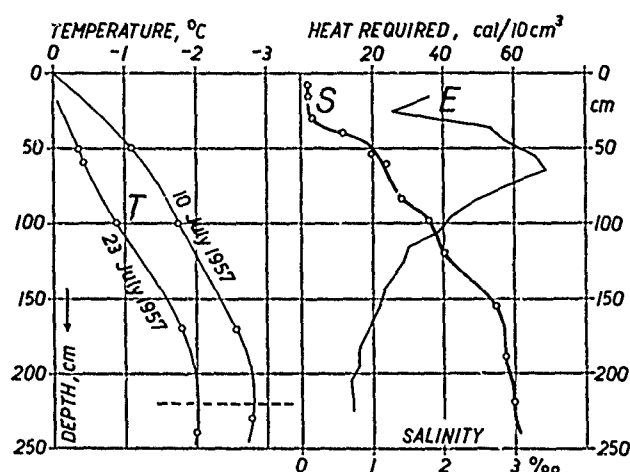


Fig. 11. The distribution of energy (E) required to raise the temperature (T) of ice with a given salinity (S) is used to compute the extinction coefficient for short wave radiation (see Table 6)

that, at depths between 50 and 150 cm, the temperature gradients and therefore the heat fluxes by conduction on 10 and 23 July were approximately the same which means that conduction did not contribute to the heating of this layer. Under these circumstances it seems justified to ascribe the heating of this layer entirely to the absorption of short-wave solar radiation. In any case, the error by neglecting the effect of conduction will be small. From the ratio of the amounts of energy transmitted through each 10-cm-layer the coefficient of extinction may be computed. The results (Table 6) are surprisingly similar to the ones obtained by AMBACH [1] by direct measurements on glacier ice. For depths $> 15 \text{ cm}$ AMBACH finds a mean value of 0.018 cm^{-1} while the present indirect method leads to an average extinction coefficient between 50 and 150 cm depth of 0.015 cm^{-1} . In view of the apparently great importance of penetrating radiation for the total heat budget, more accurate measurements, under inclusion of selective absorption,

N. UNTERSTEINER:

are desirable. If absorption at deeper levels does not differ greatly from the one in the intermediate layer, the amount of energy penetrating an old ice floe of 3 m thickness (without snow cover) in July would be of the order of 1 cal/cm² per day.

3.5. Components of the Heat Budget

The total heat budget during the period 10 to 23 July, 1957, is summarized in Table 7. Approximately 0.5 cm of solid precipitation fell

Table 6. *Absorption of Short-wave Radiation by Sea Ice, as Computed from the Energy Required for an Observed Increase of Temperature and Brine Volume (see Fig. 11)*

Depth cm	Energy 10-23 July, 1957 cal/cm ²	Extinction coefficient 10 ⁻³ cm ⁻¹
surface	1844	..
10	695	..
20	650	..
30	625	..
40	576	..
50	522	14
60	457	15
70	390	16
80	334	15
90	288	15
100	247	16
110	211	14
120	184	13
130	161	15
140	138	18
150	116	..
160	96	..
170	77	..
180	59	..
190	43	..
200	28	..
210	14	..

during that time. If this amount is added to the observed 11 cm of surface ablation (water equivalent) the difference between observed and computed ablation becomes 19%. The limited accuracy of ablation measurement as well as small variations in the distribution of salinity may easily account for such a difference.

In accordance with the results of YAKOVLEV [37], although to an even higher degree, solar radiation is shown to be the dominating factor in the ablation of ice during the summer. The smallness of the convective heat fluxes is undoubtedly caused by the fact that, along the great distance between the station and the nearest coast, heat and water vapour of the warm continental air have been given off to the ice. The remaining gradients of temperature and vapour pressure are too small to render appreciable fluxes. The warm air at higher levels manifests itself primarily by the high degree of cloudiness and its influence on radiation.

During overcast conditions in summer practically the entire short-wave radiative energy received at the surface is available for ablation. Under clear conditions the drop of atmospheric radiation may, even in July, result in a negative total heat balance (freezing). Evaporation between 10 and 23 July, 1957, was very small (154 cal/cm²). Its contribution to ablation was less than 0.3 mm. The same goes for ablation by rain [19]. It seems important to note (Table 7) that 38% of the positive heat budget are

On the Mass and Heat Budget of Arctic Sea Ice

transformed in the interior of the ice and contribute to the build-up of the great heat reserve previously discussed.

In a study of radiation data from the ice island T-3 in the Arctic ocean (1953: 85° N, 90° W) FRITZ [14] points out difficulties in reconciling the high values of net radiation with the fact that practically no surface ablation was observed. The short-wave net radiation in July, 1953, was about 100 cal/cm² day. According to FRITZ, 15% of this energy were used to heat the ice, and the rest was supposedly removed by convection. FRITZ bases his explanation on the fact that the top of the cloud

Table 7. *Energy Balance of the Ice During Maximum Melting Conditions, and Total Heat Reserve of the Ice Sheet*

10-23 July, 1957, cal/cm ²		mean, cal/cm ² day	
net radiation	short-wave + 1983	+ 142	
	long-wave — 108	— 8	
sensible heat	+ 120	+ 9	
latent heat	— 151	— 11	
<u>total + 1844</u>		From this, the following	
amounts are used for:			
surface ablation	1144	=	62%
heating and internal melting	700	=	38%
Heat reserve in August, with		ponds	600
reference to the ice temperature		brine	2400
in March, in cal/cm ² (ice thickness ~ 300 cm).		cooling	1700
		<u>total:</u>	<u>4700</u>

cover continually gives off heat by long-wave radiation. This he assumes to result in super-adiabatic lapse rates at lower levels and a corresponding upward transport of heat. Indeed, the radiosonde observations from T-3 [6] frequently showed such lapse rates in the lowest 100 m of the atmosphere. In the previous year (July, 1952) this was, however, not the case [6]. At Drifting Station A, too, only few such observations were recorded. Above the shallow layer with unstable lapse rates there was in all cases an almost isothermal zone of 1000 m thickness [6] in which the convective heat flux must have been downwards. The loss of heat from the cloud top can, therefore, not be compensated from below. In view of the high percentage of radiation penetrating clean ice it seems possible that, during July, 1953, a good part of the net short-wave radiation on T-3 only increased the porosity of the ice and was not realized as surface ablation. The shorter the period of ice ablation the more likely becomes an effect of that nature. However, according to Crary [11] an appreciable amount of ice ablation in summer seems to be the rule on T-3.

N. UNTERSTEINER:

4. Yearly Totals of Heat. Comparisons

The present data may be used for an estimate of the yearly turnover of heat in the Arctic pack ice. Unfortunately, no measurements of the turbulent flow of heat in the ocean could be made at Drifting Station A. According to YAKOVLEV [37], the ice receives an amount of 5.5 kcal/cm² year from below, 0.9 from May to August, and 4.6 from September to April. From the data of the Soviet Drifting Station NP-II the following energy budget for the months May-August was derived [37]:

Net radiation	+ 11.0 kcal/cm ²
Latent heat	— 5.7
Sensible heat	— 2.2
Heat of melting	— 2.9
Heat reserve of the ice ...	— 1.5
Heat flow from the ocean.	+ 0.9

The total of heat received at the upper and lower surface was 11.9 kcal/cm². It compensates for the heat loss by evaporation and convection and provides the energy for ablation and the build-up of the heat reserve. The atmosphere loses 3.1 and the ocean 0.9 kcal/cm² in the process. The conspicuous features of this energy budget are the very large amount of evaporation and the small amount of the heat reserve. The smallness of the latter (1.5 kcal/cm²) suggests that it may have been computed with the specific heat of pure ice, and that internal melting has not been allowed for. Since YAKOVLEV determined evaporation as a residual value its overestimation seems to be caused by an underestimation of the heat reserve. The ice temperatures at Station A were well within the range of previous observations [36], and the maximum total brine volume (end of August) as calculated from temperature and salinity is supported by the direct observations of SCHWARZACHER [29]. The value of the heat reserve given in chapter 3.4 should, therefore, be essentially correct. If we introduce our value of 4.7 kcal/cm² in YAKOVLEV's energy budget and deduct the increase of 3.2 kcal/cm² from evaporation, the latter becomes 3.8 kcal/cm² from May to August or, on an average, 31 cal/cm² day, a much more probable value.

It is, at present, not possible to give a detailed analysis of the atmospheric and solar components of the heat budget at Drifting Station A. However, from the observation of the mass budget, ice temperature, and salinity a cumulative heat budget can be obtained. Its constituents are denoted as follows:

- S = heat for melting of snow cover,
- A_s = heat for run-off part of surface ice ablation,
- A_b = heat for bottom ablation,
- R = heat reserve of the ice sheet, as defined in Table 7,
- B = heat released by bottom accretion,
- Q_w = total heat drawn from solar and atmospheric sources during the "warm" season, May-August,
- Q_c = total heat given off to the atmosphere during the "cold" season, September-April,

On the Mass and Heat Budget of Arctic Sea Ice

q_w = heat drawn from the ocean during the warm season,
 q_c = heat drawn from the ocean during the cold season.

It must be emphasized that the division of the year in a period with a positive and one with a negative heat budget of the ice surface is only a crude approximation. During the warm season the ice sheet receives heat from both sides. Its cumulative heat budget can be written

$$S + A_s + A_b + R = Q_w + q_w. \quad (6)$$

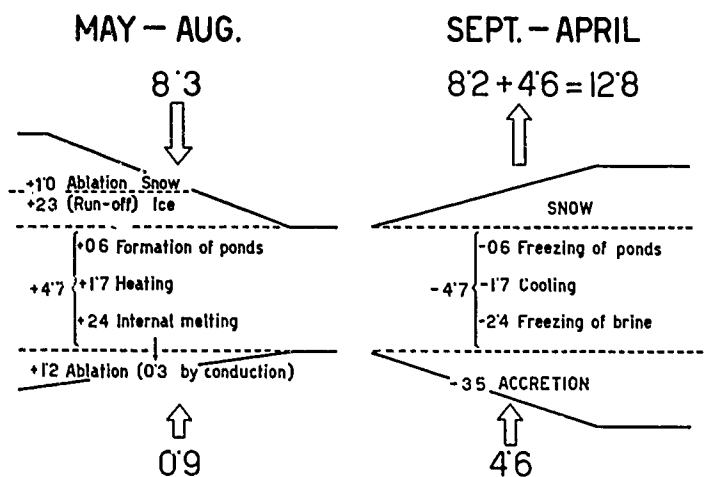


Fig. 12. Totals of heat exchange at the boundaries and in the interior of the ice, in kcal/cm²

During the cold season it receives heat at the lower and loses heat at the upper surface. The total upward heat flow is

$$R + B + q_c = Q_c. \quad (7)$$

The condition of stationary ice thickness is

$$A_s + A_b = B. \quad (8)$$

By combination of eqs. (6), (7), and (8) it is seen that

$$q_w + q_c - S = Q_c - Q_w. \quad (9)$$

The deposition of snow on the ice is an increase of mass which is not associated with a transformation of heat at the earth's surface. Eq. (9) shows that the net annual amount of heat provided to the atmosphere is equal to the upward heat flux in the ocean less the heat required for melting of the snow cover.

Average values of S , A_s , A_b , and R are known from the observations previously discussed. Using the values for the heat flux in the ocean given by YAKOVLEV, a cumulative heat budget as presented in Fig. 12

N. UNTERSTEINER:

is obtained. The temperature at the ice-ocean interface is normally -1.7°C . During a short time in late summer the heat flux by conduction in the ice downward at all levels (see Fig. 11). An estimated amount of 0.3 kcal/cm^2 reaches the lower surface and causes, together with the upward heat flux in the ocean, bottom ablation [22]. Its observed amount seems to substantiate YAKOVLEV's value of the summer heat flux in the ocean. A new instrument ("turbulimeter") described by KOLESNIKOV et al. [23] should be particularly effective in measuring turbulent heat flow in the ocean.

According to Fig. 12 the ice receives during the warm season 8.3 kcal/cm^2 from solar and atmospheric sources. A total of 12.8 kcal/cm^2 is returned during the cold season. In the course of a year the atmosphere in the Central Arctic receives 4.5 kcal/cm^2 which originate from oceanic advection. Further evaluation of the data obtained at Drifting Station A should provide a more detailed understanding of the solar and atmospheric components of the heat budget and their relative importance, as well as clues to the possible effect of climatic variations on the maintenance of the ice cover.

Acknowledgements

I am indebted to the late Dr. R. C. HUBLEY who initially coordinated the scientific program for Drifting Station A. My particular thanks are due to Dr. P. E. CHURCH, Executive Officer, Department of Meteorology and Climatology, University of Washington, and his staff for encouragement and support during all phases of our program. The untiring collaboration and companionship of Mr. A. HANSON and Mr. W. CAMPBELL, field assistants at Drifting Station A, deserves special credit. The unselfish co-operation and help received from many civilian and military personnel at the station as well as Point Barrow and Fairbanks is acknowledged with gratitude. The 3-hourly synoptic observations and the aerological data used in this paper were put at our disposal by the US Weather Bureau. We are indebted to the Geophysics Research Directorate, AFCRC, Cambridge, Mass., for the communication of their navigation data. Dr. F. I. BADGLEY has kindly helped with the translation of the manuscript.

References

1. AMBACH, W., und H. MOCKER: Messungen der Strahlungsextinktion mittels eines kugelförmigen Empfängers in der oberflächennahen Eisschicht eines Gletschers und im Altschnee. *Arch. Met. Geoph. Biokl.*, B, 10, 84-99 (1959).
2. ANDERSON, D. L.: A Model for Determining Sea Ice Properties. *Proc. Arctic Sea Ice Conf.*, Nat. Acad. Sci. Publ. No. 598, 148-152, Washington, D. C. (1958).
3. ANDERSON, D. L., and W. F. WEEKS: A Theoretical Analysis of Sea Ice Strength. *Trans. Amer. Geoph. Union* 39, 632-640 (1958).
4. ARMSTRONG, T.: *The Russians in the Arctic*, 182 p. London, 1958.

On the Mass and Heat Budget of Arctic Sea Ice

5. ASSUR, A.: Composition of Sea Ice and its Tensile Strength. Proc. Arctic Sea Ice Conf., Nat. Acad. Sci. Publ. No. 598, 106-138, Washington, D. C. (1958).
6. BELMONT, A. D.: Upper Air Temperatures, 1952-1954. (Sci. Studies at Fletcher's Ice Island, T-3, 1952-1955, Vol. 2, 11-41.) Geoph. Res. Papers No. 63, GRD, Cambridge, Mass. (1959).
7. BENER, P.: Untersuchung über die Wirkungsweise des Solarigraphen Moll-Gorczyński. Arch. Met. Geoph. Biokl., B, 2, 188-249 (1950).
8. BOCHOW, H., W. HÖHNE und A. RAEUBER: Über die Bestimmung der für einen repräsentativen Mittelwert notwendigen Anzahl von Einzelwerten. Angew. Met. 3, 170-173 (1958).
9. BROWNE, I. M., and A. P. CARY: The Movement of Ice in the Arctic Ocean. Proc. Arctic Sea Ice Conf., Nat. Acad. Sci. Publ. No. 598, 191-207, Washington, D. C. (1958).
10. CHERPANOW, N. W.: Opredeľeniye vozrasta dreyfuyushchik l'dov metodom kristalloopticheskogo issledovaniya. Problemy Arktike 2, 179-184 (1957).
11. CARY, A. P.: Arctic Ice Island Research. Advances in Geoph. 3, 1-41 (1956).
12. DEVIK, O.: Ein Registrierinstrument zur Messung der Ablation. Kongl. Norske Vid. Selskab, Forh. 2, 112-114 (1929).
13. ENGLISH, T. S.: Persönliche Mitteilung.
14. FRITZ, S.: Solar Radiation Measurements in the Arctic Ocean. (Sci. Studies at Fletcher's Ice Island, T-3, 1952-1955, Vol. 2, 7-10.) Geoph. Res. Papers No. 63, GRD, Cambridge, Mass. (1959).
15. GORDIENKO, P.: Arctic Ice Drift. Proc. Arctic Sea Ice Conf., Nat. Acad. Sci. Publ. No. 598, 210-222, Washington, D. C. (1958).
16. HALTINER, G. J., and F. L. MARTIN: Dynamical and Physical Meteorology, p. 116. New York, 1957.
17. HANN, J., and R. SÜRING: Lehrbuch der Meteorologie, 5. Aufl., p. 72. Leipzig, 1939.
18. HISDAL, V.: The Diurnal Temperature Variation during the Polar Night. Quart. J. Roy. Met. Soc. 86, 104-106 (1960).
19. HOINKES, H., und N. UNTERSTEINER: Wärmeumsatz und Ablation auf Alpengletschern. Geogr. Ann. 34, 99-158 (1952).
20. HOINKES, H.: Studies of Solar and Net Radiation in the Antarctic, 1957/58. IAMAP, Radiation Symposium, Oxford (1959).
21. HUNKINS, K. L.: Persönliche Mitteilung.
22. KOLESNIKOV, A. G.: On the Growth Rate of Sea Ice. Proc. Arctic Sea Ice Conf., Nat. Acad. Sci. Publ. No. 598, 157-160, Washington, D. C. (1958).
23. KOLESNIKOV, A. G., N. A. PANTELEJEV, J. G. PIRKIN, W. P. PETROV und W. N. IVANOV: Apparatura i metodika registratsii turbulentnich mikropulsazii temperaturi i skorosti tetsdenia v morje. Izvestiya Akad. Nauk SSSR, Ser. Geof. 3, 405-413 (1953).
24. LAKTIONOV, A. F.: Recent Soviet Investigations in the Pole Regions. Sea Transport Publishing, 347-423, Moscow (1955). Trans. Air Univ. Doc. Res. Study, Maxwell AFB (1956).
25. MALMGREN, F.: On the Properties of Sea Ice. The Norw. Polar Exped. "Maud", Sci. Res. 1 a, No. 5, 1-67 (1933).
26. MODEL, F.: Wärmeumsatz zwischen Meer und Atmosphäre im atlantischen Südpolarmeere und im Nordpolarmeere. Ann. Meteor. 7, 64-66 (1955/56).

N. UNTERSTEINER: On the Mass and Heat Budget of Arctic Sea Ice

27. MÖLLER, F.: Die Wärmebilanz der freien Atmosphäre im Januar. *Met. Rdsch.* 3, 97—108 (1950).
28. PETROV, I. G.: Physical-Mechanical Properties and Thickness of the Sea Ice Cover. *Materialy nauchno-issledovatel'skoi dreyfuyushchei stantsii 1950/51 goda*, Sect. 6, Art. 3, 310 p., Leningrad, Izd. "Morskoi Transport" 1954-55. (Transl. Amer. Met. Soc., ASTIA Doc. No. AD 117137.)
29. SCHWARZACHER, W.: Pack-Ice Studies in the Arctic Ocean. *J. Geoph. Res.* 64, 2357-2367 (1959).
30. SCHULZE, R.: Über ein Strahlungsmeßgerät mit ultrarotdurchlässiger Windschutzhaube. . . . *Geof. Pura e Appl.* 24, 107—114 (1953).
31. SVERDRUP, H. U., M. W. JOHNSON and R. H. FLEMING: *The Oceans*, p. 656. New York, 1942.
32. UNTERSTEINER, N.: Glazial-meteorologische Untersuchungen im Karakorum, II. Wärmehaushalt. *Arch. Met. Geoph. Biokl.*, B, 8, 137—171 (1957).
33. UNTERSTEINER, N., and F. I. BADGLEY: Preliminary Results of Thermal Budget Studies on Arctic Pack Ice during Summer and Autumn. *Proc. Arctic Sea Ice Conf., Nat. Acad. Sci. Publ. No. 598*, 85-95, Washington, D. C. (1958).
34. UNTERSTEINER, N.: Drifting Station A, eine schwimmende Station im Packeis des Nordpolarmeeres. *Umschau* 13, 385—389 (1959).
35. WEEKS, W. F.: The Structure of Sea Ice: A Progress Report. *Proc. Arctic Sea Ice Conf., Nat. Acad. Sci. Publ. No. 598*, Washington, D. C. (1958).
36. YAKOVLEV, G. N.: The Thermal Regime of the Ice Cover. *Materialy nauchno-issledovatel'skoi dreyfuyushchei stantsii 1950/51 goda*, Sect. 7, Art. 4, 350 p., Leningrad, Izd. "Morskoi Transport" 1954-55. (Transl. Amer. Met. Soc., ASTIA Doc. No. AD 117138.)
37. YAKOVLEV, G. N.: Solar Radiation as the Chief Component of the Heat Balance of the Arctic Sea. *Proc. Arctic Sea Ice Conf., Nat. Acad. Sci. Publ. No. 598*, 181-184, Washington, D. C. (1958).
38. ZINGG, TH.: Die Bestimmung der Schneehöhenverteilung auf photogrammetrischem Wege. *UGGI, Ass. Gén. Rome 1954, Compt. Rend. Comm. Neiges et Gl.* 4, 33-37 (1956).

Heat Balance at the Surface of the Arctic Ocean

F.I. Badgley

Paper presented at the
WESTERN SNOW CONFERENCE,
April 1961

}

HEAT BALANCE AT THE SURFACE OF THE ARCTIC OCEAN

Franklin I. Badgley
Department of Atmospheric Sciences
University of Washington, Seattle

Abstract

A resumé of available data on the components of the heat budget of the Arctic Ocean surface shows that radiative interchange with the environment is the dominant factor. The presence or absence of an ice cover influences the nature of this interchange and also the relative importance of evaporation to the heat budget. On the basis of these figures a conjecture is made as to the course of events in the event of the artificial removal of the ice cover. It is shown that the ice would re-establish itself under presently existing conditions.

Introduction

Starting with the voyage of the Fram in 1893-1896 and continuing to the present there have been at least sporadic measurements of those physical variables (meteorological, oceanographic and radiative) which determine the heat balance of the Arctic Ocean. The Russians began their systematic work with floating North Pole stations in 1937 and have continued work at each of their floating stations up to N.P. 9 at the present time. There have been four U.S. floating ice stations starting with "Fletcher Ice Island" which has been occupied several times during its known existence and has been variously called "T-3" and "Bravo". Station Alpha was established in 1957, Charlie in 1959, and ARLIS I in 1960. The thick ice of T-3 does not lend itself to heat budget studies but the other American stations have been used for this purpose. In the following sections data from both Russian and American sources have been used.

The measurements do not agree in all details but they are in general agreement and in the following an attempt will be made to resolve what differences do appear.

Most of the Arctic Ocean is ice-covered but there is an appreciable amount of open water and the responses of these two differing surfaces to their environment are

appreciably different. Most of the measurements have been made over ice so much of the over-water information must be inferred.

In treating the heat budget of the ice-covered ocean surface we will consider the entire thickness of the ice. One of the questions to be answered is whether this will increase or decrease with time. In treating a water surface we will consider the upper layers only and one of the questions is whether or not an ice cover will begin to form.

Components of the Heat Budget

The components to be treated are, in order, (1) visible radiation, (2) infra-red radiation, (3) conduction from surface to air, (4) latent heat transferred from surface to air or vice-versa by evaporation or condensation, (5) heat conducted from the ocean towards the surface. In the case of the ice surface it will be necessary to consider the energy stored in the melt water and liberated when this water freezes.

(1) The visible radiation which originates in the sun may reach the surface of the ocean directly or after single or multiple scattering and reflection from clouds, snow and ice. Having reached the surface it may be absorbed, transmitted, or reflected. At U.S. stations Kipp or Eppley pyranometers have been used to measure both the incoming and outgoing radiation streams. Similar devices have been employed by the Russians.

(2) Infra-red radiation is emitted from the surface, whether it be snow, ice, or water at a rate very close to that of a perfectly black body at the temperature of the surface. Some recent work (W. F. Murcray, unpublished) seems to show that when a very steep temperature gradient exists at the top of a snow layer, that the emission from that layer originates partly at levels slightly below and therefore warmer than the surface. Consequently the total radiative flux is somewhat greater than that of a black body at surface temperature. This effect will be neglected in the discussion below.

A downward flux of infra-red energy is received at the surface from the air and clouds overhead.

Either or both of these fluxes may be measured with an appropriate radiometer (Beckman and Whitley, Agmet,

and Schultze radiometers have been used at U.S. stations); alternatively the fluxes may be estimated from the temperature and emissivity of the surface and the atmosphere. Both of these methods have been used over snow and ice surfaces and give results which compare well with each other. Few actual measurements have been made over Arctic water so only the computed estimates are available for water surfaces.

The data below come from U.S. and Russian sources and refer to the latitude belt from 82° to 86° . The figures shown in Table 1 for the infra-red balance over the snow surface are the averages for 3 or 4 years taken from instrumented measurements. Not shown are calculated values for comparable months but these agree well with the measurements. The values computed for the water surfaces of open leads were made on the hypothesis that back radiation from the atmosphere would be the same over leads as over floes. This would be badly in error for large water surfaces but not for narrow leads and small open areas.

(3) Turbulent transfer of heat (enthalpy) may be directed either away from the ice flow or downward toward the flow depending on the gradient of temperature. During most of the year an inversion exists over the ice and the heat flow is from atmosphere to ice.

So far as is known, no one has yet measured the fluctuation of temperature and vertical air movement near the ice surface with the speed and precision necessary for a direct determination of the turbulent heat flux. The next best method is to measure the average gradients of wind speed and temperature near the surface and from these to estimate the heat flux. Without going into details this method uses the wind gradient to establish a coefficient of eddy diffusivity analogous to the molecular thermometric conductivity. This and the temperature gradient establish an estimate of the heat flux.

A third method is an approximation to the second. It uses the wind at one level and the temperature at two levels to estimate the gradients and from these the flux is established as in the second method.

Both the Russians and ourselves have used the second and third methods. They make no statement about how precise they believe their estimates to be but they are probably no better than ours which we think are within

± 35% of the true values. The various Russian investigators do not agree among themselves. Laikhtman's estimates run several times greater than do Jakovlev's. Ours are in closer agreement with the latter's but even smaller on the average. Our disagreement with Jakovlev's figures is minor and probably due to the high average roughness length (0.5 cm) that he assumes for the flow compared to our 0.02 cm. Our disagreement with Laikhtman is a major one, however; I see no way of reconciling the two estimates and believe his to be wrong.

The estimates in Table 1 are therefore based on Jakovlev's figures for NP2 and ours for Station Alpha.

The eddy flux of heat is many times smaller than either the upward or downward stream of radiation (by a factor of 30 or more) and is even small compared to the difference between these streams, that is to the net radiative flux. It is in this latter comparison that we and Jakovlev differ from Laikhtman. He finds the eddy flux to be of the same magnitude as the net radiative flux, even exceeding it in some months. I see no way in which our results could be interpreted to coincide with this.

(4) The estimation of the energy flux associated with evaporation and condensation at the floe surface can be made in a manner quite analogous to estimations of eddy heat flux and subject to even greater uncertainties because of the difficulties of measuring the vertical gradient of water vapor. An entirely different approach is to measure the amount of evaporation or condensation occurring from a representative area of the floe. This means measuring the change of weight of a pan of known area and containing a sample taken from the surface being tested. This method is subject to quite different but just as serious uncertainties as the other, including weight changes due to precipitation, blowing snow, water leakage, and others. We do feel that our estimates are accurate to within a factor of two, that is that the real value probably lies within the range from 1/2 to 2 times the computed value for evaporation-condensation. The figures in the Table 1, should be considered as the roughest of estimates meant to show the order of magnitude.

Again we find ourselves in substantial agreement with Jakovlev whose results, however, only extend from June through October. We find Laikhtman's results for the

winter period quite reasonable but for the summer period from five to ten times the magnitude of our results, although usually having the same sign.

(5) The final term to be estimated, the flow of heat from the ocean to the surface, is a small one but interesting because it maintains the same sign and presumably the same magnitude year around. At some hundreds of meters below the ocean surface the water is characteristically at a temperature of about $+1^{\circ}\text{C}$. The top surface is -1.7°C . Due to the ice cover there should be only minor variations in the turbulence from winter to summer.

Two methods suggest themselves for estimating this flux. In late summer the lower layers of ice become almost iso-thermal, there should be little heat conduction through it and little radiation reaching the bottom of the floe. Any wastage of the bottom then should be due to heat from the ocean.

This wastage has been measured on U.S. Ice Station Charlie and found to be on the order of 2 cm per month in September. This is equivalent to a heat flow of $.003 \text{ cal/cm}^2 \text{ min}$.

Another approach is to look for a time when there is no wastage or freezing at the bottom surface and a linear temperature gradient in the ice near the bottom. These conditions are met in December. Estimating the conductivity of ice at $5.5 + 10^{-3} \text{ cal/cm sec deg}$, and the temperature gradient as $2 + 10^{-2} \text{ deg/cm}$, the heat flow would be $11.0 + 10^{-5} \text{ cal/cm}^2 \text{ sec}$ or 6.6×10^{-3} or $.006 \text{ cal/cm}^2 \text{ m}$.

If expressed on a yearly basis the above estimates give 1600 to 3100 calories per sq. cm per year. This is in the range suggested by Laikhtman who arrives at estimates of between 850 and 5000 $\text{cal/cm}^2 \text{ year}$ by two different methods.

Many of the figures in Table 2 are estimates and should not be taken too seriously. In any case they refer to conditions over narrow leads or small ponds in an otherwise frozen surface. Even though the estimates are crude they show that the heat loss from an open surface over the period of a year far exceeds that which occurs from a frozen surface. During all months except May, June, July, and August all cracks and ponds would tend to freeze. This jibes with the observed facts.

It has been occasionally proposed that if the present ice sheet were destroyed, that it would not spontaneously reappear and that the Arctic Ocean would remain open. This is based on the assumption that the low albedo of the open water would allow enough energy to be absorbed during the summer so that ice would not re-establish itself with sufficient thickness to be self-sustaining during the coming year or years.

The figures of Table 2 immediately raise doubts that this would be true but they cannot be said to disprove the possibility. If the ocean, or large parts of it, were free of ice many of the assumptions on which the table is based would be invalid. For example the cloudiness and humidity would be increased, thereby changing the radiative fluxes. Changes in humidity and temperature profiles would change the turbulent fluxes of heat and momentum and the consequent changes in the temperature regime could in turn affect the larger scale circulation.

One way to reach a reasonable estimate of the over-all effect is to postulate for the winter months a purely radiative exchange between the ocean surface at about 0°C and an opaque atmospheric layer (idealized cloud layer) at some lower temperature which is to be computed. This cloud layer is to remain in quasi-equilibrium between the energy it gains and loses by radiation and that which it gains by advection from outside the arctic. This advective term remains the same as it is at present, about 10^{22} calories per year. When this computation is carried out, it shows a net loss of $.155 \text{ cal/cm}^2\text{min}$ or $6.7 \times 10^3 \text{ cal/cm}^2\text{mo}$. This flux is enough to remove all the excess energy supplied by the sun over a period of about 10 months. In the succeeding two months an ice cover could re-establish itself. Just how thick this might become before the next melt season is problematical but thicknesses of a meter or more could be expected. With an ordinary snow cover this thickness of ice could easily maintain itself for future seasons.

It has also been suggested that an increased flow of Atlantic water into the Arctic Ocean would dissipate the ice cover. This increased flow could conceivably occur naturally or be produced by pumping water across an artificial barrier at Bering Straits.

Although the quantitative arguments will not be presented here it may be somewhat obvious that the ice floes

will approach some limiting thickness which depends on the net heat flow out the top and in at the bottom. When these two are balanced over a long period of time the ice will be in a quasi steady state. If the influx of heat at the bottom were increased, the floe would thin until a new equilibrium was reached. In order for the ice to disappear in the summer it should not be much more than 1/2 meter thick, one sixth of its present thickness. Assuming that the snow cover, which represents about 1/3 of the resistance to heat flow, would remain unchanged, this means that the total resistance to heat flow would be reduced to 4/9 of its present value. This would mean that the heat flow from the ocean should be increased by 9/4 or 2.25 times its present value, an increase of approximately .004 ca./cm²min. Assuming Atlantic water were drawn in at +1°C and discharged at -1.7°C this would call for an increased flow of $2.4 \times 10^8 \text{ m}^3/\text{min}$; equivalent to a river a mile wide and 200 feet deep flowing at about 1 1/2 miles per minute.

The conclusion is that no artificial means is feasible to produce the desired effect. It is conceivable that some natural cause could increase the present flow by a factor of two or three and thereby cause the dissipation of the ice but this remains in the realm of conjecture.

TABLE 1

Heat Budget of Ice and Snow Surfaces 82° - 86°N

(+) indicates energy added to floe (-) indicates energy leaving floe
average flux in cal/cm² min

	Jan	Feb	Mar	Apr	May	Jun	Jul	Aug	Sep	Oct	Nov	Dec	Annual
1)	0	0	.014	.046	.077	.107	.087	.052	.009	0	0	0	.033
2)	-.030	-.035	-.042	-.051	-.034	-.035	-.035	-.007	-.025	-.025	-.045	-.042	-.034
1+2)	-.030	-.035	-.028	-.005	+.043	+.072	+.052	+.045	-.016	-.025	-.045	-.042	-.001
3)	+.016	+.013	+.014	+.000	-.013	-.014	-.000	-.004	-.007	+.002	+.006	+.009	+.002
4)	0	0	0	0	-.010	-.013	-.010	-.001	+.005	+.006	+.004	+.001	-.0015
5)	+.003	+.003	+.003	+.003	+.003	+.003	+.003	+.003	+.003	+.003	+.003	+.003	+.003
Total	-.011	-.019	-.011	-.002	+.023	+.048	+.043	+.043	-.015	-.014	-.032	-.029	+.002

1)	Net Visible Radiation (incident minus reflected)	2)	Net Long Wave Radiation (incident minus emitted)
1+2)	Net Radiation (visible plus long wave)	3)	Turbulent Heat Flux
4)	Latent Heat Flux	5)	Heat Flux from ocean

TABLE 2

Heat Budget of an Ice Free Surface (estimated 82° - 86°N)

(+) indicates energy flux toward surface (-) energy flux from surface

	Jan	Feb	Mar	Apr	May	Jun	Jul	Aug	Sep	Oct	Nov	Dec	Annual
	average flux in cal/cm ² min												
1)	0	0	.050	.207	.382	.368	.280	.162	.054	.002	0	0	.125
2)	-.164	-.153	-.222	-.160	-.086	-.035	-.023	-.029	-.134	-.159	-.216	-.291	-.139
1+2)	-.164	-.153	-.172	+.047	+.296	+.333	+.257	+.133	-.080	-.157	-.216	-.291	-.014
3)	-.450	-.400	-.310	-.200	-.100	-.014	.000	-.004	-.100	-.200	-.300	-.400	-.206
4)	-.150	-.160	-.150	-.100	-.050	-.007	0	-.002	-.050	-.100	-.120	-.160	-.089
5)	+.003	+.003	+.003	+.003	+.003	+.003	+.003	+.003	+.003	+.003	+.003	+.003	+.003
Total	-.761	-.710	-.629	-.250	-.149	+.315	+.260	+.130	-.227	-.454	-.633	-.848	-.306

1) Net Visible Radiation (incident minus reflected)	2) Net Long Wave Flux (incident minus emitted)
1+2) Net Radiation (visible plus long wave)	3) Turbulent Heat Flux
4) Latent Heat Flux	5) Heat Flux from Ocean

Remarks on the Cooling Power in Polar Regions

N. Untersteiner

Translated from the
WETTER UND LEBEN,
Vol. 13, No. 3/4, pp. 70-73, 1961

Remarks on the Cooling Power in Polar Regions

SUMMARY

Using recent observational data it is shown that the mean meridional distribution of the cooling power in Antarctica reaches extremely high values in a zone near the edge of the ice cap. In the central Arctic the distribution shows small variations. Conditions during the antarctic summer approximately correspond to those of the arctic winter (except Greenland).

In an investigation of the global distribution of Hill's cooling power, Lauscher (1) gives the mean meridional distribution of this quantity for the months of January and July. In the past decade, new data have become available which allow certain corrections for high latitudes.

By definition, Hill's cooling power is

$$H = (0.13 + 0.47\sqrt{v}) (36.5 - T) \text{ mgcal/cm}^2 \text{ sec}$$

where v is the wind velocity (m/sec) and T the temperature ($^{\circ}\text{C}$). Mean monthly values of both quantities for some Arctic and Antarctic stations are summarized in Table 1. The data for the Antarctic stations are taken from (2, 3, 4) and cover 1 to 3 years. The values for the Arctic are taken from (1, 6).

Figure 1 shows the mean meridional distribution of H with the high-latitude corrections. In the central Arctic, H varies little. The mean for January (76 mg cal/cm² sec) corresponds to conditions found on Alpine peaks of about 3000 m

Table 1. Monthly and Yearly Averages of Wind Velocity, Temperature, and Hill's Cooling Power (H) for Some Arctic and Antarctic Stations

	January			July			Year		
	m/sec	°C	H	m/sec	°C	H	m/sec	°C	H
Antarctic									
12 Coastal stations (2) mean latitude 72°S	7.2	-3.2	55	8.0	-25.1	90	8.2	-15.9	83
Pionirskaja, 2700 m 330 km from coast, 70°S, 95°E	10.7	-23.2	100	11.5	-46.9	144	10.7	-37.9	124
Komsomolskaja, 3400 m 800 km from coast, 74°S, 98°E	5.5	-31.6	84	2.7	-65.3	92	3.8	-52.5	93
Wostok, 3500 m 1300 km from coast, 78°S, 100°E	4.6	-31.3	76	4.6	-71.8	124	4.6	-55.4	105
Amundsen Scott, 2800 m 1300 km from coast, 90°S	5.6	-27.0	67	7.0	-59.7	133	6.3	-50.0	113
Arctic									
Average in 72° latitude (1)			76			36			55
Average over Arctic Ocean	4.0	-32.0	73	4.6	-3.0	42	3.8	-20.0	59

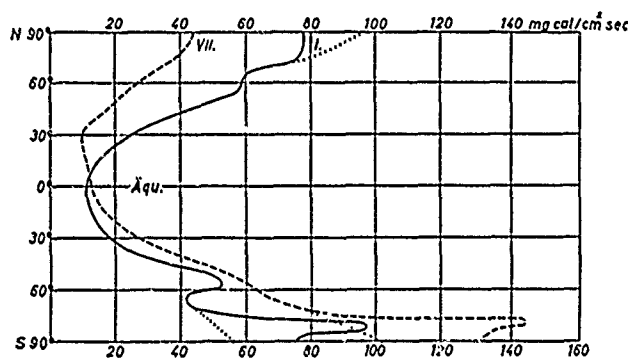


Figure 1. Mean Meridional Distribution of Hill's Cooling Power in January and July (After Lauscher (1)). The values between 72 and 90 degrees N and S latitude have been corrected according to newer observations (Lauscher's values are dotted lines)

(for example, Sonnblick, Austria, 3106 m, January: $72 \text{ mg cal/cm}^2 \text{ sec}$). The high values of H in the interior of Greenland are suppressed by the averaging process. According to (7), "Eismitte" has an H of about 52 in summer and 90 in winter, which is similar to conditions along the coast of Antarctica. The summer in the central Arctic is mild ($H \approx 45$). This is primarily due to the low wind velocities. In contrast, Antarctica is "colder" even at 72°S than the North Pole, although the values along the Antarctic coast have a wide range. For example:

	Jan.	Aug.	Year	
Little America (4 years)	53	75	76	$\text{mg cal/cm}^2 \text{ sec}$
Port Martin (3 years)	85	128	105	

Port Martin has a mean wind velocity of 75 km/h and is one of the windiest spots on earth. Extreme values of H are found only several hundred kilometers inland, with a slight decrease toward the center of the continent.

In general, the mean meridional distribution of H indicates that, only a short distance away from the coast, the Antarctic continent provides a climatic stress during the warmest season which is comparable to that in the Arctic during the coldest season. In terms of heat requirements, the climate of the Arctic Ocean is hardly different from that of some permanently inhabited, or inhabitable, mountainous regions in middle latitudes.

Literature

- 1 Lauscher, F., Ueber die Verteilung der Hill'schen Abkuehlungsgroesse auf der Erde. Arch. Met. Geoph. Bioklim., Ser. B., 3, 275, 1951
- 2 Meteorology of the Antarctic, Weather Bureau Pretoria, 1957
- 3 Nudelman, A. V., Soviet Antarctic Expeditions 1955 - 1959, Publ. Acad. Sci. Moscow, 1959 (in Russian).
- 4 Météorologie Antarctique, La Météorologie, 57, 1960.
- 5 Observational Data of the Scientific Research Drifting Station of 1950 - 1951, vol. 3, sec. 8, Leningrad 1954/55 (translated from the Russian ASTIA Doc. AD 117137).
- 6 Untersteiner, N., On the Mass and Heat Budget of Arctic Sea Ice. Arch. Met. Geoph. Bioklim., Ser. A, 12, 151, 1961.
- 7 Wissenschaftliche Ergebnisse der Deutschen Groenland Expedition Alfred Wegener, 4, 2, 1939.
- 8 Steinhauser, F., Die Meteorologie des Sonnblicks, Vienna 1938.

Seismic Studies of Sea Ice

K.L. Hunkins

Reprinted from the
JOURNAL OF GEOPHYSICAL RESEARCH,
Vol. 65, No. 10, pp. 3459-3472, 1960

Seismic Studies of Sea Ice¹

KENNETH HUNKINS

*Lamont Geological Observatory
(Columbia University)
Palisades, New York*

Abstract. During the International Geophysical Year, elastic wave propagation in sea ice was studied near Drifting Station Alpha in the central Arctic Ocean. Velocities of longitudinal and transverse waves in ice showed a marked seasonal change which is largely attributable to variations in ice temperature. With these velocity data, plus additional data on density, the calculation of various elastic constants of sea ice throughout the year can be made.

Flexural wave dispersion was investigated for different ranges, charge sizes, and ice parameters. Experimental results are in general agreement with theory. Thickness, as determined from the dispersion of flexural waves and from air-coupled flexural waves, is characteristically lower than that found by direct measurement.

Both longitudinal and flexural waves crossing leads suffer severe attenuation. Transmission across leads shortened the duration of the normal air-coupled flexural wave train.

Introduction. As a part of the scientific program of the IGY a station was maintained on the pack ice of the central Arctic Ocean from April 1957 to November 1958 by the United States Air Force. Fields of investigation included meteorology, microclimatology, sea ice physics, biology, underwater sound, and marine geophysics. The investigations in marine geophysics were carried out by Lamont Geological Observatory of Columbia University under contract with Air Force Cambridge Research Center. This program included ocean current measurements, celestial navigation, magnetic and gravity measurements, ocean bottom coring and photography, dredging, seismic depth sounding, seismic refraction, and seismic studies of elastic wave propagation in ice. Only the wave propagation studies are reported here.

Drifting Station Alpha was located on a large floe about 3 meters thick which drifted constantly under the influence of wind and current. Between June 8, 1957, when celestial navigation began, and November 1, 1958, when the scientific program ceased, a total track of 2945 km was covered—an average rate of 5.8 km/day.

Previous experimental studies. Elastic wave

propagation in lake ice has been the subject of several previous investigations [Ewing and Crary, 1934; Ewing, Crary, and Thorne, 1934; Kishinouye, 1943; Kohler, 1929]. Longitudinal, transverse, and flexural waves were studied in these experiments and used to determine elastic constants of ice. Press, Crary, Oliver, and Katz [1951] first showed the existence of air-coupled flexural waves and used them for determining ice thickness. In all these studies, good agreement was generally found between the experimental data and theory.

Only a few observations have been made of wave propagation in ice floating on the ocean [Anderson, 1958; Bogorodskii, 1958]. In the Arctic Ocean, Crary [1954] investigated seismic waves in the floating ice island T-3. The ice island is a tabular sheet of fresh ice about 50 meters thick which has apparently broken from an ice shelf. Oliver, Crary, and Cotell [1954] studied elastic waves in arctic pack ice at several locations in the Beaufort Sea in 1951. This has remained almost the only published seismic study of pack ice to the present. They studied longitudinal and transverse waves, calculated the elastic constants, and found them to be considerably less than those of lake ice. Oliver, Crary, and Cotell also studied flexural and air-coupled flexural waves and used them to determine ice thickness. The ice investigated was primarily young sea ice (less than 1 year old).

¹ Lamont Geological Observatory Contribution No. 438. This paper is a portion of a thesis submitted to Stanford University as partial fulfillment of the requirements for the Ph.D. degree.

KENNETH HUNKINS

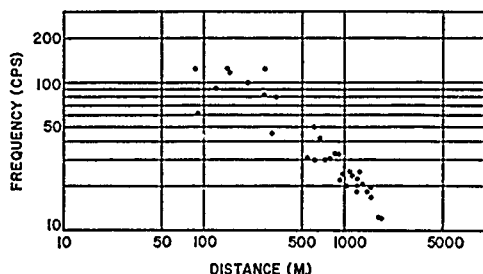


Fig. 1. Variation of apparent frequency with distance for longitudinal plate waves.

Previous theoretical studies. The propagation of elastic waves in a free plate was first investigated by Lamb [1889, 1916], who found modes of propagation corresponding to symmetric and antisymmetric behavior of the plate. For long wavelengths these modes correspond to longitudinal and flexural waves, respectively.

The complete theory of elastic waves in an ice sheet floating on water, neglecting gravitational effects, was worked out independently by Sató [1951] and by Press and Ewing [1951a], and their results are used here. The studies showed that, although the waves do not reduce to the simple symmetric and antisymmetric solutions of a free plate, there are solutions which correspond closely to these.

In addition to these complete solutions, Ewing and Crary [1934] investigated flexural waves for the case of steady-state, plane waves with wavelengths long compared with ice thickness. They included the finite depth of water and the effect of gravity in their calculations.

The theory of flexural waves was generalized by Press and Ewing [1951b] to include the case of an impulsive point source located in the air or in the water beneath the ice. This yielded the theory for the air-coupled flexural waves which had been observed previously.

Seismic instruments and experimental procedure. The principal instrument used throughout these investigations was a Houston Technical Laboratory 7000-B seismograph system. Two types of geophones were used. The Electro-Tech model EVS-2B vertical seismometers, with a natural frequency of 14 cps and 0.53 critical damping, were used for some ice studies. For lower-frequency ranges the Houston Technical Laboratory S-36-2 horizontal-component and vertical-component seismometers were used. They have a

natural frequency of 2 cps and 0.5 critical damping. Air waves were recorded by a microphone and water waves by a hydrophone.

The geophones were usually set on the surface of the ice and arranged in various profiles. Two horizontal-component geophones at right angles and a vertical geophone at the same location were used in some instances to study three components of ground motion.

Explosives, hammer blows, and swinging weights were used as sources of energy. Dynamite, TNT, and blasting caps were used for explosions. Shots were made above the ice, in the ice, and in the water below.

The tuning fork was checked periodically against radio station WWV and it proved to have very uniform frequency. The nearly constant velocity of sound in sea water compared with the changing velocity in ice also gave good indication that the timing was uniform.

Longitudinal waves. Longitudinal waves were the first recorded arrival except at distances so large that they could not be observed. The apparent frequency of the first observed arrival decreases with distance from the shot point, probably because of the selective attenuation of the high-frequency wave components (Fig. 1). The apparent frequency in this case refers to the inverse of the peak-to-peak or trough-to-trough time of the first complete cycle.

The velocity of the longitudinal wave was measured frequently during the occupation of Station Alpha. Measurements were made over a spread distance of 335 meters with geophones spaced at 61-meter intervals. One-quarter pound of dynamite exploded in a hole at a depth of 3 meters furnished the energy for these velocity

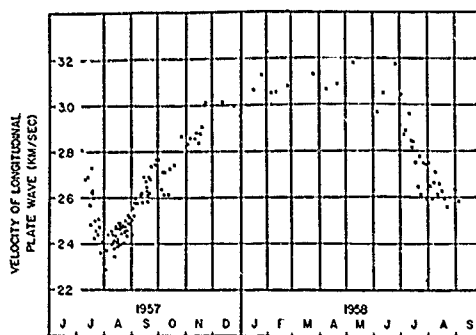


Fig. 2. Seasonal variation of longitudinal plate velocity.

SEISMIC STUDIES OF SEA ICE

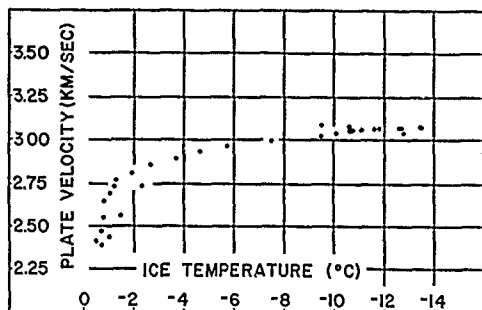


Fig. 3. Longitudinal plate velocity versus ice temperature. Temperatures are averaged from readings at four depths in the ice.

determinations. Points on the time-distance graphs were plotted to an accuracy of $\frac{1}{2}$ msec and 30 cm. Straight lines were fitted by inspection and the velocity was determined. A few standard deviations computed from random selected records were found to be ± 30 to ± 50 m/sec.

The longitudinal velocities so determined exhibit a marked seasonal change ranging from low in the summer to high in the winter (Fig. 2). During the summer of 1957 a velocity minimum of about 2.4 km/sec was found, but during 1958 the minimum was about 2.6 km/sec. The winter maximum was about 3.1 km/sec. These velocity changes are undoubtedly linked with variations in ice temperature. The ice exhibits a layered temperature structure which varies seasonally, but, for simplicity, average temperatures were determined and plotted against longitudinal velocity (Fig. 3). The long wavelengths must tend to travel at the average ice velocity. In general, the curves show the strong change of velocity at temperatures close to the melting point. This steepening of the temperature-velocity curve near the melting point has been noted in the laboratory by Lotze [1957]. Lotze studied fresh ice, however, and no direct comparison of absolute velocities can be made.

The longitudinal wave described and measured appears to correspond to the longitudinal plate wave. The velocity of this wave is given by

$$V_p = 2\beta(1 - \beta^2/\alpha^2)^{1/2} \quad (1)$$

where V_p = longitudinal plate wave velocity.
 α = bulk longitudinal wave velocity.
 β = shear wave velocity.

For the precision required here, Saló's [1951] curves show that this velocity applies for wavelengths longer than about 5 times the thickness of the ice. Because of dispersion, shorter wavelengths will be slower, but for all the above measurements the wavelengths were longer than 5 times the ice thickness.

At short distances from the shot point a faster arrival is sometimes detected which probably corresponds to the longitudinal body wave. This impulsive arrival is observable out to about 100 meters, where the changing slope of the time-distance curve indicates the loss of the faster wave which is replaced as first arrival at large distances by the plate wave (Fig. 4). Although a continuous curve may be more appropriate, two straight lines were used as an approximation in Figure 4. The bulk wave has a zero distance intercept, but the plate wave has a positive distance intercept which may result from mode conversion. Bulk wave velocity is difficult to measure accurately, since this wave is found only at short distances. A comparison is made in Table 1 of this measured bulk wave velocity with the bulk wave velocity calculated from the longitudinal plate velocity and shear velocity. Good agreement between the measured and calculated velocities tends to support the identification of the bulk longitudinal wave.

Graphs of particle velocity at the surface of the ice were prepared from the records of longitudinal-horizontal-component and vertical-component geophones (Fig. 5). All instruments have similar response curves, but, since phase shift is a function of frequency, the diagrams do not indicate true particle motion. The diagrams do show the sense of particle motion and for longitudinal waves, which are made up of a

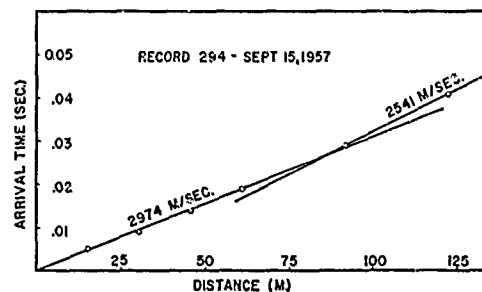


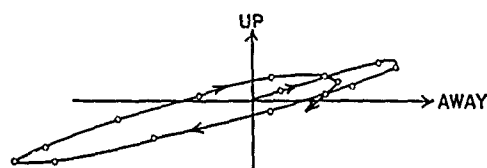
Fig. 4. Time-distance curve for longitudinal waves at short distances.

KENNETH HUNKINS

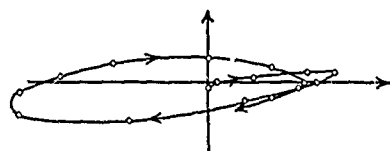
TABLE 1. Comparison of Measured and Calculated Bulk Longitudinal Wave Velocity.

Date	Measured Longitudinal Plate Wave Velocity V_p , m/sec	Measured Shear Wave Velocity β , m/sec	Measured Bulk Longitudinal Wave Velocity α , m/sec	Calculated Bulk Longitudinal Wave Velocity from V_p and β
1957				
Aug. 25-27	2457	1552	2802	2946
Sept. 15-16	2541	1578	2974	2661
1958				
Jan. 3-4	3181	1862	3401	3584
Mar. 24-31	3129	1826	3504	3544
Apr. 17-20	3088	1857	3504	3342

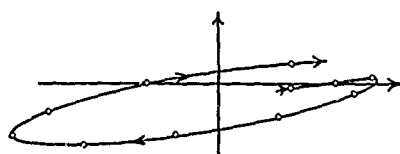
narrow band of frequencies, must closely approximate true particle motion. The plotted motion at the surface is prograde elliptical, with the major axis at an angle of 10° to 20° with the horizontal, as shown in Figure 5. The ratio of the minor to major axis ranges



NO. 738 - 29 APRIL 1958 - 177 M.



NO. 746 - 2 MAY 1958 - 135 M.



NO. 852 - 14 JUNE 1958 - 152 M.

Fig. 5. Particle velocity at the ice surface in vertical plane for longitudinal waves. Units are arbitrary.

from 5 to 10. These observations agree essentially with the results of *Sato's* corrected theory [1951, 1955] which predicts the flat ellipse and prograde motion. Only the slight inclination of the axis which is consistently observed is not predicted by simple theory.

Transverse waves. Impulsive shear waves were not generated by the explosive sources, and special methods were used for their investigation. A hammer or large weight was used to strike the side of a pit. The motion or the hammer or weight was horizontal and perpendicular to the line of geophones. This produced a strong, horizontally polarized shear, or *SH*, wave which was well recorded on transverse-horizontal-component geophones (Fig. 6). Correspondence between the direction of first motion of the wave and the direction of the blow confirms the identification. Good recordings of *SH* waves were obtained out to 250 meters, but not much beyond this. The wave arrives as a strong impulse of 1 or 2 cycles followed by a wave train of lower amplitude.

Ten determinations of *SH* wave velocity were made during 1957 and 1958 (Table 2). The *SH* wave used for these measurements may be considered to be the Love wave of zero mode for a plate. This is a nondispersive mode with a velocity β .

Theory for Love waves in a floating ice sheet has been worked out by *Sato* [1951] and by *Press and Ewing* [1951a]. They show that Love waves, corresponding to higher modes, should commence at infinitely high frequency with a velocity β (Fig. 7). The wave train then decreases in frequency and reaches a minimum frequency after an infinitely long time. For ice

SEISMIC STUDIES OF SEA ICE

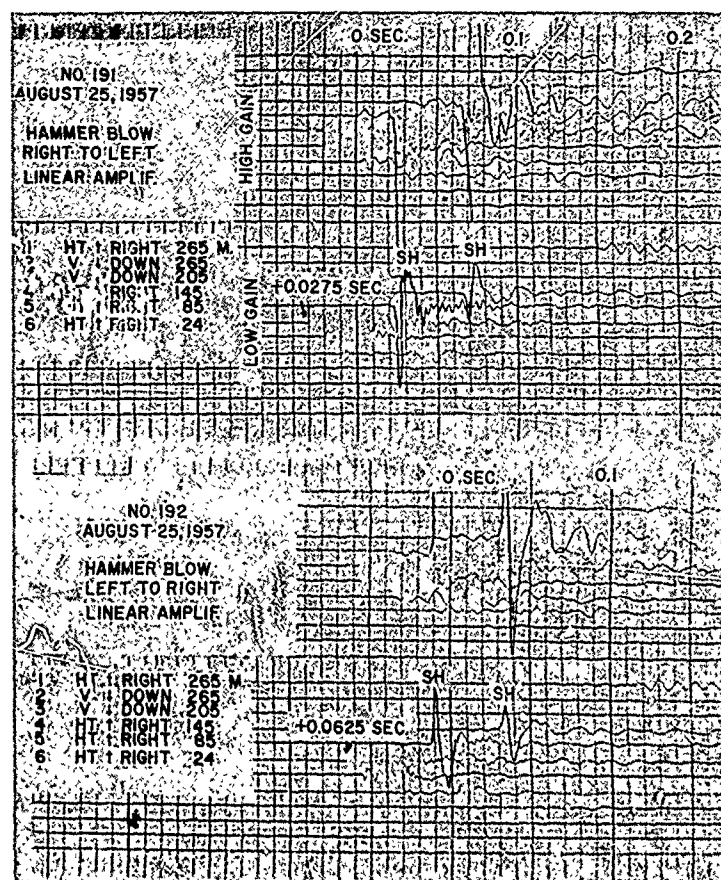


Fig. 6. Records 191 and 192. Shear waves generated by hammer blows. Trace 1 was inoperative. Note that the arrival of SH corresponds to a downward trace deflection in 191 and an upward trace deflection in 192. This corresponds to the opposite directions of the hammer blows.

TABLE 2. Measured Velocities of SH Waves in Sea Ice

Date	SH Wave Velocity, m/sec
1957	
Aug. 25	1552
Aug. 29	1419
Sept. 3	1540
Sept. 16	1578
1958	
Mar. 31	1325
Apr. 17	1856
June 3	1890
June 8	1719
June 10	1694
Aug. 21	1349

3 meters thick, with $\beta = 1500$ m/sec, the minimum frequency is 250 cps for the first mode and 500 cps for the second mode. On certain records (Fig. 6), waves are recorded which agree with those described by theory. The method of calculation of observed dispersion is that of Press and Ewing [1952]. The observed points are plotted with the theoretical curves in Figure 7 and show good agreement. These waves cannot leak into the water and so would be expected to propagate well if excited, but they are not observed on all records. The irregularity of ice thickness may tend to scatter the waves, and this effect probably combines with the effect of insufficient excitation to account for the scarcity of observations.

KENNETH HUNKINS

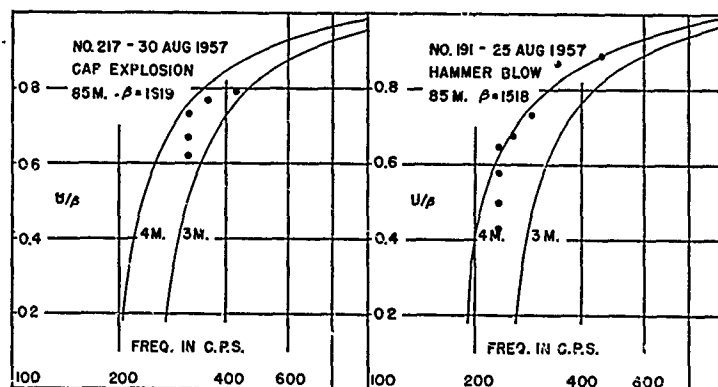


Fig. 7. Theoretical and observed dispersion of *SH* waves in a floating ice sheet. Dots indicate observations.

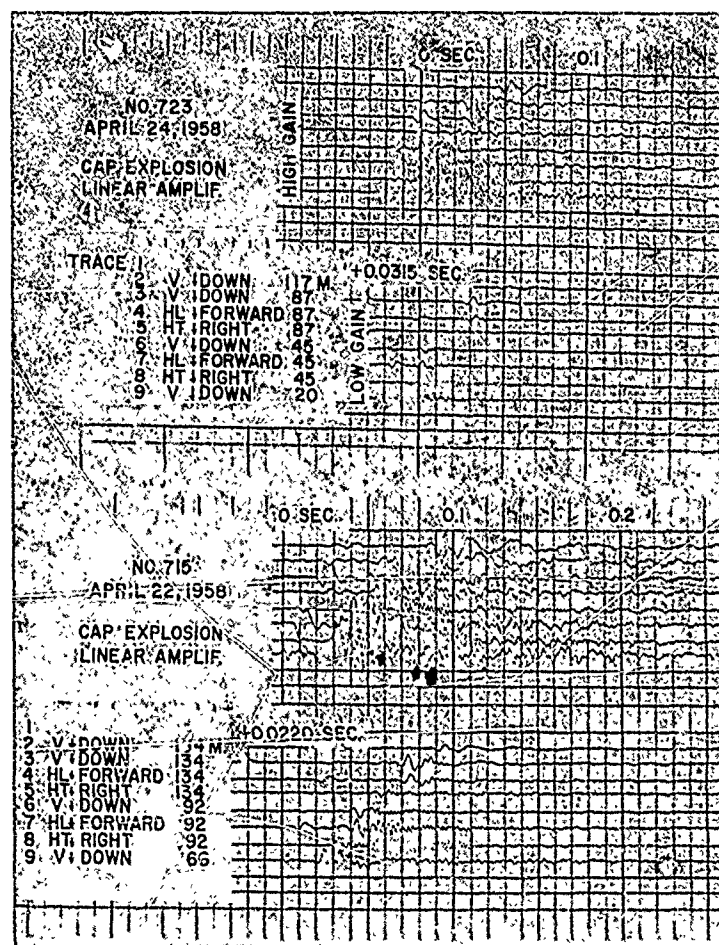


Fig. 8. Records 723 and 715. Elastic waves generated in pack ice by a blasting cap explosion. Note elliptical wave packet on trace 8.

SEISMIC STUDIES OF SEA ICE

TABLE 3. Measured Densities of Sea Ice

Date	Number of Samples	Average Density, * g/cm ³
1957		
July 23	4	0.873
July 23	5	0.890
Sept. 21	7	0.858
1958		
Apr. 10	3	0.904
Apr. 21	3	0.877
Aug. 25	4	0.928
Aug. 26	11	0.915
Sept. 2	11	0.903
Sept. 3	5	0.904
Sept. 8	15	0.893
Sept. 10	12	0.863
Sept. 11	9	0.913
Total	89	0.89 ± 0.02

* Three significant figures are carried through the calculation, with final rounding to two.

Under certain conditions, records taken close to the shot point show the arrival of an unusual elliptical packet of high-frequency waves (Fig. 8). This arrival is recorded almost entirely on the horizontal-transverse-component geophone with a frequency between 400 and 500 cps. The waves at the beginning of the train have a group velocity of about 1300 m/sec, and waves at the end of the train have a velocity of about 600 or 700 m/sec. These waves may correspond to the second mode of *SH* waves in a plate. The frequency is of the right order for the end of the wave train, and the elliptical envelope makes it appear that an interference phenomenon exists. However, the early

part of the train arrives with a frequency too high to fit the theory.

Elasticity of sea ice. If the longitudinal and shear wave velocities and the density are known, all other elastic constants can be determined, provided the simplifying assumptions of homogeneity and isotropism are made.

Density of the ice ρ was found by weighing a sample in air and finding its volume from measurement. The samples consisted of sections of cores cut into cylinders 20 to 30 cm in length. Twelve density profiles were taken, each based on samples from various depths in the ice (Table 3). Density of sea ice varies with temperature, salinity, and air content. Air content in the form of bubbles is an important factor because of its variability. Sea ice also contains liquid brine, and one of the principal errors in determining density comes from the drainage of brine from pore spaces in the sample. To reduce this error samples were weighed as soon as possible after being cored.

Most of the determinations were made during the summer, but the few results obtained in April under winter conditions do not show any significant difference from the summer results. For the purpose of computing elastic constants the average value of 0.89 g/cm³ was used.

From the measured values of the longitudinal plate velocity V_p and shear velocity β the bulk longitudinal velocity α is calculated by means of equation 1. From the α , β , and ρ , thus determined, all other elastic constants may be calculated. The elastic constants were calculated for five different dates when both longitudinal and shear wave velocities had

TABLE 4. Elastic Constants of Sea Ice

Symbol	Constant	8/29/57	3/31/58	4/17/58	6/10/58
V_p	Longitudinal plate wave velocity, m/sec	2500	3070	3080	3050
α	Longitudinal bulk wave velocity, m/sec	2997	3380	3344	3381
β	Shear wave velocity, m/sec	1419	1825	1856	1694
ρ	Density, g/cm ³	0.89	0.89	0.89	0.89
σ	Poisson's ratio	0.355	0.294	0.382	0.382
μ	Lamé's constant, dynes/cm ² (shear modulus)	2.0×10^{10}	3.0×10^{10}	3.1×10^{10}	2.6×10^{10}
λ	Lamé's constant, dynes/cm ²	4.9×10^{10}	4.3×10^{10}	10.0×10^{10}	8.5×10^{10}
K	Bulk modulus, dynes/cm ²	6.2×10^{10}	6.3×10^{10}	12.1×10^{10}	10.2×10^{10}
E	Young's modulus, dynes/cm ²	5.4×10^{10}	7.8×10^{10}	8.6×10^{10}	7.2×10^{10}

KENNETH HUNKINS

been determined nearly simultaneously (Table 4). The constants determined represent average values for pack ice. In general, ice has a layered structure, but the long wavelengths used in the measurements presented here tend to average the small details of structure. Such average values are of practical importance for many calculations relating to pack ice. The shear modulus μ given here applies to stresses acting horizontally, since only the *SH* wave velocity was measured.

Flexural waves. Flexural waves form the most prominent arrivals on most seismograms of waves in floating ice. At some distance from the shot point they are observed as a wave train with gradually decreasing frequency. Since the thickness of the ice sheet and its elastic constants were determined with some accuracy, comparisons may be made of the observed flexural wave arrivals with those calculated from theory.

The various theoretical phase-velocity curves which are discussed below are illustrated in Figure 9. *Press and Ewing* [1951a] developed the period equation for the case of an ice sheet floating over infinitely deep water. They assumed σ (Poisson's ratio) = $\frac{1}{4}$ for ice and neglected gravity. This equation is difficult to evaluate analytically but may be reduced

to approximate cases for waves very long and waves very short with respect to ice thickness. The very short waves do not concern us here because they involve frequencies beyond the range of the instruments used. For the case of very long waves the equation is easy to evaluate, but it has some error for the waves of intermediate length recorded at Station Alpha. For comparison with observations of those waves of intermediate length a curve was used which was computed numerically by *Satō* [1951]; he assumed infinitely deep water and used the following parameters.

$$\rho_2/\rho_1 = 1.09; \quad \alpha/\beta = 2, \\ (\sigma = 1/3); \quad \beta/V_w = 1.20$$

where ρ_1 = density of ice.

ρ_2 = density of water.

V_w = velocity of sound in water.

Another similar curve was evaluated by James Dorman (personal communication) on an IBM 650 computer using a general Rayleigh-wave equation for layered media. The constants were chosen to be as close as possible to those of the pack ice at Station Alpha under winter conditions. The constants are $\alpha = 3.307$ km/sec, $\beta = 1.829$ km/sec, $V_w = 1.440$ km/sec, and $\rho_1/\rho_2 = 1.138$. For Dorman's curve, group

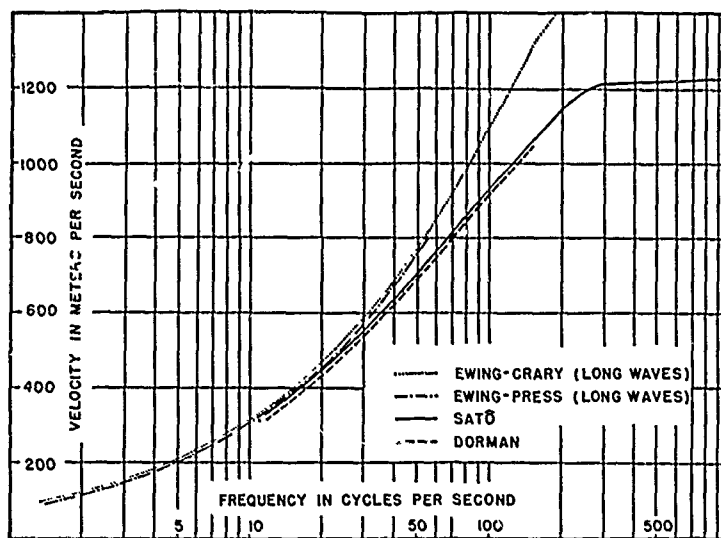


Fig. 9. Comparison of various theoretical flexural wave dispersion curves for ice of 3-inch thickness. Values used are: $\alpha = 3.60$ km/sec and $\beta = 1.80$ km/sec, except for Dorman's curve where $\alpha = 3.31$ km/sec and $\beta = 1.83$ km/sec. $V_w = 1.44$ km/sec in all cases.

SEISMIC STUDIES OF SEA ICE

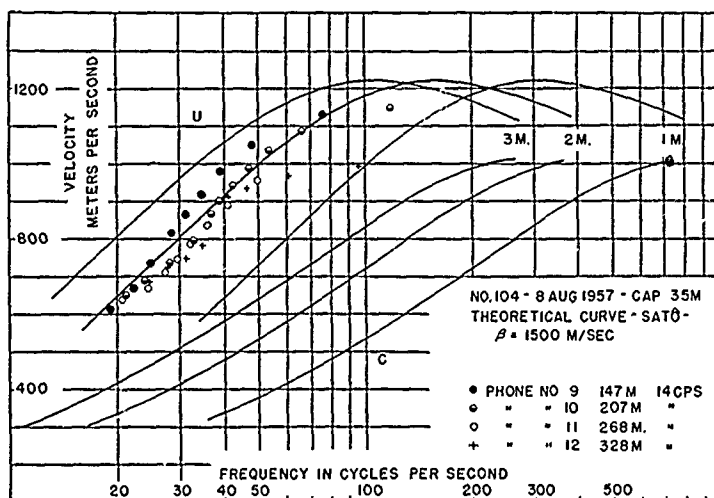


Fig. 10. Comparison of observed and theoretical dispersion for record 104, August 8, 1957.

velocity was evaluated numerically, but in all other cases group velocity was found graphically from the phase velocity.

For this study several different theoretical curves were computed by using different values of elastic constants based on the work discussed above, and these are plotted in Figures 10, 11b, 12, and 13. Several curves are drawn for each case, with ice thickness as the varying parameter. By comparing observed dispersion with these curves an ice thickness is found which may then be compared with the ice thickness found by direct measurement.

Thickness of the ice was measured directly through holes bored in the ice. This process permitted only a limited number of measurements to be made. Pack ice is irregular in thickness, departing from the plane sheet

assumed in the theory. Forty-six random measurements taken on level ice near Station Alpha in 1958 ranged from 263 to 423 cm, with a mean of 311 cm. Measurements taken at geophone sites along the most used lines are listed in Table 5.

A typical set of data taken in August 1957 is shown in Figure 10, where flexural waves indicate an average thickness of about 2 meters. Average measured thickness from six holes drilled along this line was 2.55 meters. This tendency for directly measured thickness to be larger than thickness found from dispersion is discussed later.

During March and April 1958, flexural waves were measured at short distances (Figs. 8 and 11a). For record 660, the average measured thickness was 2.55 meters, showing good

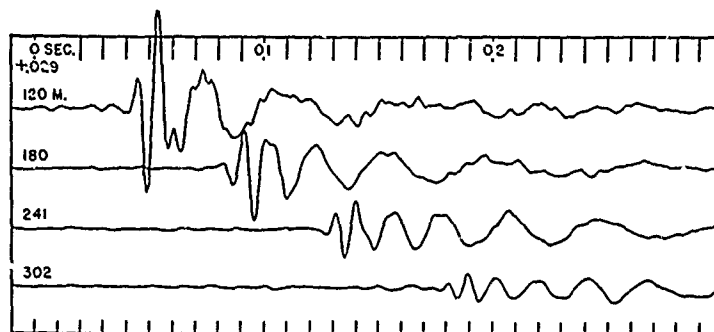


Fig. 11a. Record 660, March 31, 1958. Elastic waves in pack ice generated by a vertical hammer blow (14-cps vertical geophones).

KENNETH HUNKINS

TABLE 5. Measurements of Ice Thickness at Geophone Locations

Area	Geo- phone Number	Number of Measure- ments	Average- Thick- ness, cm
First camp 1957	1-6	6	308
	7-12	6	254
Second camp 1958	1-6	6	308
	7-12	6	438

agreement with thickness of about 2.5 meters from dispersion measurements (Fig. 11b). Some records taken in April 1958 showed waves corresponding to the high-frequency as well as the low-frequency branch of the flexural wave dispersion curve. The first flexural wave arrival on these records has a frequency of about 150 cps, corresponding to the group-velocity maximum (Fig. 12). High- and low-frequency branches are superimposed on the following portion of the record.

In June 1958, record 874 was made with geophones spaced 10 meters apart. From this record, phase velocities were found which agree well with the results for ice thickness found from group velocities (Fig. 13).

The orbital motion of the observed flexural waves was determined by comparing the three components of motion as recorded by the geophones. Particle motion is found to be retrograde, i.e., in the same sense as that of Rayleigh waves. Retrograde motion was found in both the high- and low-frequency branches of flexural waves (Fig. 14). Wherever flexural waves are well defined this sense of rotation prevails; however, there are many locations at which no systemic orbit can be found from the jumbled waves. Retrograde motion for flexural waves can also be seen on records taken by *Oliver, Crary, and Coté* [1954], but they did not discuss orbital motion in their paper.

Air-coupled flexural waves. An explosion fired in the air or on the surface of an ice sheet will produce a constant-frequency train of flexural waves preceding the air wave. This wave train begins at time $t = d/2.2 V_a$, where d = distance from shot point to receiver and V_a = velocity of sound in air. The frequency

of this train corresponds to that of flexural waves whose phase velocity equals the velocity of sound in air. This frequency is simply related to thickness through the equation

$$V_a^2 = \frac{1/3\pi^2\gamma_a^2 V_p^2}{1 + (\rho_1/\rho_2)/2\pi\gamma_a(1 - V_a^2/V_w^2)^{1/2}} \quad (2)$$

where $\gamma_a = hf_a/V_a$, f_a = frequency of air-coupled wave. Thus from a knowledge of V_p , V_a , V_w , and ρ_1/ρ_2 , a value of γ_a may be found. Once γ_a is fixed, the thickness h is found directly from the frequency f_a . In the following discussion, constants used are $V_w = 1440$ m/sec and $\rho_1/\rho_2 = 0.878$. V_p is found from Figure 2 and V_a is found by direct measurement (Table 6) or computed from the relation

$$V_a(\text{m/sec}) = 331 + 0.60T(^{\circ}\text{C})$$

In September 1957, surface shots at distances up to about 1 km produced good air-coupled flexural waves (Fig. 15). Since no direct measurement of sound velocity in air was made, a velocity of 329 m/sec was assumed and longitudinal plate velocity was taken to be 2590 m/sec, giving a value of 0.1125 for γ . The results of several direct measurements along the profile were averaged for comparison with theory (Table 7).

Data for a series of shots in June 1958 are also shown in Table 7. The path for these waves was over more irregular ice than the previous series, and the wave trains were more irregular. The appropriate sound velocity in air was measured for each shot, and $\gamma_a = 0.105$. Thicknesses determined from air-coupled waves are generally lower than those determined

TABLE 6. Measurement of Sound Velocity in Air

Record	Date	Average V_a , m/sec
233	1957 Sept. 2	326
	1958	
904-909*	June 28	320
914, 915*	June 28	307

* Records 904 to 909 were shot in the opposite direction from 914 and 915. Wind, as well as temperature changes during the day, may account for the velocity difference in the two directions.

SEISMIC STUDIES OF SEA ICE

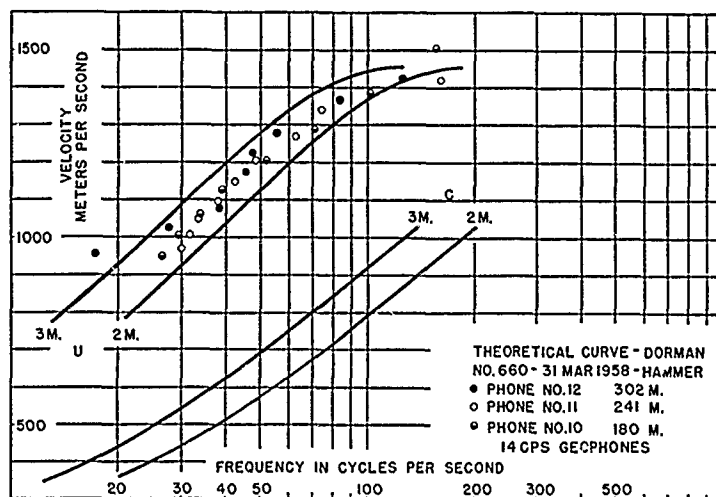


Fig. 11b. Comparison of observed and theoretical dispersion for record 660. $\alpha = 3.31$ km/sec, $\beta = 1.83$ km/sec.

directly. Air-coupled flexural waves also exhibit retrograde particle motion (Fig. 16).

Such systematic differences are also seen in results by *Oliver, Crary, and Colell* [1954]. The average thickness from their direct measurements was 1.60 meters, compared with an average of 1.19 meters from flexural wave dispersion. Their direct measurements in air-coupled wave studies average 1.67 meters, compared with 1.47 meters from the air-coupled wave dispersion. This discrepancy appears to be general for arctic pack ice.

An explanation of the discrepancy may lie in the anisotropic nature of sea ice. Although no direct measurements of the velocity of the vertically polarized shear wave *SV* were made, it is probable that this wave has a lower velocity than the *SH* wave for which velocity was measured. Since *SV* velocity is more important for flexural waves, the theoretical flexural wave curves will come into closer agreement with observed dispersion.

Nearly simultaneous arrival of water waves, first flexural waves, and *SV* waves makes

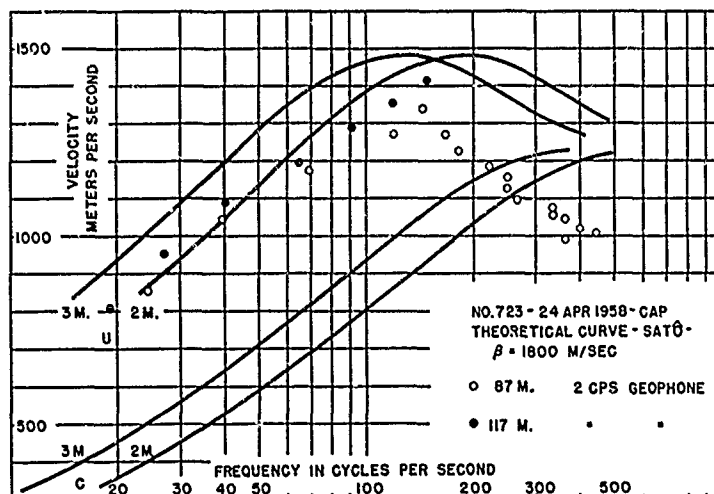


Fig. 12. Comparison of observed and theoretical dispersion for record 723, April 24, 1958.

KENNETH HUNKINS

TABLE 7. Comparison of Directly Measured Ice Thickness with Ice Thickness Calculated from Air-Coupled Wave Frequency

Date	Shot Number	Distance from Shot Point to Receiver	Frequency of Air-Coupled Waves, cps	Ice Thickness, m	
				Calculated from Air-Coupled Wave	Average of Direct Measurements
1957 Sept. 9	261	394	16.3	2.26	2.63
	263	546	17.2	2.14	2.61
	266	699	16.3	2.26	2.61
	268	851	17.5	2.11	2.72
1958 June 28	904	684	12.3	2.73	3.02
	909	409	15.9	2.12	3.05
	915	420	12.7	2.54	3.48

TABLE 8. Duration of Air-Coupled Wave Train from Distant Shots

Record	Distance from Shot Point to Receiver, km	True Azimuth from Receiver to Shot Point, deg	Duration of Air-Coupled Wave Train, sec
1032	7.17	157	0.848
1034	2.36	162	0.840
1081	9.17	267	0.555
1063	8.26	267	0.375
1064	2.90	278	0.460
1066	11.38	270	0.500

identification of SV difficult. However, the structure of sea ice suggests that the shear modulus for stresses acting vertically is less than the shear modulus for stresses acting horizontally. Sea ice consists largely of vertical plates separated by brine pockets. The plates are randomly oriented horizontally over areas greater than 50×50 cm [Schwarzacher, 1959]. Thus any vertical shear stress would act along the many lines of weakness presented by the vertical brine pockets, but any horizontal shear stress would meet the resistance of the interlocking, randomly oriented grains. Measurements using static methods have shown the

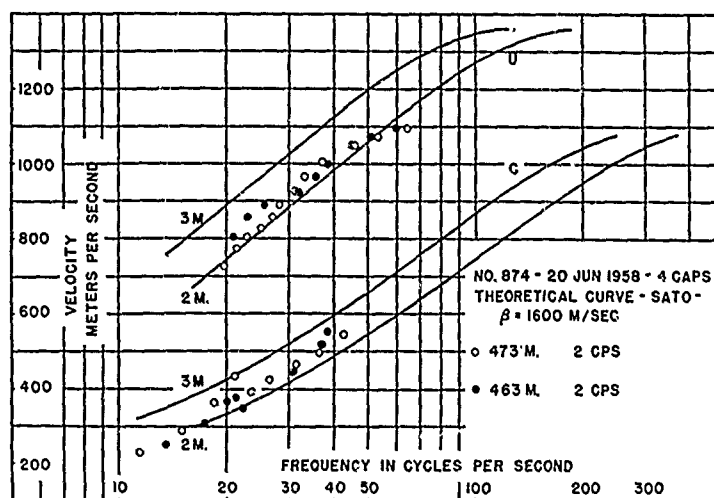


Fig. 13. Comparison of observed and theoretical dispersion for record 874, June 20, 1958.

SEISMIC STUDIES OF SEA ICE

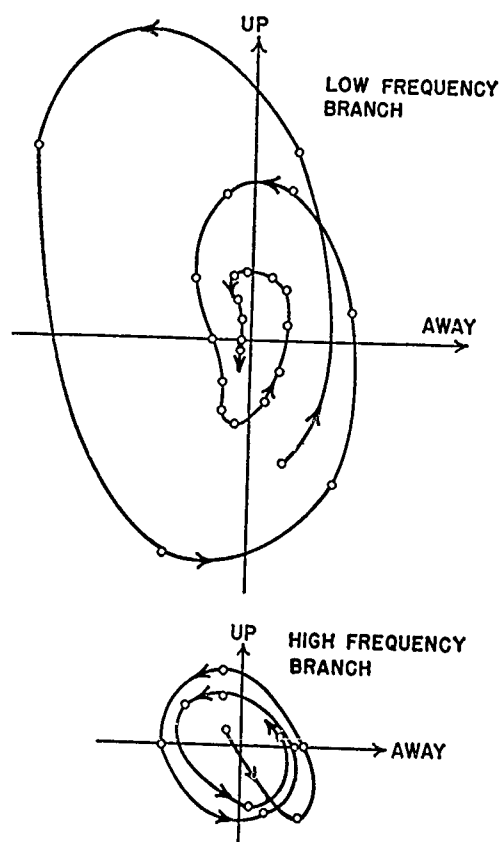


Fig. 14. Particle velocity at ice surface in vertical plane for flexural waves (record 715, April 22, 1958, 34 m).

anisotropic behavior of ice. *Butkovich* [1954] found that the strength of lake ice is not isotropic, and *Tabata* [1958] found indications that the elasticity and viscosity of sea ice are not isotropic. The flexural wave studies reported in this paper indicate that the *SV* velocity is probably 10 to 15 per cent below the *SH* velocity in pack ice.

Several large shots were made at distances up to 11.4 km. No longitudinal or flexural waves were recorded. The only waves recorded whose propagation depends on the ice were air-coupled waves. They appear as a train of waves of much shorter duration than would be expected for air-coupled waves from a shot at this distance. They increase in amplitude until the arrival of the direct air wave and then suddenly cease. The early part of the air-coupled train, as well as other waves, must be lost, partly through attenuation and partly by reflection at leads which lie between the shot point and receiver. However, the air-coupled wave is continuously generated by the air impulse as it propagates outward from the shot point. When the impulse crosses the last lead between it and the receiver, the progress of the air-coupled waves is no longer impeded. The length of the wave train will be only that which would be expected from a shot occurring at the lead nearest the receiver in the direction of the shot.

From Table 8 it is evident that there is a close correlation between the duration of the

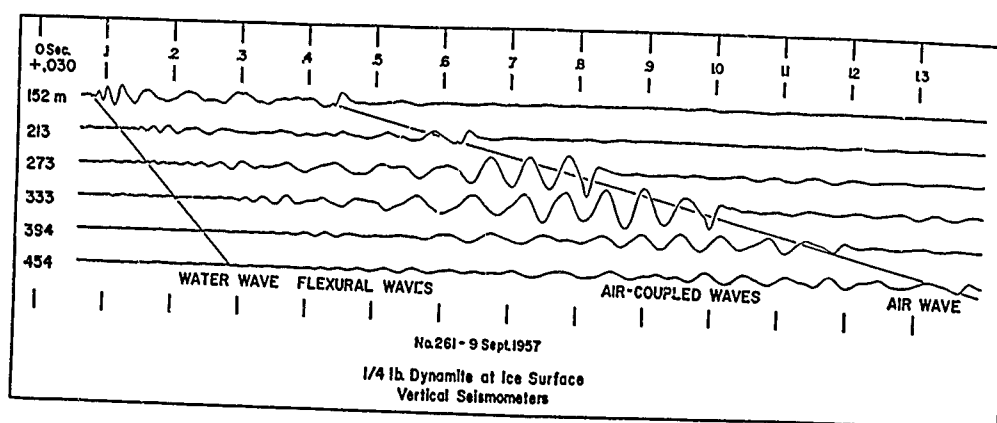


Fig. 15. Record 261, September 9, 1957. Elastic waves produced by a surface explosion.

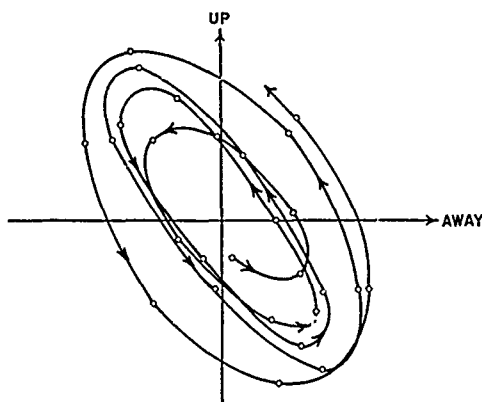


Fig. 16. Particle velocity at the ice surface in the vertical plane for air-coupled flexural waves (record 263, Sept. 2, 1957, 546 m).

train and the azimuth to the shot. However, there is little correlation between duration of the train and shot distance. Ordinarily, a direct correlation between the duration of the air-coupled wave train and shot distance is expected. The duration of the air-coupled wave train is given by

$$T = R/V_a - R/2.2 V_a = 0.545 R/V_a$$

where T = duration of air-coupled wave train.
 R = distance from receiver to shot point or to nearest lead in direction of shot.

For a wave-train length of 0.844 second, (Table 8) the distance to the nearest lead in azimuth 157° to 162° is calculated to be 513 meters. The nearest lead in this direction lay beyond the end of a 335-meter seismic spread and was estimated to be about 500 meters.

For a wave train of 0.500-second duration, the calculated distance is 364 meters, which agrees well with an estimated distance of 300 meters to the nearest lead in azimuth 160° .

Acknowledgments. I am indebted to all persons at Station Alpha who assisted me. Gary Latham and Bryan Isacks of Lamont Geological Observatory provided much assistance on the project in 1958. Dr. Norbert Untersteiner furnished helpful data on ice temperature and Dr. Walther Schwarzscher furnished much ice-thickness and density data. James Dorman kindly calculated flexural wave dispersion curves under Nonr Contract 266 (53). Dr. Jack Oliver provided assistance in the analysis of data and critically read the manuscript. This research was supported by Geophysics Research Directorate of Air Force Cambridge Research Center under Contract AF 19 (604) 2030.

REFERENCES

- Anderson, D. L., Preliminary results and review of sea ice elasticity and related studies, *Trans. Eng. Inst. of Canada*, 2, 116-122, 1958.
- Bogorodskii, V. V., The elastic characteristics of ice, *Soviet Physics-Acoustics*, 4, 17-21, 1958.
- Butkovich, T. R., Ultimate strength of ice, *SIPRE Research Paper 11*, 1954.
- Crary, A. P., Seismic studies on Fletcher's Ice Island, T-3, *Trans. Am. Geophys. Union*, 35, 293-300, 1954.
- Ewing, M., and A. P. Crary, Propagation of elastic waves in ice, 2, *Physics*, 5, 181-184, 1934.
- Ewing, M., A. P. Crary, and A. M. Thorne, Jr., Propagation of elastic waves in ice, 1, *Physics*, 5, 165-168, 1934.
- Kishinouye, F., Studies of lake ice, *Bull. Earthquake Research Inst., Tokyo Univ.*, 21, 298-306, 1943.
- Köhler, R., Beobachtungen an Profilen auf See-eis, *Z. Geophys.*, 5, 314-316, 1929.
- Lamb, H., On the flexure of an elastic plate, *Proc. London Math. Soc.*, 21, 70-90, 1889.
- Lamb, H., On waves in an elastic plate, *Proc. Roy. Soc. London, A*, 93, 114-128, 1916.
- Lotze, W., Schallgeschwindigkeitsmessungen von Eis in Abhängigkeit von Druck und Temperatur, *Z. Geophys.*, 23, 243-249, 1957.
- Oliver, J., A. P. Crary, and R. Cotell, Elastic waves in arctic pack ice, *Trans. Am. Geophys. Union*, 36, 282-292, 1954.
- Press, F., A. P. Crary, J. Oliver, and S. Katz, Air-coupled flexural waves in floating ice, *Trans. Am. Geophys. Union*, 32, 166-172, 1951.
- Press, F., and M. Ewing, Propagation of elastic waves in a floating ice sheet, *Trans. Am. Geophys. Union*, 32, 673-678, 1951a.
- Press, F., and M. Ewing, Theory of air-coupled flexural waves, *J. Appl. Phys.*, 22, 892-899, 1951b.
- Press, F., and M. Ewing, Crustal structure and surface wave dispersion, 2: Solomon Islands earthquake of 29 July 1950, *Bull. Seism. Soc. Am.*, 42, 215-325, 1952.
- Satō, Y., Study on surface waves, 2. Velocity of surface waves propagated upon elastic plates, *Bull. Earthquake Research Inst., Tokyo Univ.*, 29, 223-261, 1951.
- Satō, Y., Analysis of dispersed surface waves by means of Fourier Transform, 1, *Bull. Earthquake Research Inst., Tokyo Univ.*, 33, 33-48, 1955. (Errata and appendix to Study on Surface Waves, 2, is included at end of this paper.)
- Schwarzscher, W., Pack-ice studies in the Arctic Ocean, *J. Geophys. Research*, 64, 2357-2368, 1959.
- Tabata, T., Studies on visco-elastic properties of sea ice, *Natl. Acad. Sci. U. S. Publ.* 598, 139-147, 1958.

(Manuscript received February 10, 1960;
 revised July 15, 1960.)

Pack - Ice Studies in the Arctic Ocean

W. Schwarzacher

Reprinted from the
JOURNAL OF GEOPHYSICAL RESEARCH,
Vol. 64, No. 12, pp. 2357-2367, 1959

Pack-Ice Studies in the Arctic Ocean¹

W. SCHWARZACHER²

*Department of Meteorology and Climatology
University of Washington
Seattle, Washington*

Abstract—The annual stratification of pack ice has been examined. Summer layers are formed either by arrested growth or by thin layers of fresh-water ice. The crystal structure and the salt content of the ice reflect the seasonal cycle. During the growth of ice a pronounced orientation of crystalline structure develops; it is determined by vertical as well as by horizontal temperature gradients.

There is a marked and systematic increase of salinity with depth, ranging from about 0.1 per mil at the surface to 4.0 per mil at a depth of 300 cm. This salinity distribution remains unaltered during the summer melt season.

A tentative attempt has been made to reconstruct the growth history of the ice at Drifting Ice Station A. This shows that the winter growth is strongly related to the thickness of the ice, that the floe on which the station was located was probably eight years old, and that during each of the winters of 1955-1956, 1956-1957, and 1957-1958 the thickness of the ice increased nearly 60 cm.

Introduction—As part of the scientific program on Drifting Ice Station A an investigation of the heat budget of pack ice was proposed. The main problem appeared to be the study of the growth of floe ice under arctic conditions and, in particular, the study of the history of the floe on which the station was situated. The field work commenced towards the end of May 1958 and lasted until the middle of September 1958. The ice drifted during this period from 84°N, 150°W to 85°N, 140°W.

Nansen [1897] observed that in the Arctic Ocean the formation of pack ice takes place every year from December to June, approximately, by freezing on the underside of floes. During the summer, part of the old ice is removed by melting from the surface of the floes. Russian scientists state that the annual layers of winter ice can be recognized in section through the ice floes. Shumsky [1955] found evidence on North Pole III of at least four winter accretions, representing the years 1950 to 1954. The layers,

found on the underside of the floe, had an average thickness of 35 cm. Shumsky believes that some ice is also formed at the surface, leaving layers 10 cm thick every year. Savelev [Cherepanov, 1957] tried to estimate the age of the ice on North Pole IV, but, unfortunately, no published data are available. Cherepanov [1957] investigated the same floe; by studying thin sections he found evidence of at least nine annual layers, with an average increment of 33 cm.

The previous investigations of the stratification in pack ice were based on only a few sections; in the investigation reported here a SIPRE ice corer was used to obtain complete cores running from the top to the bottom of the ice pack. Each core was inspected and measured; photographs of thin sections and salinity samples were taken from most of the cores.

The macroscopic description of standard ice—The ice examined near Station A was most variable in origin. Each floe was itself a mosaic of older fragments, linked sometimes by pressure ridges and sometimes by stretches of relatively young ice. The boundaries of the floes changed continuously.

For a study of the variation within the ice, cores were taken along predetermined straight lines at intervals of 10 or 20 meters. Even though

¹This research was supported by the Office of Naval Research under Project NR 307 244, Contract Nonr-477(18).

Contribution No. 46, Department of Meteorology and Climatology, University of Washington.

²Present address: Department of Geology, Queen's University, Belfast, Ireland.

areas which showed signs of old pressure ridges were avoided, it was found that only 25 per cent of the cores consisted of old undisturbed ice. Twenty-five such cores were used to compile a standard section, the average thickness of which was 345 cm.

For a study of the details of the stratification the cores were placed on a dark background. This showed quite clearly that the ice increases in age from the lower surface upwards, and the winter ice of 1957-1958 therefore formed the lowest 50 cm. Until July this freshly formed ice was strikingly transparent and in sharp contrast to the older ice, which was milky-grey in color. Later in the summer the recent winter ice became grey and slightly clouded like the older ice, from which it was separated by a thin layer of milky white ice. This layer, which is interpreted as marking the previous summer, had a thickness of 2 to 5 mm, a sharp top, and an irregular, diffuse lower boundary. The interpretation of this layer is well supported by the following: The amount of winter ice formed during 1957-1958 at one locality was determined by direct measurement as being 55 cm (N. Untersteiner, personal communication). The average thickness, determined by the position of the summer layer in the standard section, compared well with this and gave a value of 59.6 cm. Furthermore, a thin layer was repeated at 53.5 cm above the 1957 layer and a third sharp boundary was at 58.9 cm above the 1957 layer. The summer line of 1956 was again only a few millimeters thick, very similar to the summer line of 1957. The summer layer of 1956 was almost always very strongly developed in the form of white opaque ice up to 10 cm in thickness. Usually the upper boundary of this layer was diffuse; the lower boundary was sharp and was frequently underlain by a few centimeters of very clear ice, which, as will be shown, was frozen fresh water. In the 25 cores of the standard section the three summer layers of 1957 to 1955 were well developed and easily correlated; the stratification closer to the surface was, however, less complete and more difficult to interpret. Only seven cores showed a good development of summer layers for 1954 to 1951, and three cores showed layers for 1950. The higher layers followed one another more closely, at intervals of 30 to 25 cm; the ice was very

cloudy, and the summer layers showed up as white opaque ice. Particularly during the later parts of the summer, liquid inclusions seem to be concentrated in the higher parts of the ice profile and to obscure the older ice stratification. The top 50 cm may contain ice which has formed on the surface, the most noticeable being layers of very transparent fresh-water ice, obviously formed in surface pools. This ice can be recognized by the vertical orientation of the crystal axes which is in contrast with that of the sea-water ice. Snow that has fallen into such pools freezes to form very characteristic layers of fine-grained ice. It has been impossible, however, to find any annual stratification of superimposed ice similar to the one described by *Shumsky* [1955], and it seems that most of such surface ice disappears during the summer melting period.

The petrology of the ice—For petrological examination of the cores, horizontal and vertical thin sections were cut with an electric band saw. In vertical sections the individual crystals of the winter ice appeared as 20- to 30-cm-long spindle-shaped grains with their vertical axes at right angles to the surface of the floe. In horizontal sections the grains were more or less isometric with cross sections of 2 to 3 cm. Grain boundaries were often difficult to see, as neighboring grains frequently had a very similar crystallographic orientation, and an intimate intergrowth between adjacent grains occurred. The most characteristic feature of all salt-water ice is a pronounced horizontal orientation of all crystal axes. This has been explained by *Weeks* [1957] in the following way: Freezing of salt water leads to a separation of pure ice and concentrated brine. The pure ice grows in thin plates parallel to the basal plane of the crystal, the impurities being concentrated between the platelets at regular intervals. The brine enclosures have a marked influence on the thermal conductivity of the single crystal, and it is estimated from theoretical considerations that the thermal conductivity at right angles to the crystal *c* axis is 25 to 50 per cent greater than that parallel to the *c* axis. Crystals with their axes in the horizontal therefore have the direction of their highest conductivity parallel to the direction of maximum heat flow and will, in consequence, grow faster.

PACK-ICE STUDIES IN THE ARCTIC OCEAN

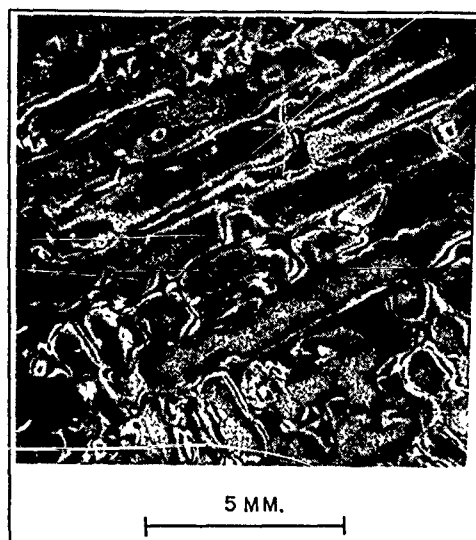


FIG. 1—Sea-ice section parallel to the crystal axis showing plate structure.

In horizontal sections the lamellar structure of salt-water ice can be clearly seen. Along the boundaries of the thin ice plates are the brine enclosures, the shapes of which vary considerably with the temperature of the ice. The distribution and size of the brine enclosures have a significant influence on the physical properties of sea ice; they have been studied in detail by Assur [1958] and Anderson and Weeks [1958]. It is noteworthy that all measurements of the thickness of ice plates in the present study gave a value of 0.902 mm (average from 500 measurements). This is just twice the value given by Weeks, who found the thickness of ice lamellas to be 0.45 mm. In the examined ice, which includes old ice as well as freshly frozen ice, it may be that only alternate 'selected' planes are used for storing brine. Artificial melting can bring out the incipient subdivisions of the observed lamellas (Fig. 1).

A special study was made of the azimuthal orientation of crystal axes. For this purpose pencil rubbings of large horizontal ice sections were prepared and the strike of the plates in each grain measured. The distribution of these directions from a section 25×20 cm is plotted in Figure 2. It can be seen that the directions of the crystal axes in the horizontal were not random, and that there was one main maximum

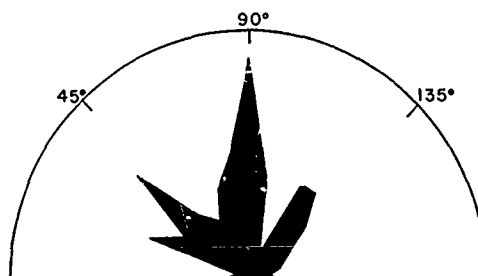


FIG. 2—Strike directions of 280 crystal axes in a horizontal section of 20×25 cm.

with two subsidiary maxima roughly 45° on either side. Detailed analysis showed that the neighbor of any grain was likely to have a similar orientation or one in which the grain orientation differed by either 45° or 90° . If we extended the orientation analysis over larger areas, 50×50 cm, for instance, then the preferred orientation disappeared, but the relationship between the neighboring grains persisted. This seems to indicate that the azimuthal orientation of a newly formed crystal is determined by the crystals surrounding it. It is suggested that the brine enclosures in a single crystal effect an anisotropic thermal conductivity in the horizontal planes which contain the crystallographic axis. The highest temperature gradients will occur parallel to the strike of the platelets, and new crystals will therefore grow parallel to it. The directions 90° or 45° inclined to the plates are also favored, as they can be the shortest distances between isolated brine enclosures, depending, of course, on their distribution. Unfortunately, this study could not be made in more detail because the temperatures at Station A were too warm during the period of investigation.

The grain-to-grain relationship became very obvious when one studied the intergrowth of crystals. Intergrowth was very common, and it was almost always those crystals with their axes approximately at right angles to each other which showed mutual penetration. The resulting texture had a distinct chessboard appearance, reminiscent of certain twinning patterns in feldspars (Figs. 1 and 3). The slight variability of angles at which intergrowth occurred suggests again a similar mechanism to the one outlined

above rather than any direct crystallographic preference. Chessboard texture has been found to be the normal development of ice which has not been disturbed mechanically during growth. The cross sections of such grains were roughly square in outline, with diameters of 1 to 2 cm.

Active growth of ice occurs from November to June [Untersteiner, 1958, and Untersteiner and Badgley, 1958]. In the middle of May, when the ice study was started, the underside of the floe showed the development of a so-called skeletal layer [Weeks and Anderson 1958]. This layer indicated that freezing was in progress. Disconnected platelets of pure ice protruded from the underside into the water. At this time the uncemented layer had a thickness of 1 to 2 cm; it gradually became thinner and was last observed on June 16. Throughout the remainder of the summer the underside of the ice floe was perfectly smooth; in fact, a small amount of melting took place. At one locality where repeated cores were taken the thickness of the winter ice of 1957-1958 decreased by 2 cm from the beginning of August to the beginning of September.

Thin sections through the summer layer of 1957 showed that the winter-ice growth of 1957-1958 was the direct continuation of that formed during the previous winter. In most instances no new generation of crystals formed, and the crystals of the previous winter which may have been truncated by the summer ablation took up growth again with the same crystallographic orientation. Sometimes the grain boundaries in the vertical sections showed minute offsets, and only occasionally did crystals with slightly different orientations develop. Artificial melting, however, always brought out the summer line and showed that this line was a potential grain boundary, even if the optical orientations of the pre- and post-summer ice was the same. Summer layers, in particular the summer layer of 1955, often showed a different development. In a vertical section one could see that the long spindle-shaped crystals had suddenly decreased in size until they had horizontal diameters of 0.5 to 1 cm and a length of only 2 to 3 cm, forming a layer 1 to 10 cm thick. The preferred orientation of the crystal axes was still horizontal, but deviations up to 30° from this occurred. This ice shows no platy

structure in horizontal sections, and its salinity was from 1 to 1.5 per mil, which was considerably lower than that of the surrounding ice. It is therefore believed that this ice formed as fresh-water ice on the underside of the floes during summer. Nansen [1897] first observed this phenomenon when he measured the growth of a one-year-old ice sheet which formed over a lead. During one winter the lead grew to a thickness of 231 cm, and the growth continued during the following summer. Nansen explained that this further growth resulted from the freezing of surface melt water which reached the underside of the floe. Due to its low salinity this water froze when cooled by the sea water. Untersteiner [1958] and Untersteiner and Badgley [1958] made the same observation in the camp area of Station A during the summer of 1957 when melt water was artificially introduced under the ice by holes bored to drain the camp area. Examination of the distribution of fresh-water ice during the summer of 1958 showed clearly that it was mainly restricted to the camp area and that it occurred under natural conditions only where the ice was thinner than normal, 200 to 250 cm. Further, this condition was often observed close to open leads, which collect a good deal of melt water during the summer. The petrographical examination of cores showed that, apart from exceptional years, summer ice did not significantly contribute to the ice growth. Partly depending on how much drift took place during the summer, fresh water collected only in restricted areas underneath the thinner ice and probably arrived there after it had drained into leads. The lower density of the melt water would inhibit it from percolating through the floe even if the ice became permeable during the summer.

Both types of annual layering (interrupted growth of large winter-ice crystals and the formation of layers of small crystals, interpreted as summer ice) have been recorded by Cherepanov [1957], a fact which seems to indicate that annual layering is generally present in the arctic pack ice. For practical purposes it should be noted that most stratifications could be seen more easily by gross inspection than by microscopic examination.

The salinity of the ice—To obtain a continuous record of the variation of salinity in the ice, many cores were cut into sections 7 cm long

PACK-ICE STUDIES IN THE ARCTIC OCEAN

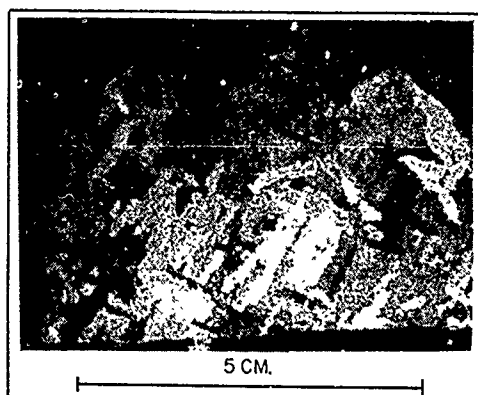


FIG. 3—Horizontal section through sea ice with chessboard-like intergrowth.

and then melted. The salinity of this water was determined by measuring its density at 15°C with a hydrometer. The instrument used was from a standard salinity-measuring kit calibrated in per mille salinity which, with

proper care and temperature corrections, was readable to 1/10 per mil. A few hydrometric measurements were checked by titration on the station, and two cores were analyzed under more favorable conditions at the Oceanography Department of the University of Washington. The hydrometric measurements compared very well with the titrations.

Plots of vertical salinity profiles (Fig. 4) showed a systematic increase of salinity with depth and, superimposed on this, periodic fluctuations which could be correlated with the annual stratification. In order to study systematic variations the mean salinity of 40 profiles has been computed with the surface as the reference level. In order to eliminate short periodic fluctuations the values have been smoothed by using the weighted mean of the graphed value with the salinity from above and below it. The resulting curve (curve A in Fig. 5) shows how the salinity from the bottom of the floe to a depth of approximately 170 cm has the

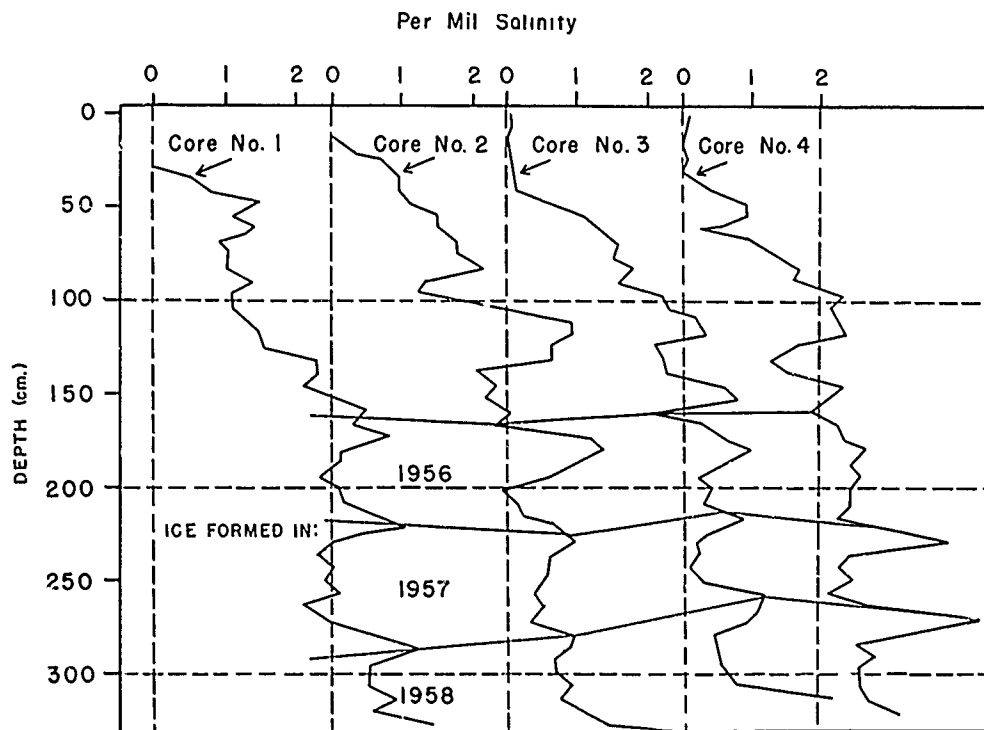


FIG. 4—Salinity profiles of four cores taken at 10-meter intervals. The correlation is based on the ice stratification.

W. SCHWARZACHER

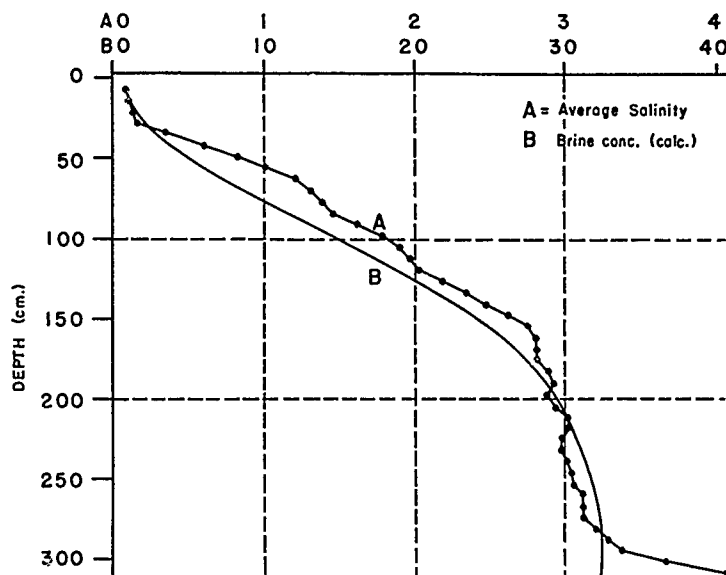


FIG. 5—Curve A: Average salinity of 40 cores based on 2060 salinity determinations, horizontal scale (A) per mille salinity. Curve B: Calculated brine concentration, horizontal scale per mille salinity.

nearly constant value of 2.8 per mil, and from there to the surface it falls rapidly to nearly 0.1 per mil. The lowest part of the curve is the least reliable part of the distribution because not all profiles were of equal length. The general shape of the salinity distribution remains unaltered from June to September. When the first salinity profiles were taken in May the ice was still well below freezing, and it is therefore reasonable to assume that the winter salt distribution was unchanged; unfortunately no reliable winter salinity measurements were available. Before interpreting the salinity it is necessary to consider the brine concentration in the ice. This concentration will depend entirely on the temperature within the ice, if we make the reasonable assumption that everywhere within the ice the enclosed brine is at its freezing point. Assur [1958] has tabulated this dependence for sea ice. Ice temperatures have been recorded at the station at 50-cm intervals. To supplement these, temperature measurements were taken on several cores directly after they were brought to the surface. The ice temperatures, compiled from all available data, are given in Table 1.

From the temperatures the concentration of the brine enclosures was calculated and is shown in Figure 5, curve B. Because the relation

TABLE 1—Ice temperatures on September 1

Depth below sur- face, cm	Temper- ature, °C	Depth below sur- face, cm	Temper- ature, °C
10	-0.05	170	-1.36
20	-0.07	180	-1.41
30	-0.12	190	-1.45
40	-0.19	200	-1.48
50	-0.27	210	-1.51
60	-0.35	220	-1.54
70	-0.44	230	-1.55
80	-0.54	240	-1.57
90	-0.64	250	-1.58
100	-0.75	260	-1.59
110	-0.85	270	-1.60
120	-0.95	280	-1.61
130	-1.05	290	-1.62
140	-1.15	300	-1.62
150	-1.23	310	-1.62
160	-1.30		

between concentration and temperature in this range is practically linear, both temperature and concentration follow the same distribution, which is best approximated by a gaussian probability function in the cumulative form. The function is part of the solution to the differential equation of either heat flow or diffusion

PACK-ICE STUDIES IN THE ARCTIC OCEAN

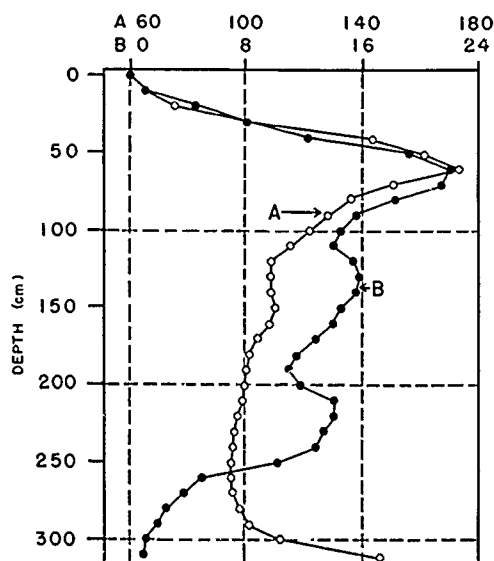


FIG. 6—Curve A (open circles): brine volume given in per mil. Curve B (full circles): frequency of macroscopic brine enclosures in 100 cores. Vertical scale depth in centimeters.

through an infinite plate. As can be seen from Figure 5, the observed salinity distribution could almost be explained as being due to saturated brine-filled enclosures making up about 10 per cent of the total volume of ice at all levels. There were, however, significant deviations from this; curve A in Figure 6 shows the vertical distribution of the volume of brine enclosures as calculated from the salinity of the ice and the theoretical brine concentration. It is seen that the level at which the largest brine enclosures occurred is 60 cm below the surface of the ice. This was confirmed by observation; the summer ice frequently contains large liquid inclusions, sometimes holes of up to 2 cm in diameter and sometimes irregular pockets of brine, and they are always easily seen in the cores. Curve B in Figure 6 shows the frequency with which such enclosures occurred for each 10-cm level from one hundred cores taken from June to September. There was, as expected, a maximum of liquid enclosures at a depth of 60 cm below the surface. Two deeper maxima at approximately 130 and 210 cm were probably caused by the periodic salinity fluctuations. It was observed that most of the recorded lower brine pockets formed

shortly after the cores were brought to the surface.

In many cores the lowest 5 to 10 cm had a salt content of 4 to 6 per mil, which is much higher than the salinity of the rest of the core. This increase of salinity developed particularly after the ice stopped growing in thickness (after the middle of June). At this time the temperature of the ice was very close to the ocean temperature and the brine volume was correspondingly high (curve A, Fig. 6). Diffusion of sea water probably took place and increased the salt concentration. It appears that part of this excess salt is retained in the ice when the winter freeze starts again, and the salinity profiles therefore show a periodic fluctuation with high salt contents corresponding to the summer layer. In Figure 4 four selected profiles have been correlated by their annual stratification. It is clearly seen that the summer line for 1957 and 1956 came close to a salinity maximum of 3 to 4 per mil. The summer line of 1955, on the other hand, coincided with a salinity minimum. A study of thirty such correlated profiles showed that the salinity maximum of 1957 was slightly below the summer line, with an average displacement of 2.0 cm. The displacement in 1956 was 3.7 cm, which seems to indicate that excessive salt concentrations in the ice migrate downwards at the rate of approximately 2 cm a year. This downward migration explains the observation (already mentioned) that the upper surface of the last two summer layers is developed as a sharp boundary, whereas the lower surface is diffuse. The summer layer of 1955 is more difficult to interpret, because most profiles showed that fresh-water ice was formed during this summer. From the available data it appears that the salinity minimum caused by such fresh-water ice migrates upwards only as indicated by the rather diffuse top boundary and the very sharp bottom boundary of such layers. Salinity distributions can be used for dating the ice but are more difficult to interpret than the ice structure. A summer can be represented either by a salinity minimum or maximum, and both maxima and minima migrate slowly with time.

The salinity distribution of all profiles indicated a progressive loss of salt. This has been explained by purely gravitational drainage or by migration of brine enclosures with the thermal gradient

(Sverdrup, 1956). The exact mechanism of salt loss, however, is still unknown. In general, gravitational drainage of brine would be expected to take place only during the winter months when the base of the ice is warmer than the surface, and the lower brine enclosures would therefore have a lower density. In winter, however, the total brine volume is small and the permeability of the ice is low, a condition which would slow drainage. During the melting period the brine density decreases from the base to the surface of the ice and is therefore gravitationally stable. Whitman [1926] showed experimentally that isolated brine enclosures migrate towards warmer surfaces, and involved in the process is melting at the warmer end of the enclosure and freezing at the colder end, together with a continuous mixing, probably by diffusion, of the brine in the enclosure. During summer, brine would be lost at the upper surface, whereas during winter, when the temperature gradients are much steeper, the migration would be downwards. It is very likely that the downward shift of salinity peaks is due to this process, which, however, seems to be very slow. A comparison of curves *A* and *B* in Figure 5 shows that during the summer the brine content was approximately constant at 10 per mil throughout the ice, and excess salt over the temperature equilibrium concentration can be removed only by diffusion towards the upper surface of the ice. This upper surface is kept fresh by precipitation and melt water from ice which has been raised above the level of the floe (pressure ridges). A striking confirmation of salt redistribution by diffusion, which is considered a most important factor, is given by the salinity profiles of two cores in the camp area. One was taken before the melting period started; the second was taken after four weeks during which time fresh water was continuously pumped under the ice surface. Within this time the salinity at a depth of 280 cm had been reduced from 4 per mil to 0.5 per mil, and at 240 cm, from 3.7 per mil to 2.9 per mil. This indicates that diffusion operates to produce a decrease of salinity in the lower ice.

Disturbed ice—In this study the sampling of ice profiles was selective, inasmuch as most cores were taken from areas which superficially showed no signs of ice disturbance. Neverthe-

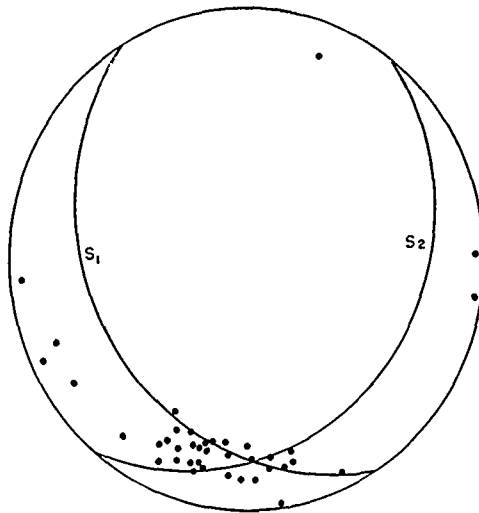


Fig. 7—Orientation of 39 optic axes of ice which has been tilted during growth.

less, petrological examination showed that it was very common for ice floes to become slightly tilted at various stages of their development. Under such circumstances a very pronounced azimuthal orientation of ice crystals develops. In the cores, one can recognize tilting by an inclination of the stratification and by the fact that the longest grain axes are perpendicular to the stratification. The crystal growth is influenced by two factors: First, crystals will continue to grow in the same direction as the crystals grew before tilting occurred, and, second, the maximum heat flow will still be directed vertically upwards. Grains which have their *c* axes parallel to the axis of tilt are obviously in the most favored position, and a strong preferential orientation of crystals which have their plates parallel to the dip direction will occur. Figure 7 shows the orientation of crystal *c* axes from a core taken approximately 10 meters from a pressure ridge. The ice must have tilted twice in different directions; *S*₁ is the summer layer of 1956, *S*₂ the summer layer of 1957. The ice between the two summer layers took the only possible orientation in which the plates are perpendicular to both boundaries.

Whenever such preferential azimuthal orientation occurred the grain shape was also affected. The horizontal cross section of the grains became elongated in the direction of the plates. The

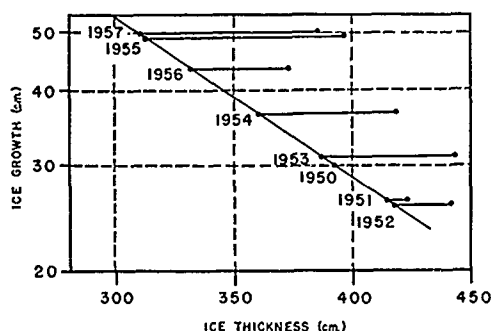


FIG. 9—Thickness of ice from 1951 to 1957. Points at the right side mark the pre-summer thickness, points on the left the post-summer thickness. The vertical scale gives the amount of ice growth in the following winter.

of the summer of 1957 and W is the winter growth. Similar results were obtained when the correlation for the winter ice of 1956–1957 was investigated, but allowance had to be made for the ice loss during the summer of 1957. From the data the loss was estimated to be approximately 60 cm.

To get some idea of how the winter growth varied from year to year, measurements were made on selected profiles which showed at least three years' undisturbed growth. The data are the same that were used for the standard ice profile previously discussed. The results are given in Table 2. It is interesting to note that the coefficient of variation for the last three years ranges from 17 to 25 per cent, which is almost twice the variation of the total thickness of the ice. This indicates that there was probably an additional process which regulated the ice thickness, apart from the correlation with the winter increment. A relation between ice thickness and summer loss could be such a mechanism. Completely neglected in establishing the relation of ice growth to ice thickness has been the effect of snow cover, which probably acts as a very effective insulating blanket and may lead to different relations in different winters. Data on growth of ice are rare in the literature; Nansen [1897] gives values of winter growth for ice 208 and 336 cm thick, and from Cherepanov's [1957] two profiles two further points can be derived. These data are also plotted in Figure 8 for comparison with the data from Station A.

It appears that the thickness-growth relation can be used for determining the ice thickness before and after the melt periods of the last seven years. In Figure 9, the points on the right side show the ice thickness before the melting started, and the points on the left, the thickness after the melting was completed. The horizontal distance between the points gives the summer loss, and on the vertical scale the growth of the following winter is given. The oldest ice is 8 to 9 years old. In the years 1950 to 1953 the ice is estimated to have been thick and to have had an annual increment of 25 to 30 cm (a similar value of 30 cm was found by Cherepanov on North Pole IV for the years 1949 to 1955). In 1955 the thickness of the ice decreased greatly. The ice loss during this summer was exceptionally great, and the large quantities of melt water may account for the low salinity and the layers of fresh-water ice which were recorded that year.

It is tempting to correlate the changes of ice thickness with the circulation in the Arctic and to conclude that the ice is again increasing in thickness, but to substantiate such a conclusion would require much more observational data from different latitudes than is now available.

Acknowledgments—This investigation was sponsored by the Office of Naval Research and was directed by P. E. Church. The staff of the Department of Meteorology and Climatology of the University of Washington, W. Weeks, and the U. S. Army Snow Ice and Permafrost Research Establishment have given valuable advice and helped with the preparations for the field work. The author is further indebted to all colleagues at Station A, in particular to A. Assur and G. Frankenstein who generously shared their equipment and provided a number of salinity determinations which have been used for comparison. The Department of Oceanography of the University of Washington analyzed some ice samples brought back from the field. Quite invaluable has been the cooperation of the Air Force personnel at Station A.

REFERENCES

- ANDERSON, D. L., AND W. F. WEEKS, A theoretical analysis of sea-ice strength, *Trans. Am. Geophys. Union*, 39, 632–640, 1958.
- ASSUR, A., Composition of sea ice and its tensile strength, in *Arctic Sea Ice*, *Natl. Acad. Sci. Natl. Research Council, Publ. 698*, 106–138, 1958.
- CHEREpanov, N. W., *Opredeleniye vozrasta dreyfuyushchikh l'dov metodom Kristalloopticheskogo issledovaniya* (Age determination of drift-

PACK-ICE STUDIES IN THE ARCTIC OCEAN

- ing ice by optical study of the crystals), *Problemy Arktiki*, 2, 179-184, 1957.
- NANSEN, F., *Farthest North*, 2 vol., A. Constable, London, 1897.
- SHUMSKY, P. A., Kirzucheniye l'dov Severnogo Ledovitoga okeana (Study of the ice of the Arctic Ocean), *Vestnik Akad. Nauk SSSR*, 2, 33-38, 1955.
- SVERDRUP, H. U., *Arctic Sea Ice, the Dynamic North*, vol. 1. United States Chief of Naval Operations, 1956.
- WEEKS, W. F., Study of the growth of sea ice crystals, *Bull. Geol. Soc. Am.*, 68, 1811, 1957.
- WEEKS, W. F., AND D. L. ANDERSON, An experimental study of strength of young sea ice, *Trans. Am. Geophys. Union*, 39, 641-647, 1958.
- WHITMAN, W. G., Elimination of salt from seawater ice, *Am. J. Sci.*, 9, 126-132, 1926.
- UNTERSTEINER, N., Arctic sea-ice studies, *IGY Bulletin* 12, 11-15, 1958.
- UNTERSTEINER, N., AND F. I. BADGLEY, Preliminary results of thermal budget studies on Arctic pack ice during summer and autumn, in *Arctic Sea Ice*, *Natl. Acad. Sci. Natl. Research Council, Publ. 598*, 85-95, 1958.
- (Manuscript received May 29, 1959; revised September 4, 1959.)

The Deuterium Concentration in Arctic Sea Life

I. Friedman
B. Schoen
J. Harris

Reprinted from the
JOURNAL OF GEOPHYSICAL RESEARCH,
Vol. 66, No. 6, pp. 1861-1864, 1961

The Deuterium Concentration in Arctic Sea Ice

IRVING FRIEDMAN, BEATRICE SCHOEN, AND JOSEPH HARRIS¹

U. S. Geological Survey, Washington 25, D. C.

Abstract. Samples taken from cores of sea ice collected near Ice Island T-3 at 80°18'N, 113°W, and on US-IGY Drifting Station Alpha at approximate locations of 85°40'N, 127°W, and 83°N, 165°W, were analyzed for their relative deuterium content. A plot of deuterium concentration vs. depth in the ice, from the T-3 ice core, shows three positions of minimum deuterium concentration.

These minima are interpreted as being due to the formation in the summer, and freezing in the early winter, of a surface layer of water of low deuterium concentration. This layer forms by the mixture of sea water with water from melted precipitation that is low in deuterium. The sea ice floats on this deuterium-poor layer, and this layer is the first material to be added to the ice floe when accretion by freezing begins in the early winter.

Several samples of surface water collected by the submarine U.S.S. *Skate* during the summer of 1958 at 86°44'N, 77°55'W, and 89°18.5'N, 45°00'W, prove the existence of such a deuterium-depleted layer at these locations.

Two cores taken on US-IGY Drift Station Alpha at approximate locations of 82°N, 165°W, and 85°N, 127°W, show no such clear deuterium variation. This is interpreted to indicate that no deuterium-depleted layer formed because (1) in the 2 or 3 years preceding ice collection on Drift Station Alpha precipitation was much less than at the other locations sampled, or (2) vertical mixing under Drift Station Alpha was greater than at the other locations.

During an investigation of the separation of deuterium during the freezing of ice, a number of natural environments were sampled. In a previous paper by Friedman and Redfield [1956] deuterium analyses of coexisting ice and water from Hopedale Bay, Labrador, and ice forming in the sea off Woods Hole, Massachusetts, were given, and it was shown that when water freezes at approximately 0°C, the ice will contain 2 per cent ± 0.4 per cent more deuterium than the water from which it is freezing. These results are in agreement with unpublished laboratory experiments of Epstein and Friedman.

Details of the technique of the deuterium analysis are given in previous papers [Friedman, 1953; Friedman and Woodcock, 1957]. The deuterium concentration is expressed as per cent relative to a standard sea water, approximately equal to mean sea water. A sample expressed as + 1 per cent indicates that the sample contains 1 per cent more deuterium than does the standard sea water, while -1 per cent indicates that the sample contains 1

per cent less deuterium than does our standard sea water. Expressed algebraically, relative deuterium concentration in per cent

$$= \frac{D/H \text{ sample} - D/H \text{ standard}}{D/H \text{ standard}} \times 100.$$

The deuterium results have an error of ± 0.1 per cent.

An ice core collected by Maurie Davidson from Drift Station Alpha (83°N, 165°W) in early July 1957 was subsequently analyzed. The results appear in Figure 1, where both the deuterium and salt concentration of the ice is plotted as a function of depth in the ice. Most of the ice has a relative deuterium value of -0.2 per cent. The sea water under the ice has a relative deuterium concentration of -2.0 per cent. The ice is thus enriched in deuterium by approximately 1.8 per cent, in good agreement with the 2 per cent previously found.

The snow cover on the ice had a relative deuterium concentration of -18.4 per cent, while the sample 10 cm down analyzed -6.7 per cent. This sample can be explained by mixing of 'normal' sea ice of -0.2 per cent with snow of approximately -18 per cent.

The bottom of the ice in contact with the sea

¹ Publication authorized by the Director, U. S. Geological Survey.

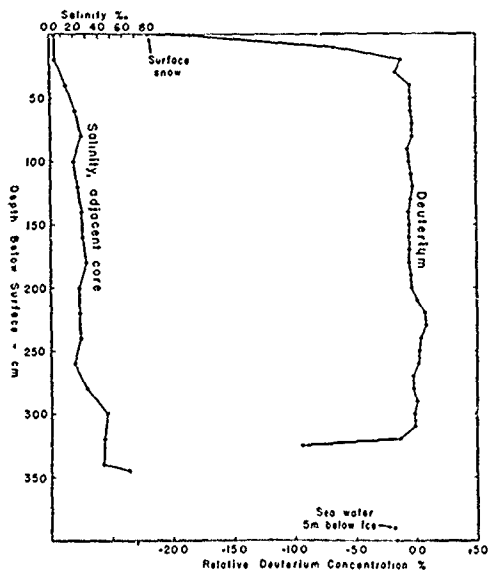


Fig. 1. Deuterium and salinity distribution in an ice core collected July 1957 on Drift Station Alpha.

has a relative deuterium concentration of -9.4 per cent, and the sample 5 cm above the bottom of the ice, -1.4 per cent. We initially believed that these low concentrations were due to contamination of the core by surface melt water running down into the hole. However, subsequent measurements on other samples, herein described, have caused us to change our opinion. We now believe that these low-deuterium concentrations are caused by the freezing of a layer of water of lower-deuterium concentration than normal sea water, caused by the melting of snow and the runoff of this low-deuterium water from the sea ice into the sea. This fresh water, being of lower density than the sea water, will float on the sea surface. The sea ice will in turn float on this fresh-water layer. If vertical mixing, probably due in the main to turbulence caused by wind action, does not dissipate this layer, a layer of low-deuterium ice will form under the ice floe when freezing and accretion of ice begins in the late summer or early fall.

Although the annual precipitation in the areas of the Arctic basin under consideration probably does not exceed 4 inches, this melted precipitation is concentrated, owing to runoff from the permanent sea ice, into small areas of

relatively open water. It is in these small leads and 'lakes' that the formation of the low-deuterium and salinity layer is proposed. In areas of more open water the annual precipitation is (1) of insufficient volume to yield a layer thick enough to get under the permanent ice, and (2) mixed by wind-induced turbulence with a large amount of sea water and loses its identity.

The next ice core to be examined was collected by Robert Le Blanc on an ice floe adjacent to Ice Island T-3 at $80^{\circ}18'N$, $113^{\circ}W$, on April 20, 1958. The deuterium and chlorinity data are given in Figure 2. Again, the ice of -1.4 to -0.5 per cent is in approximate equilibrium with sea water under the ice of -2.8 per cent, a difference of 1.4 to 2.3 per cent, which agrees closely with the established value of 2 ± 0.4 per cent.

Since this ice core was collected during the Arctic winter, the layer of 'light' water had already frozen and was incorporated into the floe approximately from 57 to 102 inches in depth, followed by 'normal' sea ice from 102 inches to the bottom of the floe at 108 inches. Inasmuch as several months of cold weather were still to be expected, during which more ice would be added to the bottom of the floe, the figure of 51 inches is the minimum accretion

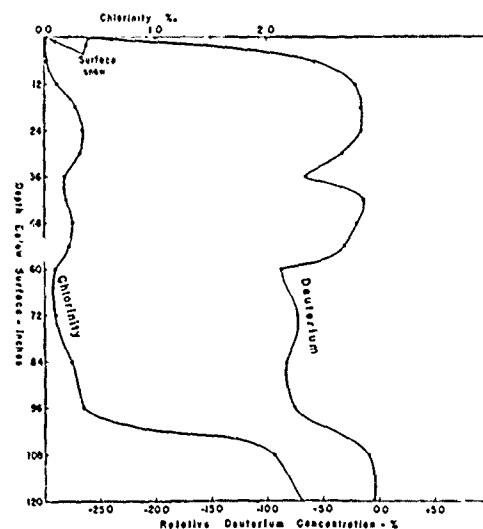


Fig. 2. Deuterium and chlorinity distributed in an ice core collected April 20, 1958, on Ice Island T-3.

DEUTERIUM CONCENTRATION IN ARCTIC SEA ICE

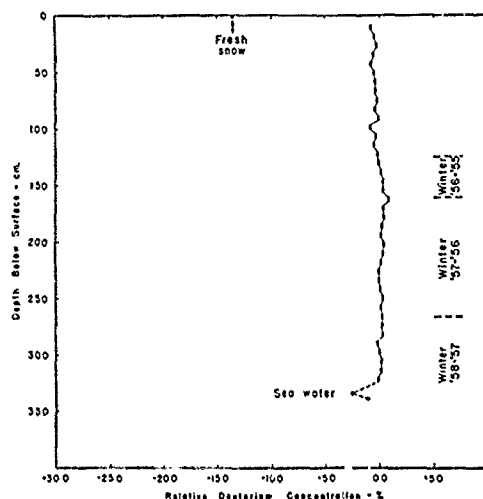


Fig. 3. Deuterium distribution in ice core collected Sept. 6, 1958, on Drift Station Alpha.

of ice on this floe during the Arctic winter of 1957-1958.

The deuterium (and chlorinity) minimum at 36 inches is believed to represent the remainder of the previous winter's ice. The relatively small section of ice having a low-deuterium concentration might be due to the deuterium-depleted water layer having been thin the previous year, owing perhaps to the factors mentioned previously under the discussion of Drift Station Alpha.

Recently a second core from Drift Station Alpha (85°40'N, 127°W) collected September 6, 1958, by Kenneth Hunkins and W. Schwarzsacker, was analyzed. The data are presented in Figure 3. Although the samples from 200 cm to the bottom have a slightly lower deuterium concentration than those above 200 cm, and the last sample has several per cent less deuterium than those above, there is little evidence

of a deuterium minimum at the levels assigned as the beginning of winter accumulation or the evidence of a visual examination of the core by the collector, Kenneth Hunkins (written communication). As in the case of Figure 1, the deuterium-depleted layer was not present at the beginning of the winter accretion.

Samples recently secured by the submarine U.S.S. *Skate* during a summer voyage under the ice to the North Pole proves the existence of a surface layer in local ice-free areas that is depleted in deuterium at the two stations where surface (0.3 m) samples were taken. The data are given in Table 1. The water of approximately -7.4 per cent deuterium concentration at the surface will give ice of approximately -5.4 per cent upon freezing. This is in contrast to the water of -2.1 per cent encountered at 6 meters, which would give ice of approximately -0.0 per cent upon freezing.

In conclusion, we have demonstrated the existence of a relatively thin layer of deuterium-depleted water on parts of the surface of the Arctic Ocean during the summer. This layer is believed to form by the melting of snow, which is known to be highly depleted in deuterium, and the mixing of this melt water with sea water. Owing to vertical mixing, this layer may mix with the deep water and will often completely disappear before the Arctic winter begins. However, in some cases a deuterium-depleted layer apparently persists until winter, when it is incorporated into the bottom of the ice that has persisted over the summer, floating on this deuterium-depleted layer.

In leads and other areas of open water, this deuterium-depleted layer will freeze and will constitute a deuterium-depleted layer at the surface of the floe. However, the snow cover—in itself depleted in deuterium—will tend to obscure this feature during the winter. During

TABLE 1. Water samples collected by U.S.S. *Skate*, Summer, 1958

I.F. No.	Relative Deuterium Concentration, ‰	Position		Depth meters	Salinity, per mil
		Latitude	Longitude		
3044-15	-7.3	86°44'N	77°55'W	0.3	3.12
3044-16	-2.1	86°44'N	77°55'W	6	31.63
3044-17	-7.5	89°18.5'N	45°00'W	0.3	5.98

FRIEDMAN, SCHOEN, AND HARRIS

the following summer, melting of the surface may further obscure or remove this feature.

Acknowledgment. This research was financed in part by the U. S. Atomic Energy Commission, Division of Research, and by the U. S. Air Force Cambridge Research Center, Terrestrial Sciences Laboratory, Geophysics Research Directorate. We gratefully acknowledge the aid that we received from Mrs. Irene Browne Cotell of the latter Institution in arranging for the collection of ice core samples. A great debt is due the collectors of the ice samples who collected these cores under trying conditions and at no small personal risk.

REFERENCES

- Friedman, I., Deuterium content of natural water and other substances, *Geochim. et Cosmochim. Acta*, 4, 89-103, 1953.
- Friedman, I., and A. C. Redfield, Deuterium-hydrogen fractionation during freezing of water (abs.), *Internat. Geol. Cong.*, 20th, Mexico City, *Resúmenes de los trabajos presentados*, p. 214, 1956.
- Friedman, I., and A. H. Woodcock, Determination of deuterium-hydrogen ratios in Hawaiian waters, *Tellus*, 9, 553-556, 1957.

(Manuscript received March 10, 1961.)

Waves on the Arctic Ocean

K.L. Hunkins

Reprinted from the
JOURNAL OF GEOPHYSICAL RESEARCH,
Vol. 67, No. 6, pp. 2477-2489, 1962

Waves on the Arctic Ocean

KENNETH HUNKINS

*Lamont Geological Observatory, Columbia University
Palisades, New York*

Abstract. A continuous vertical oscillation of the ice of the Arctic Ocean has been observed at four U. S. drifting research stations. In the period range of 15 to 60 sec, the oscillations were detected with seismometers and gravity meters, and the displacement amplitudes were about $\frac{1}{2}$ mm at 30 sec. Amplitudes increase roughly as the square of the period. These oscillations are, in part at least, generated by wind action. In one case, oscillations in this period range have been identified as propagating waves. Theoretical dispersion curves for propagating flexural-gravity waves are presented. Oscillations in the 10- to 100-min period range were detected with a tide recorder operating at a grounded ice station, T-3, on the continental shelf, 130 km northwest of Point Barrow, Alaska. Displacement amplitudes were about 1 cm at a period of 30 min and were roughly proportional to period. The Arctic Ocean wave spectrum contrasts with that of other oceans. The spectral peak due to sea and swell is absent, and the present data indicate a monotonic increase in displacement amplitude as the periods range from about 0.1 to 60 sec in deep water or from about 0.1 sec to 100 min on the continental shelf.

Introduction. The ice cover of the Arctic Ocean is an exceptional boundary between air and ocean which has certain effects on wave motion. To the visual observer, it is evident that the sea and swell of open oceans are absent on the ice-covered Arctic Ocean. However, recent studies have shown that ice floes and ice islands are in nearly continuous oscillation, with amplitudes so small as to be detectable only with instruments. These oscillations are of particular interest for their bearing on the understanding of ocean wave generation and propagation in general.

Early observations of natural ice vibrations were reported by *Crary, Oliver, and Cotell* [1952], who made a series of landings on ice floes in the Beaufort Sea for geophysical studies. Using a gravity meter as a seismometer, they observed oscillations with a maximum vertical amplitude of about 0.05 cm in the period range of 5 to 40 sec. Later, an extensive series of gravity meter readings were made at Fletcher's ice island (T-3), a 60-m-thick section broken from an ice shelf [*Crary, 1956; Bushnell, 1959*]. On this drifting ice island similar oscillations were noted that had a maximum vertical motion in the 35- to 45-sec period range of 0.02

to 0.03 cm and a seasonal variation in both amplitude and period. The largest amplitudes occurred during the winter months, but the longest predominant periods occurred in the summer.

The present paper reports new investigations of natural vibrations at four floating ice stations: Alpha, Charlie, Fletcher's ice island, and Arlis II. The oscillations discussed here occur when the ocean is almost entirely covered with ice. Recording instruments used were a gravity meter, a long-period seismometer, and a tide gage. It is of interest that these three instruments were intended, respectively, for the study of gravity, earthquakes, and tides in the Arctic Ocean and that they yielded data on ice oscillations as an auxiliary result. Discussed here are (1) the spectral composition of this motion, (2) the relationship between amplitude and wind speed, and (3) the theory of long waves in a floating ice layer.

Waves with 15- to 60-sec periods. During 1957 and 1958, observations of ice motion were made with a gravity meter at drifting station Alpha, a floating ice research site maintained by the United States Air Force in cooperation with the United States National Committee of the International Geophysical Year. The drift track of the station is shown in Figure 1. Water depths are about 2 to 3 km along this track.

KENNETH HUNKINS

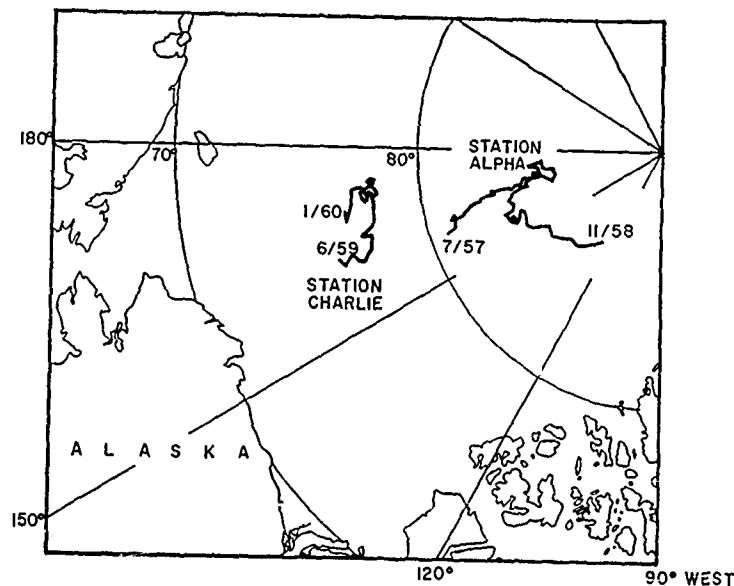


Fig. 1. Drift tracks of stations Alpha and Charlie in the Arctic Ocean.

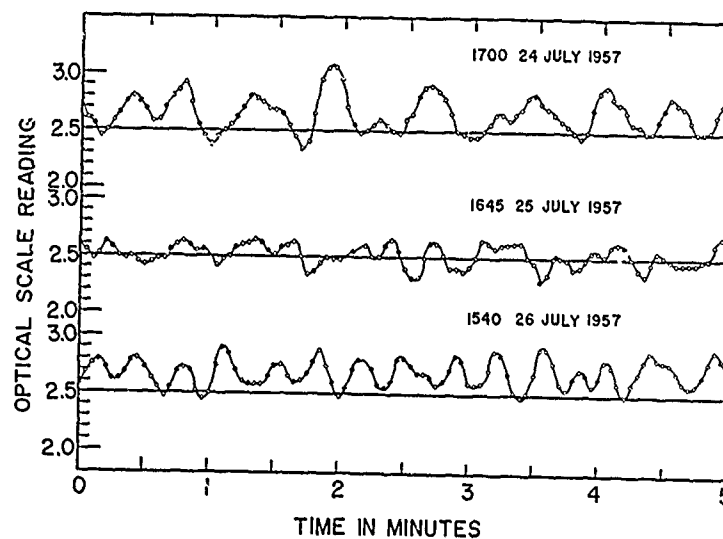


Fig. 2. Wave records taken with gravity meter at station Alpha in 1957. Dots indicate readings.

The Frost gravity meter, C-1-15, used at station Alpha, was nearly identical with the North American meter used at Fletcher's ice island. A horizontal boom is supported by a zero-length spring and enclosed in a double case with two thermostatically controlled sections. The boom is compensated for atmospheric pressure changes, and its position, magnified by an

optical lever, is viewed through an ocular. The practice was to read the boom position at 3-sec intervals for a period of 4 to 5 min. The sampling schedule was chosen to span nearly all the visually observable periods, so that the problem of 'aliasing' is small. The amplitudes were frequently great enough to cause the boom to strike the stops. It was possible to read the

WAVES ON THE ARCTIC OCEAN

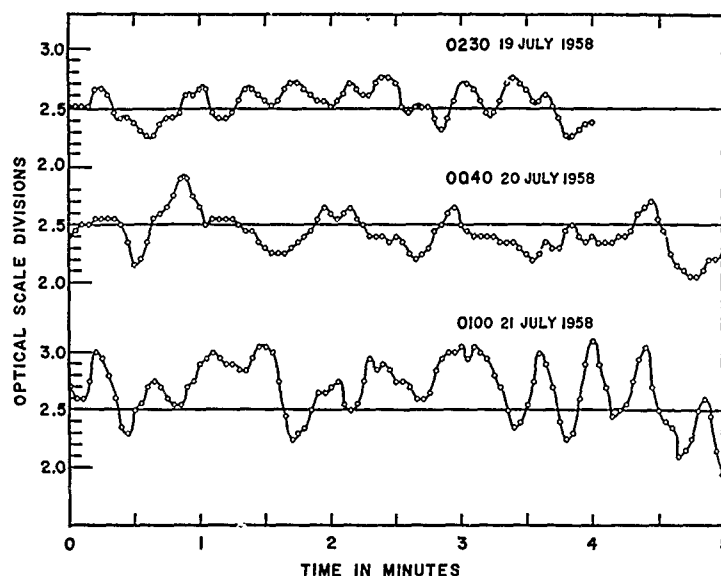


Fig. 3. Wave records taken with a gravity meter at station Alpha in 1958. Dots indicate readings.

TABLE 1. Wind Speeds at Station Alpha

Hour AST	Date	Wind Speed, m/sec
1330	7/24/57	2
1630	7/24/57	1
1930	7/24/57	3
1330	7/25/57	2
1630	7/25/57	3
1330	7/26/57	3
1630	7/26/57	4½
0100	7/19/58	1
0400	7/19/58	2
0100	7/20/58	1½
0400	7/20/58	2½
2200	7/20/58	2
0100	7/21/58	2½
0400	7/21/58	3

instrument only during periods of calm or of light winds when maximum ice amplitudes were about 0.04 cm in the 30-sec period range. This contrasts with conditions on Fletcher's ice island, where the amplitudes were rarely sufficient to cause the boom to strike the stops [Crary and Goldstein, 1957].

Six typical records from Alpha are shown in Figures 2 and 3, and the contemporaneous wind data are contained in Table 1. Numerical Fourier analyses of these records were made with an

IBM 650 computer. In preparation for analysis, linear drift was removed from the records with a ramp function, and the ends of the record were

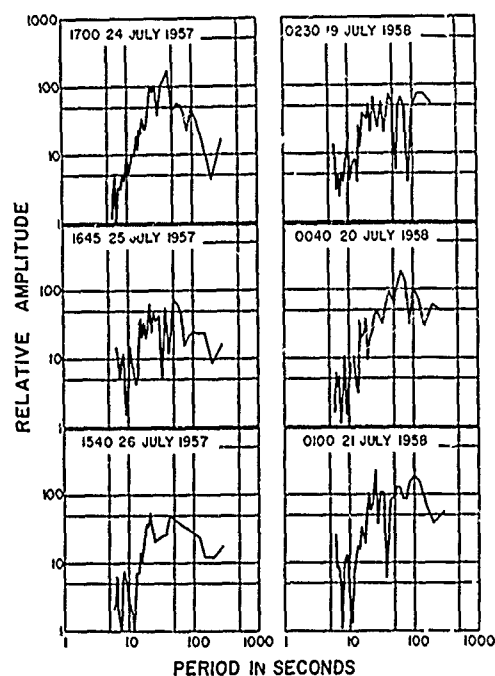


Fig. 4. Fourier spectra of records in Figures 2 and 3 plotted in terms of displacement. Log-log scale.

KENNETH HUNKINS

chosen as the points of first and last zero crossings. The uncorrected Fourier spectra are plotted in Figure 4, but it is necessary to examine these results in light of the instrument response. They were corrected for the displacement re-

sponse of the instrument (Fig. 5). This response curve was calculated on the basis of the 17-sec natural period and 0.70 critical damping of the gravity meter. The corrected Fourier spectra (Fig. 6) are plotted from periods of 6 sec out to periods equal to the record length (240 or 300 sec), but the central period range from about 15 to 60 sec is the most reliable. The reliability of the spectral amplitudes at the shortest periods is limited by the sampling interval, and at the longest periods by the record length. A general increase of displacement amplitude with increasing period is the most outstanding feature of all records. This increase in displacement amplitude corresponds to nearly constant acceleration. Superimposed on the general amplitude increase is a fine structure which does not show sufficient correspondence between records for a definite interpretation. It should be noted that station Alpha was situated on different ice floes in the years 1957 and 1958. In 1957 the floe was about $1\frac{1}{2}$ km wide and 3 km long, and in 1958, about 1×1 km. The thickness was approximately 3 m both years.

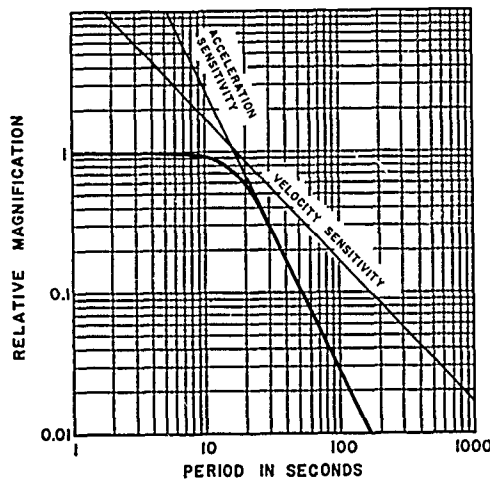


Fig. 5. Calculated response curves for Frost gravity meter. Log-log scale.

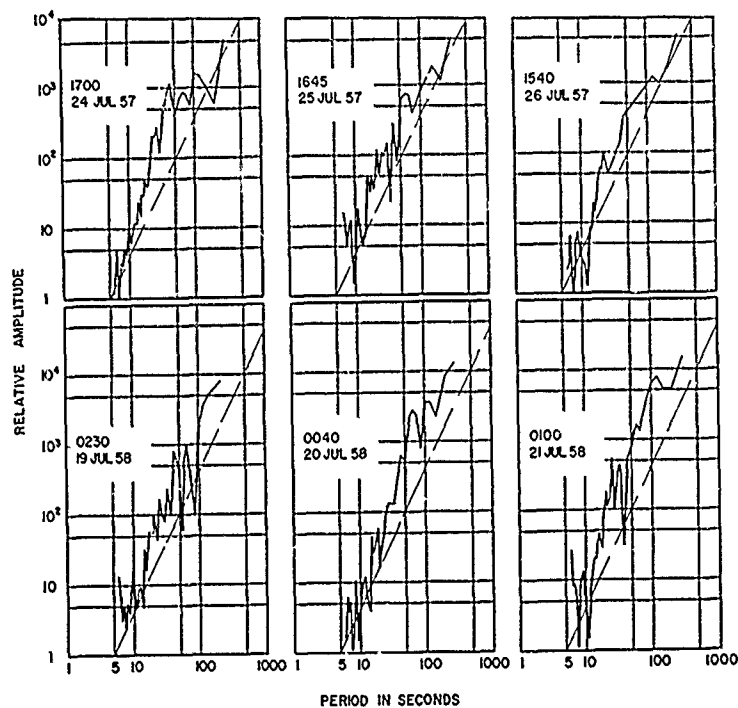


Fig. 6. Fourier spectra of records in Figures 2 and 3 plotted in terms of displacement. Dashed line is constant acceleration. Log-log scale.

WAVES ON THE ARCTIC OCEAN

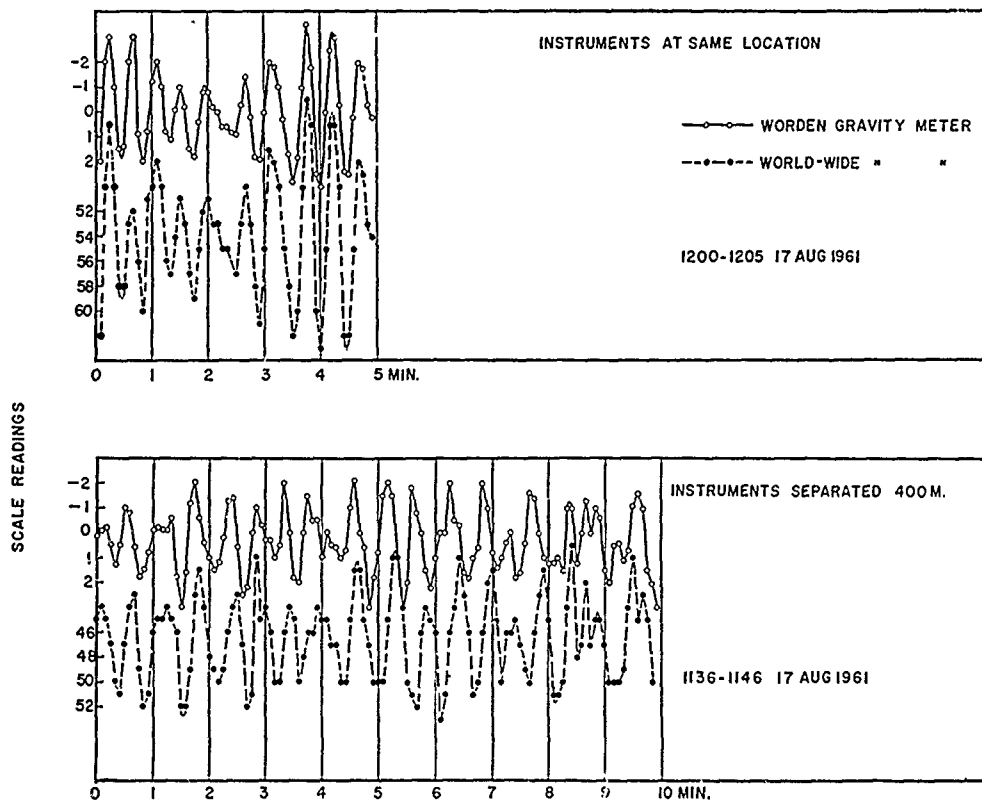


Fig. 7. Records taken with two gravity meters at ice island Arlis II. The upper records were taken simultaneously at the same location. The lower records were taken simultaneously with a 400-m instrument separation. Readings at 5-sec intervals are indicated with dots.

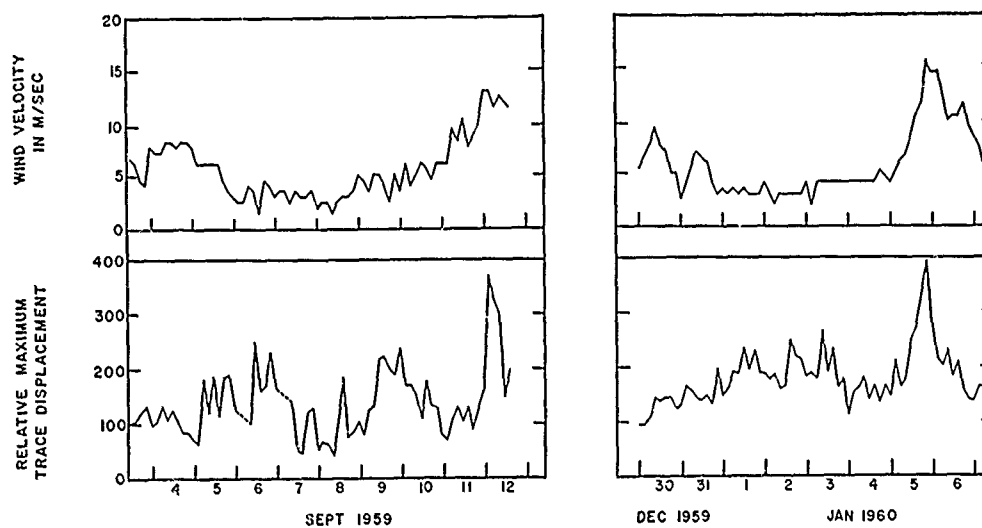


Fig. 8. Comparison of wind speed and peak-to-peak trace amplitude for long-period seismometer at station Charlie. Seismometer natural period is 10 sec for left diagram and 40 sec for right diagram.

KENNETH HUNKINS

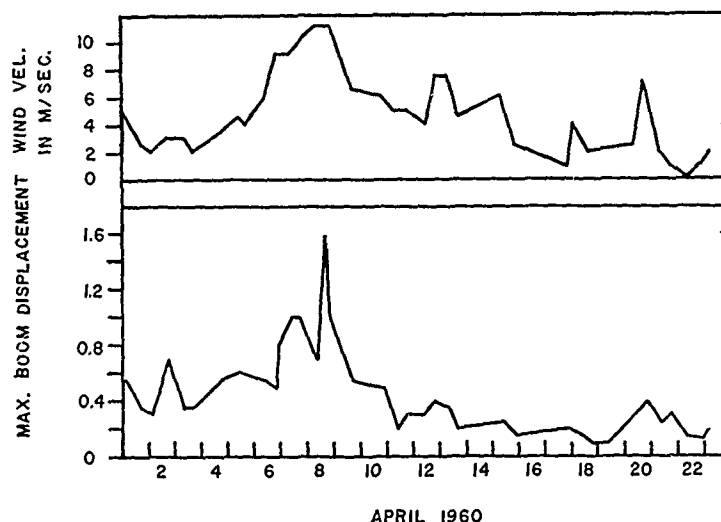


Fig. 9. Comparison of wind speed and wave amplitude at Fletcher's ice island. Peak-to-peak boom displacement in terms of optical scale divisions.

Oscillations similar to these were also recorded at ice island Arlis II, a floating research station operated by the Arctic Research Laboratory under support of the Office of Naval Research. The ice island dimensions were about $3\frac{1}{2} \times 3\frac{1}{2}$ km and 20 m in thickness. Arlis II was at $74^{\circ}33'N$, $162^{\circ}33'W$, at the time in 1500-m water depth. Two gravity meters, a World-Wide and a Worden model, were read simultaneously at two locations which were separated by an interval of 400 m (Fig. 7). The meters were about 300 m from the island edge, and the waves must have traversed only a small portion of island ice. Most of the records of peaks and troughs can be correlated over this distance, but they exhibit a phase difference between the locations. When the two meters are read simultaneously at the same location, no phase differences are observed. We are clearly observing progressive waves in this case. A Fourier analysis was made of the records in Figure 7, and the phase velocities between the two meters were determined. Velocities are 37.3 m/sec at a period of 40 sec, 30.5 m/sec at 36 sec, and 24.7 m/sec at 27.7 sec (Fig. 13). Since only two instruments were used, this is an apparent phase velocity and is an upper limit of the true phase velocity. Before the measurements were made, winds had been blowing in the direction of the line between the two instruments, from the Worden toward the

World-Wide meter, and the velocity measured may be close to the true phase velocity in this case.

Wave amplitude and wind speed. A long-period seismometer was operated at station Charlie, a drifting ice research station which traveled along the track in Figure 1 during 1959 and early 1960 [Cromie, 1961]. The station was located on an ice floe which originally measured 7×10 km and 3 m in thickness, but the area was considerably reduced during the drift. The U. S. Air Force supported the station as a contribution to the International Geophysical Cooperation-1959.

The seismometer, a Sprengnether long-period vertical instrument, was placed directly on the ice surface and enclosed in a protecting shelter. Seismometer output was filtered to remove high frequencies, electronically amplified, and recorded with a pen and ink oscillograph. The response of the instrument was peaked near the natural period, and variation in period is small on the records. Local wind speed and maximum peak-to-peak trace displacement are plotted in Figure 8 for two different intervals which included storms. The natural period of the seismometer was adjusted to 10 sec in one case and 40 sec in the other. Correlation between wind and oscillation amplitude is notable only during periods when winds exceed 10 or 12 m/sec. This is evidently a threshold wind

WAVES ON THE ARCTIC OCEAN

speed which is necessary for efficient excitation of the oscillations. It is also notable that surface waves from the earthquake on August 18, 1959, at Hebgen Lake, Montana, were recorded above the natural ice background with this instrument.

Gravity meter recordings at Fletcher's ice island in 1960 also show a similar type of correlation between wind speed and wave amplitude. At this time the island was drifting between $72^{\circ}11'N$, $154^{\circ}02'W$, and $71^{\circ}43'N$, $157^{\circ}27'W$. The maximum boom displacement found in a

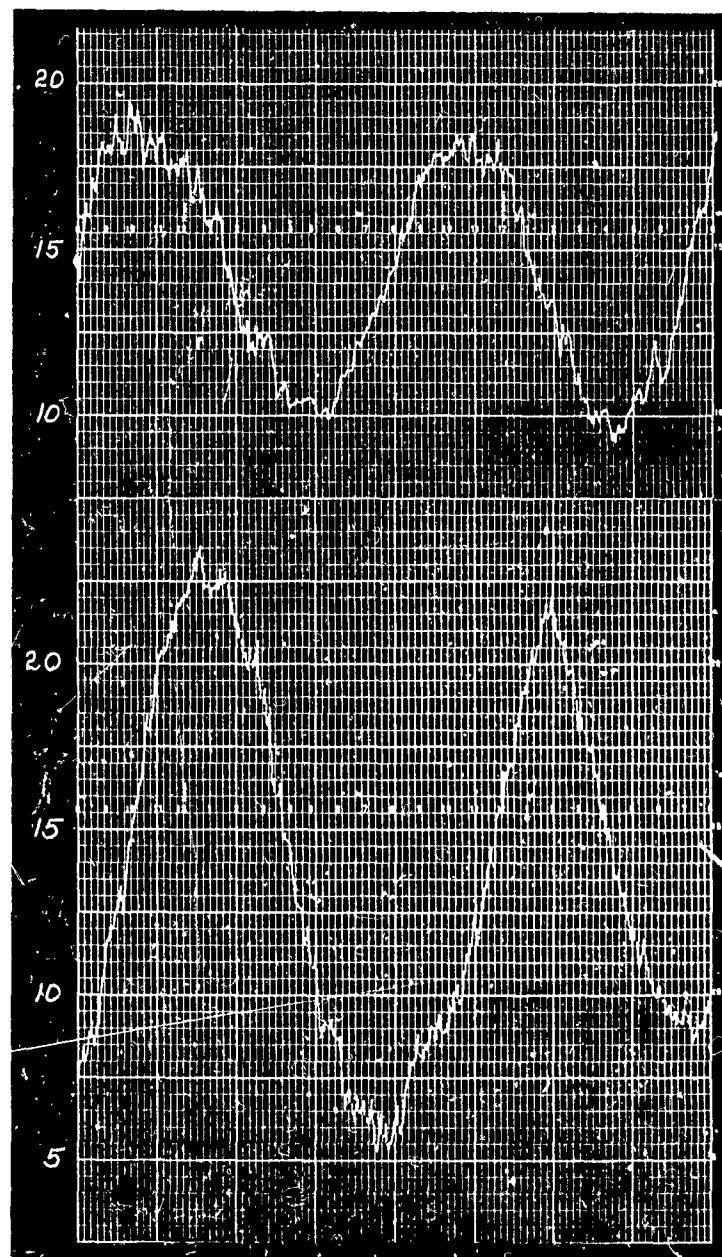


Fig. 10. Tide records at T-3 from 0800 AST 5/27/61 to 0800 AST 5/28/61 (top) and 0800 AST 5/16/61 to 0755 AST 5/17/61 (bottom). Amplitude scale in centimeters.

KENNETH HUNKINS

5-min interval versus local wind speed is shown in Figure 9. Again the correlation is most notable for higher wind speeds.

For high wind speeds, maximum amplitudes of ice oscillation show no marked tendency to lead wind speed maxima, indicating that the waves are generated at a relatively close distance. Only slight correlations are found between light local winds and the oscillations which accompany them. It is possible that the oscillations during periods of calm or light wind are generated in distant storm centers where wind speeds exceed the threshold value and then propagate to other areas of the ocean.

TABLE 2. Wind Speeds at Fletcher's Ice Island (T-3)

Hour AST	Date	Wind Speed, m/sec
0750	5/16/61	8
1050	5/16/61	10
1350	5/16/61	8
1650	5/16/61	11
1950	5/16/61	7
0750	5/17/61	8
0750	5/27/61	8
1050	5/27/61	10
1350	5/27/61	9
1650	5/27/61	10
1950	5/27/61	9

Waves with 10- to 100-min periods. Waves in a much longer period range were also observed at Fletcher's ice island, which became grounded in 1960 on the continental shelf at $71^{\circ}55'N$, $160^{\circ}20'W$, about 130 km northwest of Point Barrow, Alaska (Fig. 1). A tide gage was operated on 2-m-thick pack ice in Colby Bay, adjacent to the island. A cable was anchored to the bottom with a large weight in 37 m of water. The other end of the cable was led over the pulley of the tide gage and a small weight suspended from it. The records thus represent changes in ice level with respect to the ocean bottom. The chart drum was clock-driven at a rate of 8 inches per 24 hours. Trace displacement was equal to actual changes in ice level. The short-period resolutions of the instrument were limited to about 5 min by the chart speed and trace width.

Three general groups of water-level changes are revealed in the tide records (Fig. 10; wind data, Table 2). The tidal effects are the most evident, having a maximum amplitude of 18 cm at spring tide. Irregular water-level changes extending over several days are associated with atmospheric pressure and wind changes. This effect is not noticeable on the daily records in the illustration. Finally, there are 'short-period' waves ranging in period from 5 min to several hours and appearing as small fluctuations su-

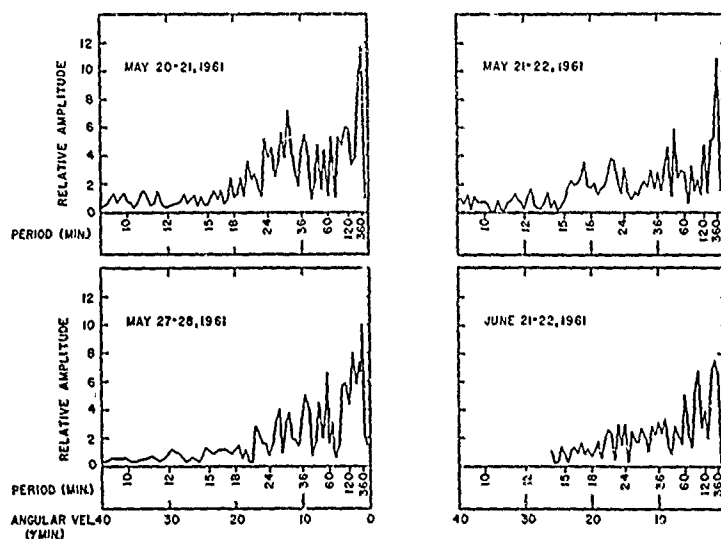


Fig. 11. Fourier analyses of four T-3 tide records. Waves of tidal period have been removed. Linear scale in angular velocity and in displacement.

WAVES ON THE ARCTIC OCEAN

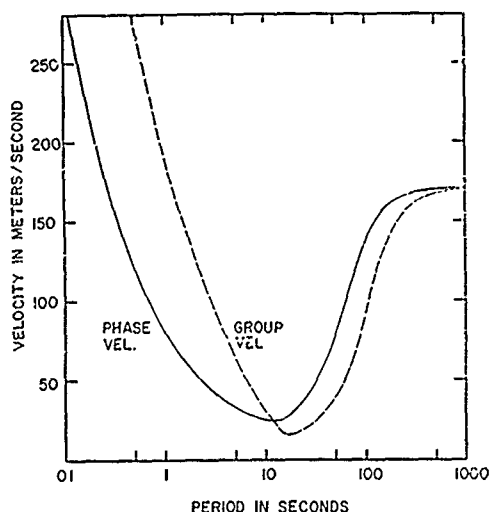


Fig. 12. Group and phase velocity dispersion for long waves in 3-m ice layer floating on water 3000 m deep. Semilog scale.

superimposed on the tides and on the long-period water-level changes. *Becl* [1957] also observed these three types of oscillations with a tide gage operated in a similar manner close to shore near Point Barrow. The advantage of the ice island installation is its location far from the influence of the irregular shoreline. The fact that tides were well recorded at the ice island gives evidence that the ice was responding faithfully to water-level changes. No differential movements between ice and water level were noted at the recording site.

The 'short-period' waves are of interest in this study; the tides and long fluctuations will be the subject of a later publication. A Fourier analysis of four daily tide records was made. The records were first converted to digital form with an instrument built for this purpose by Paul Pomeroy of Lamont Geological Observatory. The record is placed on a drum, and when the drum is set in rotation the record trace is followed manually with a lens and target which are free to move laterally. The position of the target is digitally encoded at periodic intervals by an encoder which operates on an IBM card punch. A series of three digit numbers proportional to trace amplitude are thus punched on IBM cards for further analysis. In each case a 24-hour record was analyzed with a drum speed and punching interval which

correspond to sampling at 52- or 53-sec intervals in real time. The remaining analysis was performed by Professor Yasuo Satô, using a program he devised for the IBM 7090 computer. The tides were removed from the digitized data by making a least squares fit of tidal components to the record, then synthesizing a tidal curve from these components. Five tidal components were used: M_2 (principal lunar, semidiurnal), S_2 (principal solar, semidiurnal), O_1 (principal lunar, diurnal), S_1 (solar, diurnal), N_2 (larger lunar elliptic, semidiurnal). The synthesized tide curve was then subtracted from the original data, leaving a residual curve. A Fourier integral analysis was then made of the residuals, and the results are plotted in Figure 11. The periods between 10 and 100 min are the most reliable section of these spectra. The most outstanding feature of the spectra is again a general increase of displacement amplitude with period in all cases. Superimposed on the general increase in this range is a fine structure which shows only a slight correspondence between records. Some of the increase with period may be due to tidal contamination, but this is not considered to be important since the tides have been largely removed. Also, waves with periods of up to 1 hour are clearly evident on the records.

The origin of these long waves is not yet well understood. This long-period wave background is present even on records made during almost complete calm. Such long-period waves on open continental shelves have been identified with seiches and with edge waves by various authors [Marmer, 1951; Munk, Snodgrass, and Carrier, 1956]. Seiches should be identifiable as peaks of corresponding period on the various records but are not evident in these spectra. It is possible that these very long waves originate in response to atmospheric pressure changes and then propagate from the source as edge waves or gravity waves; however, there is no assurance that this is so.

Waves with periods of several minutes, unlike the longer-period waves, are evidently generated by local wind action. Only tide records from periods of calm or light wind were Fourier analyzed, since storms produced irregular water level changes which would be difficult to eliminate. But it is evident from a visual examination of tide records made in storm periods that

KENNETH HUNKINS

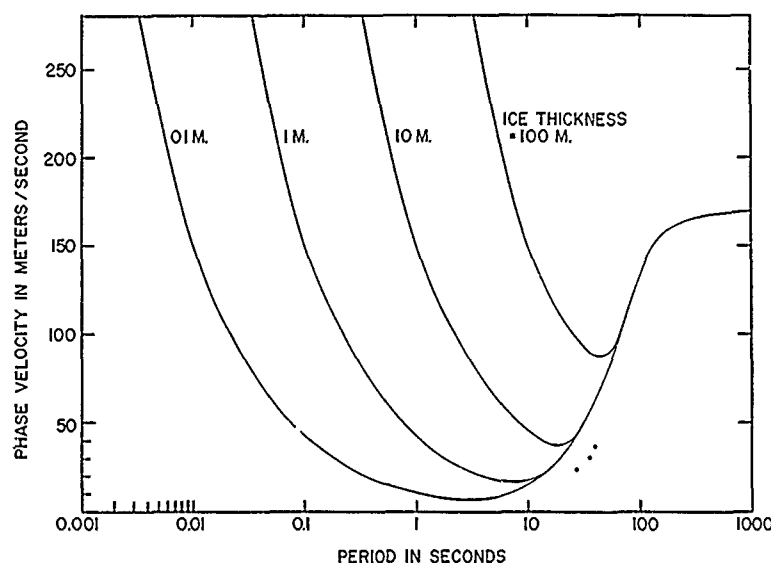


Fig. 13. Phase velocity dispersion for long waves in ice of various thicknesses floating on water 3000 m deep. Dots indicate apparent phase velocities measured at Arlis II. Semilog scale.

periods of the order of several minutes are enhanced by strong local wind.

Theoretical flexural-gravity waves. These observations of oscillations on the Arctic Ocean lead to the study of waves on a floating ice layer. Progressive waves are treated here, since records from Arlis II suggest that they may be the most important type. Long waves in a floating ice sheet under steady-state, plane-wave conditions were investigated by *Ewing and Crary* [1934]. They assumed an infinite, perfectly elastic ice sheet floating on a body of water having a plane, rigid bottom, and they included the effect of gravity in their calculations. For waves which are extremely long in comparison with ice thickness, their results reduce to the case of gravity waves on water. For short waves, the results apply to flexural vibrations and are valid down to a frequency of 20 cps when the ice sheet is 3 m thick [Hunkins, 1960]. These two wave types exhibit contrasting behavior. Deep water gravity waves are normally dispersed with a prograde orbital motion; flexural waves are inversely dispersed with an orbital motion which is retrograde at the ice surface and prograde at the ice-water interface.

The transition region between flexural and gravity waves was examined numerically using the period equation of Ewing and Crary which,

for infinitely deep water, may be written in the form

$$G\lambda^4 - D(c^2/\alpha)\lambda^3 - \rho^2\lambda^2 + F = 0$$

where

λ = wave length.

c = phase velocity.

ρ = ice density = 0.90 g/cm³.

ρ_1 = water density = 1.025 g/cm³.

h = ice thickness = 3 m.

g = acceleration due to gravity = 983 cm/sec².

$G = g\rho_1/4\pi^2h$.

$D = \rho_1/2\pi h$.

$F = \frac{1}{3}\pi^2h^2\rho V_p^2$.

$\alpha = (1 - c^2/V_w^2)^{1/2}$.

V_w = sound velocity in water = 1440 m/sec.

V_p = longitudinal plate velocity of ice = 2800 m/sec.

This is a quartic equation in λ , and it was solved in terms of λ for various assigned values of c . The other parameters were given the constant values listed above, which are representative of the Arctic Ocean [Hunkins, 1960].

The equation was solved on an IBM 650 computer with a program for quartic equations which yields all four roots, real or complex. For values of c greater than a certain minimum

WAVES ON THE ARCTIC OCEAN

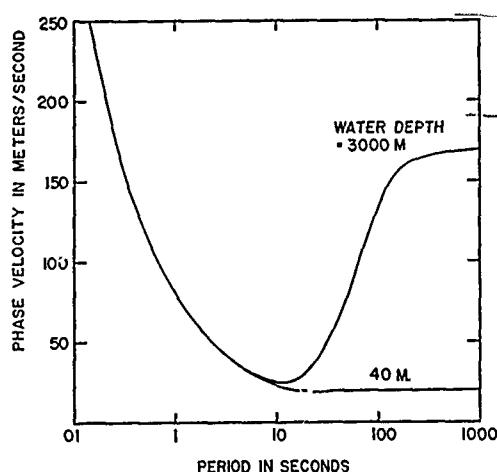


Fig. 14. Phase velocity dispersion for long waves in 3-m ice layer floating on water 3000 m and 40 m deep. Semilog scale.

value, the equation yields two real roots corresponding to the two types of wave motion, and the results are plotted in Figure 12 in terms of period, T . At very long wavelengths the assumption of infinite water depth causes the wave velocity to approach infinity. To correct this, the long-wave portion of the curve was calculated from the gravity wave formula,

$$c = \left(\frac{g\lambda}{2\pi} \tanh \frac{2\pi h}{\lambda} \right)^{1/2}$$

and added later.

The short-period flexural waves and the long-period gravity wave branches meet at a point of minimum phase velocity, $c = 22$ m/sec and $T = 12$ sec. Group velocity was derived graphically and has a minimum at $c = 15$ m/sec and $T = 16$ sec. The velocity minimum in this case is analogous to that for surface waves on water where a minimum occurs between the capillary and gravity wave branches. The ice layer and the layer of surface tension both act to produce inverse dispersion at short wavelengths. It is to be noted that the phase-velocity minimum in this type of dispersion corresponds to the minimum wind speed capable of producing simple resonant coupling between the atmosphere and the ocean.

Some of the constant parameters in the previous calculation may vary under natural conditions, particularly ice thickness and water depth. Changes in ice thickness alter the flex-

ural wave branch of the dispersion curve, the velocity minimum occurring at progressively higher velocities and longer periods as ice thickness increases (Fig. 13). Changes in water depth alter the gravity wave branch if ice thickness remains constant (Fig. 14). Dispersion in water 40 m deep is compared with the 3000-m depth of Figure 12. The velocity minimum virtually disappears in shallow water, and the flexural wave branch joins the shallow water gravity wave branch of constant velocity.

Standing waves on individual ice floes or ice islands may also occur. They should be identifiable as a series of sharp spectral peaks corresponding to the various modes. Although such a series is not evident in the present data, mention may be made of two possible types of standing waves. The simplest type is the bobbing of ice under the influence of gravity and buoyancy alone. The period of the oscillation, T , is given by

$$T = 2\pi(h\rho/g\rho_i)^{1/2}$$

and, using the previous constants, the value is 3.25 sec for ice 3 m thick and 14.55 for ice 60 m thick. The damping effect of the water will modify these periods under actual conditions and the system may be overdamped. Flexural standing waves on an ice floe or ice island may exist in analogy with the flexural vibrations of a free elastic plate.

Discussion. Observations with various recording instruments on different ice floes and ice islands in the Arctic Ocean all indicate that the ice oscillates almost continually. Some properties of these oscillations have been determined. On the ice floes of station Alpha, the displacement amplitudes of these oscillations generally increase with period in the range of 15 to 60 sec. The amplitudes increase from a fraction of a millimeter to several millimeters, roughly in proportion to the square of the period. On the ice island Arlis II, oscillations in this period range have been identified as propagating waves. Although only apparent phase velocities were determined, the values show fair agreement with the gravity wave branch of the theoretical flexural gravity-wave dispersion. These oscillations are at least partially generated by wind action. The fact that the local wind speed must reach a threshold value of 10 or 12 m/sec before large amplitudes are developed suggests

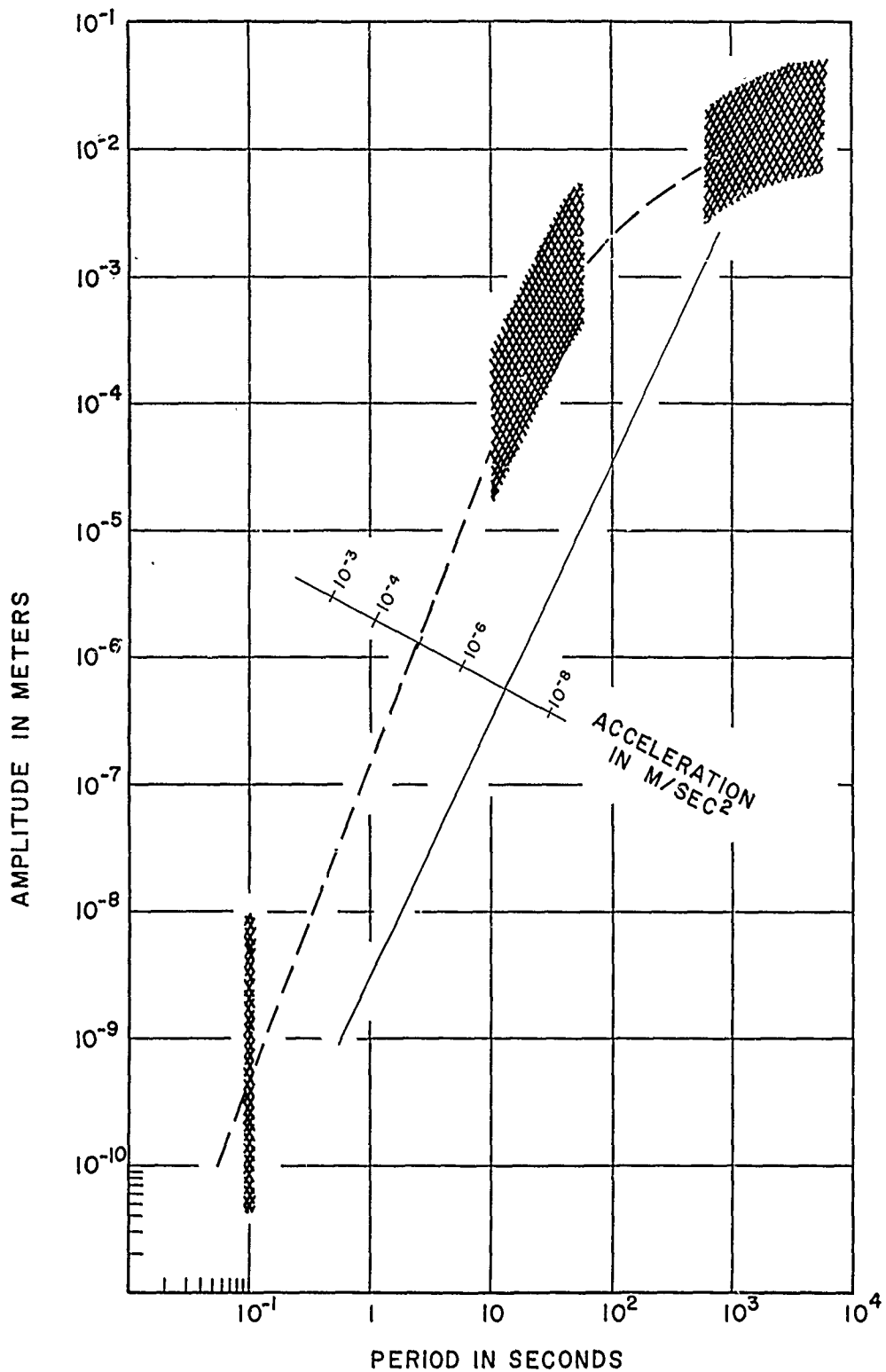


Fig. 15. Generalized spectrum of wave amplitudes on the Arctic Ocean. Crosshatching indicates observed period ranges with approximate limits of variation under average conditions. Dashed lines are interpolations. Log-log scale.

WAVES ON THE ARCTIC OCEAN

that some form of resonant coupling may be the method of excitation.

There is evidence that the general amplitude-period relationship found for 15- to 60-sec waves extends to very short periods. Observations of vertical oscillations of pack ice in the period range of 5 to 200 cps with exploration seismograph systems indicate that the general background is about the same as that on land. According to Brune and Oliver [1959], average displacement amplitudes of background motion on land are about 2 $m\mu$ at 5 cps and decrease with increasing frequency.

Another group of oscillations has been recorded in the period range of 10 to 100 min, but so far they have been observed only on the continental shelf in the Arctic Ocean. Amplitudes are in the centimeter range and increase slightly with period.

The Arctic Ocean spectra differ from those of other oceans. On an open ocean the typical wave spectrum is distinguished by an amplitude peak in the period range of 5 to 20 sec. This is the region of sea and swell which propagates as gravity waves [Roll, 1957]. On the ice-covered Arctic Ocean amplitudes in this range are small; sea and swell are effectively prohibited by the ice layer. A tentative diagram of the typical Arctic Ocean spectrum based on the results presented here is sketched in Figure 15. Large gaps exist and the known sections need to be verified at many more locations, but the broad features of a pattern can be seen.

Acknowledgments. This study was supported by the Geophysics Research Directorate of the Air Force Cambridge Research Laboratories, Office of Aerospace Research, and by the Office of Naval Research as a part of the Advanced Research Projects Agency project Vela. I am indebted to those who assisted in collecting the data. Arnold Hansen, Bryan Isaacs, William Cromie, Gerry Cabaniss, David Craven, Stephen den Hartog, and Henry Kutschale were particularly helpful. The Air Force

commanders and their men at the various stations provided assistance without which this study could not have been completed. Dr. Mark Landisman made available his Fourier analysis program for the IBM 650 computer. Dr. John Kuo made available his computer program for the solution of quartic equations. Prof. Yasuo Satô analyzed the tide records with his special program for this purpose. Profs. Maurice Ewing and Jack Oliver provided helpful criticism and encouragement.

REFERENCES

- Beal, M. A., Barrow Sea valley study and tide gauge installations, *AINA final rept., Scripps Inst. Oceanog., Ref. 67-38*, 1957.
- Brune, J., and J. Oliver, The seismic noise of the earth's surface, *Bull. Seism. Soc. Am.*, **49**, 349-353, 1959.
- Bushnell, V., ed., Scientific studies at Fletcher's ice island, T-3, 1952-1955, vol. 1, *Geophys. Research Paper 63*, Geophysics Research Directorate, Air Force Cambridge Research Laboratories, Bedford, Mass., pp. 183-219, 1959.
- Crary, A. P., Arctic ice island research, in *Advances in Geophysics*, **3**, Academic Press, New York, 1956.
- Crary, A. P., R. D. Cotell, and J. Oliver, Geophysical studies in the Beaufort Sea, 1951, *Trans. Am. Geophys. Union*, **33**, 211-216, 1952.
- Crary, A. P., and N. Goldstein, Geophysical studies in the Arctic Ocean, *Deep-Sea Research*, **4**, 185-201, 1957.
- Cromie, W. J., Preliminary results of investigations on arctic drift station Charlie, in *Geology of the Arctic*, University of Toronto Press, pp. 690-708, 1961.
- Ewing, M., and A. P. Crary, Propagation of elastic waves in ice, **2**, *Physics*, **6**, 181-184, 1934.
- Hunkins, K., Seismic studies of sea ice, *J. Geophys. Research*, **65**, 3459-3472, 1960.
- Manner, H. A., Tidal datum planes, *USC&GS Spec. Publ. 135*, U. S. Dept. of Commerce, Washington, 1951.
- Munk, W., F. Snodgrass, and G. Carrier, Edge waves on the continental shelf, *Science*, **123**, 127-132, 1956.
- Roll, H. U., Oberflächen-Wellen des Meeres, *En cycl. Physics*, **48**, Springer-Verlag, Berlin, pp. 671-733, 1957.

(Manuscript received March 2, 1962.)

Seismic Studies of the Arctic Ocean Floor

K.L. Hunkins

Reprinted from the
GEOLOGY OF THE ARCTIC,
Vol. 1, pp. 645-665, 1961

Seismic Studies of the Arctic Ocean Floor¹

KENNETH HUNKINS

ABSTRACT

Reflection and refraction seismic measurements from drifting station Alpha in the Arctic Ocean revealed details of a prominent submarine rise, called the Alpha Rise. This rise trends across the Arctic Ocean subparallel to the Lomonosov Ridge. The minimum depth sounded in its central portion was 1426 m at 85°03' N and 171°00' W. The rise descends to depths of over 3000 m to the north and south. Sub-bottom reflections revealed a characteristic echo from a depth of several hundred metres below the ocean floor in the eastern area of the rise. This reflection was not pronounced in the western area. The eastern area also had a rougher bottom texture than the western area.

Several short unreversed refraction profiles were made. Dips and strikes of the ocean floor from reflection records aided interpretation. An average of three measurements showed the upper "unconsolidated" layer to be 0.38 km thick. One profile revealed a 2.80 km thick layer of 4.70 km/sec velocity. Below this lay the "oceanic" layer with a velocity of 6.44 km/sec and an undetermined thickness.

REFLECTION AND REFRACTION seismic techniques were used to study the Arctic Ocean floor from drifting station Alpha during the International Geophysical Year. Reflection measurements were made on a daily schedule from July 1957 to November 1958. Refraction measurements were made during the summer of 1958. The station drifted along an irregular track in the North Canadian Basin under the influence of ocean currents and wind (Figure 1). The track lies in the area between 83° to 86° N and 115° to 175° W. Position of the station was determined daily by astronomic fixes when cloud conditions permitted. Location was determined to better than one-half mile in most cases. The bathymetry of the Arctic Ocean in this area, the various types of sub-bottom reflections, and the refraction studies of the sediments are discussed in this paper.

This paper is condensed from a thesis submitted to Stanford University in partial fulfillment of the requirements for a Ph.D. degree. The work was carried out under Contract No. AF 19 (604)-2030 from the Geophysical Research Directorate of Air Force Cambridge Research Center. Assistance in the field work was provided by Maurice Davidson, Franz van der Hoeven, Gary Latham, and Bryan Isaacs, all of Lamont Geological Observatory. Other scientists and Air Force personnel as well as the Air Force station commanders gave valuable co-operation and assistance. Discussions with Dr. Jack Oliver, director of the Arctic geophysics project at Lamont, were invaluable in analysing and interpreting the results.

INSTRUMENTATION

The recording instrument for all the work was a Houston Technical Laboratory 7000-B seismograph with twelve amplifiers. The signals from an array of twelve geophones were recorded photographically on dual channels. The upper twelve

¹Lamont Geological Observatory (Columbia University) contribution no. 489.

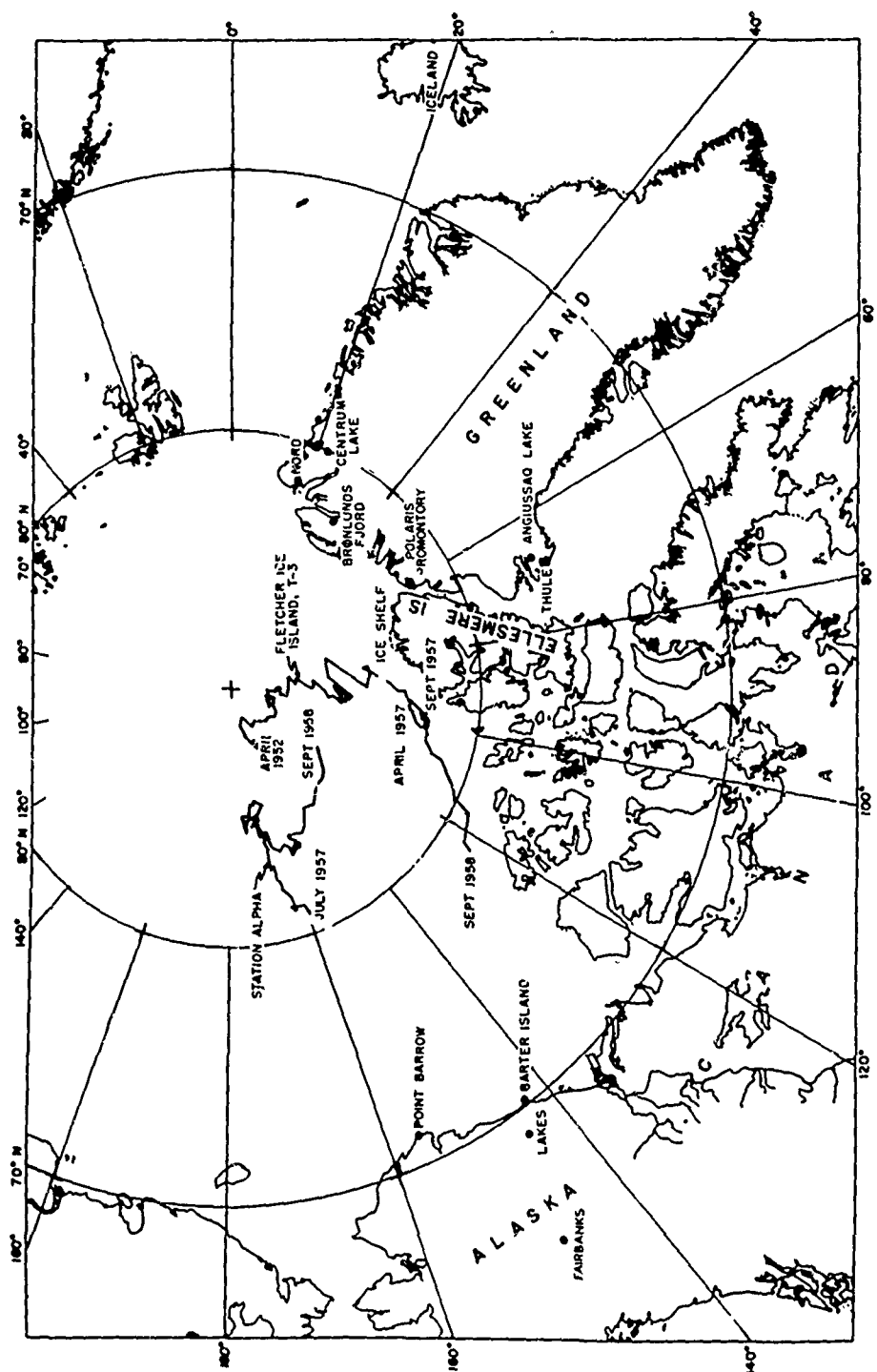
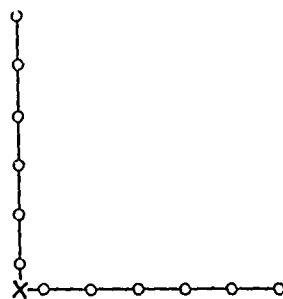


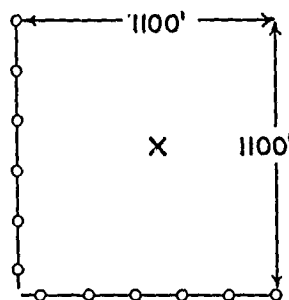
FIGURE 1. Track of drifting station Alpha in the Arctic Ocean (after Irene Browne Cotell).

KENNETH HUNKINS

traces on the record were at high gain. The lower twelve traces duplicated the upper set at one-half the amplitude. Three paper speeds were available: 6.6, 13, or 32.4 inches per sec. The amplifier response was relatively flat from 5 to 500 cycles per sec. The camera and amplifiers were operated in the laboratory hut and connected to the geophones outside by cable. Electro-tech model EVS-2B vertical geophones with a natural frequency of 14 cycles per sec. and 0.53 critical damping were used. They were placed firmly on the ice surface. A right-angle array was used with six geophones on each line. For reflection work, two different shot positions with respect to the array were used (Figure 2). The change from the first to second arrangement was made in May 1958 when the camp had to be moved to a new ice flow. The second shooting arrangement allowed reflection computations to be made more easily. True orientation of the array was determined from the daily astronomic shots. The timing tuning fork was checked periodically against



JULY 1957 - MAY 1958



MAY 1958 - NOVEMBER 1958

○ GEOPHONE

X SHOT POINT

FIGURE 2. Arrangement of geophone spreads.

ARCTIC OCEAN BASIN

a chronometer which had been rated against WWV radio time signals. During all shooting, the camp electrical generators were shut down to prevent mechanical and electrical noise pickup.

REFLECTION STUDIES

Vertical reflection soundings were made daily during the winter and twice daily during the summer. As the average drift of the floe was three-and-one-half miles per day, these soundings were usually spaced from one to four miles apart along an irregular track. Unusual calm or windy periods resulted in closer or wider spacing. The sounding positions were interpolated between astronomic fixes and were in most cases accurate to one-half mile. During periods of persistent cloud cover several days passed between fixes and the accuracy of the sounding position dropped to one or two miles.

For the reflection shots, one-quarter-pound charges of dynamite were exploded at a depth of ten feet below the water surface. Firing was done electrically and the cap break was recorded. A short pulse blaster insured that the cap did not fire late. The delay between the electrical impulse and the cap detonation was found to be 0.0025 sec. Correction was made in the computations for this delay. The recording

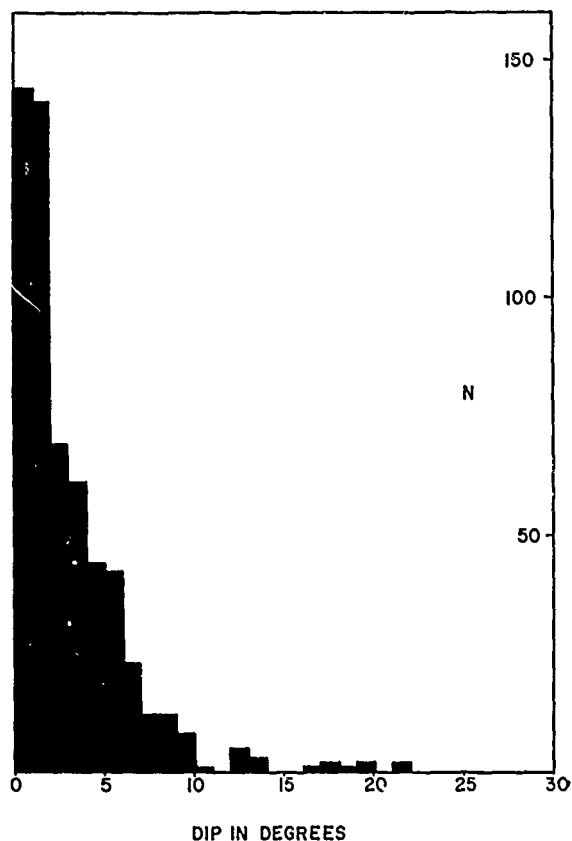


FIGURE 3. Frequency distribution of measured ocean bottom dips.

KENNETH HUNKINS

paper was run at a speed of 13 inches per sec for the early part of the record. After about two seconds, the speed was manually increased to 32.4 inches per sec in time to record the reflections at high speed. This method conserved photographic paper but gave fine detail in the reflection portion of the record. Two sounding records were usually made in quick succession, the first with automatic gain control and the second with linear amplification.

Bottom Reflections

The array of geophones allowed the dip and strike as well as the depth of the bottom to be found. A total of 623 sonic soundings were made and, of these, 555 yielded dip and strike information. Calculation of the dip and strike was made using standard formulas (Nettleton, 1940). Straight-line ray paths were assumed. The measured dips and strikes represented the attitude of a portion of the ocean floor one-half the length of the spread on each side, that is, $500' \times 500'$. Dip of the bottom ranged from 0° to 22° . The average dip was 2.70° with a standard deviation of 2.25° . The frequency distribution (Figure 3) showed that most dips lay between $\frac{1}{2}^\circ$ and $1\frac{1}{2}^\circ$. The depths represented the slant distance to the nearest reflector and are accurate to less than one m. Sound velocity corrections to the depth measurements were made with Matthew's tables (1939). Wire soundings taken at Station Alpha are in close agreement with the sonic soundings.

Paper speeds were high enough to permit determination of the initial trace motion for reflections. All bottom reflections observed were compressional or positive; they appear to indicate in all cases that the characteristic impedance (density \times sound velocity) of the topmost sediment is greater than that of water. The frequency of the first bottom reflection is roughly 400 cycles per second, measured peak to peak on the record. Thus the wavelength in water is about three-and-one-half m. If any sediment layer with an impedance less than water exists, it probably has a thickness less than about four m.

During its occupation, drifting station Alpha sailed over a submarine feature which has been named the Alpha Rise after the station. At the beginning of operations, the station was immediately south of the rise in over 3000 m of water. The maximum depth recorded was 3671 m at $82^\circ 48' \text{ N}$ and $167^\circ 01' \text{ W}$. The northward movement carried the station over the rise at almost right-angles to its trend. After a northernmost point of $85^\circ 32' \text{ N}$ and $171^\circ 10' \text{ W}$ was reached, the station moved southward nearly retracing its previous track. The station then turned northeastward and moved nearly along the trend of the rise. Near the end of the occupation of the station the shallowest depth of 1140 m was recorded on the eastern end of the rise at $86^\circ 09' \text{ N}$ and $114^\circ 08' \text{ W}$.

The drift of station Alpha provided detailed bathymetry for several areas of the rise (Figure 4). The bathymetric chart was contoured with the aid of dips, strikes, and depth information. The broad outline of the Alpha Rise was known previously from the drift of Russian station NP-4 and from soundings of the High Latitude Aerial Expeditions (bathymetric chart of the Arctic Ocean, as of 1956 approx.; Hope, 1959). It trends northeast-southwest across the Arctic Ocean from the edge of the shelf north of Wrangel Island to the shelf off Ellesmere and Axel Heiberg islands. The Alpha Rise is subparallel to the Lomonosov Ridge and is twice as

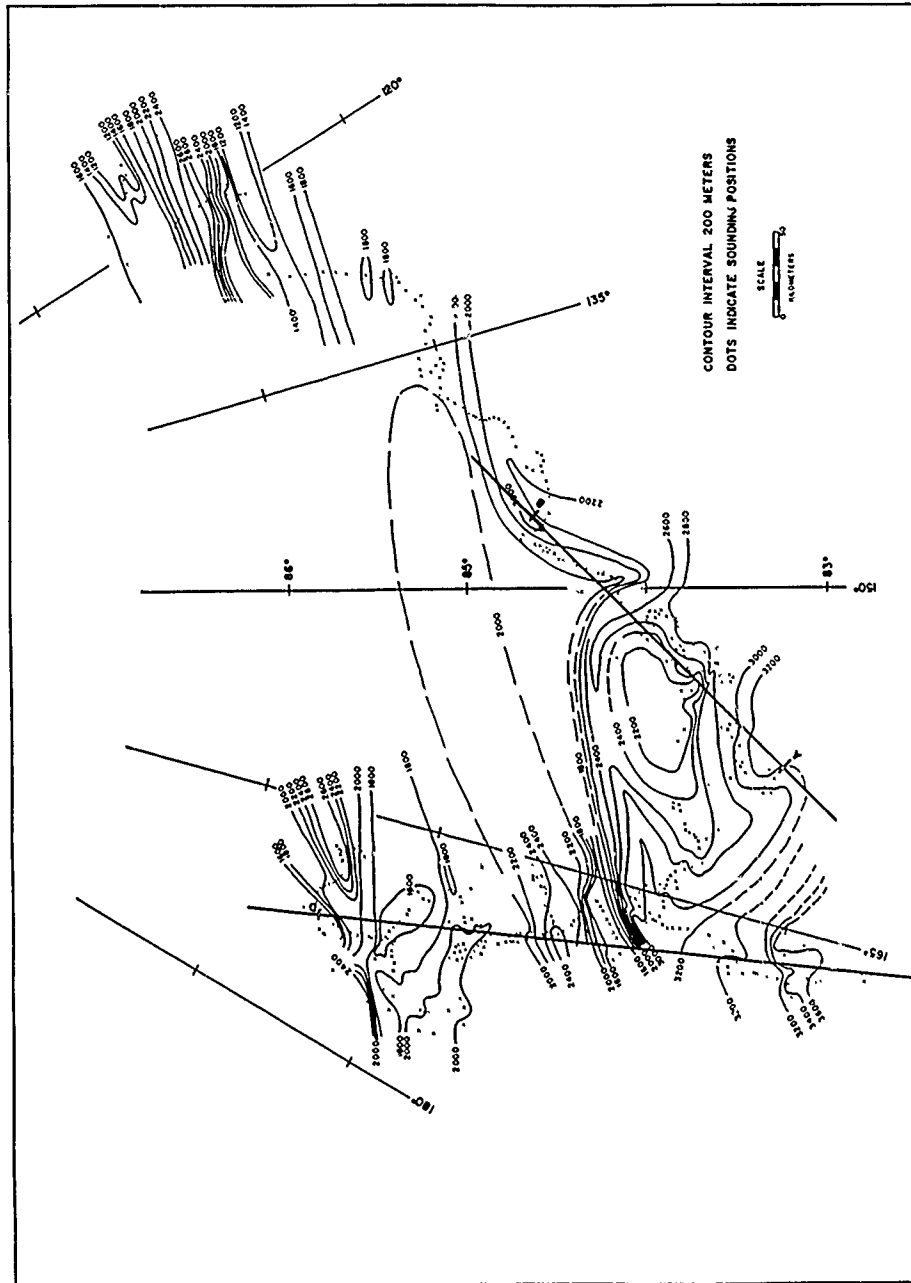


FIGURE 4. Bathymetric chart of the Arctic Ocean along the track of drifting station Alpha

KENNETH HUNKINS

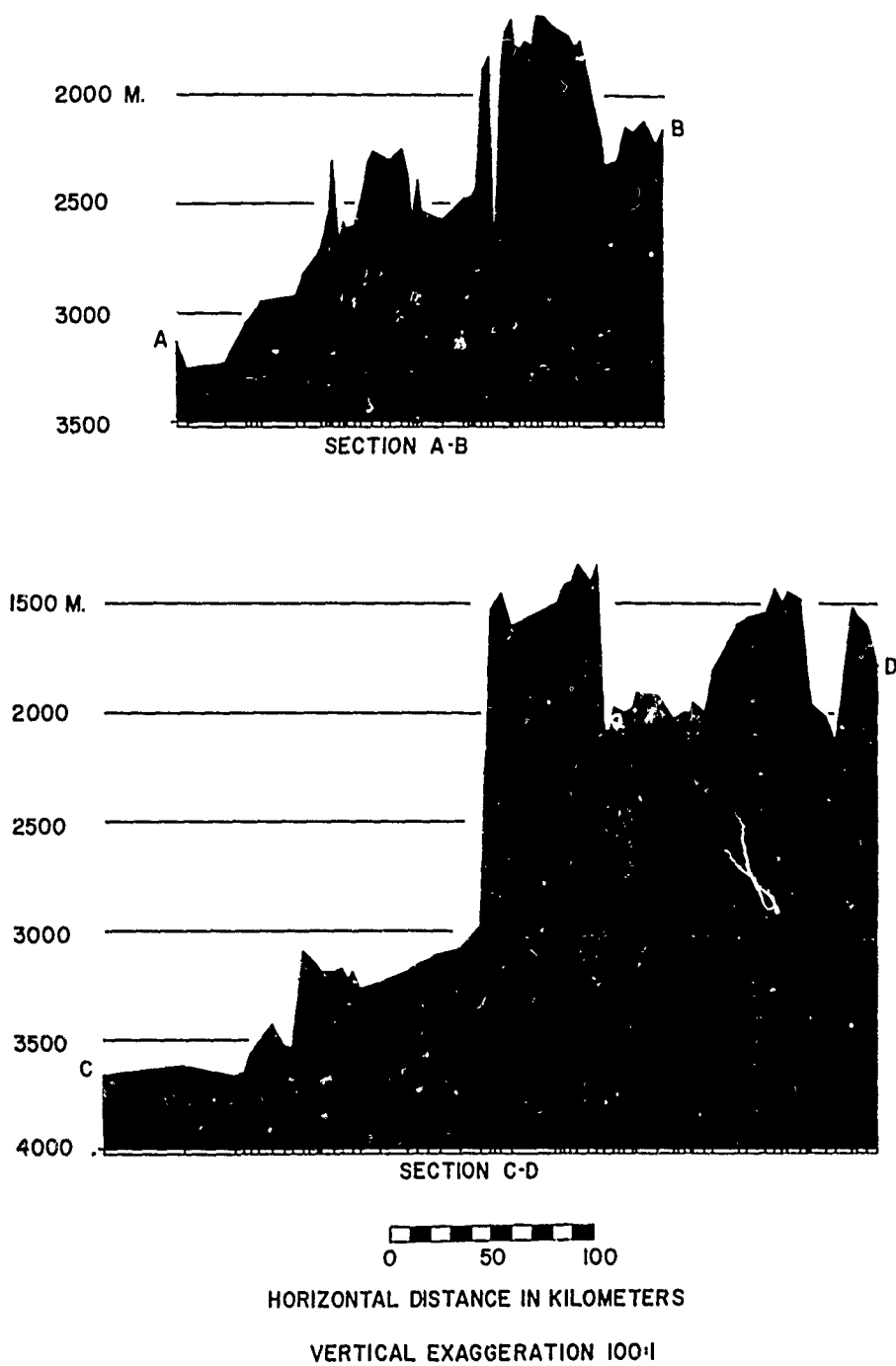


FIGURE 5. Bathymetric profiles across the Alpha Rise.

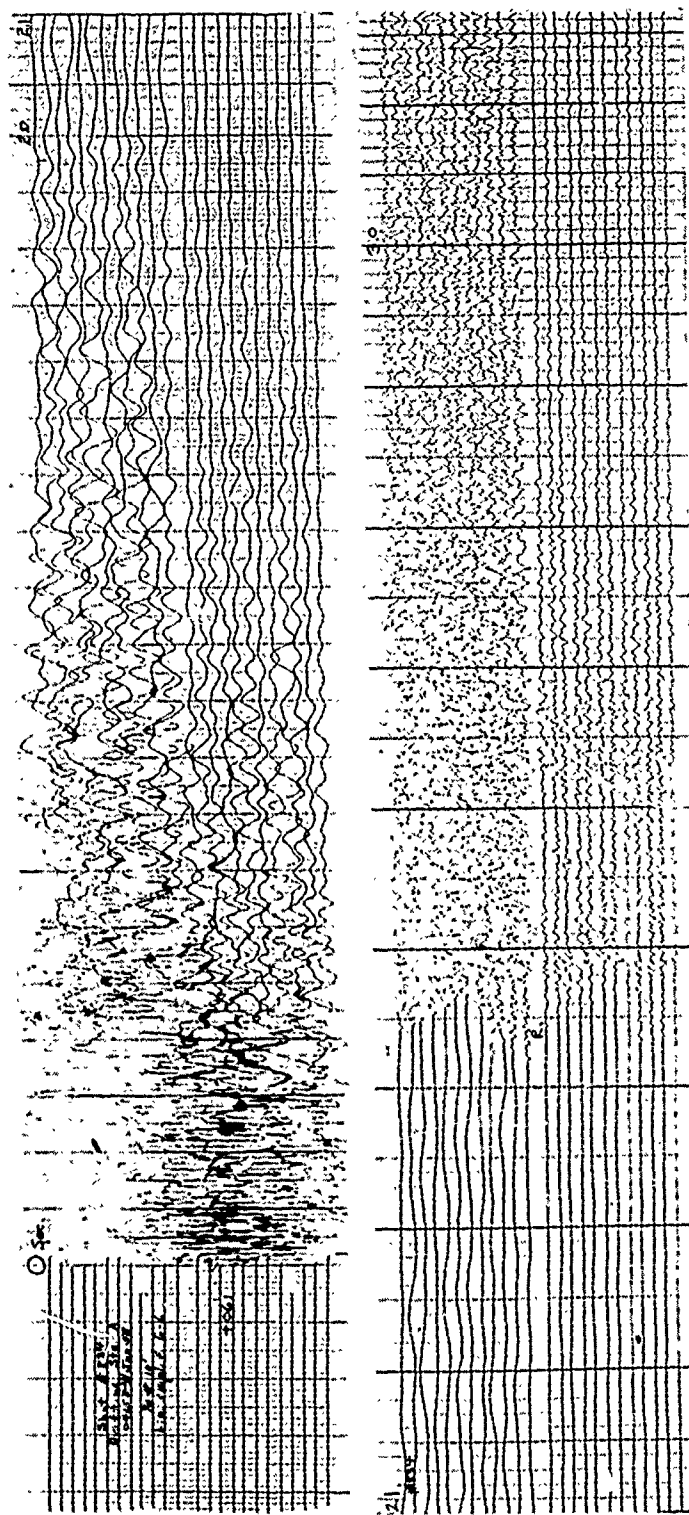


FIGURE 6. Type R-T reflection record. $84^{\circ}11.9' \text{ N}$, $149^{\circ}26' \text{ W}$, 2356 m. Linear amplification. No filters.

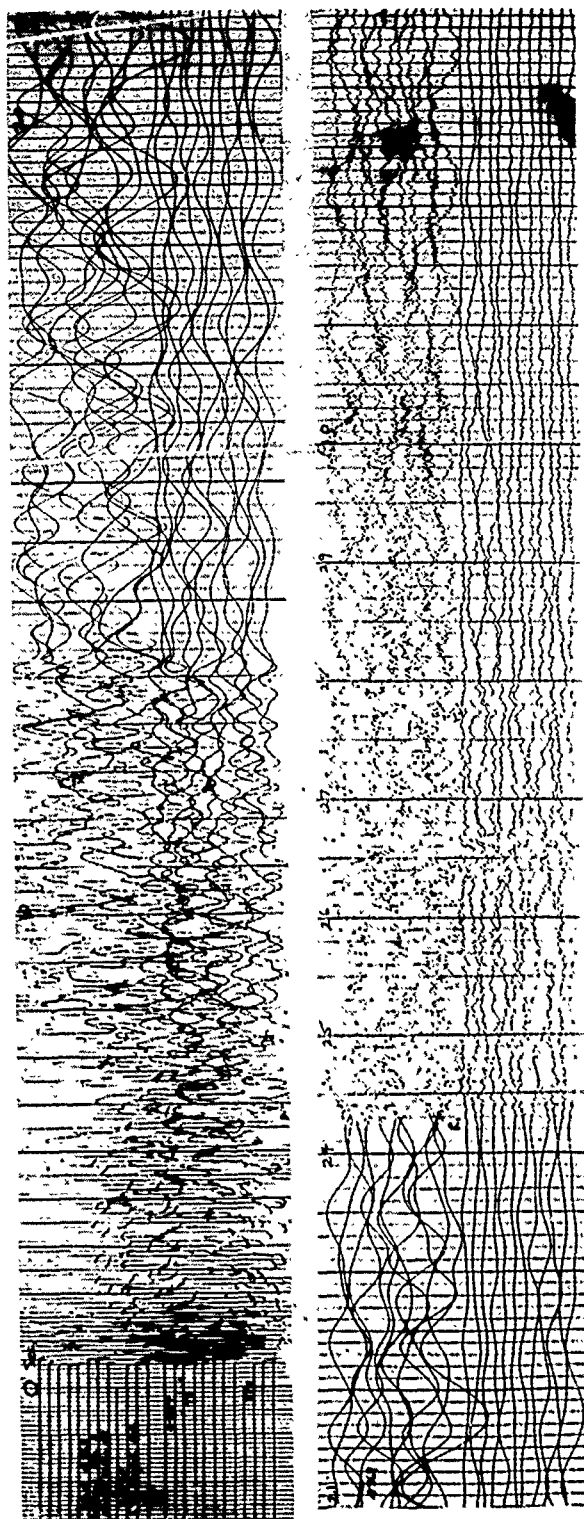


FIGURE 7. Type M-T reflection record. 84°32' N, 147°53' W, 1781 m. *M*-reflection is at 225 m (*r*). Bubble pulse reflection at *r*. Linear amplification. No filters.

ARCTIC OCEAN BASIN

broad as that feature, or about 200 km wide. It is shallower than current maps indicate. A minimum sounding over the central portion of the rise was 1426 m at $85^{\circ}03' \text{ N}$ and $171^{\circ}00' \text{ W}$. To the north and south of it lie basins with depths over 3000 m. The dip information and bathymetric profiles show that the topography of the rise is rugged (Figure 5). The profiles strongly suggest that this is an area of fault block mountains. The Alpha Rise is not tectonically active at the present time because it lies in an aseismic area of the Arctic Ocean (Gutenberg and Richter, 1954).

Topographic Echoes and Sub-bottom Reflections

Several bottom echoes or topographic echoes are present on many records. They occur in areas of rugged topography where several reflectors return echoes from different locations (Figure 6). Characteristically, the first reflection is low in amplitude and shows steep dip because it comes from a topographically elevated area having little reflective area. The principal bottom echo arrives shortly after and is of greater amplitude and flatter dip. The topographic echoes can be identified by their high frequency content. Sub-bottom echoes suffer high frequency attenuation in the sediments and have a lower frequency composition.

Sub-bottom reflections are present on the majority of the reflection records. They occur as lower frequency events after the bottom reflection. The quality of these reflections was high, good reflections being obtained with linear amplification and no filtering (Figure 7). The level, stable ice floe, lack of background noise, and low attenuation of sound in water all contributed to the good reflection quality.

No confusion between sub-bottom reflections and second bottom reflections was encountered because the water was deep enough so that the second bottom reflection arrived after the deepest sub-bottom reflection. However, bubble pulses produced some undesired complications in the records. The reflection shots produced a bubble pulse which appeared at 0.09 to 0.11 sec after the main explosion. This pulse produces a duplication of sub-bottom echoes but allowance was made for this when interpreting the records.

The records were classified by a system similar to that used by Hersey and Ewing (1949). Records with multiples bottom echoes or topographic reflections are of Type T. Those showing only one strong sub-bottom reflection, or possibly several weak reflections and one strong reflection, are type M. The type M reflection frequency is usually 50 to 100 cycles per sec measured peak to peak on the record and often has a larger amplitude than the bottom reflection (Figure 7). A sediment velocity of 2 km/sec is assumed in computing depths of reflections. This makes the two-way time in milliseconds equal numerically to the depth in metres of the reflector below the bottom. Where several sub-bottom reflections of about the same amplitude are present, the record is of the structural or S type (Figures 8 and 9). Records with no coherent sub-bottom reflections are reverberation or R type (Figure 6). Type R records may indicate either a lack of deep acoustic reflectors or confusion of sub-bottom reflections by rough topography. Although type R records occur in areas of both low and high relief, it is only in areas of low relief that reflectors can be said to be lacking. Either M, R, or S records may also be T type records (Figure 10). The type T record is a good index to rough bottom texture.

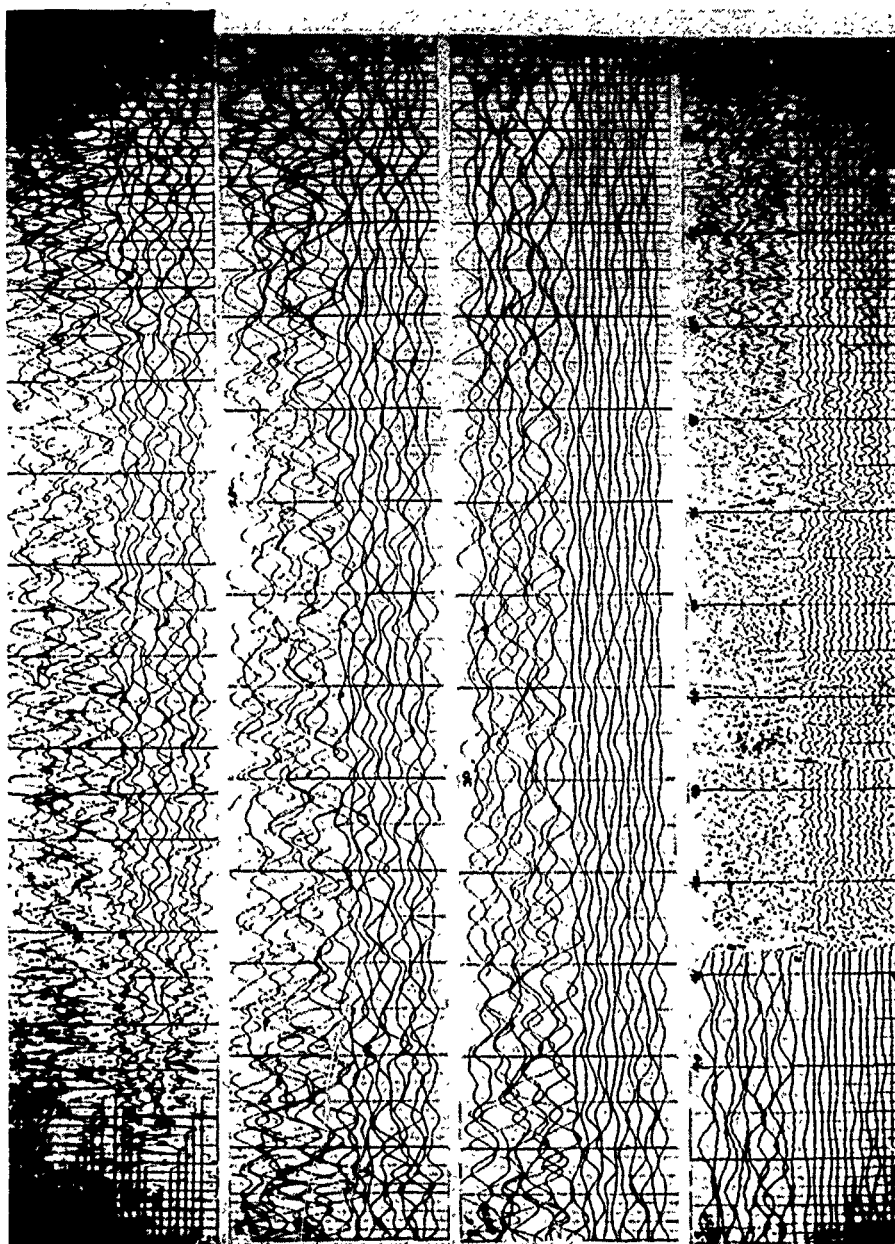


FIGURE 8. Type S reflection record, $83^{\circ}24.0' N$, $158^{\circ}07' W$, 3096 m, automatic gain control. Pass band from 15 to 218 cycles per second.

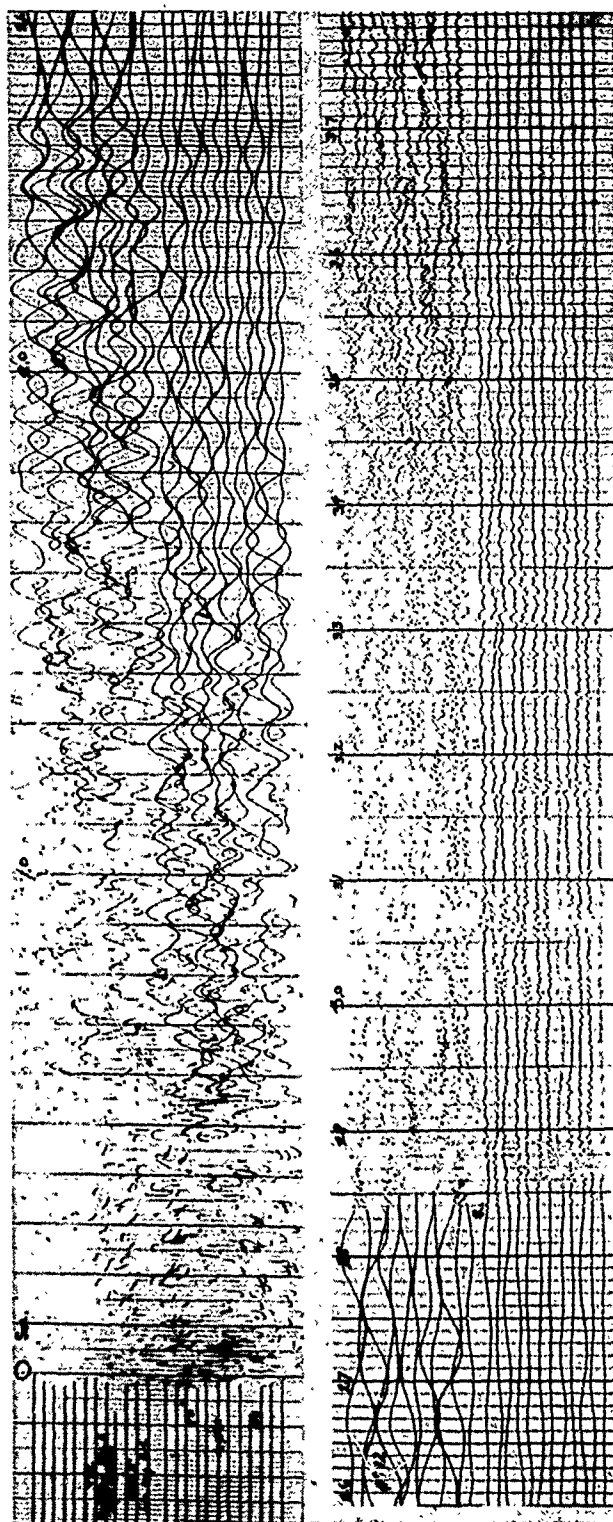


FIGURE 9. Type S-T reflection record. 84°31.0' N, 144°34' W, 2144 m. Linear amplification. No filters.

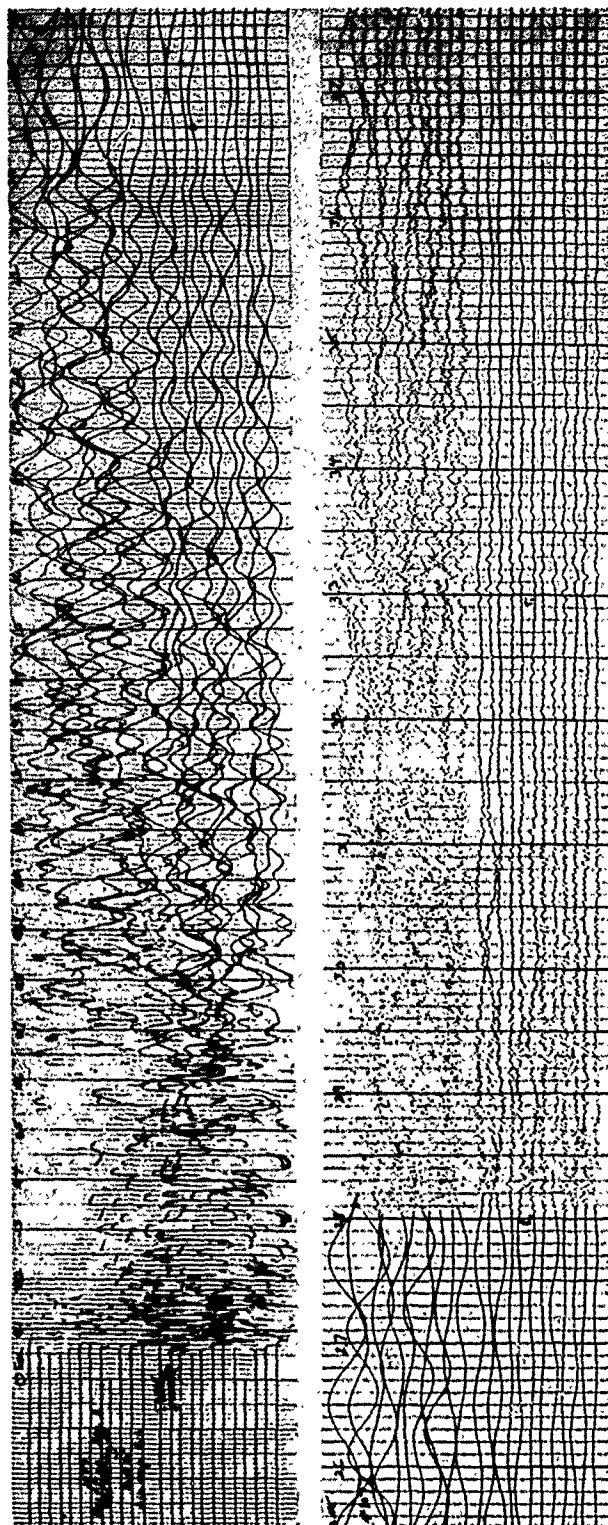


FIGURE 10. Type M-T reflection record. $85^{\circ}01.9' \text{ N}$, $138^{\circ}46' \text{ W}$, 2063 m. Linear amplification. No filters.

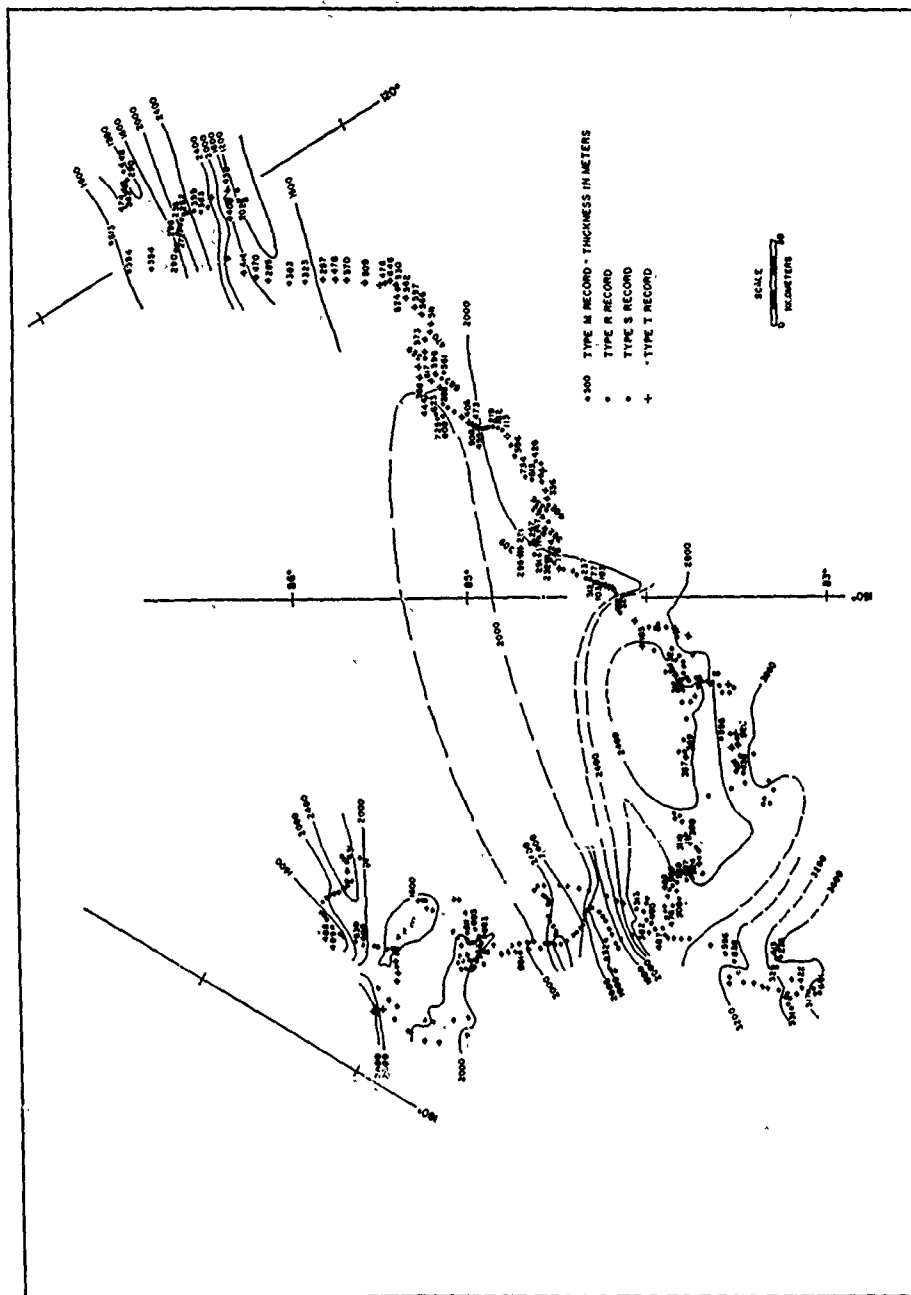


FIGURE 11. Map showing types of reflection records observed.

It is evident from the map of reflection types (Figure 11) that all these types are found on the Alpha Rise. Only type R and T records are strongly correlated with bottom dip, being found on the steepest slopes. Type M and S records are found on all but the steepest slopes, but are usually best developed in level areas. The most striking feature of the reflection distribution is the contrast between the eastern and western crossings of the Alpha Rise. On the western crossing, type S reflections are principally seen with few topographic echoes. The oblique eastern crossing produced principally type M-T records. This variation in record type cannot be due to instruments or technique, as the same instruments and shooting technique were used for all the field work, but must indicate a stratigraphic or structural difference between the eastern and the western ends of the Alpha Rise. The type T records show that bottom texture is rougher in the eastern area. The M reflection in the eastern area probably corresponds to the "second reflection" observed by Crary and Goldstein (1957) from T-3 in the area from 84° to 88° N and from 70° to 100° W. This "second reflection" lies from 210 to 340 m below the bottom. It is likely that the type M reflections found on the eastern Alpha Rise

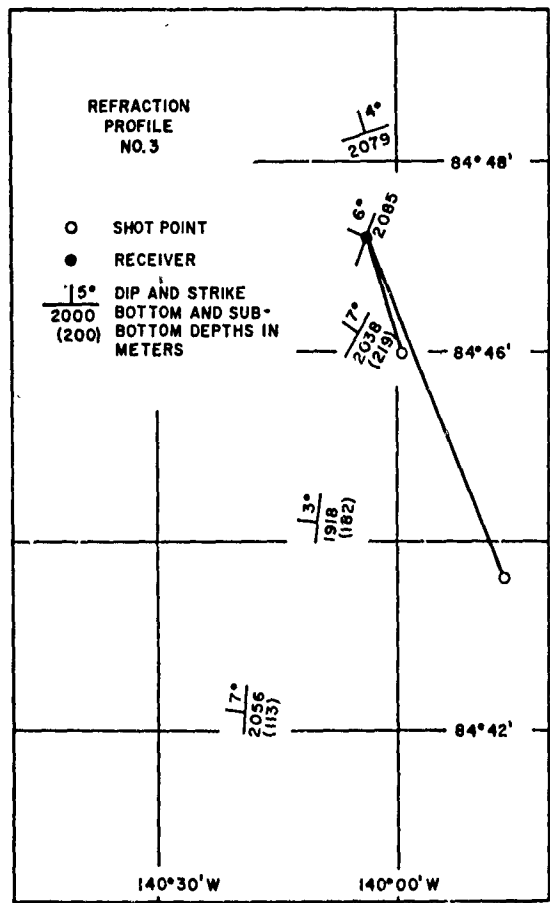


FIGURE 12. Map of refraction profile 3.

ARCTIC OCEAN BASIN

by station Alpha continue eastward to the area mapped by T-3. The strong type M echo indicates a good impedance contrast. It is quite possible that this reflection represents in some cases the base of the unconsolidated sediments in areas where there is a strong impedance contrast between these sediments and the underlying rock. In the western area, where a single strong reflection is absent, it may be that the impedance contrast at the base of the sediment is low owing to a different underlying rock which has properties little different from the overlying sediment. The reflections of the type S record would, if this were the case, be due to layering within the unconsolidated sediment.

REFRACTION STUDIES

During the spring and summer of 1958, five unreversed refraction stations were made at drifting station A. Of these stations, only the last three recorded the

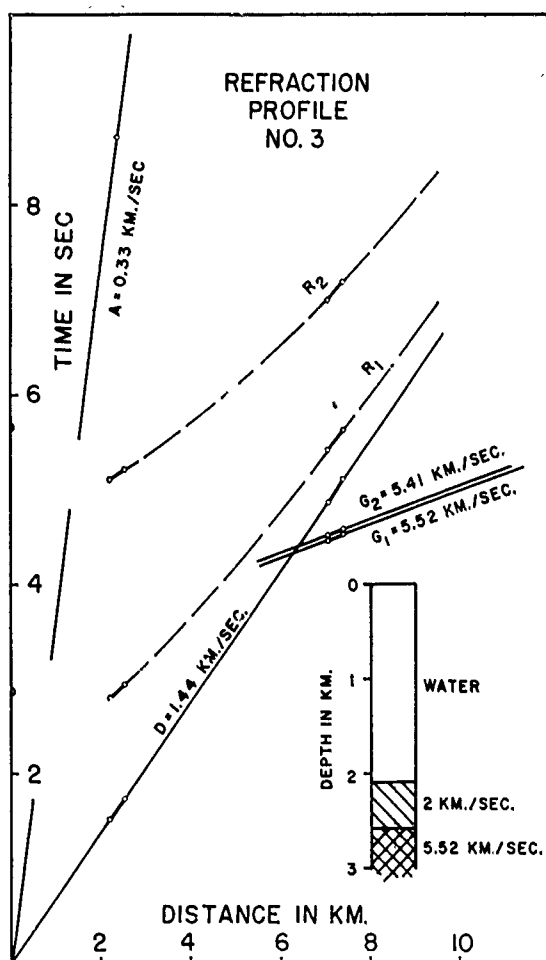


FIGURE 13. Travel time curves and interpreted structure section for refraction profile 3.

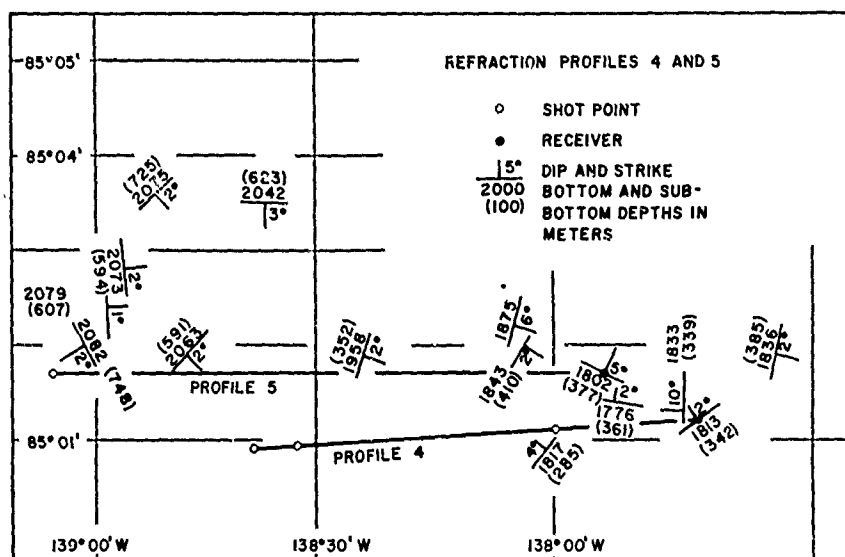
KENNETH HUNKINS

refracted ground wave as a first arrival. Only these three stations are discussed here. For the refraction work, explosives were sledged and back-packed to locations on the ice where they were detonated. The various arrivals were recorded by the HTL 7000-B seismograph at the camp. The difficulties of crossing pack ice with its many open leads and hummocks prevented using this technique for long refraction shots.

The charges ranged from 25 to 75 lbs. of TNT fired about five to eight feet below the water surface. In all cases the charges blew out preventing bubble oscillations. The arrivals were recorded on a right-angle array of fourteen cycles per sec geophones. This array permitted the measurement of the apparent velocities and azimuths of the arrivals. Recording speed was 6.6 inches per sec. Attempts at wire and radio communication were unsuccessful and time breaks were not recorded.

Distance from the shot point to the receiver was determined indirectly using the air and water arrivals which were respectively detected with a microphone and hydrophone. The relationship $t = r/0.33 - r/1.44$ was used to find the distance, r , in kilometres where t was the time difference in seconds between the direct water and the air arrivals. This method is approximate and an error in distance of up to 5 per cent may result from uncertainties in the air and water velocities used.

Depth of water beneath the receiver was measured by vertical reflection at the time of the refraction shot. This reflection record gave the depth, dip, and strike of the bottom as well as of sub-bottom layers when present. Other reflections were taken in the vicinity of the profile when the drift of the station allowed. These showed the bottom to be quite irregular at all the stations. The measured dips were apparently only of local significance. For this reason, the apparent velocity of the refracted wave across the array was corrected using the dip of the bottom



ARCTIC OCEAN BASIN

and sub-bottom beneath the receiver. However, all interpretations were made with the assumption of horizontal bedding between the shot point and receiver. This was considered justified because depths were irregular but did not deviate widely.

In making the interpretations, straight-line ray paths were assumed. Also assumed was an upper layer with a velocity of 2 km/sec. No direct evidence of this layer was seen in the refraction work as it would be masked by the water layer at all the stations. However, from previous work it seems reasonable to assume such a layer with an average velocity of 2 km/sec for depths on the order of 0.5 km (Crary and Goldstein, 1957; Nafe and Drake, 1957). All structural interpretations apply to the area immediately below the receiver. The notations for the various arrivals are those of Ewing and Ewing (1959), with the addition of the symbol "A" for the direct air wave.

Refraction profile 3 (Figures 12 and 13). On July 25, 1958, a refraction station was made which consisted of two shots at distances of 2.36 and 7.19 km. The

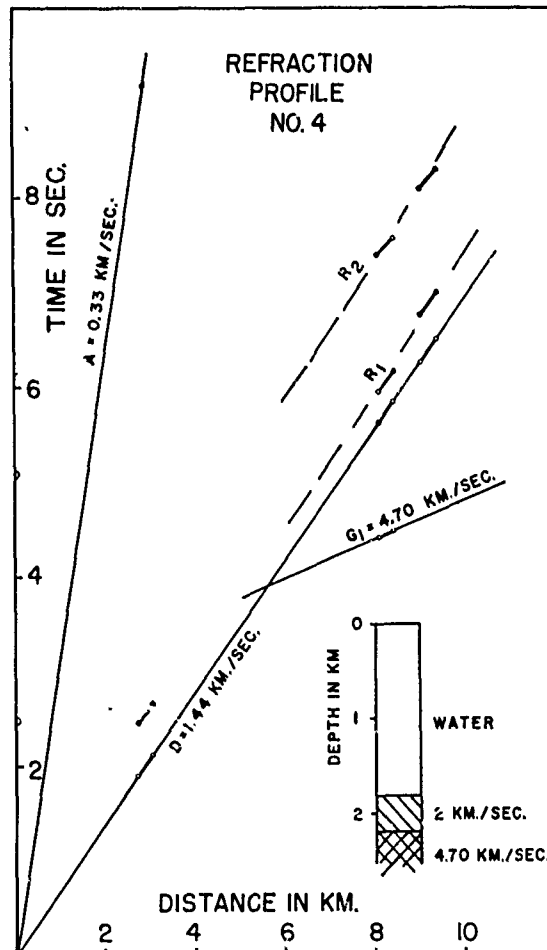


FIGURE 15. Travel-time curve and interpreted structure section for refraction profile 4.

KENNETH HUNKINS

ocean bottom beneath the receiver was at a depth of 2085 m with a dip of 6° . The apparent dip in the line of the shot was 4° away from the shot. R_1 and R_2 indicate that the depth along the profile was somewhat less than that under the receiver, but this latter depth was used for computations. The apparent velocities of the refracted waves in the line of the shot were 4.43 and 4.33 km/sec. These values were corrected for dip to 5.52 and 5.41 km/sec. The interpreted structure sections shows 2085 m of water underlain by 0.48 km of sediment with a velocity of 2 km/sec. Below this lies an undetermined thickness of 5.52 km/sec material.

On several reflection records taken in the vicinity, a type M sub-bottom reflection appears. The depth of the horizon below the bottom is noted in parentheses in Figure 12. This depth assumes a sediment velocity of 2 km/sec. In the vicinity of the profile, the depth to the horizon is about 200 m. Thus this prominent reflector apparently lies above the base of the layer of low velocity sediment.

Refraction profile 4 (Figures 14 and 15). A profile of three shots was made on August 2, 1958. These were at distances of 2.90, 8.26, and 9.18 km from the receiver. The vertical reflection record at the receiver showed 1813 m of water and a bottom dip of 2° . A sub-bottom reflection at 342 m was also shown. This sub-bottom horizon dipped more steeply than the bottom and its dip was used to correct the apparent velocity of the refracted wave. The low-angle reflections indicate high topography between the closest shot point and the receiver. The apparent velocity across the spread in the line of the shot was 5.30 km/sec. This was corrected to 4.70 km/sec by a 2° apparent dip. The interpreted structure is 1813 m of water, a 2 km/sec. layer which is 0.37 km thick, underlain by an undetermined thickness of 4.70 km/sec material.

The prominent reflection horizon was at 342 m at the receiver site and around this site it was in the vicinity of 350 m. This agrees closely with the 370 m thick-

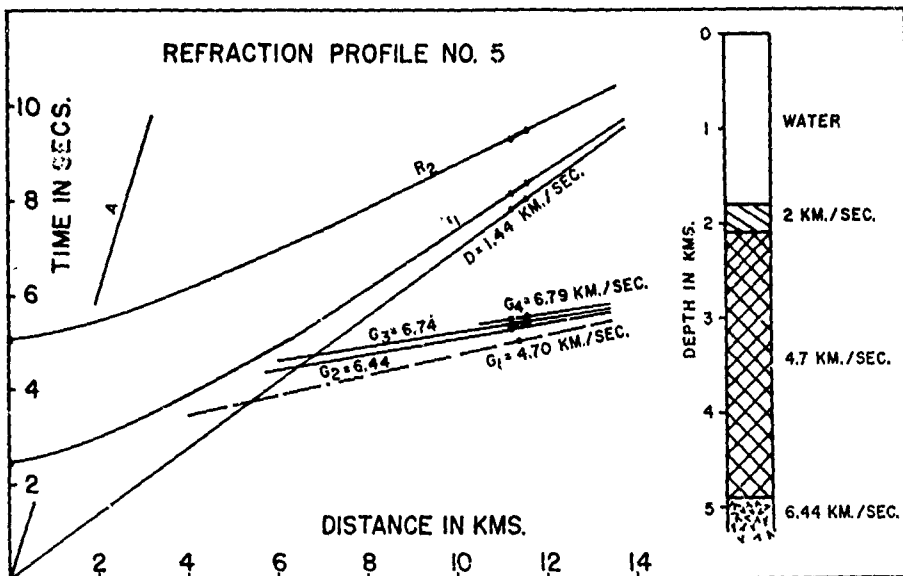


FIGURE 16. Travel time curves and interpreted structure section for refraction profile 5.

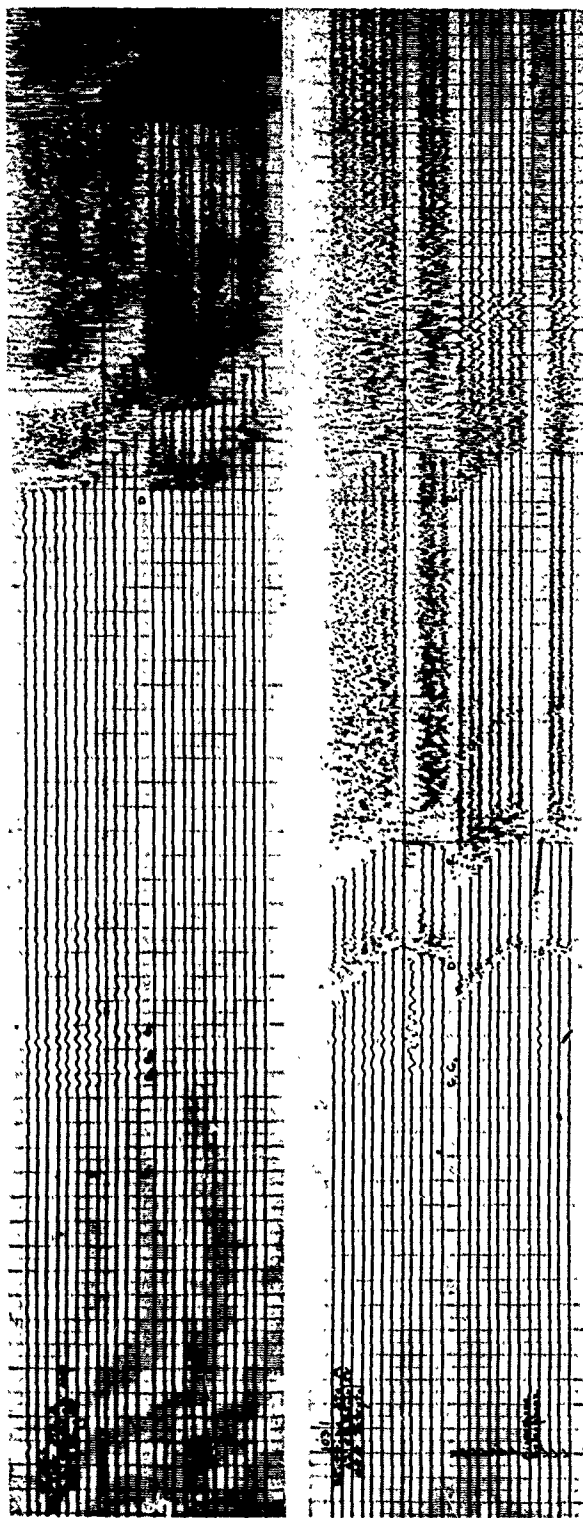


FIGURE 17. Refraction records. The upper record is from profile 5. The lower record is from profile 3. Linear amplification. No filters. Late phases of the record, including the air wave, are not shown.

KENNETH HUNKINS

ness of the 2 km/sec layer found by refraction. Apparently this prominent reflector is the base of the upper low velocity sediment in this area.

Refraction profile 5 (Figure 16). A profile consisting of one shot at a distance of 11.38 km was made on August 3, 1958. On this record, G_1 is too low in amplitude for its apparent velocity to be determined. As this station is very close to profile 4, it is assumed that this is the 4.70 km/sec layer. G_2 , G_3 , and G_4 are all recorded with good amplitudes. The apparent velocities of these arrivals are 5.74, 6.01, and 6.05 km/sec respectively. The corrected velocities, using the dip of the sub-bottom horizon, are 6.44, 6.74, and 6.79 km/sec. These arrivals are apparently from the "oceanic" layer. Interpretation of the results shows 0.29 km of 2 km/sec sediment and 2.80 km of 4.70 km/sec material. Below this lies the 6.44 km/sec layer of unknown thickness. Here the prominent sub-bottom reflection is at a depth of 377 m beneath the bottom at the receiver site. Here the reflector is apparently below the base of the layer of low velocity sediments.

CONCLUSIONS

The Alpha Rise is one of the large positive features of Arctic Ocean topography and must be considered in any discussion of the tectonics or physical oceanography of this region. Relief on the rise is rugged and is apparently the result of block faulting. Although only three short refraction profiles were made, they tend to show results similar to those in the North Atlantic Ocean (Ewing and Ewing, 1959). The average thickness of the upper or "unconsolidated" layer was 0.38 km as compared to the $\frac{1}{2}$ to 1 km in the North Atlantic. A single measurement of 2.80 km thickness was made for a 4.70 km/sec layer. The "oceanic" layer velocity was 6.44 km/sec which is in close agreement with the velocity of about 6.5 km/sec found in the North Atlantic.

REFERENCES

- CRARY, A. P., and GOLDSTEIN, N. 1957. Geophysical studies in the Arctic Ocean; Deep Sea Research, vol. 4, pp. 185-201.
- EWING, J., and EWING, M. 1959. Seismic refraction measurements in the Atlantic Ocean basins, in the Mediterranean Sea, on the Mid-Atlantic Ridge, and in the Norwegian Sea; Bull. Geol. Soc. Amer., vol. 70, pp. 291-318.
- GUTENBERG, B., and RICHTER, C. F. 1954. Seismicity of the earth and associated phenomena; Princeton University Press, 2nd ed.
- HERSEY, J. B., and EWING, M. 1949. Seismic reflections from beneath the ocean floor; Trans. Amer. Geophys. Un., vol. 30, pp. 5-14.
- HOPE, E. R. 1959. Geotectonics of the Arctic Ocean and the great Arctic magnetic anomaly; J. Geophys. Res., vol. 64, pp. 407-27.
- MATTHEWS, D. J. 1939. Tables of the velocity of sound in pure water and sea water for use in echo-sounding and sound-ranging; Hydrographic Department, Admiralty, London.
- NAFE, J., and DRAKE, C. 1957. Variation with depth in shallow and deep water marine sediments of porosity, density and the velocities of compressional and shear waves; Geophysics, vol. 22, pp. 523-52.
- NETTLETON, L. L. 1940. Geophysical prospecting for oil; McGraw-Hill.
- 1957. Bathymetric chart of Arctic Ocean as of 1956; compiled for Defence Research Board of Canada, Ottawa.

**Some features of Arctic Deep-Sea
Sedimentation**

K.L. Hunkins

Reprinted from the
PROCEEDINGS OF THE SECOND ANNUAL ARCTIC PLANNING SESSION,
Vol. 29, pp. 11-15, 1959

SOME FEATURES OF ARCTIC DEEP-SEA SEDIMENTATION*

Kenneth Hunkins
Lamont Geological Observatory
Columbia University

Research on aspects of sedimentation in the Arctic Ocean was carried out from Drifting Station Alpha during the International Geophysical Year. The studies are part of a broad marine geophysics program carried out at Station Alpha and now being continued at Station Charlie.

At the beginning of the work several broad questions about deposition in the Arctic Ocean were posed. What is the nature of sedimentation in an ice covered ocean and what is its rate? What can the sedimentary record from the ocean floor reveal about past climate? Since the Arctic is probably a key factor in controlling climate, it was expected that direct information from this region might aid in understanding ice age problems.

For the study of these questions, samples were taken from the ocean floor with an Ewing piston corer and with a dredge. A total of 16 cores and 10 bottom dredges were obtained. Over 100 photographs of the bottom were also taken. Plankton tows taken in the waters near the surface revealed the organisms living presently which are a modern source of sediment.

Several unique features of arctic sedimentation were revealed. From the dredge hauls and bottom photographs it was learned that rocks of various sizes are very abundant. The cores which reach down to a depth of seven feet also have pebbles distributed throughout their length. Roundness studies show these rocks to be angular and some are faceted. Glacial striae are not always immediately evident to the eye, but cellulose peel techniques reveal many of the pebbles to be striated. The conclusion is that these gravels are of glacial origin and have been rafted out from shore on sea ice or on shelf ice. A study of the molluscs brought up by dredge showed many of them to be shallow water species. This also points to the operation of ice rafting since the station was about 500 miles from the nearest coast at the time and floating over about 2000 m of water. The rocks and some of the molluscs have a manganese coating on the portion exposed above the mud. Such a coating indicates that the rocks have been there for some time but does not tell how long since the rate and conditions for manganese deposition in the deep sea are still little known. The coating on the rocks is very thin. They look as though they had been blackened by rubbing with a soft pencil. The ice rafting of these materials may be taking place today by means of such ice islands at T-3, which contains rock debris. However, the present rate of deposition from this source must be low. There are probably only a few dozen ice islands at present. The debris they hold must only be dumped during crushing on the island edges or the slow melting around the edges.

*The research reported was accomplished through AFCRC Contract AF 19(604)-2030 with Lamont Geological Observatory.

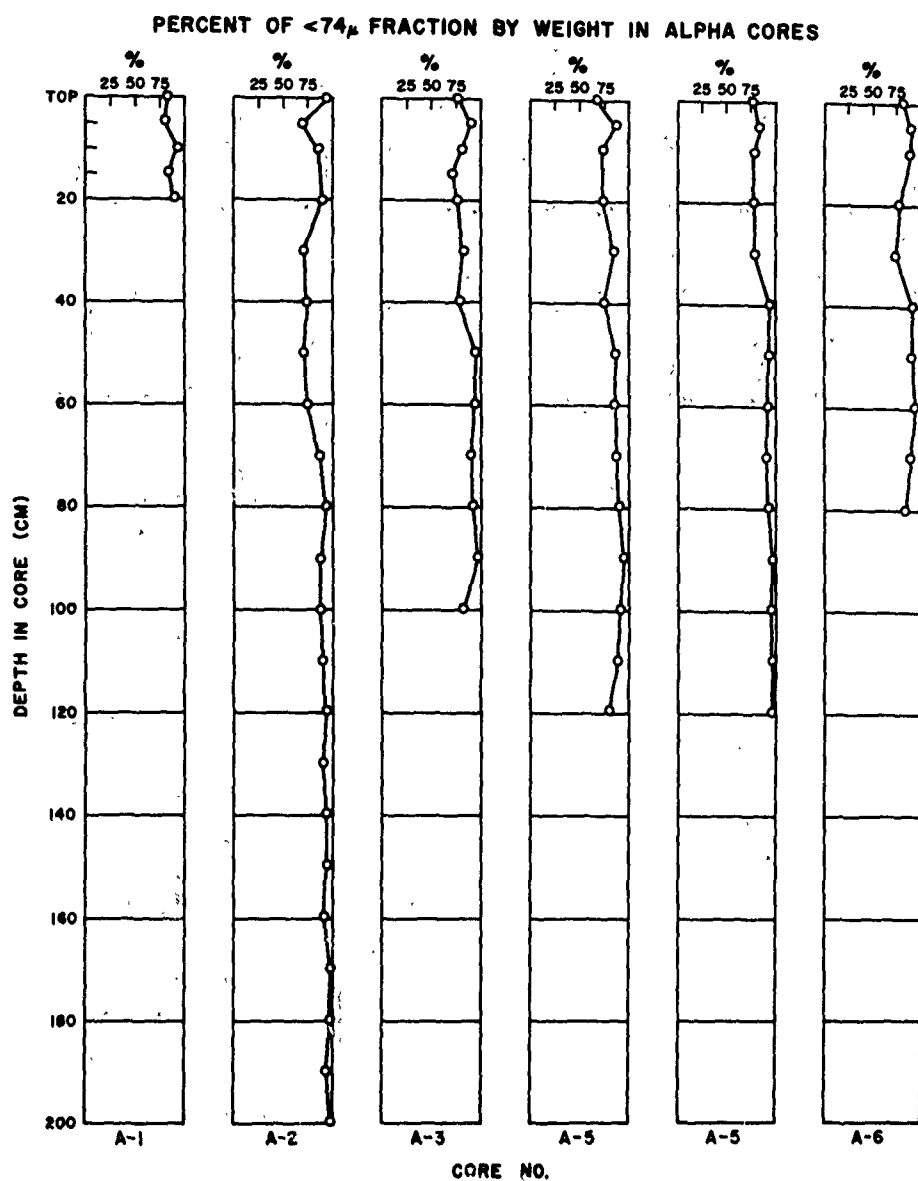


Fig. 1. Percent of fine sediment in six arctic cores.

To penetrate below the surface of the sediment and study the geological record in detail, bottom cores must be taken. Core analysis reveals that most of the sediment throughout the length is clay (fraction $<74\mu$). In the samples examined from the various cores at various depths, clay ranged from 67 to 96 % by weight of the sample. Some of this clay is undoubtedly ice rafted with the other glacial material. Some of it may be terrigenous, carried out by river and ocean currents. The coarse material from the cores (fraction $>74\mu$) is composed principally of sand and pelagic foraminiferal tests. Throughout the length of the cores only one species of planktonic foraminifera (*Globigerina pachyderma*) and only one species of pteropod (*Limacina helicina*) was found. This uniformity of fauna shows that temperature conditions in the Arctic have not changed severely for a very long time. If they had changed other fauna would have developed. Temperatures have probably not deviated by more than 10°C from the present value. Burrow mottling is also present throughout the length of the cores. Bottom dwellers tunneling through the sediment within a few centimeters of the surface produce this mottling. Bottom dwellers must have been active in the Arctic for a very long time.

In all cores, two persistent layers are seen. Correlation of these layers between the cores is good. The upper layer of sediment down to a depth of about 10 cm is dark colored and rich in forams. Below this lies a lighter colored thicker layer which is sandy and relatively barren of forams. Such a change in sediments indicates a change in the conditions of deposition. It might be expected that it is associated with the large climatic changes of the ice ages. The age of the sediments can be dated with the radiocarbon method using the carbonate of the foram tests. Dating is only practical for the upper, foram-rich layer. The first sample dated was taken with an Ekman grab at $84^{\circ}23'\text{N}$, $148^{\circ}51'\text{W}$ in water depth of 1700 m. The amount of penetration of such a grab is difficult to determine. It was estimated that the sample represented the upper 5 or 10 cm of sediment which is the upper part of the dark organic layer. The forams from this sample were dated at $9,300 \pm 180$ years BP. Another sample was then dated which was known definitely to be from a given level. This sample consisted of the 7- to 10-cm layer from Alpha cores number 3, 4, 5, and 6. This is the base of the upper dark layer. In order to obtain enough forams, the samples from these four cores were mixed.

Core Number	Date	Position	Depth
3	19 Aug 57	$84^{\circ}12'\text{N}$, $168^{\circ}33'\text{W}$	2409 m
4	20 Aug 57	$84^{\circ}21'\text{N}$, $168^{\circ}49'\text{W}$	2041 m
5	22 Aug 57	$84^{\circ}28'\text{N}$, $169^{\circ}30'\text{W}$	1934 m
6	8 Sept 57	$85^{\circ}15'\text{N}$, $167^{\circ}54'\text{W}$	1842 m

This mixed sample was found to be definitely older than 18,000 years and probably older than 25,000 years. The age does not definitely place the upper dark layer, but it must represent either the last stage of the Wisconsin or the entire period of Wisconsin glaciation. The lower sandy layer must be either the Sangamon interglacial period or the last warm period during the Wisconsin glaciation. Evidently there has been little deposition in postglacial time. Plankton tows have shown that present foram production in the Arctic is an order of magnitude less than that in the Atlantic today. The rate of deposition since the beginning of the last glacial period is very low. The maximum rate is about $1/3$ cm per 1000 years. The uncertainty in the age dates makes it possible that the rate may be much lower than this.

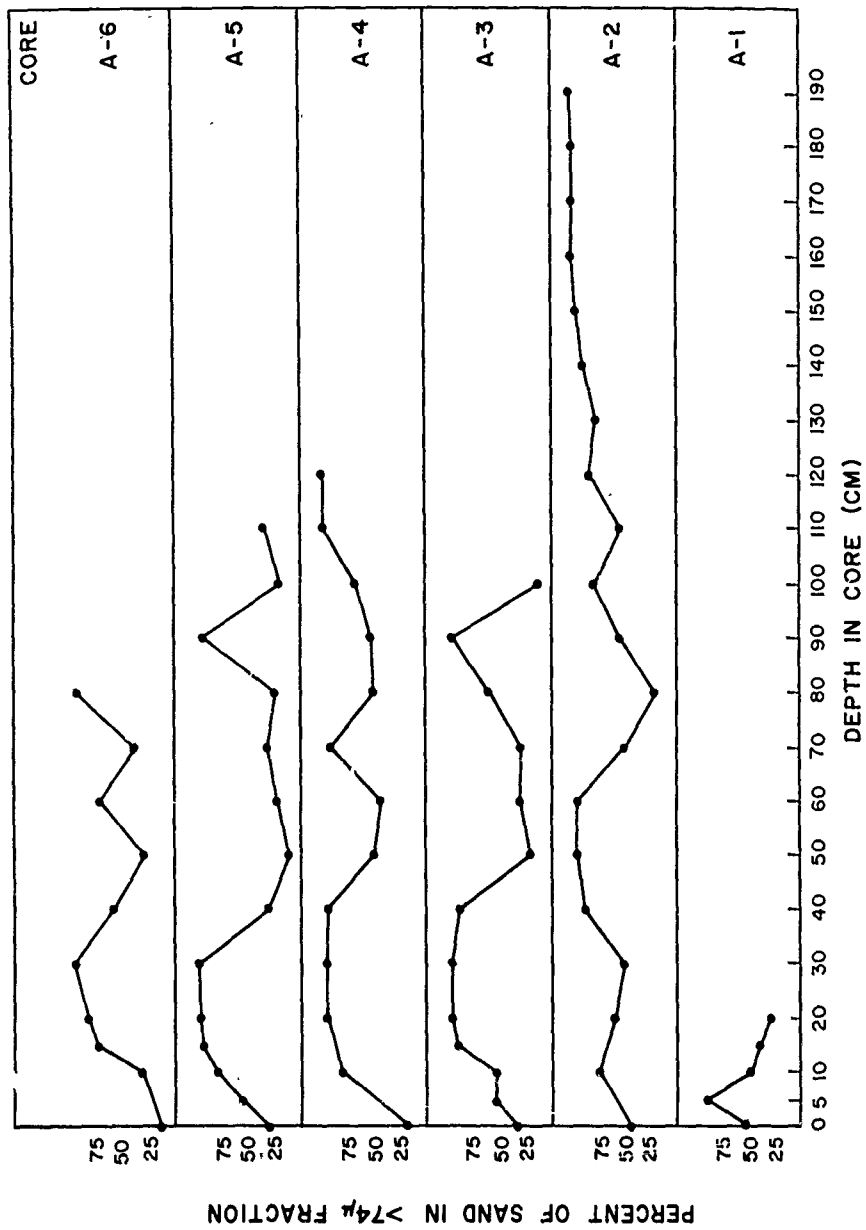


Fig. 2. Percent of coarse sediment in six arctic cores.

The conclusions reached about sedimentation in the Arctic Basin, as a result of studies from Drifting Station Alpha, may be summarized as follows:

- (1) Ice rafting has been an important source of sediment. Ice rafted gravels are seen in bottom photographs and brought up in dredges. They are found at all depths in the cores.
- (2) The majority of the sediment is composed of clay-sized particles. These are probably in part ice rafted and also carried by currents.
- (3) Some of the sediment is of organic origin, chiefly foraminiferal tests. Plankton tows show that foram production is very low today in the Arctic Ocean.
- (4) The cores indicate a climatic change took place sometime before 25,000 years ago. This event is probably either the end of the Wisconsin or the beginning of the last stage of the Wisconsin glaciation.
- (5) The upper 10 cm of the cores is dark and organic. It presumably represents the last cold period and post-glacial time.
- (6) The layer from 10 to 40 cm is sandy and relatively barren of forams. Presumably it was deposited during the Sangamon interglacial or the last Wisconsin warm period.
- (7) Radiocarbon dating shows the rate of deposition in the Arctic Ocean to have been less than 1/3 cm/1000 years during the last cold period and post-glacial time.
- (8) Temperatures in the Arctic have not fluctuated more than about 10°C throughout the length of time represented by the cores since the faunal assemblage has not changed.

**Dredged Gravels from the Central
Arctic Ocean**

W. Schwarzacher
K.L. Hunkins

Reprinted from the
GEOLOGY OF THE ARCTIC,
Vol. 1, pp. 666-677, 1961

Dredged Gravels from the Central Arctic Ocean¹

WALTER SCHWARZACHER
AND KENNETH HUNKINS

ABSTRACT

A series of nine bottom trawls was made in the Arctic Ocean from drifting station Alpha. The trawls were taken in the area between 84° and 85° N and between 138° and 152° W. All trawls produced high percentages of gravel. Macroscopic and microscopic analyses showed these gravels to be predominantly sedimentary rocks. Few igneous or metamorphic specimens were found. One fossiliferous sandstone specimen is Permo-Carboniferous in age. Bottom cores contained similar pebbles at depths in the sediment of up to 115 cm below the sea floor. Studies of the striation, roundness, and shape of the pebbles reveal them to be typical glacial material which has undergone little or no water transport.

It is concluded that these gravels have been rafted by ice from a shore containing active glaciers. Considerations of Arctic Ocean circulation, Pleistocene glaciation, and lithology make it probable that the source area was Axel Heiberg Island, Ellesmere Island, or the northern coast of Greenland.

DRIFTING STATION ALPHA was organized and maintained as a scientific research station on an ice-floe in the central Arctic Ocean by the combined efforts of the United States National Committee of the International Geophysical Year and the United States Air Force. The station was in operation from April 1957, to November 1958. Lamont Geological Observatory of Columbia University carried out a programme of marine geophysics at the station under contract AF19 (604)-2030 from Air Force Cambridge Research Centre. One aspect of the marine geophysics was the study of the ocean floor. A winch and cable allowed oceanographic gear to be operated in the same way as on board a research vessel. A total of 9 dredge samples, 14 bottom cores, and about 200 bottom photographs were obtained from the station. The most remarkable feature of sedimentation revealed by these investigations is the high percentage of gravels and sands on the ocean floor. The relative density of such gravels is most impressively seen in bottom photographs (Figure 1) (Hunkins, *et al.*, 1960). This coarse material has undoubtedly been ice-rafted and dropped to its present position.

Most of the gravel samples were taken with a small bottom trawl consisting of a net held in place by a steel frame. The mouth opening was 10 cm x 100 cm and the net had a mesh of 0.5 mm. In operation, the trawl was lowered until a decrease of tension on the dynamometer indicated bottom contact. Some extra cable was then played out and the trawl was towed by the drifting ice-floe for a period of from one to four hours. The actual distance travelled by the trawl on the bottom was from about 1,000 feet to one mile. One sample was also obtained with a bucket dredge and another with an Ekman grab. One rock was brought up

¹Lamont Geological Observatory (Columbia University) contribution no. 490.

WALTER SCHWARZACHER AND KENNETH HUNKINS

accidentally when it wedged itself into a sprocket wheel used as a weight during other operations. Material collected by these methods represents, of course, only the topmost layers of sediment. Information on the various samples is given in Table I.

TABLE I

Sample No.	Position lat.	Position long.	Depth sounding	Gear used	Period of dredging	Date
1	83°59' N	151°44' W	2590 m	bucket dredge	—	27 April 1958
2	84°09'	150°23'	2490	bottom trawl	1 hr.	8 June 1958
3	84°16'	149°11'	1658	bottom trawl	1 hr.	12 June 1958
4	84°22'	148°51'	1776	Ekman grab	—	14 June 1958
5	84°27'	148°28'	1700	bottom trawl	1 hr. 50 min.	16 June 1958
6	84°33'	146°24'	2201	bottom trawl	1 hr. 30 min.	7 July 1958
7	84°30'	145°00'	2294	bottom trawl	1 hr. 45 min.	9 July 1958
8	84°31'	143°30'	2118	accidental catch	—	11 July 1958
9	85°01'	138°00'	1840-1910	bottom trawl	4 hr. 15 min.	31 July 1958

The samples consisted generally of one to four L of brown mud mixed with various amounts of sand and gravel. As the mesh of the dredge net was 0.5 mm, the samples faithfully represent the bottom sediment only for particle sizes greater than this. The smaller fractions are best examined from core samples where they are seen to be partly normal marine sediment and partly glacial marine sediment. All dredge samples were washed and only the fraction larger than three mm was examined in detail.

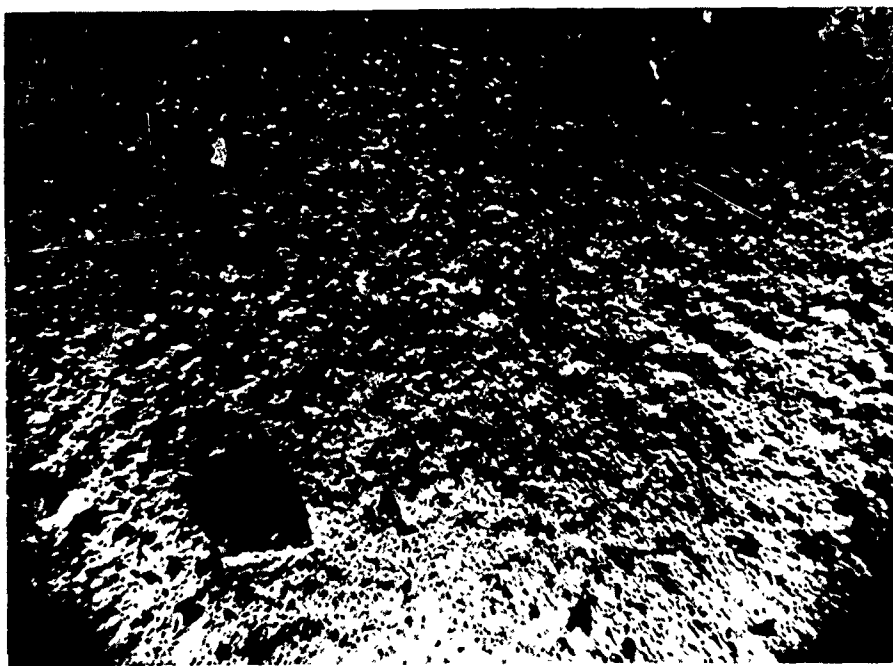


FIGURE 1. Bottom photograph taken at 83°35' N, 162°30' W in 2400 m of water. The area included in the picture is about one sq. m.

ARCTIC OCEAN BASIN

After sieving the samples, the fraction greater than three mm was examined under the binocular microscope. Sandstone, shale, metamorphic, and igneous rock types were separated by inspection; limestones and dolomites were differentiated by staining with alizarine red S (Friedman, 1959). Gravels larger than twenty mm were thin-sectioned and examined under the polarizing microscope.

The composition of the various sieve fractions seems to change with some regularity. Especially notable is the increase of shale and sandstone in the fraction smaller than four mm and the maximum occurrence of dolomite in the fraction between four and ten mm. It appears that the size is determined to a degree by the rock type.

In the following descriptions the weight percentage of the different rock types in the material greater than three mm are given. The gravels with a diameter greater than twenty mm are described in some detail. As a definite source area has not yet been located for these samples, it is hoped that these descriptions may lead to a more positive identification of their source.

<i>Sample 1:</i> fraction greater than 3 mm 135 gm			
no pebbles greater than 20 mm			
limestone			15 per cent
dolomite			26 per cent
sandstone and shale			50 per cent
igneous and metamorphic			9 per cent
<i>Sample 2:</i> fraction greater than 3 mm 1029 gm			
fraction greater than 20 mm 253 gm			
limestone			32 per cent
dolomite			36 per cent
sandstone and shale			27 per cent
igneous and metamorphic			5 per cent

The limestone in this sample is all of the same type. In hand specimen it is light grey to blue-grey. Under the microscope it is a true calcitute with some patches of coarser recrystallized calcite mosaic. Shell fragments and occasional crinoid ossicles occur, but they constitute only a small proportion of the rock. Specks of limonite after pyrite are present in some sections.

The dolomite in all dredge samples appears to be of the same type. It is either white or white-brown and is invariably recrystallized into a dolomite marble with crystal sizes of 0.01 to 0.5 mm. The crystals occur in a mosaic in which rhombic crystal shapes are rarely seen. In two specimens, a preferred orientation of the fabric was noted, suggesting that the rock has undergone some tectonic deformation. In some of the dolomites, a slight grading of the grains produces a lamination 0.5 to 1.0 mm thick. Occasional small unconformities occur within the laminae and in one instance small scale channelling is well developed. Clastic quartz grains occur interspersed throughout the dolomite and as small lenses of sandstone. The quartz grains are subangular with grain diameters ranging from 0.04 to 0.06 mm. Fossil remains are rare and unidentifiable. It is probable that these dolomites are derived from an extensive series which was deposited under shallow-water conditions and which may have been interbedded with sandstone.

WALTER SCHWARZACHER AND KENNETH HUNKINS

In this sample, only one sandstone pebble is found. It is a dark grey, greywacke type with angular quartz grains of 0.01 to 0.05 mm diameter in a fine-grained cement of mica and chlorite. The quartz grains show signs of strain.

Only one metamorphic pebble, a chloritoid schist, was found in this sample. It is a fine-grained quartz mica schist containing porphyroblasts of chloritoid and sharply defined patches of calcite.

Sample 3:	fraction greater than 3 mm	30 gm	
	no pebbles greater than 20 mm		
	limestone		13 per cent
	dolomite		29 per cent
	sandstone and shale		43 per cent
	igneous and metamorphic		15 per cent
Sample 4:	fraction greater than 3 mm	23 gm	
	no pebbles greater than 20 mm		
	limestone		21 per cent
	dolomite		22 per cent
	sandstone and shale		44 per cent
	igneous and metamorphic		13 per cent
Sample 5:	fraction greater than 3 mm	3307 gm	
	pebbles greater than 20 mm	2698 gm	
	limestone		11 per cent
	dolomite		33 per cent
	sandstone and shale		54 per cent
	igneous and metamorphic		2 per cent

One limestone pebble is light grey to yellow and contains a large number of shell fragments in a calcilutite matrix. Among others, fragments of pseudo-punctate brachiopods, tentatively identified as chonetids and productids, are present. In addition, shells of gastropods, crinoid ossicles, and some bryozoans occur. The limestone is probably Permo-Carboniferous in age. Dolomites are as described in sample 2.

One large sandstone specimen with a calcareous cement is present. The quartz grains are subangular, ranging from 0.02 to 0.1 mm in diameter. The cement is recrystallized and large areas show common extinction. This specimen is highly fossiliferous. The following brachiopods have been identified by Professor A. Williams: *Lingula* sp., *Neospirifer* sp., *Spiriferina* sp., *Aulosteges* sp., Chonetid. The following bryozoans have been identified by Dr. R. S. Boardman: *Rhombo-trypella* sp., *Rhazdomeson* sp., ? *Polypora* sp., In addition, crinoid ossicles and gastropods also occur. Both the brachiopods and the bryozoans indicate a Permo-Carboniferous age, more likely Permian.

One large pebble of greywacke type sandstone is dark green with black shale wisps parallel to the bedding plane. Quartz grains are very well rounded with diameters from 0.02 to 0.3 mm. Many of the quartz grains show well-developed strain lamellae and the mica matrix exhibits "flow structure" deformation. Low grade metamorphism is likely. Another similar sandstone pebble is more highly metamorphosed and has interpenetrating grain boundaries.

ARCTIC OCEAN BASIN

Three sandstone specimens, with a relatively unaltered appearance, vary in colour from yellow to dark brown and are cemented with carbonate. Only one, which contains a fair amount of bitumen and some unidentifiable organic remains, is distinctive.

One specimen of *conglomerate* is present. Well-rounded pebbles of dark grey to black chert and a few quartzite pebbles occur in a matrix of quartz sandstone and chert. The chert is recrystallized and contains no organic remains.

In sample 5, one loose piece of chert occurs. It contains a large amount of calcareous organic detritus and some rare quartz grains. Noteworthy are several glauconite grains. The quartz grains have an average diameter of 0.05 mm.

<i>Sample 6:</i>	fraction greater than 3 mm	93 gm	
	no pebbles greater than 20 mm		
	limestone		14 per cent
	dolomite		42 per cent
	sandstone and shale		36 per cent
	igneous and metamorphic		8 per cent

<i>Sample 7:</i>	fraction greater than 3 mm	156 gm	
	no pebbles greater than 20 mm		
	limestone		16 per cent
	dolomite		45 per cent
	sandstone and shale		35 per cent
	igneous and metamorphic		4 per cent

Sample 8: This sample contains only one dolomite pebble which weighs 103 gm. It is the same type as the dolomite described in sample 2.

<i>Sample 9:</i>	fraction greater than 3 mm	8739 gm	
	pebbles greater than 20 mm	8692 gm	
	limestone		8 per cent
	dolomite		5 per cent
	sandstone and shale		3 per cent
	igneous and metamorphic		84 per cent

One specimen of yellow-grey limestone, unlike any previously described type, occurs. It is a calcilutite with small recrystallized areas. It contains many poorly preserved fossils, probably brachiopod shells and foraminiferal tests. A few pyrite crystals are present. Small limestone mud pebbles in this limestone suggest a shallow-water origin. A second limestone pebble is dark grey in colour with a pellet texture. A few quartz grains (0.02 to 0.04 mm) are interspersed in it.

One large dolomite pebble of the same composition as those described in sample 2 is present.

A pink sandstone specimen consists of close-fitting, well-rounded quartz grains with diameters of 0.1 to 0.3 mm. The grains are cemented with calcite.

One diabase cobble weighing 7,300 gm forms the largest part of this sample and greatly affects the percentage composition. Under the microscope it is seen to consist of a mass of lath-shaped feldspars with a labradorite to andesine composition. Large plates of pyroxene are in ophitic intergrowth with the feldspar. Some skeletal crystals of magnetite are present. Small amounts of amphibole

WALTER SCHWARZACHER AND KENNETH HUNKINS

occur marginal to the pyroxenes and in the mesostasis. Some quartz occurs as rounded, slightly corroded, grains.

In addition to the material described above, pebbles were also found at various depths in the core samples. The cores were taken with a small Ewing piston corer having a diameter of one-and-a-half inches. A full description of these cores will be published later. In many respects these pebbles resemble those dredged from the top layer of sediment. They are generally small, the largest being 17 mm in diameter.

Core 2 was taken at 83°52'N, 168°12'W at a depth of 1521 m. One small pebble of a basic igneous rock was found at a depth of 115 cm in the core.

Core 4 was taken at 84°21'N, 168°49'W at a depth of 2041 m. One piece of sericite schist was found 46 cm below the sea floor.

Core 5 was taken at 84°28'N, 169°04'W in 1934 m of water. A light grey limestone with some shell fragments (brachiopods?) was found at 46 cm in the core.

Core 10 was taken at 84°19'N, 166°50'W in 2418 m of water. A dolomite pebble similar to those in the dredge samples was found at 64 cm.

Core 15 was taken at 84°10'N, 149°40'W in 2045 m of water. A fine-grained sandstone pebble was found at 69 cm.

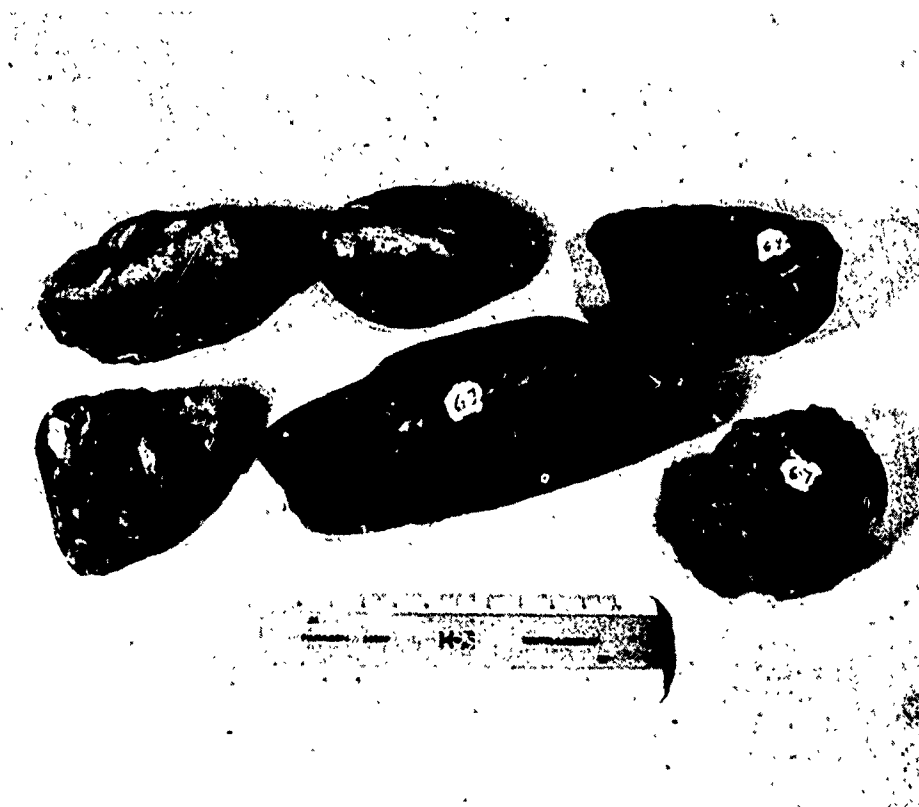


FIGURE 2. Rock specimens from dredge 6.

ARCTIC OCEAN BASIN

Many of the dredged rocks are partly covered with a thin black manganese coating which occurs in all of the specimens larger than 20 mm and on a large number of the smaller pebbles. The layer of manganese is extremely thin, probably less than 0.001 mm. It is restricted to the part of the pebble which was exposed to the sea water. The portion immersed in mud is not coated. If the specimens are oriented into their original position as indicated by the boundary of the coating, the average ratio for eighteen pebbles of the depth of the submerged portion to the height of the emerged portion is about 1 : 3. This ratio does not correlate with rock size. It is interesting that this manganese coating occurs in a similar fashion on the pebbles from cores, showing that they too were at one time exposed to sea water. Many of the dredged rocks also carry encrusting worm tubes on the manganese-coated portion. However, no living specimens were found in any of the worm tubes and the tubes themselves are in many cases coated with manganese (Figure 2).

Surface texture and roundness

Nearly half of the twenty-seven rocks larger than twenty mm in diameter show a distinct glacial striation. Wentworth (1936a) finds a similar proportion of striated rocks in moraine deposits. As expected, limestones usually preserve the best striations. Striations on dolomites are relatively short, coarse, and poorly preserved. Some of the limestone pebbles show a high degree of polish. Cellulose peels of these surfaces were made and examined under the microscope. The polish



FIGURE 3. Cellulose peel from rock specimen showing subparallel striations. Enlargement 425 times.

WALTER SCHWARZACHER AND KENNETH HUNKINS

is seen to be of abrasive origin and exhibits many minute scratches in the direction of the large striae. The cellulose peel technique proved valuable in examining all types of striations (Figure 3).

The general shapes of the pebbles have been classified using the system of Wentworth (1936a) and the results, together with the striation data, are summarized in Table II.

TABLE II
CHARACTERISTICS OF 27 PEBBLES GREATER THAN 20 MM DIAMETER

Striation						
Occurrence	Present	Subparallel to longest axis	Parallel to longest axis	Irregular		
No. of pebbles	10	8	7	3		
Snub scars						
Occurrence	Present		Marked			
No. of pebbles	7		3			
Outline of maximum projection area						
Shape	Triangular	Quadrangular	Rectangular	Trapezoidal	Pentagonal	Polygonal
No. of pebbles	3	4	3	6	7	4

Wentworth (1936b) states that the characteristic shape of the glacial pebble is the pentagonal outline, flatiron stone. This shape accounts for 26 per cent of the above sample. In contrast to this, pebbles shaped in ice-jams of periglacial rivers are essentially river pebbles on which striations are only superimposed. Snub scars are absent and are replaced by short broad bruises. Parallelism of the direction of striae to the longest axis of the pebble is less common. Irregular striation patterns occur more frequently than on glacial pebbles.

A number of authors have used the study of particle roundness for reconstructing the history of a sediment. Unfortunately, a large number of factors influence rounding and there are always two unknown quantities present: the environment in which rounding took place and the length of time for which the sediment was exposed to that environment. Further complications are presented by the use of several different roundness coefficients (Krumbein and Pettijohn, 1938).

Specimens within the size range from two to ten mm were chosen for roundness measurements. From each dredge sample twenty-five limestone and twenty-five dolomite pebbles were selected. Drawings of the maximum projection area were made by enlarging the grains through projection to a standard diameter of 7 cm. The Cailleux index was determined for all samples. This index was chosen because there are more data for comparison expressed in it than in any other.

Most water-transported sediments show a relation between the size of the pebbles and their roundness and thus only pebbles of one size group are strictly

ARCTIC OCEAN BASIN

comparable. Whether a similar relation exists for glacial material is not known. A comparison of three subsamples of twenty-five dolomite pebbles each from dredge number 2 gave 0.112 for the 3-5.4 mm fraction, 0.108 for the 7-11 mm fraction, and 0.101 for the 20-100 mm fraction. The apparent decrease of roundness with the larger sizes is not statistically significant. A comparison between the dolomite and the limestone pebbles was also made which showed no significant difference in roundness. Table III gives the roundness for the dredged material in the 3-5.4 mm range and the average for all pebbles greater than 20 mm.

TABLE III

Dredge no.	Size range (in mm)	Mean Cailleux index	Standard deviation	Sample size
2	3-5.4	0.112	0.056	50
3	3-5.4	.128	0.64	50
4	3-5.4	.116	.036	50
5	3-5.4	.128	.064	50
6	3-5.4	.112	.044	50
7	3-5.4	.124	.051	50
8	3-5.4	.112	.056	50
All pebbles	> 20	.101	.052	27

The roundness of the station Alpha material agrees well with the roundness of tills as found by various authors. Van Andel (1954) found a mean Cailleux index of 0.085 with a standard deviation of 0.059. Tricart and Schaeffer (1950) found a range of 0.100 to 0.150 and Cailleux (1952) found a range of 0.040 to 0.190.

Although the cores yielded only five pebbles for examination, these too appear to be of glacial origin. Striae are well developed on one of the pebbles and all seem to have the same degree of roundness as the dredge samples.

CONCLUSIONS

From the examination of the roundness, shape, and striae of these gravels, it is apparent that they are of glacial origin. It is also evident that this material has undergone little if any transport by water. Kuenen (1956) carried out experiments on angular sandstones from solifluction material with an average roundness of 0.044 and found that, after only 0.4 km of transport, the roundness increased to 0.113 and, after 3 km, to 0.275.

Observations by Wentworth (1922) showed that a travel distance of only 0.35 miles was sufficient to remove striae from hard limestones and greenstones. It thus appears that these gravels have been ice-rafted from a coast on which active glaciers reached the shore. It is probable that transport was by icebergs which calved directly from the glaciers. Also at least part of the material was frozen into the bottom of either grounded icebergs or sea ice. Clarke (1959) has studied the molluscan shells from the dredge samples described and concludes that, as they are shallow-water species, many of the shells have been transported

to their deep-water locations. They surely must have been picked up by grounded ice in shallow water near shore.

The known Arctic Ocean circulation in this area (Worthington, 1959; Browne and Crary, 1959) and the extent of Pleistocene glaciation (Glacial Map of Canada, 1958) limit considerably the possible source areas for these gravels. The circulation pattern in the North Canadian Basin makes it likely that the material was obtained from the northern coast of Greenland, the Canadian Arctic Archipelago, or the northern coast of Alaska. As the northern coast of Alaska and most of the northern Canadian islands are believed to have been unglaciated during Pleistocene time, we are limited to Axel Heiberg, Ellesmere Island, and the northern coast of Greenland as source areas.

Two features of the gravel composition tend to support these source areas. One sandstone specimen has been definitely identified as Permo-Carboniferous. Strata of this same age are found on Axel Heiberg and Ellesmere islands and on northern Greenland (Geological Map of North America, 1946; Geological Map of Dominion of Canada, 1945). In addition, all station Alpha dredge samples contained a characteristic white dolomite marble which may be identical with the dolomite of Precambrian to Cambrian age found in these same areas (Armstrong, 1947). In the future, comparison of the gravels with actual samples from the Arctic coast may provide more positive identification of the source areas.

A comparison of the station Alpha data with the Russian NP-2 data (1954-5) shows that the composition of the gravels in this basin of the Arctic Ocean is fairly uniform. The Russian dredge stations were located at a distance of from 200 to 600 miles from those of station Alpha (Table IV).

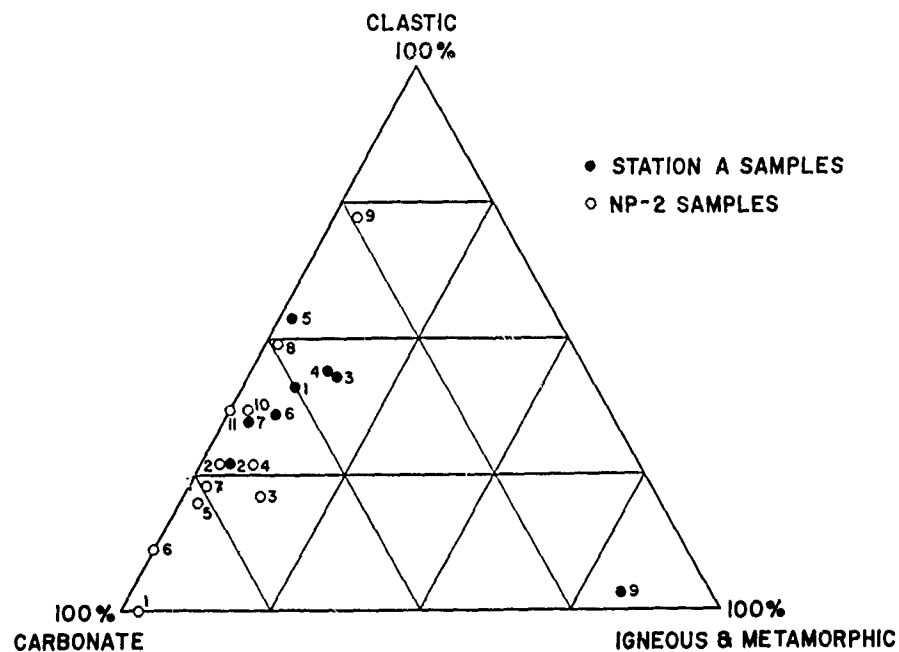


FIGURE 4. Carbonate-igneous-clastic composition of station Alpha and Russian NP-2 samples.

ARCTIC OCEAN BASIN

TABLE IV
RUSSIAN DREDGE STATIONS, NP-2 (1950-1)

Station no.	Lat.	Long.	Depth (in metres)
1	76°23' N	177°49' W	1239
2	77°44'	171°18'	2245
3	77°13'	168°49'	542
4	78°24'	168°11'	512
5	78°48'	170°52'	2788
6	78°51'	166°03'	1435
7	78°55'	162°58'	836
8	80°36'	160°25'	2861
9	80°39'	164°01'	3047
10	80°48'	162°58'	3266
11	80°48'	161°48'	3622

Figures 1 and 2 show the relative composition of the station Alpha gravels in comparison with those of Russian NP 2. A plot (Figure 4) of the three components, clastic-carbonate-igneous, reveals a close similarity between the sediments of the two stations. Agreement is not quite as good in Figure 5 where limestones, dolomites, and clastics have been plotted. No agreement is seen between the dredged gravels found by station Alpha and NP-2 and the rocks on

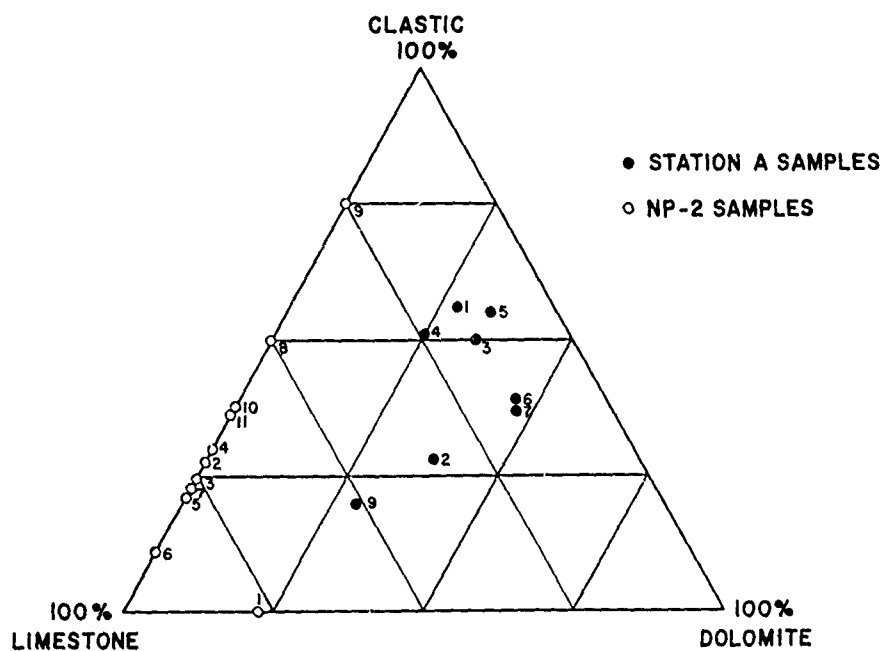


FIGURE 5. Limestone-dolomite-clastic composition of station Alpha and Russian NP-2 samples.

WALTER SCHWARZACHER AND KENNETH HUNKINS

the surface of T-3, Fletchers Ice Island, where mainly schists and gneisses were found with a noticeable absence of limestone and other sedimentary rocks (Shorey, 1953; Stoiber, *et al.*, 1956).

REFERENCES

- ARMSTRONG, J. E. 1947. The Arctic Archipelago, in *Geology and economic minerals of Canada*; Department of Mines and Resources, Ottawa.
- BROWNE, I. M., and CRARY, A. P. 1959. The movement of ice in the Arctic Ocean, in W. R. THURSTON, ed., *Arctic sea ice*; National Academy of Sciences, Washington, D.C.
- CAILLEUX, A. 1952. Morphoskopische Analyse der Geschiebe und Sandkörner und ihre Bedeutung für die Paläoklimatologie; *Geologische Rundschau*, vol. 40, pp. 11-19.
- CLARKE, A., JR. 1959. Abyssal benthic Arctic mollusca, in *Biological aspects of Arctic deep-sea sedimentation*; a final report to the Arctic Institute of North America; Lamont Geol. Obs.
- FRIEDMAN, G. M. 1959. Identification of carbonate minerals by staining methods; *J. Sed. Petrology*, vol. 29, pp. 87-97.
- GEOLOGICAL MAP OF NORTH AMERICA. 1946. Geol. Soc. Amer.
- GEOLOGICAL MAP OF THE DOMINION OF CANADA. 1945. Map 820A, Geol. Surv. Canada.
- GLACIAL MAP OF CANADA. 1958. Geol. Assoc., Canada.
- HUNKINS, K. L., EWING, M., HEEZEN, B., and MENZIES, R. 1960. Biological and geological observations on the first photographs of the Arctic deep-sea floor, *Limn. and Oceanography*, vol. 5, pp. 154-61.
- KUENEN, PH. H. 1956. Experimental abrasion of Pebbles; II, Rolling by current; *J. Geol.*, vol. 64, pp. 336-68.
- KRUMBEIN, W. C., and PETTIJOHN, F. J. 1938. *Manual of sedimentary petrology*; Appleton-Century-Crofts.
- SHOREY, R. R. 1953. Fletcher's island rocks; unpublished report, Terrestrial Sciences Laboratory, Geophysical Research Directorate, Air Force Cambridge Research Center.
- SOMOV, M. M., ed. 1954-5. Observational data of the scientific research drifting station of 1950-1951, 1; *Izd. Morskoi Transport*, 3 vols. (trans. Amer. Met. Soc., Boston).
- STOIBER, R. E., LYONS, J. B., ELBERTZ, W. T., and MCCREHON, R. H. 1956. The source area and age of Fletcher's ice island, T-3; Dartmouth College.
- TRICART, J., and SCHAEFFER, R. 1950. L'indice d'érosion des galets: Moyen d'étude des systèmes d'érosion; *Rev. Geomorph. Dynam.*, vol. 1, pp. 151-79.
- VAN ANDEL, T. J. H., WIGGERS, A. J., and MAARLEVALD, G. 1954. Roundness and shape of marine gravels from Urk (Netherlands), a comparison of several methods of investigation; *J. Sed. Petrology*, vol. 24, pp. 100-16.
- WENTWORTH, C. K. 1922. The shapes of beach pebbles; *U.S. Geol. Surv., Prof. Paper* 131-C.
- 1936a. An analysis of the shapes of glacial cobbles; *J. Sed. Petrology*, vol. 6, pp. 85-96.
- 1936b. The shapes of glacial ice jam cobbles; *J. Sed. Petrology*, vol. 6, pp. 97-108.
- WORTHINGTON, L. V. 1959. Oceanographic observations, in V. BUSHNELL, ed.; *Scientific studies at Fletcher's Ice Island, T-3, (1952-1955)*; I, AFCRC, G.R.D., Bedford, Mass.

**Biological and Geological Observations on the
First Photographs of the Arctic Ocean
Deep-Sea Floor**

K.L. Hunkins
M. Ewing
B.C. Heezen
R.J. Menzies

Reprinted from
LIMNOLOGY AND OCEANOGRAPHY,
Vol. 5, No. 2, pp. 154-161, 1960

BIOLOGICAL AND GEOLOGICAL OBSERVATIONS ON THE FIRST PHOTOGRAPHS OF THE ARCTIC OCEAN DEEP-SEA FLOOR¹

*Kenneth L. Hunkins, Maurice Ewing, Bruce C. Heezen,
and Robert J. Menzies*

Lamont Geological Observatory (Columbia University) Palisades, New York

ABSTRACT

The first series of Arctic bottom photographs give the following indications regarding conditions on the Arctic sea floor: Bottom life appears to be less abundant than in the Atlantic Ocean at similar depths. Loose rocks are more numerous. Ripples seem to be less abundant in the Arctic area photographed than they do at comparable depths in the Atlantic. A bottom current of 0.3 to 0.6 cm/sec is indicated from movements of sediment clouds. The area is abundantly supplied with curious short "tracks" of uncertain origin. Small irregular holes in the pictures probably represent holes produced by ice-rafted stones and pebbles.

INTRODUCTION

Arctic drifting Station A, established during the International Geophysical Year by the United States Air Force is a scientific research base floating in the Arctic Ocean on an ice floe of about 10-15 ft in thickness (Fig. 1). During the first year it has drifted at an approximate rate of one to three miles a day within a radius of 300 to 600 miles from the North Pole.

Observational programs in meteorology, aurora, geomagnetism, gravimetry, and oceanography were maintained. The oceanographic program included serial oceanographic measurements, current measurements, biology, seismic depth measurements, coring, and bottom photography (anon. 1957a). The great stability of the floating platform lends itself especially well to photographic operations.

The camera was a modification of the Ewing suspended automatic camera (Ewing *et al.* 1946) Model TM-III, designed and constructed by Dr. Edward Thorndike, Professor of Physics at Queens College, New York, and Research Associate at the Lamont Geological Observatory. The camera was lowered on a one-eighth inch stainless steel cable by a gasoline-driven winch, fitted with a small spring-type dynamometer. Bottom contact was determined from acoustic signal (pinger) and from the dynamometer indication.

¹ Lamont Geological Observatory Contribution No. 411.

A total of 140 exposures were taken at the bottom at two different locations by Frans van der Hoeven, then Chief Scientist at Station A. To our knowledge these are the first bottom photographs ever taken of the sea floor of the central Arctic Ocean.

The geophysical program at Station A was directed by Professor Jack Oliver. The Arctic camera project was initiated by Maurice J. Davidson. While the pictures were taken, the Station was under the command of Lt. Col. Helmuth E. Stromquist, USAF, and we acknowledge the commanding officer and his men for their aid in getting the camera in operation. We gratefully acknowledge financial support of the Air Force Cambridge Research Center of the Air Research and Development Command. Valuable advice was received from Prof. Thorndike concerning the area of the bottom covered by the various exposures.

Camera station DSA-1. Position: Lat. 83° 49'N; Long. 165° 05'W. Depth 2997 meters, wire sounding. Ninety-five exposures. Date 12-13 December, 1957; on the south flank of the newly discovered Alpha Rise. Bottom contact was indistinct, camera was laid on the bottom for much of the time; many of the pictures were taken with the camera in essentially the same position. Eighty-six exposures were made covering 30 different bottom sites.

Camera station DSA-2. Position: Lat. 83° 34'N; Long. 162° 15'W. Depth 2300 meters by wire sounding. Time 2120 GMT to 2340

PHOTOGRAPHS OF THE ARCTIC OCEAN FLOOR.



FIG. 1. Arctic Ocean. Locations of sea floor photographs shown by dots 1 and 2. The 200, 2000, 3000, 4000 and 5000 m isobaths are shown. The three major transoceanic topographic features are from east to west. A, the Mid-Oceanic Ridge; B, the Lomonosov Ridge, and C, the Alpha Rise. The photographs were taken on the Alpha Rise.

GMT; 20 December, 1957. This location is also on the south flank of the newly discovered Alpha Rise (Anon. 1957b). Seventy-four exposures were made covering 55 different bottom sites.

BIOLOGY

Life in general and the evidence for life seems rather sparse; however, one series of exposures (DSA-1-3 through DSA-1-22) all taken at about the same place, did show an erect bryozoan colony attached to the mud, an actinarian attached to the edge of an uncovered rock, what appears to be a cup-shaped sponge on the mud, and possibly a holothurian or gastropod on the surface of the mud. The kinky or angular elongate "tracks" which are not connected with one another do not seem to be biogenic (Fig. 2A) although it is difficult to imagine

another source other than biogenic. They might have been produced by some vagrant benthont such as a bottom feeding fish. The mounds that are present in some exposures are probably not biogenic because of the absence of a central cavity (*cf.* Fig. 4D from the Atlantic). These mounds seem to represent rocks covered by sediment. The general picture is one of an area with little life. The holes do not seem typical of holes produced by animals due to their irregularity and angularity. One would expect worm-holes to be in more regular patches, (*cf.* Fig. 2B from the Atlantic) often with tubes protruding. Such is not the case with these. A clam burrow would show certainly a characteristic fringe of sediment around the hole and, in many instances, a pair of holes, one for each siphon. The holes produced by a covered asteroid would be sym-

KENNETH L. HUNKINS, MAURICE EWING, BRUCE C. HEEZEN, AND ROBERT J. MENZIES

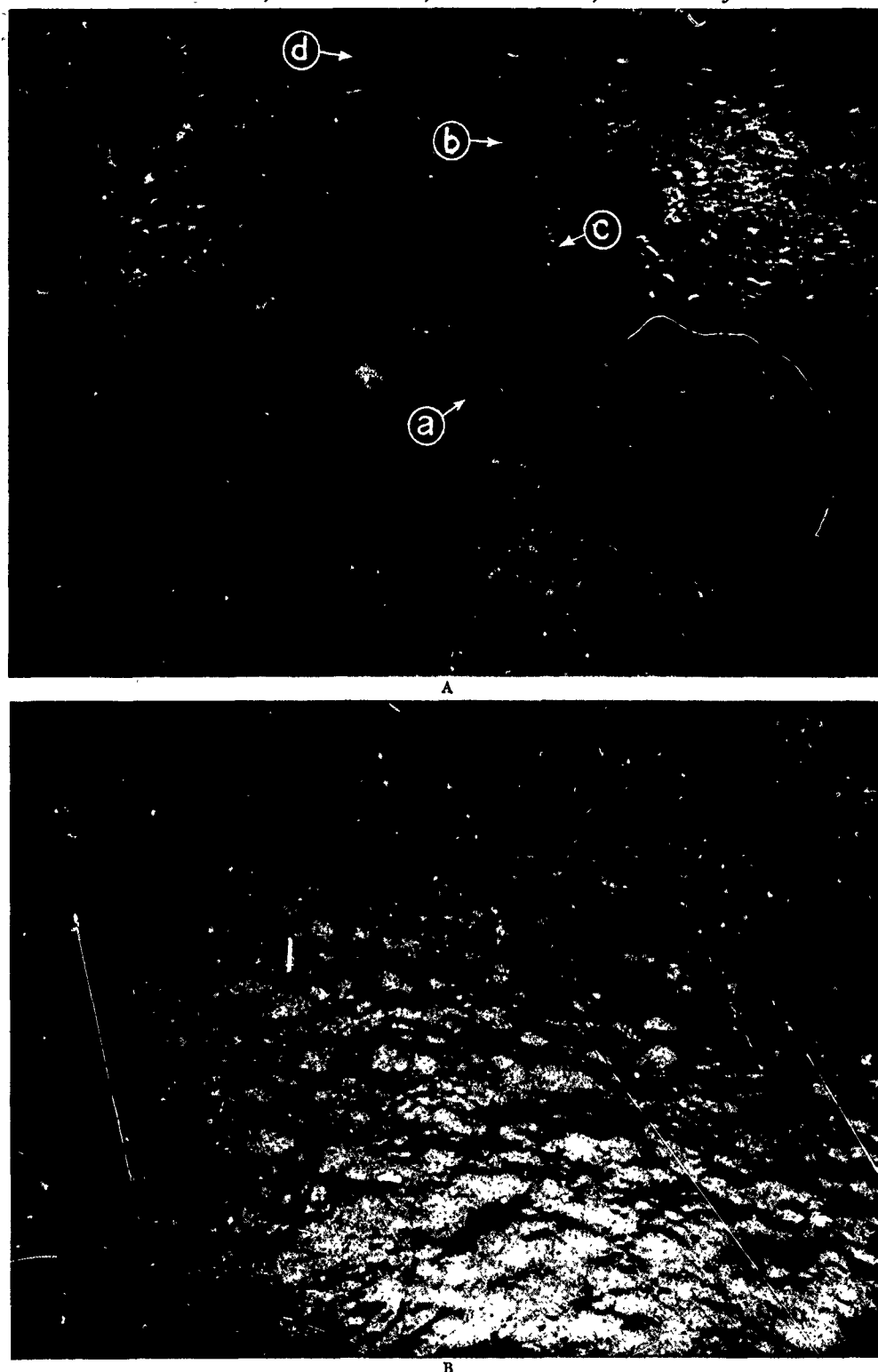


FIG. 2. A. (DSA-1-5) Bottom at Arctic Station A, 2997 m depth, Latitude $83^{\circ}49' N$, Longitude $165^{\circ}05' W$. Note sessile bryozoan colony (a), actinarian attached to rock (b), sponge (c) and gastropod (d), and "tracks" of unknown origin. B. Mounds and holes from Atlantic Station THETA 1-39-95, Latitude $28^{\circ}07' N$, Longitude $14^{\circ}09' W$, depth 800 m.

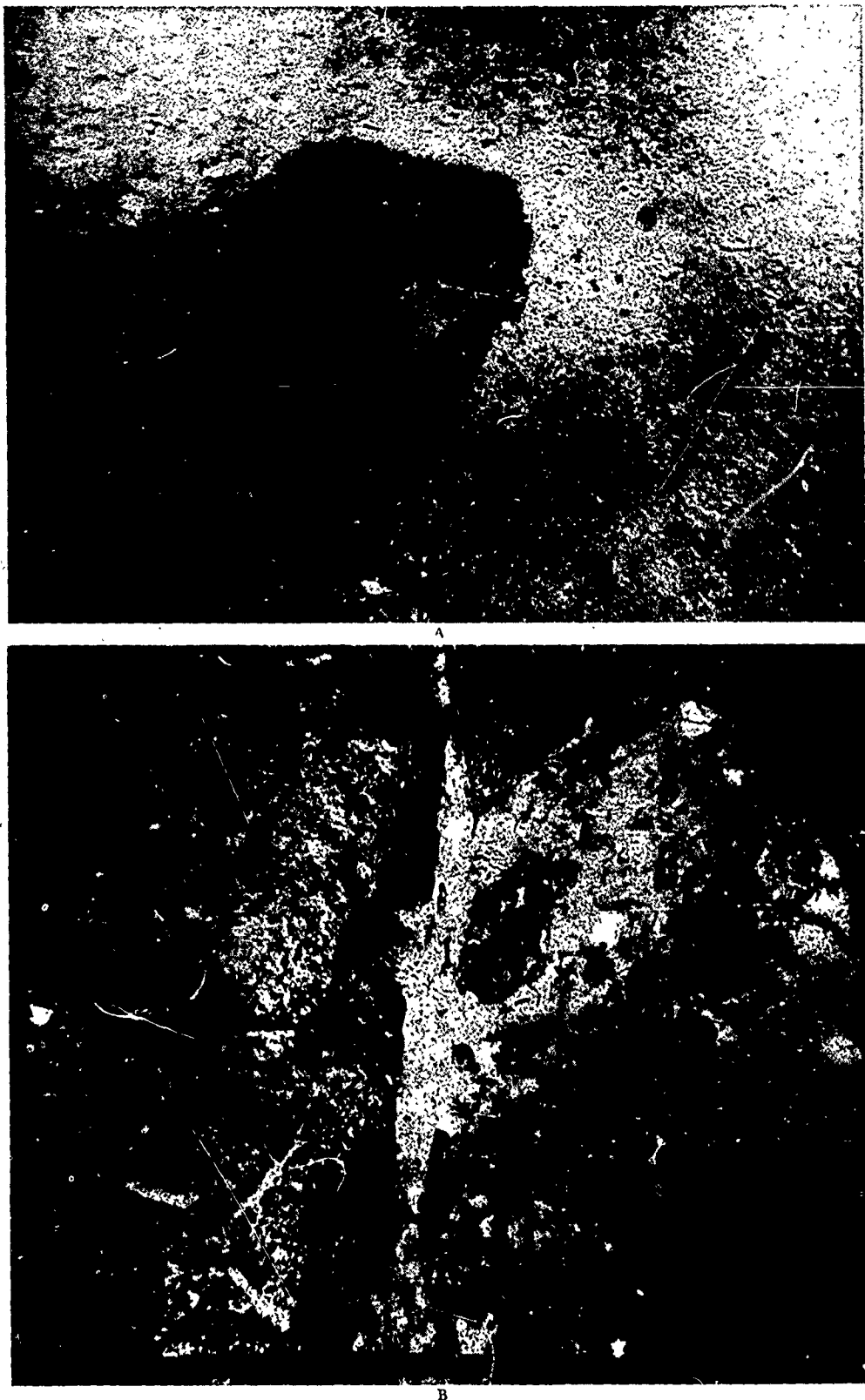


FIG. 3. A. Rock and pebbles on bottom at (DSA-2-61) Arctic Station A, 2370 m depth, Latitude $83^{\circ}34'$ N, Longitude $162^{\circ}15'$ W. Note absence of life. B. Rocks covered with sessile animal life, VEMA 4, 14-36, from Latitude $35^{\circ}12'$ N, Longitude $15^{\circ}22'$ W, and 1935 m depth. A seamount in the eastern Atlantic.

KENNETH L. HUNKINS, MAURICE EWING, BRUCE C. HEEZEN, AND ROBERT J. MENZIES

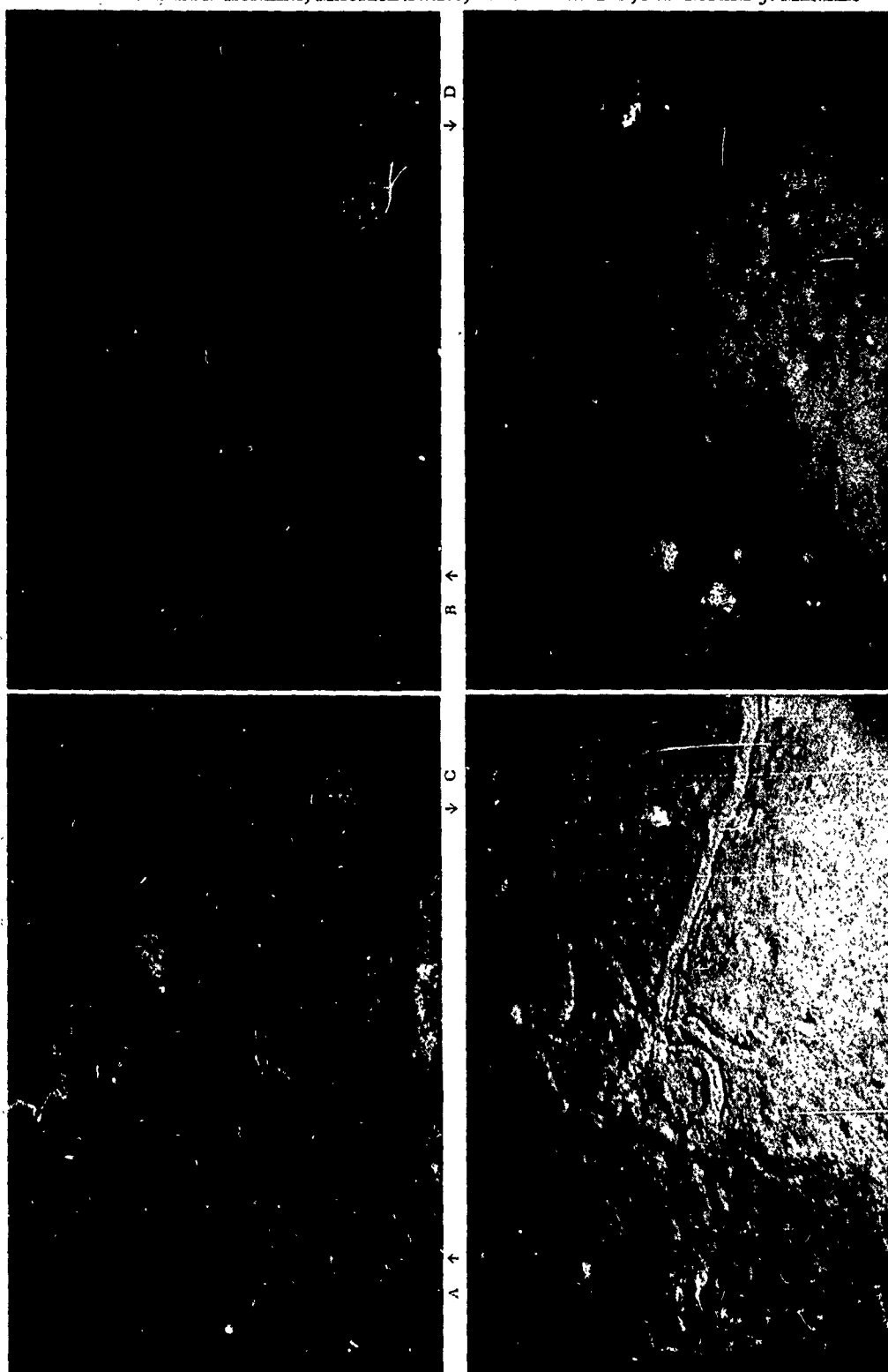


FIG. 4. A. (DSA-1-42) Angular "tracks" from Arctic Station A, at Latitude $83^{\circ}49'$ N, Longitude $165^{\circ}05'$ W; depth 2997 m. B. Mounds from Arctic Station A, (DSA-2-9) at Latitude $83^{\circ}34'$ N, Longitude $162^{\circ}15'$ W; depth 2310 m. C. Animal tracks from THETA 1-39-64, Latitude $28^{\circ}07'$ N, Longitude $14^{\circ}09'$ W; depth 2310 m. D. Animal-produced mounds and holes from THETA 1-39-27, Latitude $28^{\circ}07'$ N, Longitude $14^{\circ}09'$ W; depth 810 m.

PHOTOGRAPHS OF THE ARCTIC OCEAN FLOOR

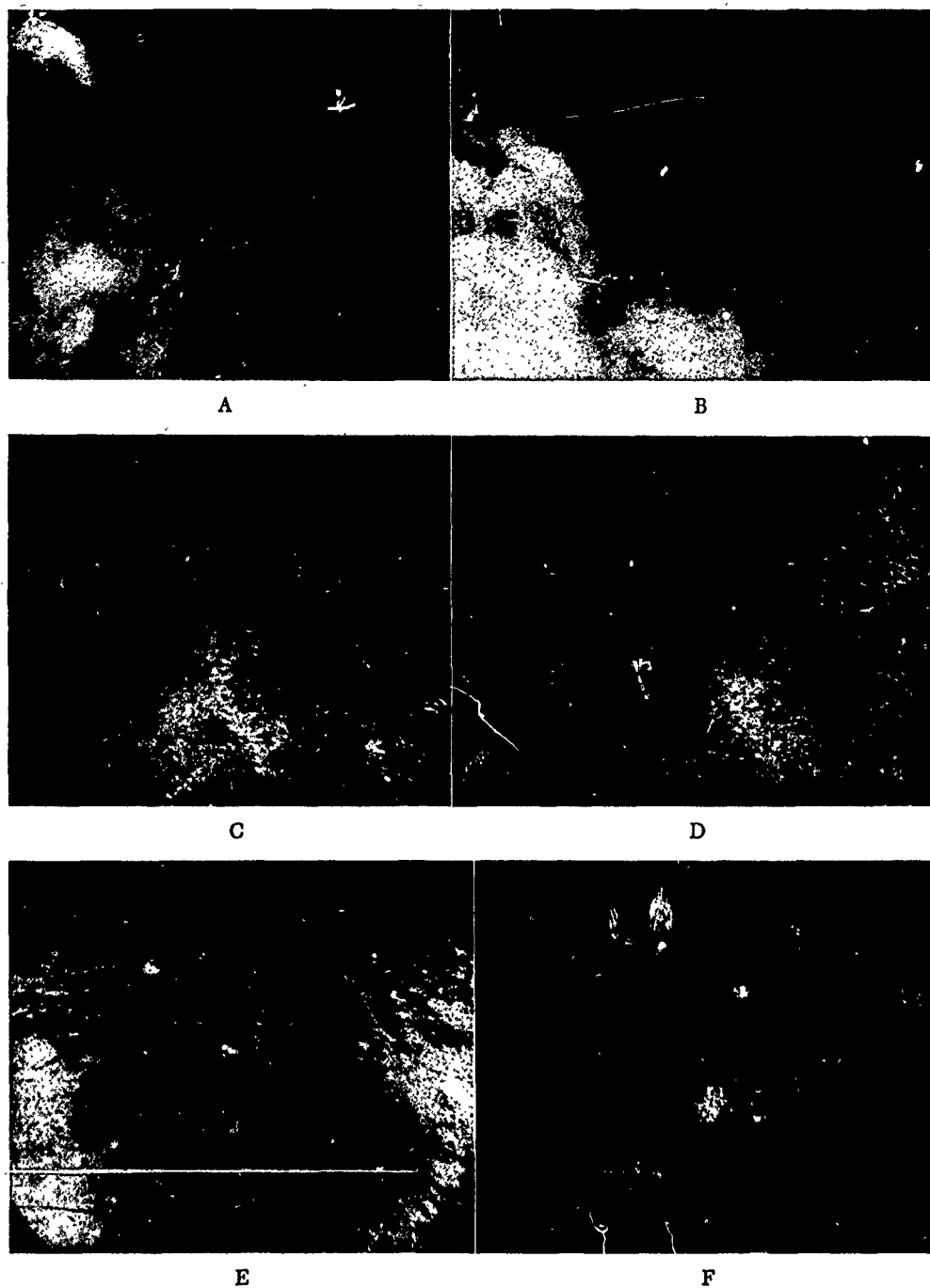


FIG. 5. A.-D. (DSA-2-62 to 65) Movement of sediment cloud across camera field of view, Latitude $83^{\circ}34'$ N, Longitude $162^{\circ}15'$ W; 2370 m depth. Sediment moves to the left and toward the camera against a fixed bottom background, finally revealing impressions, made by the camera on the bottom, in a previous position. E. Buried sea-star from THETA I-13-31; 4725 m depth, Latitude $45^{\circ}42'$ N, Longitude $20^{\circ}38'$ W. F. Atlantic ripple marks from VEMA 4-16-18, 1980 m depth, Latitude $35^{\circ}07'$ N, Longitude $13^{\circ}04'$ W.

metrical (see Fig. 4C' from the Atlantic.) None of these features are revealed in the Arctic photos.

ROCKS

The abundance of rocks on the Arctic ocean floor is one of the more striking features of these photographs. Only three out of 30 sites in DSA-1 failed to show exposed rocks. All 55 sites in DSA-2 revealed rocks. One or two large rocks (about 10 cm diam.) are seen in most of the photos. In addition, many smaller rocks (about 1 cm diam.) are shown; especially by closeups when the camera rested on the bottom. In most cases the rocks are clear of sediment, but in some exposures, partial burial by fine-grain sediment is shown. One photo, Fig. 3A, shows a tabular boulder which is one-half a meter wide and which must exceed one meter in length. This large rock is partially buried and on top of its covering of sediment smaller rocks are found. Evidently some of these rocks have been in position on the ocean floor for a long period and others are continuing to be emplaced. All rocks shown are dominantly angular and the larger ones are tabular.

Examination of dredged material from a nearby area ($84^{\circ} 40'N$, $170^{\circ} 51'W$) reveals an extremely heterogeneous group of pebbles consisting of shale, sandstone, quartzite, white quartz, rose quartz, muscovite, gneiss, etc. All are angular to sub-angular. One shows glacial striae. The angularity, heterogeneity, random distribution of the rocks in the photo and general lack of ripple marks all suggest that the rocks were rafted by ice to their present position. The partial burial of some rocks indicates that the rafting has been taking place over a long period of time.

RIPPLE MARKS

Prominent ripple marks are not shown on any of the photographs. Exposures DSA-1-21 and DSA-1-22 have features which may be interpreted as ripples, but this is not certain. Both photos were taken at low angles of a site which did not reveal ripples when photographed at the normal camera angle.

BOTTOM CURRENTS

Evidence for relatively high velocity bottom currents comes from an unusual and significant source. The camera was accidentally allowed to sit on the bottom several times and took many photographs of the same area of ocean floor. Against the background of the bottom, the mud cloud, stirred up by the camera, drifted while it was being photographed at regular intervals. Two good sequences were obtained (DSA-1-8 to DSA-1-16 and DSA-2-66 to DSA-2-69). The camera takes pictures at approximately 35 second intervals when allowed to rest on the bottom. This information, together with the dimensions of the area photographed, approximately $1.1 \text{ m} \times 0.8 \text{ m}$, allows us to estimate bottom current velocity. In DSA-1-10 through DSA-1-14 the mud cloud raised by the cable which coiled on the bottom drifts across half the picture area (Fig. 5A-D). This gives a velocity of about 0.3 cm/second. In DSA-2-67 through DSA-2-70 the mud cloud raised by the camera contacting the bottom crosses nearly the whole photo area. A velocity of about 0.6 cm/sec is indicated.

The possibility that the sediment cloud had settled instead of being moved by current was considered. Experimentation indicates this is not the case. A sample of bottom sediment from $83^{\circ} 53'N$, $168^{\circ} 42'W$ was stirred in sea water and allowed to settle. The material was extremely fine grained and at least one-half hour was required to clear a 30 cm column to transparency again. Thus it seems unlikely that the sediment cloud in the picture could have settled in a period of only several minutes, which is the length of time taken for it to disappear from the camera's field.

HOLES

All of the pictures show shallow depressions or holes on the ocean bottom. Some of these holes are round, others are linear or linear with small kinks and angular bends. The round holes average about 1 cm in diameter. The linear holes vary from 1 to 10 cm in length and are about one-

PHOTOGRAPHS OF THE ARCTIC OCEAN FLOOR

fourth to one-eighth as wide as their length. The pictures taken at Station 1 show a greater abundance of holes than those taken at Station 2.

The holes with the sharpest outline, apparently the most recent ones, all have a raised ridge around the edge.

The round holes probably are due to the fall of ice-rafted rocks. Similar holes were produced experimentally by dropping pebbles into a seawater tank having a sediment floor. The linear holes are more difficult to explain. A biological explanation is possibly indicated but no wholly satisfactory mechanism has yet been suggested.

MOUNDS

Camera Station 2 differs from Camera Station 1 in showing numerous mounds in several pictures (Fig. 4B). The mounds are all roughly similar, being shallow domes of several centimeters in diameter. It is believed that these mounds are primarily sediment-covered rocks. The absence of axial holes, characteristic of biological holes, supports this conclusion.

BOTTOM SEDIMENT

Except for rocks and pebbles, the bottom surface sediment is probably composed of foraminiferal lutite. The sediment clouds stirred up by the cable and camera striking bottom gives evidence that the sediment is soft and fine-grained. Below the fine, unconsolidated few centimeters of surface layer there must exist a fairly firm layer as shown by shallow marks left by the cable and camera when they struck bottom, (DSA-1-8 to DSA-1-16 and DSA-2-68, 69).

Surface sediment as determined by sampling in nearby areas is a brownish, weakly foraminiferal lutite. A bottom core was taken at DSA-2 but an analysis is not yet available.

COMPARISON OF ARCTIC AND ATLANTIC PHOTOS

The irregular holes shown in Figure 2A from the Arctic at a depth of 2997 m should be compared with the regular and clumped worm holes shown in Figure 2B from the Atlantic at 800 m depth. The irregular and random distribution of the holes shown in the Arctic bottom photograph argue that they are not biologic in origin.

Typical animal tracks from the Atlantic at 2310 m are shown in Figure 4C where the continuity of the tracks is quite unlike the irregular, angular and discontinuous "tracks" shown in Figure 4A (DSA-1-41) from the Arctic at 2197 m.

The mounds of Figure 4B from the Arctic are unlike typical animal-produced mounds from the Atlantic Figs. 2B and 4D which have a more angular peak and a central or axial cavity. Often in Atlantic photos one sees the pentangular holes produced by covered asteroids. This is shown in Figure 5E from 4725 m depth.

An exposed tabular rock which is from the Arctic is virtually devoid of life (Fig. 3A) should be compared with an exposed rock covered abundantly with (Fig. 3B) sessile animal life.

Ripple marks are frequently encountered in Atlantic bottom photos Fig. 5F. In the Arctic photographs no distinct ripples are shown. Since not all Atlantic bottom photos show ripples, the apparent absence of ripples at two Arctic localities is hardly conclusive proof of their absence in the Arctic.

REFERENCES

- ANON. 1957a. Arctic Program. IGY Bull. No. 4, Trans. Amer. Geophys. Union, 38: 824-830.
 ANON. 1957b. Arctic Ocean submarine ridges. IGY Bull. No. 6, Trans. Amer. Geophys. Union, 38: 1016-1019.
 EWING, M., A. VINE, AND J. L. WORZEL. 1946. Photography of the ocean bottom. Journ. Optical Soc. Am., 36: 307-321.
 HEEZEN, B. C., M. THARP, AND M. EWING. 1959. The floors of the oceans. Geol. So. Am., Special Paper 65, 122 pp.

**Some Biological Oceanographic Observations
in the Central North Polar Sea, Drift Station
Alpha, 1957 - 1958**

T.S. English

Reprinted from the
SCIENTIFIC REPORT NO. 15, CONTRACT AF 19(604)-3073,
Arctic Institute of North America, 1961
(Part II, oceanographic data, omitted. See compilers' note.)

TABLE OF CONTENTS

	<u>Page</u>
Abstract	vii
PART I	
General	1
Some Features of the Environment	3
Methods	5
Vertical Structure of the North Polar Sea	7
Seasonal Cycles in the North Polar Sea	9
Incident and Submarine Solar Radiation	13
Distribution of Chlorophyll 'a'	16
Net Phytoplankton and Standing Crop	18
Production in Leads and Ponds	18
Inorganic and Organic Nutrients	20
Studies of Photosynthesis	21
Annual Production	21
Literature Cited	25
PART II	
Oceanographic Data: June - October 1958	33
Data from Oceanographic Stations - 1958	41
Plant Pigments - 1958	53
Carbon-14 Experiments - 1958	63
Submarine Daylight - 1958	69
Temperatures by Thermistor - 1958	77

LIST OF FIGURES

	<u>Page</u>
1. Track described by Drift Station Alpha, 1957-1958.	4
2. Temperature, salinity, and dissolved oxygen from Drift Station Alpha, 23-24 June 1958. Included are temperatures obtained by thermistor.	8
3. Inorganic nutrient concentrations with depth, Drift Station Alpha, 19 August 1958.	10
4. Chlorophyll <u>a</u> concentrations in a 1 square meter water column, Drift Station Alpha, 1957. The concentration in the 5-20 meter water column is shown for all sampling dates; the concentration in the surface-5 meter water column is shown only for sampling dates when it was possible to work at a lead.	11
5. Chlorophyll <u>a</u> concentrations integrated for a 1 square meter water column from 4 to 64 meters, Drift Station Alpha, 1958. Photosynthetic potential is indicated as carbon fixation in a sample from 6 meters held at 200 foot-candles; experiments were made only on dates indicated by heavy lines.	12
6. Relationship between visible radiation, snow cover, and concentration of chlorophyll <u>a</u> , Drift Station Alpha, 1957-1958. Chlorophyll <u>a</u> concentrations were determined from samples taken at 5 meters through February 1958 and from samples taken at 6 meters thereafter.	14
7. Attenuation of 425 millimicra radiation in open water and beneath an ice floe, Drift Station Alpha, July 1958.	15
8. Chlorophyll <u>a</u> concentrations with depth for intervals through the productive season. Drift Station Alpha, 1958.	17
9. Relative photosynthesis, expressed as carbon fixation in samples held under 2000 foot-candles illumination, and relative chlorophyll <u>a</u> concentrations, Drift Station Alpha, 20 July-13 August, 1958.	22
10. Relative photosynthesis from six experiments on samples taken at 6 meters, Drift Station Alpha, 1958.	23
11. Relationship between photosynthetic potential, expressed as carbon assimilation, and chlorophyll <u>a</u> concentration, Drift Station Alpha, 1958.	24

ABSTRACT

IGY Drift Station Alpha was a base for oceanographic observations in the Central North Polar Sea in 1957 and 1958. Water masses were recognized by temperature and salinity characteristics: Arctic Upper Water of low salinity and low temperature; Arctic Intermediate Water with a sharp halocline from about 50 to 200 meters; Pacific Ocean Water of variable temperature intruding as a layer in the Arctic Intermediate Water; Atlantic Water between the upper and lower 0°C isotherms; and Arctic Deep Water below, colder than 0°C. The position of the Pacific Ocean Water was confirmed by the distributions of dissolved oxygen, nitrate-nitrogen, phosphate-phosphorus, and silicate-silicon.

Primary production is limited to the relatively dilute Arctic Upper Water which is freely convective and characterized by homogeneity of the observed variables with depth. When ice melts, water of slightly higher temperature and much lower salinity is added at the sea surface. The maximum change observed in the Arctic Upper Water was only several tenths of one degree centigrade and several tenths of one part per mille salinity. Nutrient enrichment proceeds by slow mixing across the substantial density gradient.

The major seasonal environmental change in the North Polar Sea is the amount of visible radiation penetrating into the ocean. Radiation available for photosynthesis is increased by ablation of the snow cover, a decrease in the thickness of the ice floes, the formation of ponds on the floes, any decrease in albedo, and the formation of leads. Maximal radiation in the sea lags behind surface radiation, occurring after ablation of the snow cover and the formation of ponds. An average ice floe appears to reduce the depth of the euphotic zone to less than one-half of the depth of the freely convective layer.

The concentration of chlorophyll a was used to obtain an estimate of the time of maximum phytoplankton populations and as a relative measure of production and photosynthetic potential. Maxima of chlorophyll a were in late July and early August; maxima were at and above 16 meters depth, occasionally in water between floes. A fine net retained less than 10 percent of the chlorophyll a retained by a Millipore filter, suggesting that most photosynthetic organisms were small enough to pass through the meshes.

The carbon-14 technique was used to study the variations in photosynthesis with light intensity, chlorophyll a concentration, and sampling depth. The phytoplankton population is apparently not adapted for low light intensities; there is an increasing proportion of photosynthetically inactive chlorophyll a with depth; and the ratio of carbon uptake to chlorophyll a concentration is lower than that reported for lower latitudes.

The production in ponds and leads does not add a significant amount to the annual total. There is no evidence that meltwater from the ice floes contains any substances beneficial to plant growth. Primary production in the North Polar Sea is very low relative to other ocean areas. The productive season is short and all indices of productivity are low. The limiting amount of submarine illumination can be shown to serve as a satisfactory first order explanation.

SOME BIOLOGICAL OCEANOGRAPHIC OBSERVATIONS IN THE CENTRAL
NORTH POLAR SEA, DRIFT STATION ALPHA, 1957-1958¹

PART I

The difficulties of locating and maintaining a base for scientific studies on the permanent ice pack in the North Polar Sea have severely limited work accomplished in the past. Until the International Geophysical Year, few scientific programs included biological oceanography. Studies of organisms in the North Polar Sea were made by the Norwegian North Polar Expedition, 1883-1896, the Russian expeditions beginning in 1937 with the ice floe station North Pole I, and the American outpost of Fletcher's Ice Island (T-3) first occupied in 1952.

Nansen (1902) summarized biological conditions in the North Polar Sea as they were understood after the FRAM Expedition. He said that phytoplankton was sparse because of the thick ice which passes little light into the sea and also because of the very low water temperature. He said that increased light received by the channels between the floes had slight effect because of their transience and their covering of nearly fresh water during much of the summer. In confirmation, Gran (1904) reported the phytoplankton samples of the FRAM to be deficient in species and specimens of diatoms. Nansen did not make chemical analyses, but reasoned that water under the ice was rich with accumulated inorganic nutrients (nitrogen compounds, phosphoric acid, and silicate) supplied by rivers. In support of his conclusion, he cited the enormous development of diatoms where polar currents are no longer ice-covered and meet warmer water from the south.

Sverdrup (1929), on the basis of several series of oxygen measurements in the Chukchi and East Siberian Seas from the MAUD, concluded that, "the presence of ice prevents the development of phytoplankton, but that this development suddenly increases as soon as the surface becomes free of ice."

Braarud (1935), working in the Denmark Strait south of the permanent ice pack, encountered Polar Water and studied the phytoplankton and its conditions of growth. He demonstrated that Polar Water emerging from the ice cover supported a phytoplankton increase which exhausted the supply of nutrient salts. He stated, "Since the phytoplankton production in Polar waters takes place as soon as the ice opens, without any mixture with Atlantic water, regardless of the low temperature of Polar waters, it must be the lack of light under the ice and not the low temperature which prevents a large plant production from taking

¹This work was initiated when the author was serving with the Arctic Aero-medical Laboratory, Ladd Air Force Base, Alaska. Later work was partially supported by the Office of Naval Research, Contract Nonr-1138(03) with the Arctic Institute of North America and by the National Science Foundation IGY grant, NSF Y/9.18/144, to the Woods Hole Oceanographic Institution.

place in the areas of very close pack ice." Braarud demonstrated that Nansen's belief that rivers at the periphery of the Polar Basin supplied abundant nutrients to a surface layer of the ocean is incorrect on two grounds: (1) "...the content of nutrient salts in the river water is usually much smaller than that of the deep layers in the sea," and (2) "...the surface layers of the Polar Sea...main constituent is waters from deeper strata in the Polar basin, which accordingly also contribute the main part of their content of inorganic salt."

Braarud used the observations of the Norwegian North Polar Expedition as an indication that production under the permanent ice pack probably never depletes the nutrient supply. He believed that winter mixing would re-establish the nutrient supply in the surface layer if it had been reduced in the summer and stated clearly that the source of nutrient salts in Polar Water is from waters below the productive zone. His contribution to these problems included insights into the species and sizes of phytoplankton organisms to be expected under the permanent ice pack, and the knowledge that nets would probably not capture representative samples of nanoplankton. In short, Braarud clearly indicated the direction to be taken in future work in the North Polar Sea.

Shirshov (1938 and 1944), on North Pole I, found that a seasonal cycle of phytoplankton does occur under the permanent ice pack and that the maximum population, expressed as chlorophyll in an alcohol extract of phytoplankton taken by a net, occurs in August. The early marine biological work on Fletcher's Ice Island (T-3) concentration on zooplankton collections (Mohr, 1959).

The observations of the Russian Scientific-Research Drifting Station of 1950-1951 (North Pole-II) reported by Gudkovich (1955) are a significant addition to knowledge of the physical and chemical environment of the North Polar Sea. Brodskii and Nikitin (1955) reported the biological observations, but included only seven stations at which phytoplankton was collected with a net.

The earlier work gives scant information on primary (photosynthetic) production under the permanent ice pack. Several lists of phytoplankton species are available (Gran, 1904; Shirshov, 1938; Brodskii and Nikitin, 1955), but samples were taken with nets. There was almost no knowledge of the seasonal cycles and variations in the standing crop of phytoplankton before 1957. When the opportunity to work from Drift Station Alpha became available, it appeared that a study of aspects of primary productivity and a series of phytoplankton samples taken with water-sampling bottles would be a useful addition to our understanding of the biological oceanography of the North Polar Sea. An effort was made to carry out a similar program at Fletcher's Ice Island (T-3) (Apollonio, 1959).

Some Features of the Environment²

Drift Station Alpha was an IGY camp located on a large ice floe of the permanent arctic ice pack. From the initial occupation of the station in April 1957 to the abandonment in November 1958, the drifting floe described a course in the center of the North Polar Sea (Figure 1). The center of the North Polar Sea has been called the Ice Pole and the Pole of Inaccessibility. There, rather than at the North Geographic Pole, one encounters the extreme climatic and biological conditions of the arctic seas, an area of roughly 5 million square kilometers. The apparent widespread uniformity of the environment beneath the permanent ice pack suggests that the results of these studies can be applied with some confidence over a large sea area, recognizing that polar conditions moderate toward the edge of the pack.

The average thickness of the floes of the permanent ice pack has been estimated to be 2.5 meters (Timofeev, 1960), ranging from a surface slush to regions where several floes have been superposed. Shirshov (1938) indicated that large areas of floe were about 3 meters thick, and much of the floe area near Drift Station Alpha was equally thick. Ridges of broken ice called hummocks may be as high as 10 meters, but seldom exceed 3 meters and were commonly observed to be only 1-2 meters. Observations suggest that hummocks may cover about 1 per cent of the floe surfaces. While diving under floes, areas were observed where several thicknesses of floe extended 15 meters below the sea surface, but the width of such areas was scarcely more than 10 meters. Thickness was observed to change little during the melt season, as ablation was slight; 7-10 centimeters in 1957 and about 30 centimeters in 1958.

The amount of open ocean between the floes, in channels called leads or lanes, has been estimated to be as low as 1 per cent and as high as 5-10 per cent (Transehe, 1928; Timofeev, 1958). Our observations and verbal reports of others flying over the North Polar Sea indicate that even at the season of minimum ice cover the usual extent of open ocean is much closer to the lower estimate, with less open water near the center of the ice pack and progressively more open water toward the edge. The first lead examined opened on 15 June 1957 and by 26 June the surface ceased to freeze. Slush began to form on open leads on 29 August 1957.

In the area of these studies, the ice is covered with a layer of wind-packed snow for over 10 months of the year. Ablation begins after the return of the sun and continues until the snow cover is removed and some of the underlying ice has melted at which time the ice surface becomes granular and resembles firn.

²Micrometeorologists from the Department of Meteorology and Climatology, University of Washington, provided the data on snow cover, ablation, and incident solar radiation. I am indebted to Norbert Untersteiner, Franklin I. Badgley, Arnold M. Hanson, and William J. Campbell for their generous assistance.

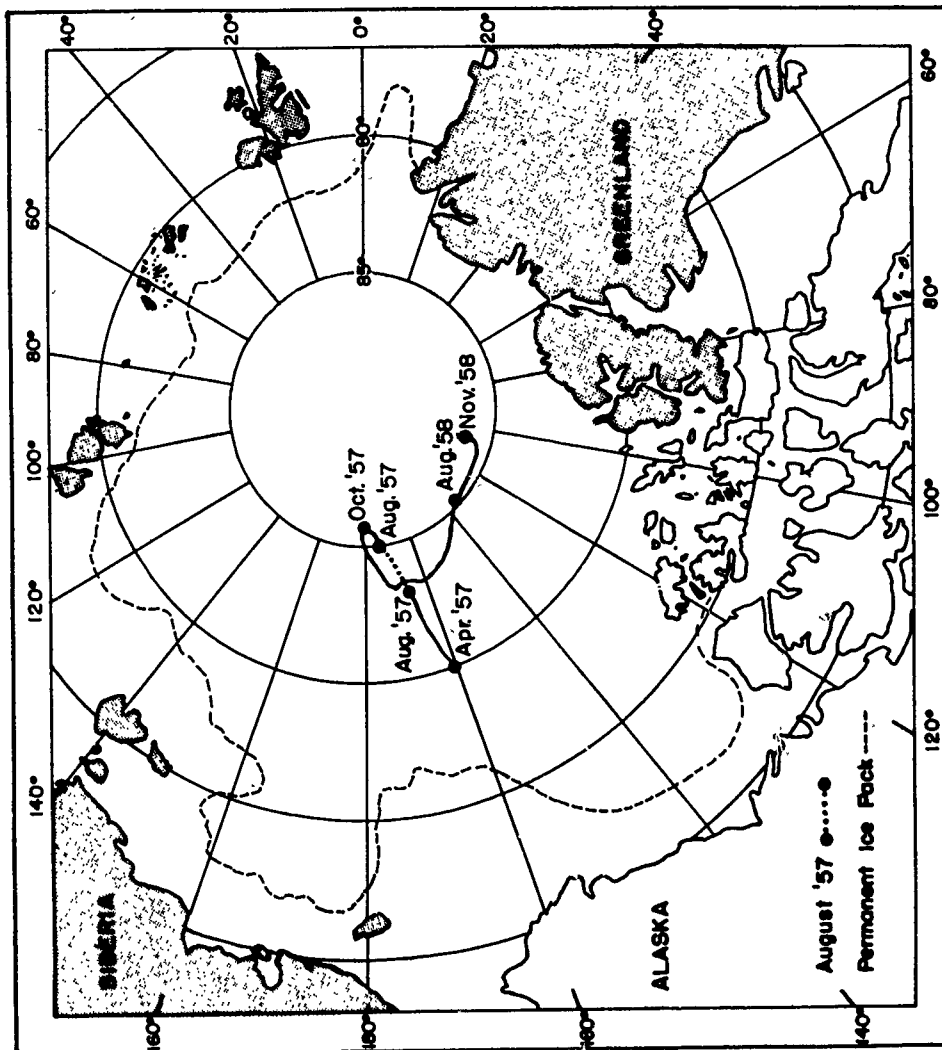


Figure 1. Track described by Drift Station Alpha, 1957 - 1958.

The amount of ice melted may vary considerably from year to year and must also vary with the position of a floe in the North Polar Sea.

Ponds of meltwater became visible on the floes in the first week of July in 1957 and 1958. By examining aerial photographs, and by flying over the pack, ponds were estimated to cover from 15-30 per cent of the floe surface in the area of study.

Meltwater runs off the floes and into cracks and leads. Near the edge of the pack, floes apparently melt through and drain into the ocean. As old pack ice is almost fresh water, with a salinity usually less than 3 per mille, the runoff forms a layer on the more dense ocean. The layer varies in thickness with the size of the watershed, the intensity of melt, floe movement, wind mixing, and the extent of the leads. The interface between the meltwater and the ocean was usually observed at a depth between 1 and 2 meters.

In late August the pond surfaces froze, the leads began to freeze, and the entire area was covered with the snow of a new winter. The effects of these seasonal changes on the biological and hydrographic cycles were a major part of the field study.

Methods³

Hydrographic stations were occupied irregularly at the beginning of the study, but weekly observations were obtained during the last summer season. Nansen bottles with deep-sea reversing type thermometers were lowered through a hole in the floe. A thermistor with a high relative accuracy was used to study the vertical temperature distribution in the near-surface water.

Salinity and total phosphorus samples were sent to the Woods Hole Oceanographic Institution for analysis. Total phosphorus was determined by the method of Ketchum *et al.* (1955). Other analyses were carried out on the ice floe station: phosphate-phosphorus by the method of Robinson and Thompson (1948); nitrate- and nitrite-nitrogen by the method of Mullin and Riley (1955); silicate-silicon by a method described by Dienert and Wandenbulcke (1923); and dissolved oxygen by the Winkler method (Thompson and Robinson, 1939).

Water samples were taken for plant pigment extraction, carbon-14 studies, and phytoplankton cell counts. In 1957 samples were obtained with a 4-liter glass snatch bottle at the surface, 1, 2, 5, 10, and 20 meters, beyond which the bottles imploded. In 1958 modified Emsworth samplers (Carruthers *et al.*, 1950) of lucite and teflon-coated metal were used to take routine samples at 4, 6, 8, 16, 32, and 64 meters. Samples were taken through holes chipped through the floe or from the side of the floe. In 1958 some samples were obtained under the ice floes while the author was swimming in self-contained underwater breathing apparatus.

³ A more thorough statement of methods employed and data obtained is contained in Part II of this report.

Plant pigments were extracted from 4-liter samples except when filtration was unusually slow. Some samples of 20 liters were concentrated by a fine-meshed (No. 20) plankton net and resuspended. Samples were filtered through 47-millimeter HA Millipore filters which were stored in a dark, evacuated desiccator at about 0° centigrade. The concentration of plant pigments was measured spectrophotometrically in an acetone extract by the method of Richards with Thompson (1952), as modified for use with the Millipore filter by Creitz and Richards (1955). Some further modifications of the procedure were necessary.

The acetone extract was cleared with a clinical centrifuge which did not uniformly and completely remove all particles from suspension. Plant pigment concentrations were so low that many of the samples had to be examined in a cell providing a 5-centimeter light path. Those samples were examined at 750 millimicra and that absorption subtracted from the absorption at other wave-lengths as a correction for non-selective scattering. This is a minimal correction which attempts to reduce the elevation of the visible spectrum caused by non-selective scattering, but does not reduce any errors introduced by selective absorption. The correction has been effective in reducing several unusually high results to values comparable with other series of observations.

Photosynthesis was determined by the carbon-14 technique of Steeman Nielsen (1952). Experimental bottles were washed with a detergent, rinsed with dilute hydrochloric acid, and given several rinses with distilled water. In 1957 bottles of 250-milliliter capacity were used; in 1958 bottles of 150-milliliter capacity were used. The carbon-14 solution was contained in sealed ampoules; it was approximately 20 microcuries/milliliter. The desired volume of solution was transferred to the bottom of the bottle with a hypodermic syringe and the bottle agitated vigorously. There was no provision for agitating the bottles during the experiments.

In 1957 in situ experiments of 12- and 24-hour duration were conducted. In 1958 the sample bottles were held in a box filled with sea water pumped from beneath the floe. They were exposed to light supplied from a bank of 10 day-light fluorescent tubes for 6- or 12-hour periods. The maximum illumination was approximately 2000 foot-candles. Dark bottles were prepared for each depth sampled or each experimental condition. A series of Wratten neutral density filters were placed over four of the light bottles to extinguish 50, 75, 90, and 99 per cent of the light.

Some experiments were made to ascertain the effects of adding dissolved inorganic nutrients to samples of sea water. One-milliliter portions were added from ampoules to increase the concentration in the sample bottle by 50 microgram atoms/liter of nitrate-nitrogen or 5 microgram atoms/liter of phosphate-phosphorus. In each experiment the nutrients were added both singly and in combination; two control samples were maintained.

At the completion of an experiment samples were filtered onto 25-millimeter HA Millipore filters and rinsed with 0.001 normal hydrochloric acid in a 3 per cent solution of sodium chloride (Ryther and Vaccaro, 1954). Filters were stored in a dark, evacuated desiccator. Standardization and sample counts were made in a gas flow Geiger counter at the Woods Hole Oceanographic Institution. The amount of photosynthesis was calculated by the method of Steeman Nielsen (op. cit.), but with no correction for respiration.

Solar radiation was measured continuously with a Moll Solarimeter manufactured by Kipp. Readings in millivolts were converted to gram calories/square centimeter/minute. This is considered to be visible radiation, although the response of the instrument actually covers a somewhat broader spectral band (0.3 to 3.0 millimicra).

Submarine daylight was measured with a photometer of the type described by Holmes (1957). The photosensitive element was a Weston 856RR Photronic cell. The output of this submarine cell was measured with a Rawson model ADEAR microammeter, an instrument with 100 ohms internal resistance on scales covering the ranges from 0-50, 0-100, 0-200, 0-500, and 0-1000 microamperes. Another cell was connected to a less sensitive microammeter and was used to detect changes in incident solar radiation. The submarine photometer was fitted with filters under the diffusing glass cover. The peak transmissions of the filters were: red, 650 millimicra; green, 525 millimicra; and blue, 425 millimicra.

A smaller light meter was carried by divers to make measurements under the ice floes in places it was difficult to carry the larger instrument. It consisted of a General Electric photographic exposure meter mounted in a water-tight lucite case.

Vertical Structure of the North Polar Sea

Nansen (1902) described the major hydrographic features of the North Polar Sea. The details of surface and deeper circulation have been rather fully, though perhaps not definitively discussed. The results from Drift Station Alpha agree with the earlier description and add some details to our knowledge of the surface water mass. Temperature and salinity, and the derived density, may be used to differentiate the water masses (Figure 2). Following Timofeev (1953), one can divide Nansen's Polar Water into Arctic Upper Water of low salinity and temperature and Arctic Intermediate Water with generally increasing temperatures and a sharp halocline ranging from about 31 per mille at 50 meters to over 34 per mille at 200 meters. The warmer mass of Atlantic Water, defined as the layer between the upper and lower 0° centigrade isotherms, lies below the Arctic Intermediate Water and above the Arctic Deep Water which continues to the ocean bottom.

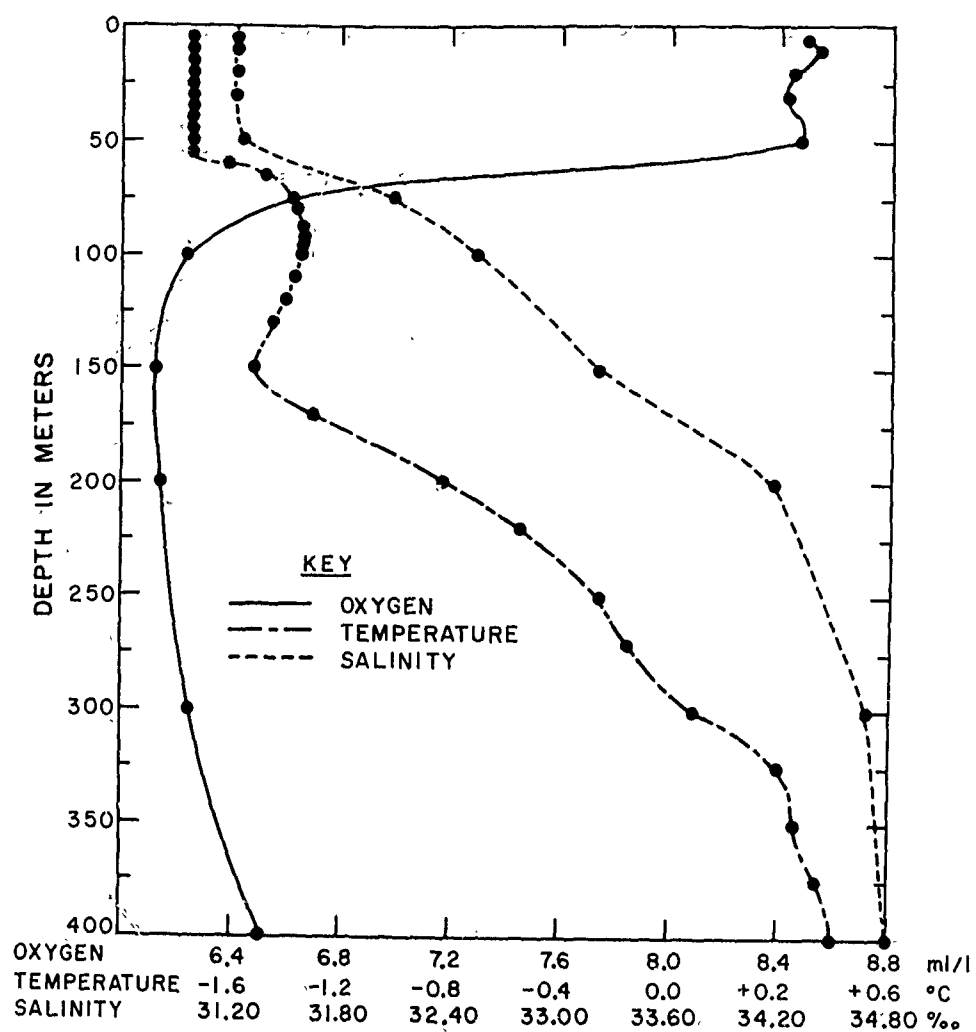


Figure 2. Temperature, salinity, and dissolved oxygen from Drift Station Alpha, 23-24 June 1958. Included are temperatures obtained by thermistor.

Gudkovich (1955) recognized a Pacific Ocean Water stratum intruding between the Arctic Upper Water and Arctic Intermediate Water. He gave an extreme temperature range of -0.7 to -1.2° centigrade and a salinity of about 32 per mille. Coachman and Barnes (in press) suggest that the intrusion of Bering Sea Water into the Arctic Ocean is responsible for both the temperature maximum (here 75-100 meters) and the temperature minimum below (here at 150 meters) as a result of mixing with appropriate amounts of shelf water in summer and winter. The latter interpretation is given strong support by the vertical distribution of dissolved oxygen and of inorganic nutrients observed from Drift Station Alpha (Figures 2 and 3).

The vertical homogeneity of observed oceanographic variables in the Arctic Upper Water, as well as the rapid attainment of uniform temperature and salinity with depth, indicate that mixing in this stratum is rapid and complete. However, nutrient enrichment of the Arctic Upper Water must proceed very slowly. The pronounced halocline (pycnocline) constitutes a substantial barrier to mixing nutrients from the observed maxima at 100-150 meters in the Pacific Ocean Water into the Arctic Upper Water. A persistent temperature minimum (about -1.7° centigrade) between the Arctic Upper Water and the Pacific Ocean Water encountered in temperature profiles from 1958 suggests that there is no mixing across that isotherm during the summer season, though there may be some years in which that barrier is broken.

Seasonal Cycles in the North Polar Sea

With the progression of the summer season changes were observed in the Arctic Upper Water. There was a slight decrease in salinity (several tenths of 1 per mille), a slight increase in temperature (several tenths of 1 degree centigrade), an increase in dissolved oxygen, and the obvious increase in the amount of solar radiation penetrating into the ocean. Accepting the assumption that the size of the phytoplankton population can be estimated from the concentration of chlorophyll *a*, the population was ten times as large in late July and early August as it was in early June (Figures 4 and 5). Results from carbon-14 experiments through most of the 1958 productive season indicate that the photosynthetic potential of the phytoplankton varies in a manner similar to that of the chlorophyll *a* concentration (Figure 5). The observations were inadequate to demonstrate any decrease in inorganic nutrients caused by the production of phytoplankton.

Shirshov (1944) noted the seasonal phenomena only in the upper 25 meters near the periphery of the permanent ice pack northeast of Greenland. This corresponds to his observation that the Arctic Upper Water extends to a depth of 20-30 meters in the south and 50-75 meters in the north. Shirshov also noted seasonal changes in the zooplankton, which remained in the "winter state" in July. The productive season is so short that the area is the extreme example of a monocyclic sea (Bogorov, 1938).

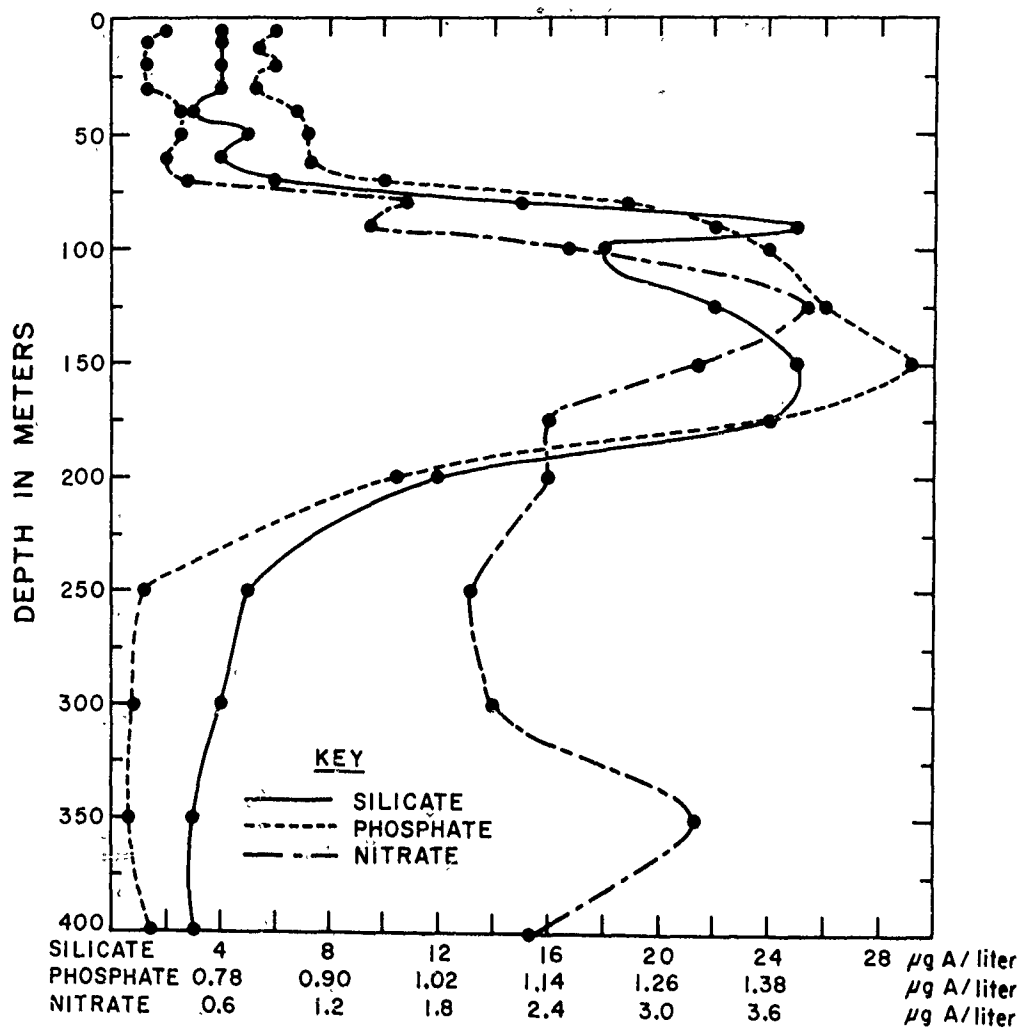


Figure 3. Inorganic nutrient concentrations with depth, Drift Station Alpha, 19 August 1958.

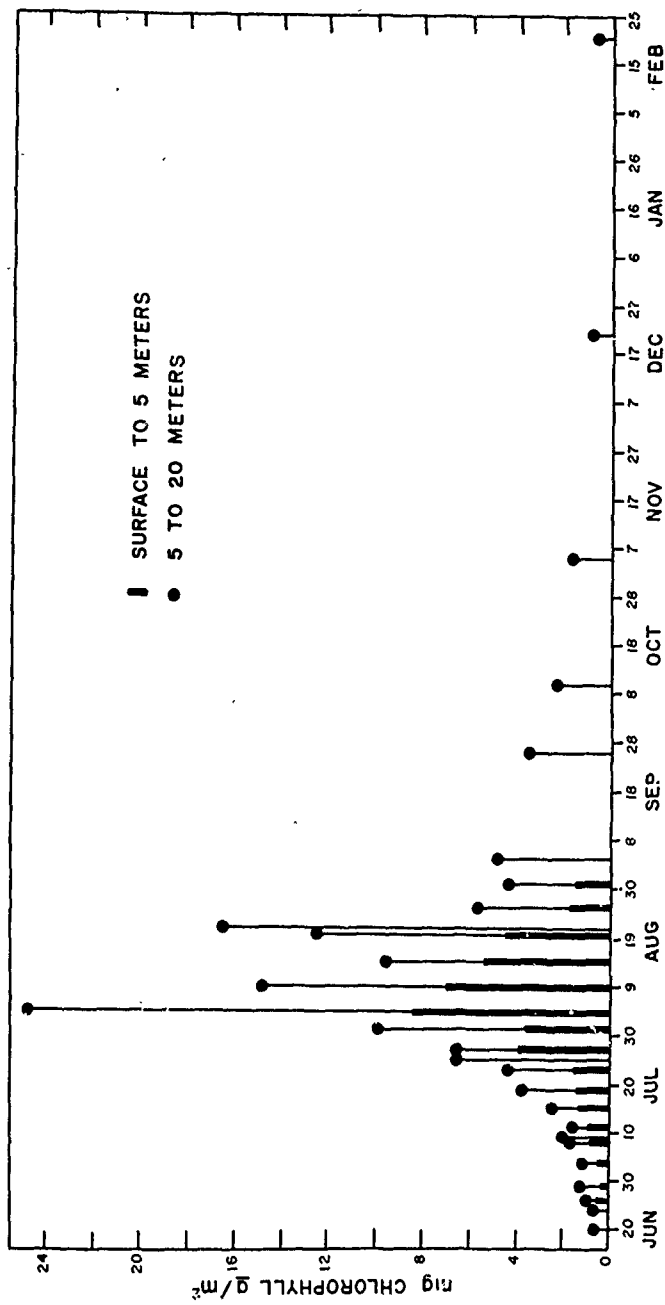


Figure 4. Chlorophyll a concentrations in a 1 square meter water column, Drift Station Alpha, 1957. The concentration in the 5-20 meter water column is shown for all sampling dates; the concentration in the surface-5 meter water column is shown only for sampling dates when it was possible to work at a lead.

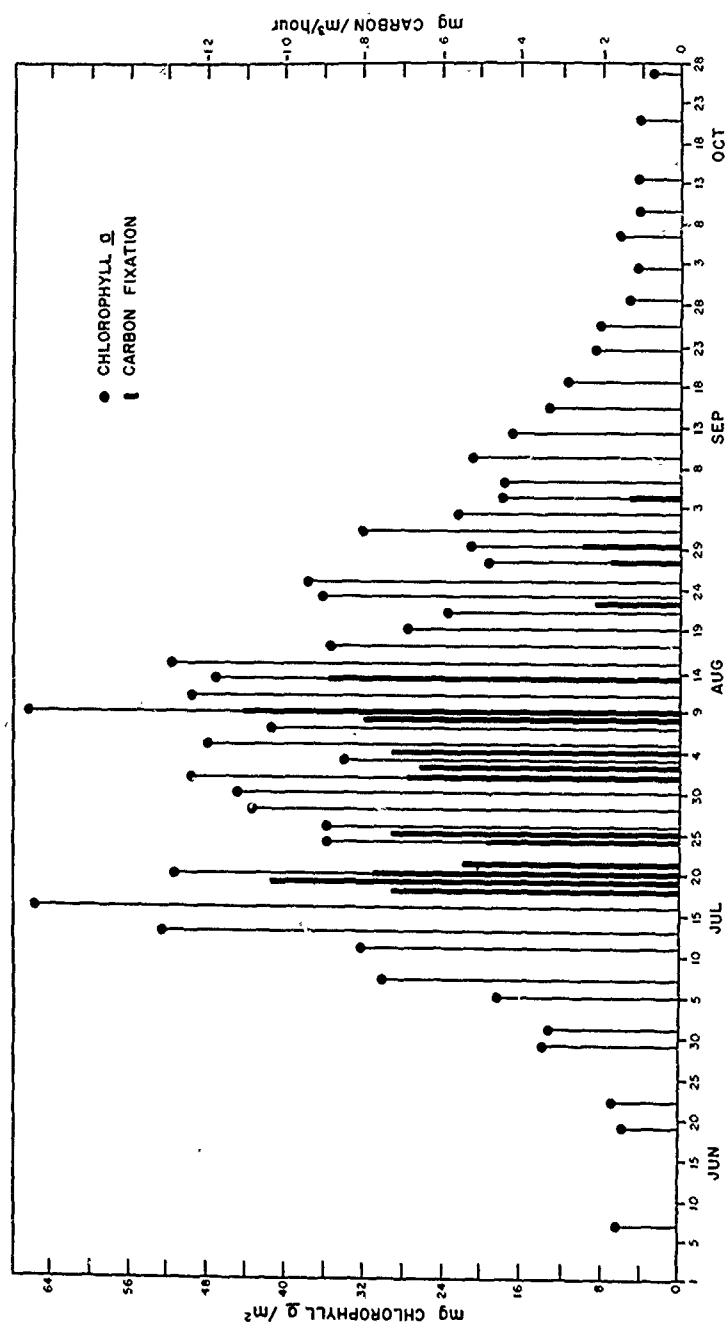


Figure 5. Chlorophyll a concentrations integrated for a 1 square meter water column from 4 to 64 meters, Drift Station Alpha, 1958. Photosynthetic potential is indicated as carbon fixation in a sample from 6 meters held at 200 foot-candles; experiments were made only on dates indicated by heavy lines.

The results from Drift Station Alpha show that the seasonal cycle was evident to a depth of somewhat over 50 meters. Results from Fletcher's Ice Island (T-3) (Collin, 1959, and Farlow, 1958) and North Pole II (Gudkovich, 1955) indicate that a similar layer covers a large area of the North Polar Sea. The complete mixing of the Arctic Upper Water ensures that the seasonal cycle will be evident to whatever depth the stratum extends in other areas.

Incident and Submarine Solar Radiation

The amount of incident solar radiation on the permanent ice pack at various latitudes can be estimated from the table given by Kimball (1928, p. 395, Table 4) or the figure from Haurwitz (1941) as given in Holmes (1957). The daily insolation, even as far south as 70°N , is negligible from early November until early February; it increases rather uniformly into May, reaches a maximum about 21 June, then decreases through the summer and autumn. The seasonal trend of visible radiation at Drift Station Alpha was clear despite variability introduced by differential cloud cover (Figure 6).

The amount of visible radiation available for photosynthesis beneath the ice is increased by the occurrence of leads, the ablation of the snow cover, a decrease in thickness of the ice floes, the formation of meltwater ponds on floes, and the decrease in the albedo of the ice surface. In June, before the snow cover had disappeared, less than 1 per cent of surface radiation penetrated through an average ice floe (about 3 meters thick) into the sea. Removing a layer of snow only a few centimeters thick more than doubled the amount of radiation received beneath an ice floe. Wetting the surface increased the radiation still more. In mid-July the radiation under a pond was about five times as high as under an ordinary expanse of an average ice floe.

Vertical extraction coefficients for the sea water were established by measuring the submarine radiation at successive depths, both in the large leads and beneath ice floes. The vertical distance between equal radiation intensities may be taken as a rough measure of the depth by which the euphotic zone is changed (Figure 7). In this case, it appears that an average ice floe reduces the depth of the euphotic zone to less than one-half the depth of the freely convective layer of Arctic Upper Water.

The snow cover vanished in early July and allowed a greatly increased amount of light to enter the sea (Figure 6). The increased penetration of light into the sea overcompensates for the decrease of incident surface radiation after the maximum about 21 June. The maximum penetration of light into the sea must occur shortly after the formation of the ponds.

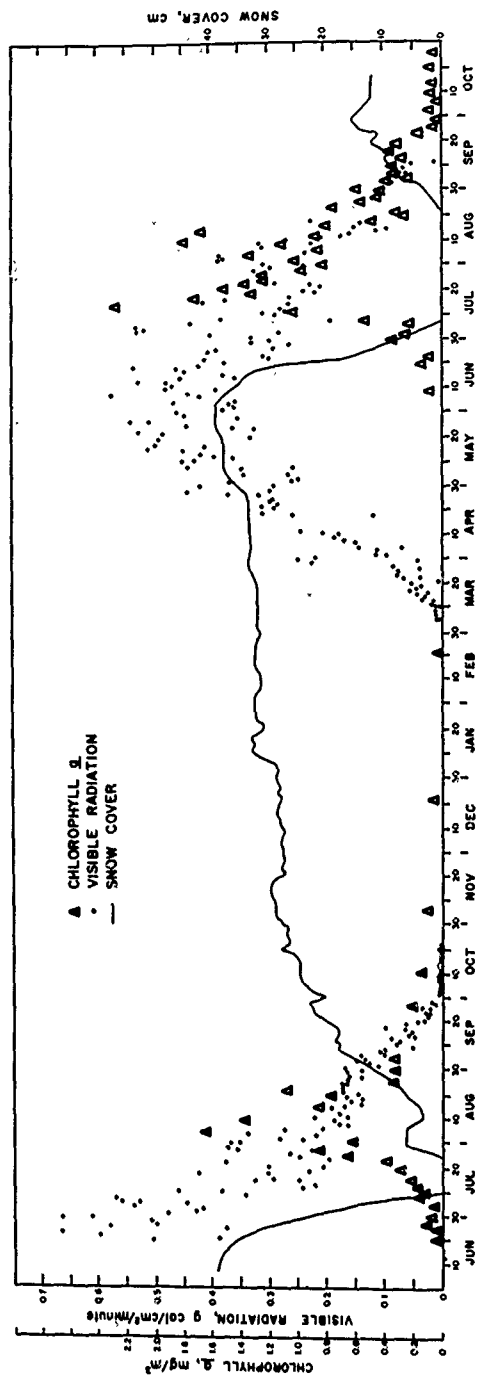


Figure 6. Relationship between visible radiation, snow cover, and concentration of chlorophyll α . Drift Station Alpha, 1957-1958. Chlorophyll α concentrations were determined from samples taken at 5 meters through February 1958 and from samples taken at 6 meters thereafter.

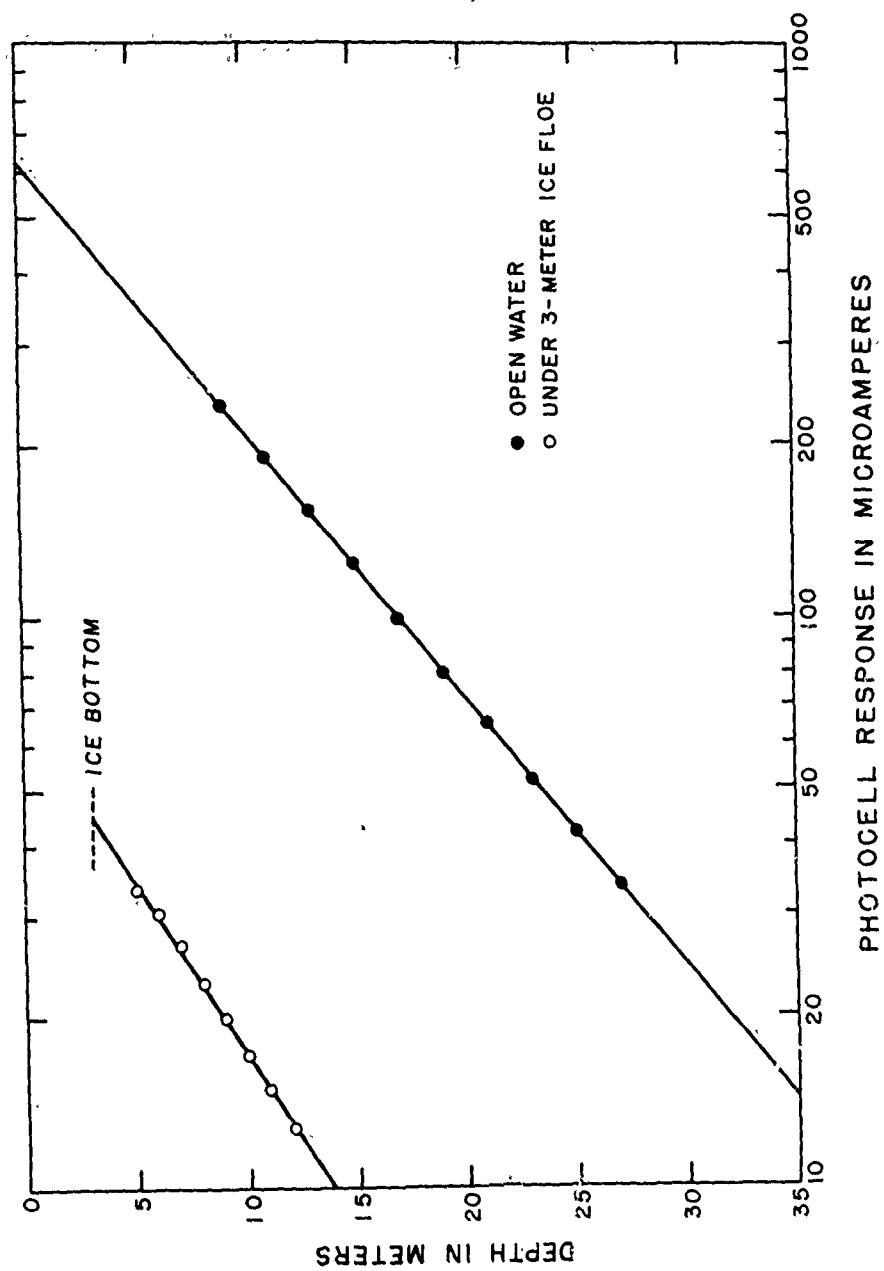


Figure 7. Attenuation of 425 millimicra radiation in open water and beneath an ice floe, Drift Station Alpha, July 1958.

The decrease in submarine radiation in August is quite abrupt. The decrease is caused by a lower angle of incidence of solar radiation and an increase in albedo brought about first by the freezing of ponds and leads and finally the new snow cover.

The time of the increase and occurrence of the maximum concentration of chlorophyll a, after the widespread formation of meltwater ponds and while the final traces of snow were disappearing, confirms the belief that the lack of sufficient solar radiation limits photosynthesis under the ice pack. The role of the ice pack itself as a physical barrier regulating the proportion of incident solar radiation penetrating into the sea is also clear. However, unlike the open ocean situation, an average depth of the euphotic zone for a large sea area under the ice pack would necessarily be based on a complex of measurements and estimates. The amount of radiation entering the sea during a productive season must be a summation of the proportions passing through leads and floes, with or without ponds or snow cover, in amounts varying seasonally, diurnally, and with meteorological conditions. The history of the radiation received by any small volume of sea water is always in doubt, and the variable ice cover moving relative to the ocean could introduce variations within rather wide limits. This knowledge prompted frequent measurements of chlorophyll a concentrations. Some of the unusually high and low values can probably be explained by a history of radiation widely divergent from the average.

Distribution of Chlorophyll 'a'

Seasonal variations in the concentration of chlorophyll a were followed through two productive seasons (Figures 4 and 5). The concentrations were integrated for water columns which conformed to sampling depths. Such a representation is assumed to give an accurate estimate of the time of maximum phytoplankton populations and a fair index, or relative measure, of production and photosynthetic potential.

The distribution of chlorophyll a with depth was considered for periods throughout the 1958 productive season (Figure 8). Chlorophyll a was found only in trace quantities at 128 and 256 meters. The shape of the concentration curves must reflect the balance between production and both mixing and sinking of the phytoplankton cells. The productivity before June must have been sufficiently low that mixing in the Arctic Upper Water could maintain an almost homogeneous distribution of chlorophyll a with depth. As the production season progressed into July the concentration of chlorophyll a near the bottom of the ice pack reached a pronounced peak, indicating that production was proceeding faster than mixing and sinking. In August the maximum values are deeper in the water column, reflecting a decrease in productivity and the effects of sinking and mixing. When the productive season was over the concentration of chlorophyll a in the water column was again almost homogeneous.

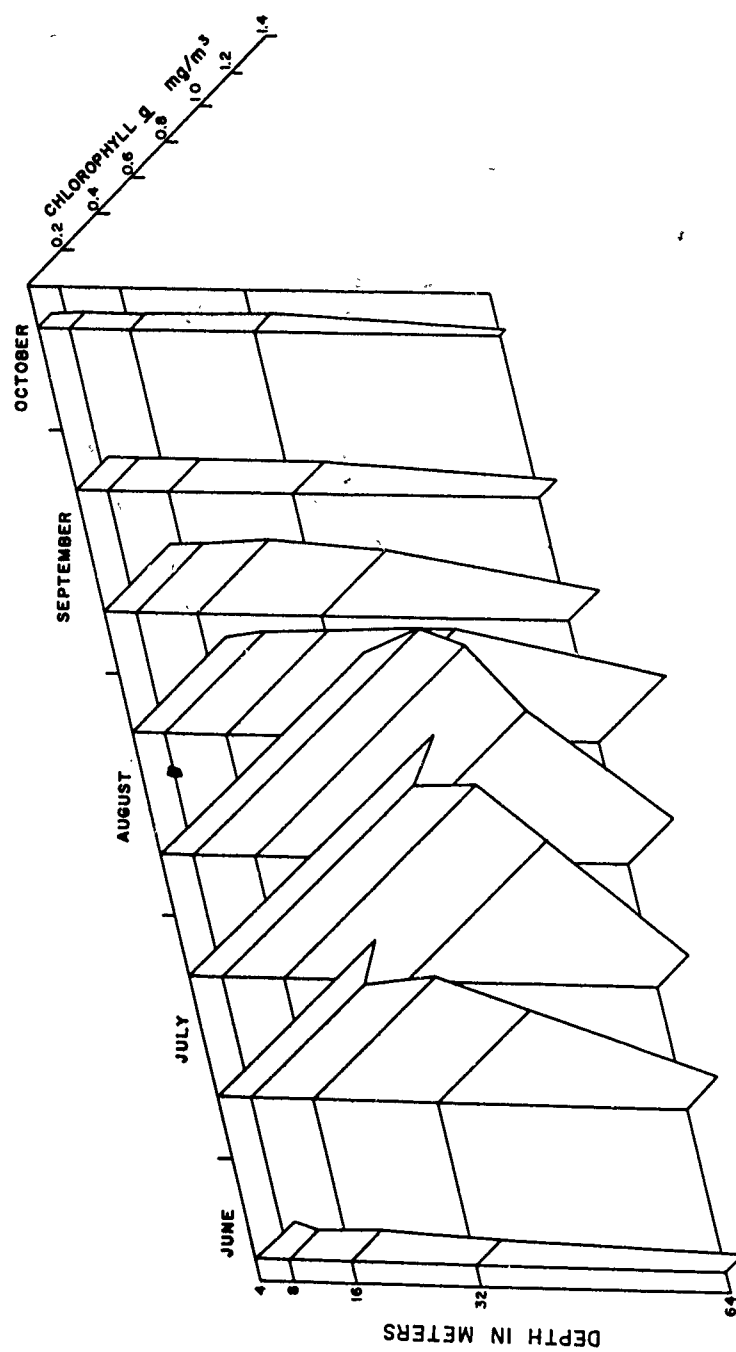


Figure 8. Chlorophyll a concentrations with depth for intervals through the productive season, Drift Station Alpha, 1958.

Net Phytoplankton and Standing Crop

Yentsch and Ryther (1959) have considered the relative importance of net plankton and nannoplankton. They got a variable, but lower, estimate of chlorophyll *a* abundance, photosynthesis, and cell counts from samples taken with a fine net (aperture size 0.065 millimeters) than from raw sea water. The differences noted were attributed to the nannoplankton. They cited other workers who found that the net plankton was often lower than 10 per cent of the nannoplankton. However, Digby (1953), working in Scoresby Sound, East Greenland, found pigment taken with a membrane filter (0.62 micron average pore diameter) was only slightly, if at all, more abundant than pigment gathered by a net (80 meshes/centimeter).

Each week of the productive season a sample was concentrated in a net to compare with a routine sample at 6 meters. The chlorophyll *a* retained by the net was in trace quantities, from 0.01 to 0.07 milligrams/cubic meter. At the time of maximum concentrations, the net retained less than 10 per cent of the chlorophyll *a* retained on a Millipore filter. A preliminary examination of preserved samples indicates that few large diatoms were present, but that small flagellates were numerous. Such a result is not unexpected on the basis of Braarud's (1935) work.

Production in Leads and Ponds

Both Nansen (1902) and Shirshov (1938) perceived that the open water trapped between ice floes was not of major importance to the production in the North Polar Sea. Although the total volume of water in leads was recognized to be small, work was needed to establish the relation of that water to the main body of the ocean.

Many samples were taken through the surface of a lead in 1957 and the integrated concentration of chlorophyll *a* under 1 square meter from the surface to 5 meters was consistently about one-half of that found from 5 to 20 meters (Figure 4). Although the water in leads received strong sunlight through July, chlorophyll *a* concentrations were not high until August. Each sample was tested and noted to be fresh, brackish, or salty. The surface water was fresh during July, but in August the runoff had abated and the wind had mixed the fresh layer with the ocean below.

In 1958 chlorophyll *a* profiles were taken through the leads and through a hole in the floe (Table 1). The surface concentration was always less than the concentration deeper in the lead, and usually less than the concentration in the ocean beneath the depth of the ice floes. Carbon-14 experiments in 1957 and 1958 showed a similar pattern of photosynthesis and photosynthetic potential with depth (Tables 2 and 3). The low surface concentrations of

chlorophyll a are taken to be a reflection of the dilution of the surface sea water with freshwater runoff, but an inhibition of photosynthesis by strong surface light could contribute to the observed effects. The high surface concentrations of chlorophyll a found in early August 1957, when runoff had diminished, suggests the dilution to be the major factor. The single sample for chlorophyll a from a pond showed only a trace, and no color was ever visually noted in a pond. Although water trapped in the spaces between the floes sometimes attained a high chlorophyll a concentration, and showed a higher photosynthetic potential than the water in the ocean below the depth of the ice bottom, there was little immediately evident effect of increased solar radiation through the leads.

While diving through a lead, the writer noticed a layer of turbid water which appeared to be a plankton bloom. A second dive was made and a sample taken with a large syringe. The concentration of chlorophyll a was 2.17 milligrams/cubic meter, well above the main body of the ocean at that time, but similar to other such areas in August.

Gran (1904) after noting the paucity of plankton diatoms from the FRAM samples, continued, "The samples taken upon the drift-ice, partly upon the ice-floes and at their edge, partly in the channels in the ice, are of greater botanical interest." As recently as 1954, Ross, considering planktonic algae in a review of cryptogamic arctic flora, stated, "In those parts of the Arctic Sea which are not ice-free during the summer, there is little true phytoplankton." Gran found traces of phytoplankton in the samples from June and October, but there were no samples between those dates. Even if the net had caught smaller phytoplankton and if the preservative had maintained them in a recognizable state, it is not surprising that planktonic algae were scarce on dates which were not near the peak of the season.

The samples which particularly interested Gran (1904) were: "(1) Free-floating lumps in the channels between the ice-floes. (2) Diatoms 'on the ice-foot,' a margin projecting from the ice-floes a foot or two below the surface of the water, and formed by the more thorough melting of the ice on the surface of the sea, where the water is comparatively warm. (3) Diatoms in cylindrical holes on the ice-floes, on the bottom of fresh water ponds not communicating with the open sea. (4) Sediment obtained by melting newly-formed sea ice."

In 1957 the free-floating lumps were observed, but no ice-foot could be found and no diatoms were noted in cylindrical holes on the ice floes. This discrepancy can be explained when the remarks from the journal of Blessing, physician and botanist to the Norwegian expedition, are examined. Blessing notes that much of the sort of plant material which interested Gran was found in 1894, but that it was very rare in 1895. Blessing suggested that the winter might have been too cold, but the observations can be explained simply by the differences associated with greater distance from the edge of the ice pack after a year of drifting.

In 1958 one area of ice-foot was discovered in a lead which persisted, and clumps of diatoms on it had melted cylindrical holes into the ice. A few bleached clumps of diatoms were discovered on the ice floe surfaces and on the bottom of ponds. No pigmented diatoms were found on the ice floes or in the ponds, and it seems likely that the clumps found were once clumps that floated in leads or were on the bottom of floes, then became frozen into floes, and finally were transported to the surface as the floes underwent ablation on the surface and accretion on the bottom.

Inorganic and Organic Nutrients

The inorganic nutrients are less abundant in the Arctic Upper Water than in the Pacific Ocean Water, but there is no evidence that a shortage limits production. The addition of inorganic nutrients failed to lead to a significant increase in photosynthesis (Table 4).

There is a persistent opinion that the melting ice pack releases nutrient materials which stimulate high production near the edge of the pack. Braarud (1935, p. 82) pointed out that melting ice produces fresh water containing very low nutrients which would check rather than increase plant production. Shirshov (1938) and Bogorov (1939) reasoned that the environmental change leading to the observed high production was the increased amount of solar radiation passing through and between the ice floes. Still, it seemed useful to accumulate a series of measurements, in addition to radiation, to further demonstrate the correctness of this view. Measurements of inorganic nutrients from a pond, a lead, and at depths in the sea demonstrate that meltwater can only dilute the Arctic Upper Water (Table 5). It will be more difficult to demonstrate the unimportance of each new and more subtle factor supposedly contributed by melting ice, such as polymerized water molecules (Dunbar, 1953). However, those who suggest an effect of meltwater, or anything it contains, are faced with the difficulty of relative concentrations; the volume of annual melt is only about one-hundredth as great as the volume of Arctic Upper Water.

Films of organic matter, predominately diatoms, but probably including flagellates, ciliates, bacteria, and detritus, can be seen on the sides and bottoms of ice floes. Those films must be incorporated into the floes from time to time, both when the meltwater runs under the floes and when the ice grows thicker in the winter. Amphipods were observed to graze along the sides and bottoms of ice floes, appearing to wear away small volumes of ice. Observation while diving revealed that the amphipods are occasionally trapped by new ice forming behind them and frozen into a hole. However, those organic inclusions must be infrequent and of small significance in the economy of the ocean. Although organic nutrients released as a result of ice melting are not likely to contribute directly to photoautotrophic production, detritus can serve as food for some of the zooplankton.

Studies of Photosynthesis

In 1957 the carbon-14 technique was used to make a rough estimate of photosynthesis in situ beneath the surface of a lead (Table 2). There was no measurable photosynthesis on 1 July. In late July and mid-August, estimates of assimilation under 1 square meter of 5-6 milligrams carbon/day were obtained for a water column of 30 meters. The water column above the bottom of the ice floes, the water "in" the lead, contributed about one-fourth of the totals.

In 1958 the photosynthetic potential of water from different depths was studied (Table 3). The decreasing photosynthetic potential with depth is similar to the decreasing concentration of chlorophyll a with depth (Figure 9). There are several possible explanations for the more rapid decrease of relative photosynthesis. Phytoplankton from greater depths could be adapted for lower light intensities, and the illumination used in the experiments might then have inhibited photosynthesis, or there could be an increasing proportion of photosynthetically inactive pigment (included here with chlorophyll a) with increasing depth.

The effect of different light intensities upon subsamples of water from 6 meters was studied (Table 6). The observations suggest a curve similar to that shown by Ryther (1956, p. 65, Figure 2) for 14 species of marine plankton algae (Figure 10). The compensation intensity is between 20 and 200 foot-candles and the saturation intensity is near 2000 foot-candles. It seems especially significant that there is no evidence of inhibition and that the population of phytoplankton under the ice does not evidence adaptation to lower light intensities than the organisms from lower latitudes which Ryther examined.

The procedure of Ryther and Yentsch (1957) for determining the ratio of photosynthesis and the concentration of chlorophyll a was followed (Figure 11). Samples were taken from the same depth, 6 meters, on the same or adjacent days. The slope of 0.6 is considerably lower than the value of 3.7 determined by Ryther and Yentsch. An explanation for the lower ratio is the extremely low temperature of the Arctic Upper Water which reduces the efficiency of carbon fixation per unit chlorophyll a. This convenient explanation is regarded with considerable doubt, but must stand until more work can be done or another interpretation of these data is suggested.

Annual Production

It is safe to assert that the annual primary production in the North Polar Sea is very low relative to other ocean areas. The production season is short and all indices of productivity are low. The limiting amount of submarine illumination can be shown to serve as a satisfactory first order explanation.

Primary production in the North Polar Sea is so low that further refinements in methods to estimate an annual total are of little interest. However, the factors operating to produce and maintain a population of photosynthetic organisms under the extreme environmental conditions observed will continue to be of interest. The behavior and special adaptations of the phytoplankton population have been suggested rather than explained.

Studies of Photosynthesis

In 1957 the carbon-14 technique was used to make a rough estimate of photosynthesis *in situ* beneath the surface of a lead (Table 2). There was no measurable photosynthesis on 1 July. In late July and mid-August, estimates of assimilation under 1 square meter of 5-6 milligrams carbon/day were obtained for a water column of 30 meters. The water column above the bottom of the ice floes, the water "in" the lead, contributed about one-fourth of the totals.

In 1958 the photosynthetic potential of water from different depths was studied (Table 3). The decreasing photosynthetic potential with depth is similar to the decreasing concentration of chlorophyll *a* with depth (Figure 9). There are several possible explanations for the more rapid decrease of relative photosynthesis. Phytoplankton from greater depths could be adapted for lower light intensities, and the illumination used in the experiments might then have inhibited photosynthesis, or there could be an increasing proportion of photosynthetically inactive pigment (included here with chlorophyll *a*) with increasing depth.

The effect of different light intensities upon subsamples of water from 6 meters was studied (Table 6). The observations suggest a curve similar to that shown by Ryther (1956, p. 65, Figure 2) for 14 species of marine plankton algae (Figure 10). The compensation intensity is between 20 and 200 foot-candles and the saturation intensity is near 2000 foot-candles. It seems especially significant that there is no evidence of inhibition and that the population of phytoplankton under the ice does not evidence adaptation to lower light intensities than the organisms from lower latitudes which Ryther examined.

The procedure of Ryther and Yentsch (1957) for determining the ratio of photosynthesis and the concentration of chlorophyll *a* was followed (Figure 11). Samples were taken from the same depth, 6 meters, on the same or adjacent days. The slope of 0.6 is considerably lower than the value of 3.7 determined by Ryther and Yentsch. An explanation for the lower ratio is the extremely low temperature of the Arctic Upper Water which reduces the efficiency of carbon fixation per unit chlorophyll *a*. This convenient explanation is regarded with considerable doubt, but must stand until more work can be done or another interpretation of these data is suggested.

Annual Production

It is safe to assert that the annual primary production in the North Polar Sea is very low relative to other ocean areas. The production season is short and all indices of productivity are low. The limiting amount of submarine illumination can be shown to serve as a satisfactory first order explanation.

Primary production in the North Polar Sea is so low that further refinements in methods to estimate an annual total are of little interest. However, the factors operating to produce and maintain a population of photosynthetic organisms under the extreme environmental conditions observed will continue to be of interest. The behavior and special adaptations of the phytoplankton population have been suggested rather than explained.

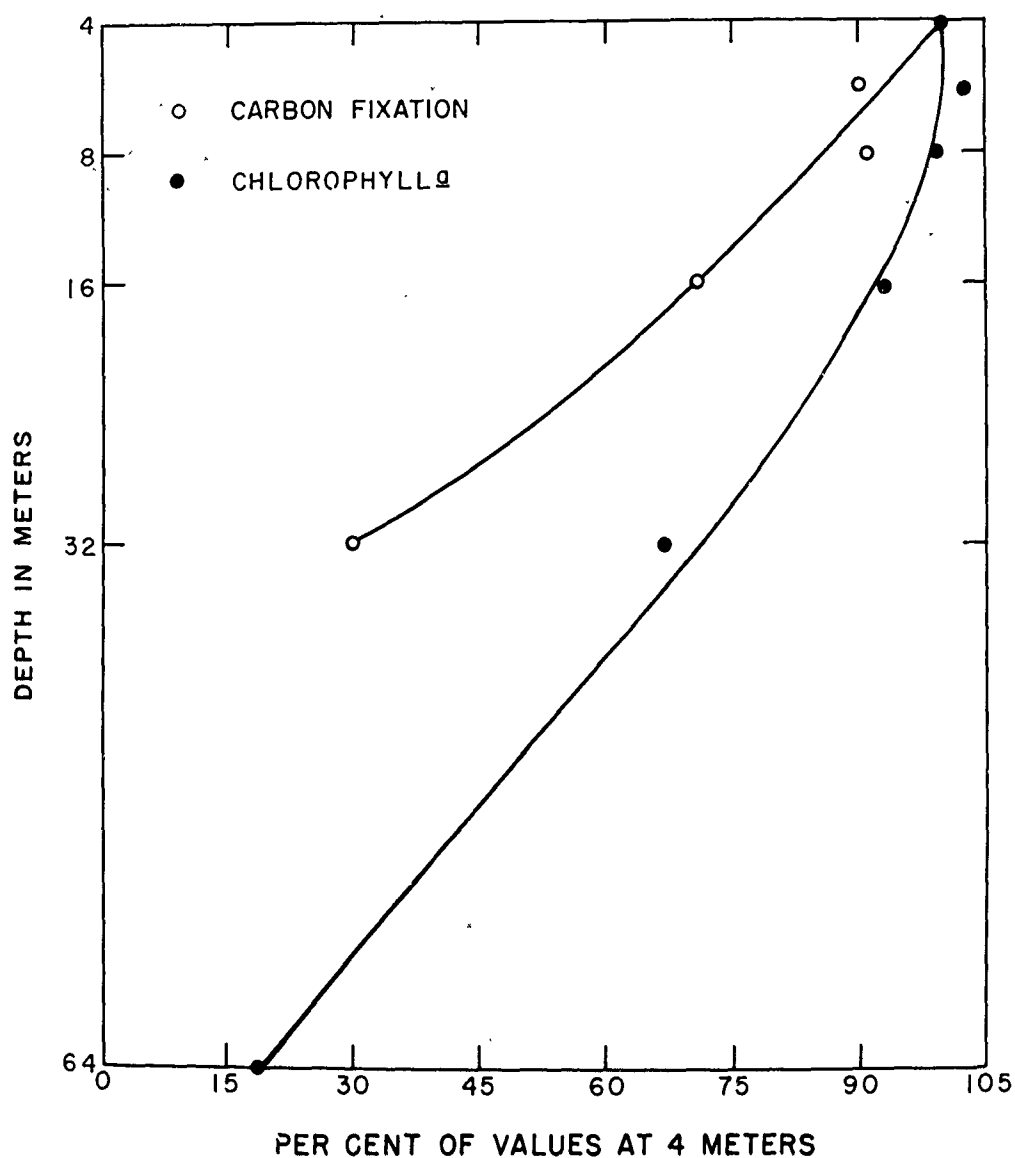


Figure 9. Relative photosynthesis, expressed as carbon fixature in samples held under 2000 foot-candles illumination, and relative chlorophyll *a* concentrations, Drift Station Alpha, 20 July-13 August, 1958.

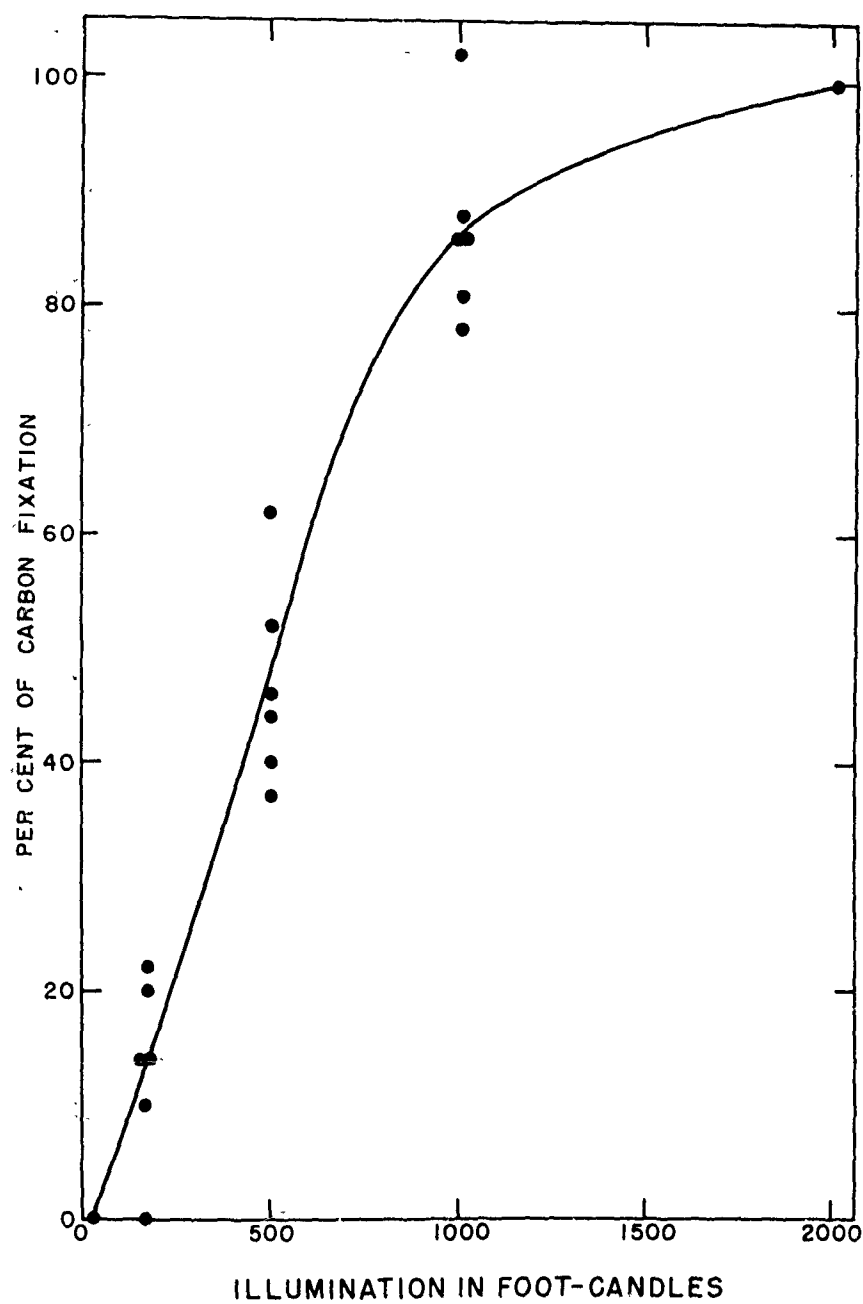


Figure 10. Relative photosynthesis from six experiments on samples taken at 6 meters, Drift Station Alpha, 1958.

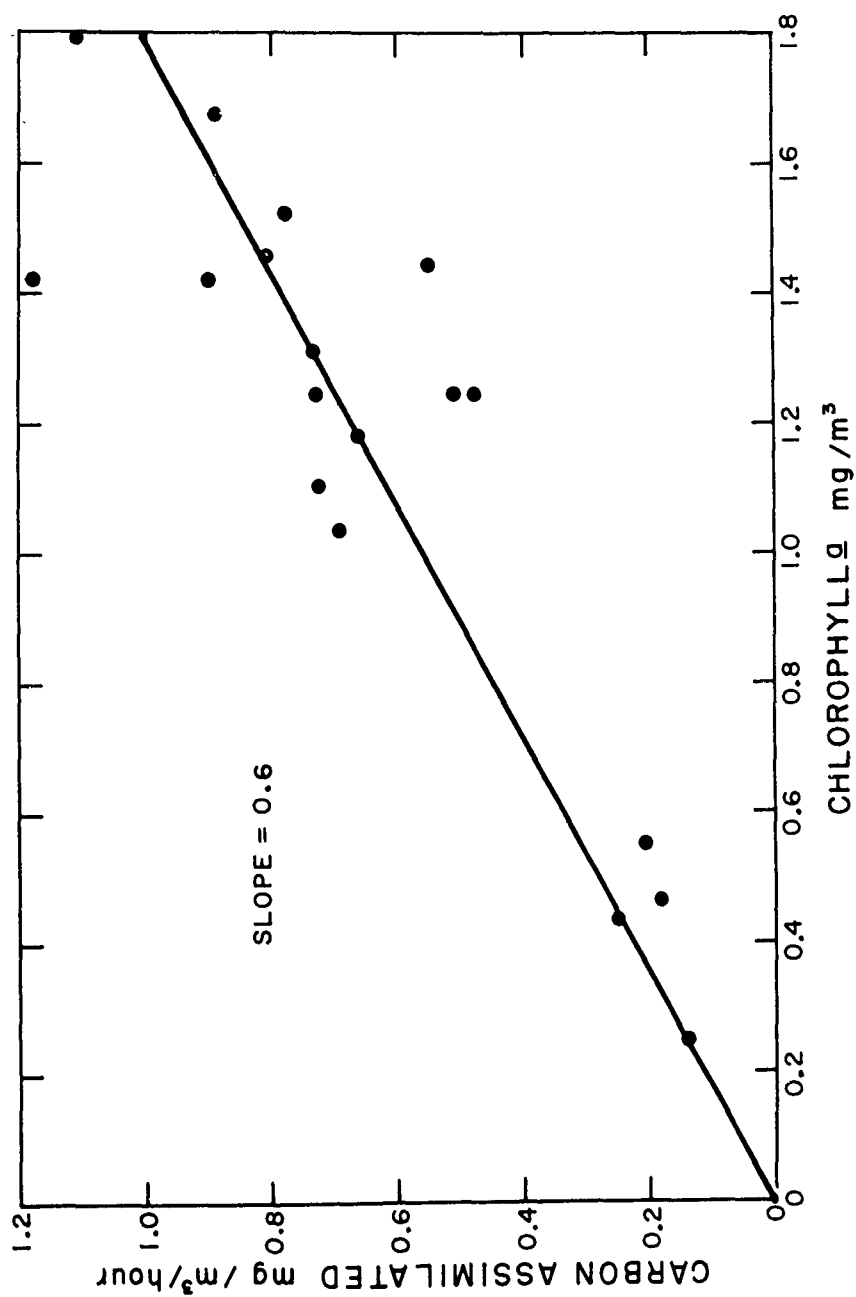


Figure 11. Relationship between photosynthetic potential, expressed as carbon assimilation, and chlorophyll *a* concentration, Drift Station Alpha, 1958.

Literature Cited

- Apollonio, Spencer. 1959. Hydrobiological measurements on IGY Drifting Station Bravo. Transactions American Geophysical Union. 40 (3): 316-319.
- Bogorov, B. G. 1938. Biological seasons of the Arctic Sea. Comptes Rendu (Doklady) de l'Academie des Sciences de l'URSS. 19(8): 641-644.
- Bogorov, B. G. 1939. The particularities of seasonal phenomena in the plankton of arctic seas and their significance for ice forecasting. Zoologicheskii Zhurnal. 18(5): 735-747.
- Braarud, Trygve. 1935. The 5th Expedition to the Denmark Strait 1929. II. The phytoplankton and its conditions of growth. Hvalrådets Skrifter. Nr. 10. 173 pp.
- Brodskii, K. A. and M. N. Nikitin. 1955. Hydrobiological work. Observational Data of the Scientific Research Drifting Station of 1950-1951. Volume I, Section 4, Article 7, 6 pp., 4 appendices. (American Meteorological Society translation.)
- Carruthers, J. N., H. G. Stubbings, and A. L. Lawford. 1950. Water sampling in estuarial waters. The Dock and Harbor Authority. December, pp. 2-12. Ward and Follow, Ltd. London.
- Coachman, L. K. and C. A. Barnes. The contribution of Bering Sea water to the Arctic Ocean. In press.
- Collin, A. E. 1959. Canadian oceanographic activities on IGY Drift Station "Bravo." Fisheries Research Board of Canada. Manuscript Report Series (Oceanographic and Limnological). No. 40.
- Creitz, G. I. and F. A. Richards. 1955. The estimation and characterization of plankton populations by pigment analyses. III. A note on the use of "millipore" membrane filters in the estimation of plankton pigments. Journal of Marine Research. 14(3): 211-216.
- Dienert, F. and F. Wandenbulcke. 1923. Sur le dosage de la silice dans les eaux. Comptes Rendu de l'Academie des Sciences de Paris. 176: 1478-1480.
- Digby, P. S. B. 1953. Plankton production in Scoresby Sound, East Greenland. The Journal of Animal Ecology. 22(2): 289-322.
- Dunbar, M. J. 1953. Arctic and subarctic marine ecology: immediate problems. Arctic. 6(2): 75-90.

- Farlow, John S., III. 1958. Project Ice Skate oceanographic data. Woods Hole Oceanographic Institution. Reference No. 58-28. 18 pp.
- Gran, E. H. 1904. Diatomaceae from the ice-floes and plankton of the Arctic Ocean. In: Nansen, F., Norwegian North Polar Expedition, 1893-1896. Scientific Results. Volume 4(11).
- Gudkovich, Z. M. 1955. Results of a preliminary analysis of the deep-water hydrological observations. Observational data of the scientific research drifting station of 1950 - 1951. 1(2):170 pp. (American Meteorological Society translation).
- Haurwitz, Bernhard. 1941. Dynamic meteorology. Mc-Graw Hill. New York. 365 pp.
- Holmes, Robert W. 1957. Solar radiation, submarine daylight, and photosynthesis. Geological Society of America. Memoir 67. 1:109-128.
- Ketchum, B. H., N. Corwin and D. J. Keen. 1955. The significance of organic phosphorus determinations in ocean waters. Deep-Sea Research. 2(3):172-181.
- Kimball, Herbert H. 1928. Amount of solar radiation that reaches the surface of the earth on the land and on the sea, and the methods by which it is measured. Monthly Weather Review. 56:393-398.
- Mohr, John L. 1959. Marine biological work. Studies at Fletcher's Ice Island, T-3, (1952-1955). 1:83-103. Geophysical Research Papers. No. 63. ASTIA Document No. AD-216813.
- Mullin, J. B. and J. P. Riley. 1955. The spectrophotometric determination of nitrate in natural waters, with particular reference to sea water. Analytica Chimica Acta. 12(5):464-480.
- Nansen, Fridtjof. 1902. The oceanography of the North Polar Basin. Norwegian North Polar Expedition, 1893-1896. Scientific Results. Vol. 3, No. 9.
- Richards, F. A. with T. G. Thompson. 1952. The estimation and characterization of plankton populations by pigment analyses. II. A spectrophotometric method for the estimation of plankton pigments. Journal of Marine Research. 11(2):156-172.

- Robinson, R. J. and T. G. Thompson. 1948. The determination of phosphates in sea water. *Journal of Marine Research*. 7(1):33-41.
- Ross, R. 1954. Algae: planktonic. In: *The cryptogamic flora of the Arctic*. *The Botanical Review*. 20(6 and 7):400-416.
- Ryther, J. H. 1956. Photosynthesis in the ocean as a function of light intensity. *Limnology and Oceanography*. 1(1):61-70.
- Ryther, J. H. and R. F. Vaccaro. 1954. A comparison of the oxygen and ^{14}C methods of measuring marine photosynthesis. *Journal du Conseil*. 20(1):25-34.
- Ryther, J. H. and C. S. Yentsch. 1957. The estimation of phytoplankton production in the ocean from chlorophyll and light data. *Limnology and Oceanography*. 2(3):281-286.
- Shirshov, P. P. 1938. Oceanological observations. *Comptes Rendu (Doklady) de l'Academie des Sciences de l'URSS*. 19(8):569-580.
- Shirshov, P. P. 1944. Scientific results of the drift station North Pole. *Akademiia nauk SSSR. Obshchee sobranie*. February 1944, pp. 110-140. (Translated February 1956 by David Kraus, GRD, AFCRC, Cambridge, Massachusetts.)
- Steeman Nielsen, E. 1952. The use of radio-active carbon (C^{14}) for measuring organic production in the sea. *Journal du Conseil*. 18(2):117-140.
- Sverdrup, H. U. 1929. The waters on the North-Siberian shelf. The Norwegian North Polar Expedition with the "Maud" 1918-1925. *Scientific Results*. 4(2):131 pp.
- Thompson, T. G. and R. J. Robinson. 1939. Notes on the determination of dissolved oxygen in sea water. *Journal of Marine Research*. 2(1):1-8.
- Timofeev, V. T. 1953. Water masses of the Arctic Basin. The High Latitude Aerial Expeditions of 1948 and 1949, *Scientific Results*. (Cited in Gudkovich, Z. M. 1955.)

Timofeev, V. T. 1958. An approximate determination of the heat balance of arctic waters. Problemy Arktiki. (4): 23-28.

Timofeev, V. T. 1960. Water masses of the Arctic Basin. Hydrometeorological Publishing House. Leningrad. 190 pp. and Appendix.

Transehe, N. A. 1928. The ice-cover of the Arctic Sea, with a genetic classification of sea ice. Problems of Polar Research. American Geographical Society Special Publication No. 7, pp. 91-123

Yentsch, Charles S. and John H. Ryther. 1959. Relative significance of the net phytoplankton and nannoplankton in the waters of Vineyard Sound, Journal du Conseil. 24(2): 231-238.

Table 1. Chlorophyll a measurements taken in leads and under the ice floe in 1958. Samples were taken through two widely separated leads on 20 July.

Depth in Meters	5 July		18 July		20 July		24 July		
	Hole	Lead	Hole	Lead	Hole	Lead	Lead	Hole	Lead
Surface	--	0.65	--	0.11	--	0.07	0.15	--	0.31
1	--	0.75	--	0.23	--	0.47	0.52	--	0.51
2	--	0.77	--	0.75	--	5.72	2.01	--	1.90
*-----									
4	0.23	0.39	1.84	1.55	1.53	2.04	1.59	0.80	1.55
6	--	--	1.31	--	1.52	--	--	1.24	--
8	0.26	0.26	1.64	1.57	1.43	1.37	1.27	0.90	1.07
16	0.45	--	--	1.44	1.54	1.48	1.60	0.76	1.07

*The ice bottom was approximately 3 meters below the ocean surface.

Table 2. In situ photosynthesis measured by the carbon-14 technique; samples taken from the edge of a lead in 1957.

Sample Depth in Meters	Milligrams Carbon/Cubic Meter/Day		
	24 July	28 July	18 August
Surface			0.34
1			0.40
2		0.54	0.48
5		0.32	0.31
10	0.21		0.08
20	0.11		0.11

Table 3. Photosynthesis measured by carbon-14 technique: samples illuminated with about 2000 foot-candles.

Depth Meters	Milligrams Carbon/Cubic Meter/Hour							
	20 July	21 July	24 July	24 July	28 July*	4 August	13 August	29 August
4	0.74	0.58	0.65	0.52	1.32	1.39	0.78	0.20
6	0.78	0.55	0.48	0.51	2.26	0.73	0.89	0.25
8	0.77	0.55	0.52	0.45	1.52	0.60	1.08	0.24
16	0.56	0.44	0.44	0.37	1.12	0.47	0.80	0.17
32	0.15	0.22	0.20	0.30	0.45	0.23	0.12	0.12

*Samples taken from lead at depths of surface, 1, 2, 4, and 8 meters.

Table 4. Photosynthesis measured by carbon-14 technique; inorganic nutrients added to sample water.

Inorganic Nutrients	Milligrams Carbon/Cubic Meter/Hour					
	25 July	26 July*	2 August	8 August	22 August	4 Sept.
Nitrate	0.90	4.79	0.88	0.83	0.20	0.11
Nitr-Phos	0.79	5.07	0.68	0.84	0.24	0.09
Phosphate	0.74	4.48	0.80	0.96	0.23	0.09
Controls	0.72	4.86	0.63	0.80	0.23	0.14
	0.74	4.90	0.70	0.79	0.20	0.12

*Sample taken at 0.5 meter in a lead.

Table 5. Approximate concentrations of inorganic ions from a lead, a pond, and water masses in the North Polar Sea, 12 August 1958.

Sample Source	Microgram Atoms/Liter		
	Nitrate	Phosphate	Silicate
Lead	0.1	0.05	0
Pond	0.1	0.1	0
Arctic Upper Water	0.4	0.8	4
Pacific Ocean Water	3.6	1.5	24
Arctic Intermediate Water	2.4	0.7	3

Table 6. Photosynthesis measured by carbon-14 technique; samples from 6 meters held under different light intensities.

Illumination Foot-candles	Milligrams Carbon/Cubic Meter/Hour					
	18 July	19 July	19 July	1 August	9 August	27 August
2000	0.73	1.18	0.90	0.80	1.11	0.18
1000	0.63	1.04	0.92	0.69	0.90	0.14
500	0.45	0.61	0.41	0.32	0.41	0.08
200	0.15	0.00	0.13	0.08	0.16	0.04
20	0.00	0.00	0.00	0.00	0.00	0.00

Some Remarks on Arctic Ocean Plankton

T.S. English

Reprinted from the
PROCEEDINGS OF THE ARCTIC BASIN SYMPOSIUM, OCTOBER 1962,
pp. 184-196, 1963

Proceedings of the Arctic Basin Symposium

SOME REMARKS ON ARCTIC OCEAN PLANKTON¹

T. SAUNDERS ENGLISH

University of Washington

Seattle, Washington

Dr. Martin W. Johnson has sustained an interest in Arctic Ocean plankton for three decades, making the most of infrequent opportunities to gather samples. In his recent treatment of the copepods as indicators of water masses and patterns of water movement, he has related hydrography and biological oceanography so that ecological implications have been emphasized. Johnson has dealt expertly with the taxonomic problems of the copepods; his studies of life histories have been helpful with problems of expatriate species, discontinuous distributions, meroplanktonic populations, and reproductive periods. The conclusions which he has been able to draw from unavoidably limited data attest to his broad knowledge of the Arctic Ocean plankton.

The contributions of Johnson—as well as those of Dr. M. J. Dunbar and his group, Dr. John L. Mohr and his associates, workers from the Arctic Research Laboratory, and the University of Washington team in the Chukchi Sea—emphasize the shortage of planned sustained observations for all seasons. It is scarcely necessary to mention that we know more about the plankton in summer than in winter. Continued sporadic biological sampling can certainly yield further information about Arctic Ocean plankton. However, it is clear that the pioneering observations of earlier workers should now be followed by more purposeful work on a continuing basis.

Several aspects of Johnson's paper, particularly the consideration of biomass and the possible sources of food for copepods, suggest comments. These two topics are closely related in the evolving, unifying concepts of the economy of the sea.

Johnson examined a specified portion of the total biomass: the plankton biomass sampled with nets (0.15 mm mesh). Therefore, he found, "... the plankton biomass of the Arctic consists overwhelmingly of crustaceans, especially copepods." Clearly, the biomass taken with a Nansen bottle or a midwater trawl would be somewhat different. Therefore, samples should be taken with gear other than a plankton net to improve our understanding of the total Arctic Ocean biomass.

In considering the maintenance of Arctic Ocean plankton, Johnson points out, "It is clear that added to the organic production taking place locally there must be a great amount of particulate food swept into the high latitudes by the prevailing current through Bering Strait." The particles of food might be living or dead; particle size could vary widely, to an upper extreme of large organisms.

Particulate food for zooplankton can come from several sources. The major source is usually photosynthesis, which is low in the Arctic Ocean.

¹Contribution No. 289 from the University of Washington, Department of Oceanography.

Hydrosphere

The production of particulate food by heterotrophic processes, involving the assimilation of carbon by micro-organisms of the nanoplankton such as bacteria, eumycetes, protozoa, and algae, might therefore be of relatively greater importance in the Arctic Ocean than in other areas. The particulate food provided by the meroplanktonic eggs and larvae of benthic invertebrates and some fishes can be important only near shore and over shelf areas. Oceanic detritus, such as chitin, fecal pellets, and fibers, was measured recently by Parsons and Strickland (1962). They found large quantities, with a wide range of chemical composition, in the northeastern Pacific Ocean. They consider the detritus to be a potential source of food for the secondary producers among marine organisms and a substrate for bacteria.

Therefore, food for zooplankton in the Arctic Ocean may be carried in by advection as well as produced locally. The copepods could food on phytoplankton, animal nanoplankton, meroplankton, and detritus. Photosynthesis replaces energy lost from the system, possibly supplemented by heterotrophic processes based on allochthonous dissolved organic matter. Any feedback

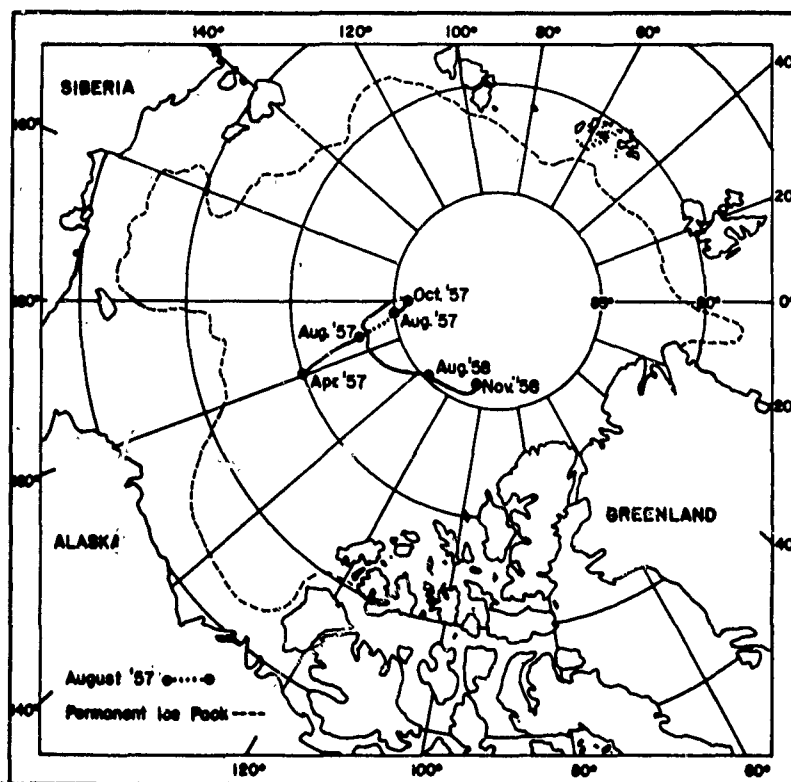


FIGURE 1 Track of Drift Station Alpha, April 1957-November 1958.

Proceedings of the Arctic Basin Symposium

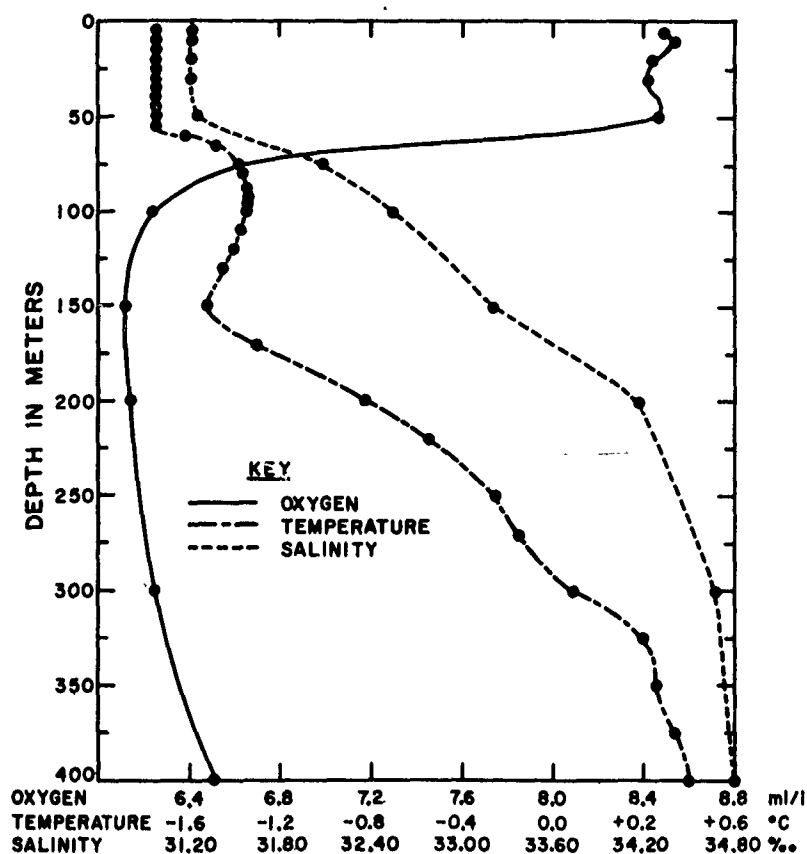


FIGURE 2 Temperature, salinity, and dissolved oxygen, Drift Station Alpha, 23-24 June 1958.

from a cycle of heterotrophic production extends the effect of energy fixed by photosynthesis. The actual balance between these factors in the Arctic Ocean is still an entirely open question.

It is of interest to consider what quantities of food are necessary, and when, to sustain the observed expatriates, to maintain the indigenous populations of high latitudes, and to support reproduction. The work of Conover (1961) on the metabolism and growth of *Calanus hyperboreus* provides several helpful insights. This herbivorous cold-water copepod spends most of its life cycle below the euphotic zone, isolated from its phytoplankton food source. Breeding occurs in midwinter. When plant food is available the copepods migrate to the surface waters to feed and their metabolic rate is high; activity and metabolic rate are reduced for the rest of the year. Conover concluded that the physiology and life cycle of the copepod are adjusted to take advantage of a single period of food abundance, perhaps only 10-20 percent of the total life span. The most extreme environment for

Hydrosphere

such adjustment by regulating metabolism should be near the Pole of Inaccessibility.

Dunbar (1946) pointed out another adaptive mechanism of the high arctic zooplankton. He found a prolongation of the life cycle, caused by an alternating breeding cycle; some northern pelagic crustaceans delayed spawning and death for one year longer than those in warmer waters.

Some results from studies north and south of the area considered by Johnson help to support his conclusions. Biological oceanographic observations were made on IGY Drift Station Alpha in 1957 and 1958². The station drifted near the center of the North Polar Sea (Fig. 1). Hydrographic observations established the distribution of properties with season and with depth (Fig. 2). When the ice surface began to melt in summer, water of slightly increased temperature and very low salinity was added at the sea surface. The maximum change observed in the Arctic Upper Water was only several tenths of one degree Celsius and several tenths of one part per thousand salinity. The distribution of inorganic nutrients with depth reflected the density stratification and indicated the extent of the Pacific Water (Fig. 3). Nutrient enrichment of the Arctic Upper Water must proceed by slow mixing across a substantial density gradient. Both the oxygen minimum and the nutrient maxima were in the Pacific Water.

Primary organic production was limited to the freely convective Arctic Upper Water. The major seasonal change in the North Polar Sea environment was the amount of visible radiation penetrating into the ocean. Radiation available to the phytoplankton for photosynthesis was increased by ablation of the snow cover, a decrease in thickness of ice floes, the formation of meltwater ponds on the floes, any decrease in albedo, and the formation of leads between floes. The period when maximum radiation entered the sea followed the period of maximum incident surface radiation, occurring after ablation of the snow cover and the formation of meltwater ponds (Fig. 4). The maximum chlorophyll *a* concentration occurred still later than the maximum submarine radiation.

The concentration of chlorophyll *a* has been used as a means of estimating the size of phytoplankton populations, as well as a relative measure of primary production and photosynthetic potential. The annual average of the standing crop of phytoplankton was quite low compared to other ocean areas, notwithstanding the increase in August. The distribution of chlorophyll *a* through the productive season indicated the relative amount of production (Fig. 5). A net of very fine mesh (0.065 mm) retained less than 10 percent as much chlorophyll *a* as was retained by a molecular filter, suggesting that the majority of the photosynthetic organisms were very small.

In summary, there is a short productive season and a low standing crop of phytoplankton in the Arctic Upper Water of the North Polar Sea; the amount of production by photosynthesis must be the smallest of any ocean area.

²The 1957 field season was supported by the Arctic Aeromedical Laboratory, Fairbanks, Alaska; the 1958 field season was sponsored by the Arctic Institute of North America under contract with the Geophysics Research Directorate, Air Force Cambridge Research Laboratories.

Proceedings of the Arctic Basin Symposium

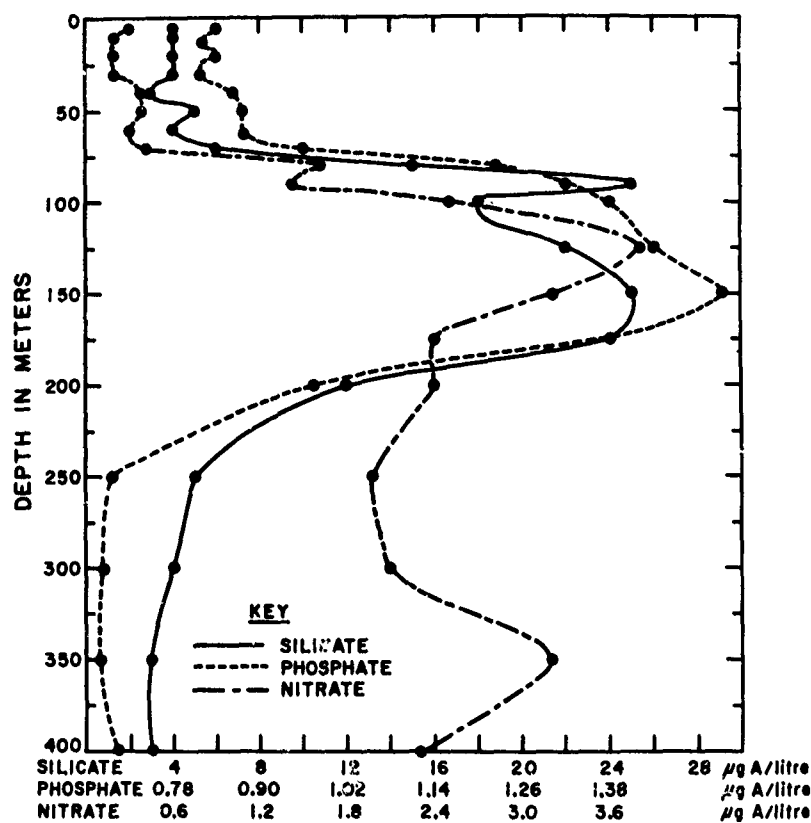


FIGURE 3 Inorganic nutrient concentrations, Drift Station Alpha, 1958.

The research vessel *Brown Bear* of the University of Washington, Department of Oceanography worked in the Chukchi Sea in 1959 and 1960³. Hydrographic and biological oceanographic observations were begun in the Bering Sea and extended to the limit of the ice pack (Fig. 6). Some preliminary results indicate the relationship of hydrography to the distribution of organisms.

Current measurements showed a flow northward of about 1 knot (Fig. 7). The isotherms paralleled the direction of the current (Fig. 8); warmer water was near the coast and colder water toward the west. The distribution of chlorophyll *a* indicated lower phytoplankton concentrations in the coastal water and to the north (Fig. 9). The distribution of zooplankton was also related to the current patterns and hydrographic variables, such as salinity

³Supported by Contract AT-45-1-540 with the Atomic Energy Commission and Contract Nonr-77(10), Project NR 083 012, with the Office of Naval Research.

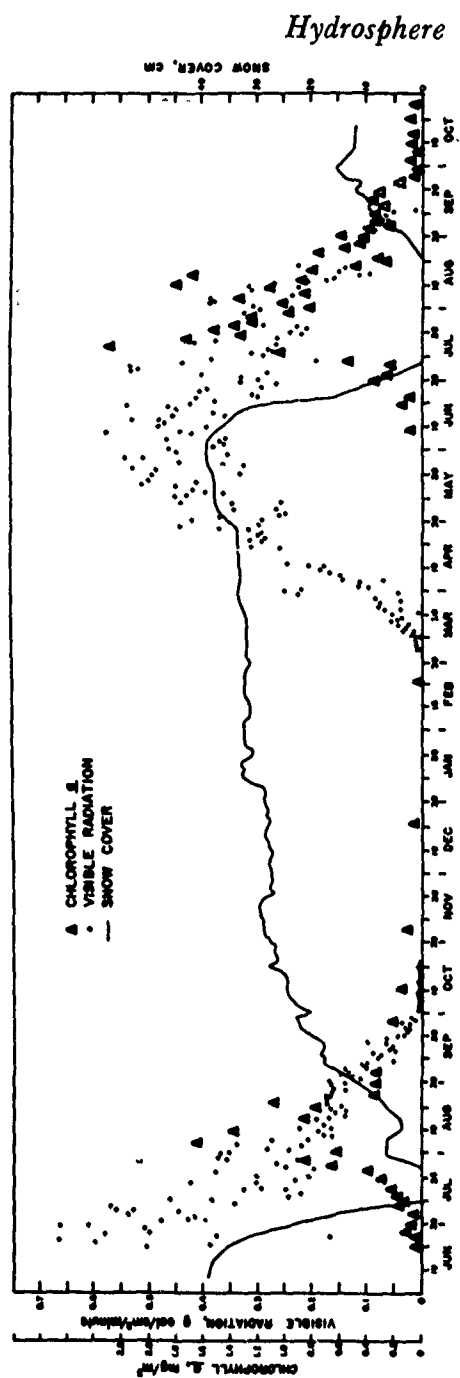


FIGURE 4 Visible radiation (0.3-3.0 microns), snow cover, and chlorophyll *a* concentration, Drift Station Alpha, 1957-1958.

Proceedings of the Arctic Basin Symposium

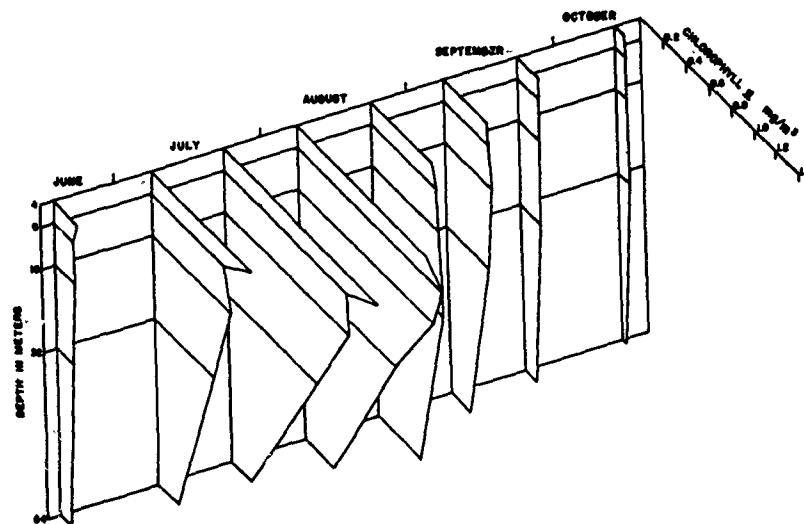


FIGURE 5 Chlorophyll *a* concentration, Drift Station Alpha, 1958.

(Fig. 10). Copepods and euphausiids were the dominant organisms in the samples of the plankton nets (0.24 mm mesh). It was possible to distinguish between the neritic species of copepods near the coast and the oceanic species farther from shore. The euphausiids were less abundant in the water as it moved to the north. Meroplanktonic organisms such as barnacle, gastropod, and lamellibranch larvae were sporadically abundant. The catches of a mid-water trawl indicated the oceanic distribution of the euphausiids and the neritic distribution of the small codfish (Fig. 11).

The water moving northward through the Chukchi Sea contributes copepods and some of their food to the northernmost areas considered by Dr. Johnson. The low primary productivity observed in the North Polar Sea may be supplemented by food carried in by advection and particles produced by heterotrophic processes, but the importance of such phenomena is still unknown.

Literature Cited

- Conover, Robert J. 1961. Metabolism and growth in *Calanus hyperboreus* in relation to its life cycle. International Council for the Exploration of the Sea. Symposium on "Zooplankton Production." Paper No. 11, 10 pp.
- Dunbar, M. J. 1946. On *Themisto libellula* in Baffin Island coastal waters. Journal of the Fisheries Research Board of Canada, 6(6):419-434.
- Parsons, T. R., and J. D. H. Strickland. 1962. Oceanic detritus. Science, 136(3513): 313-314.

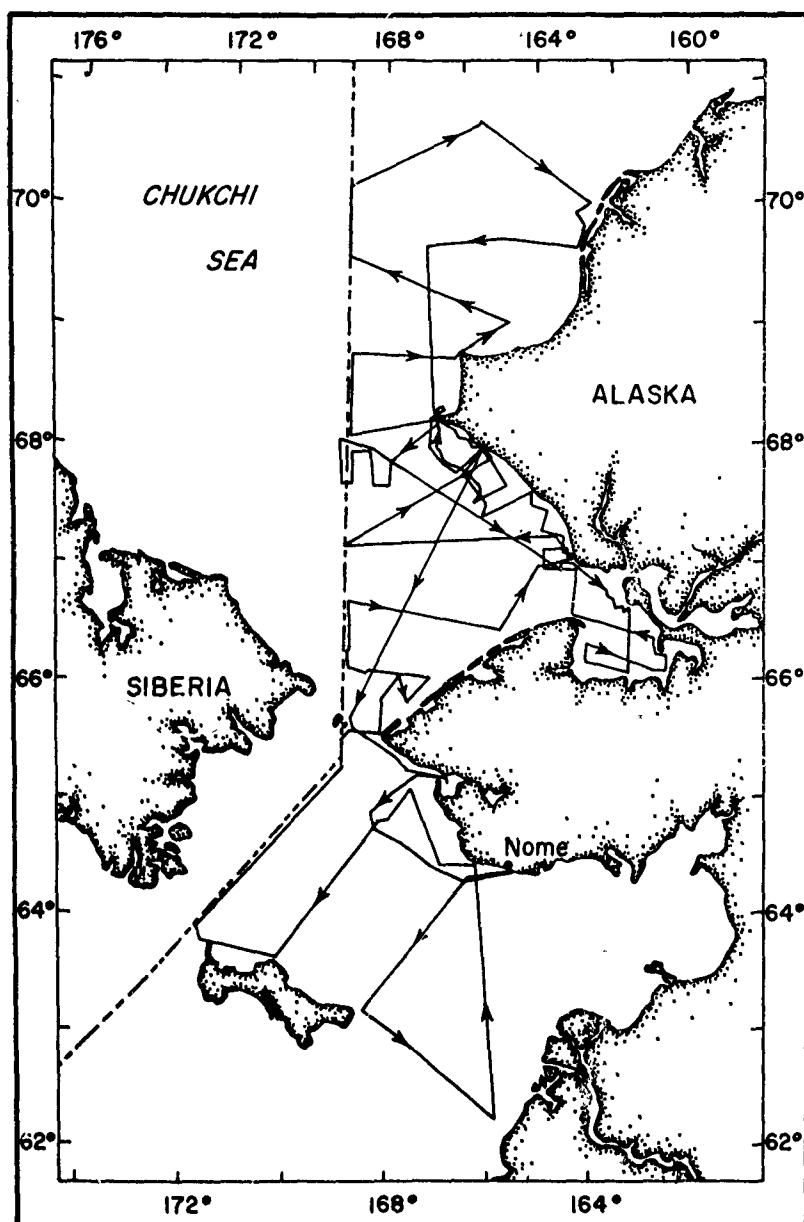
Hydrosphere

FIGURE 6 Cruise of the R. V. Brown Bear, July-August 1960.

Proceedings of the Arctic Basin Symposium

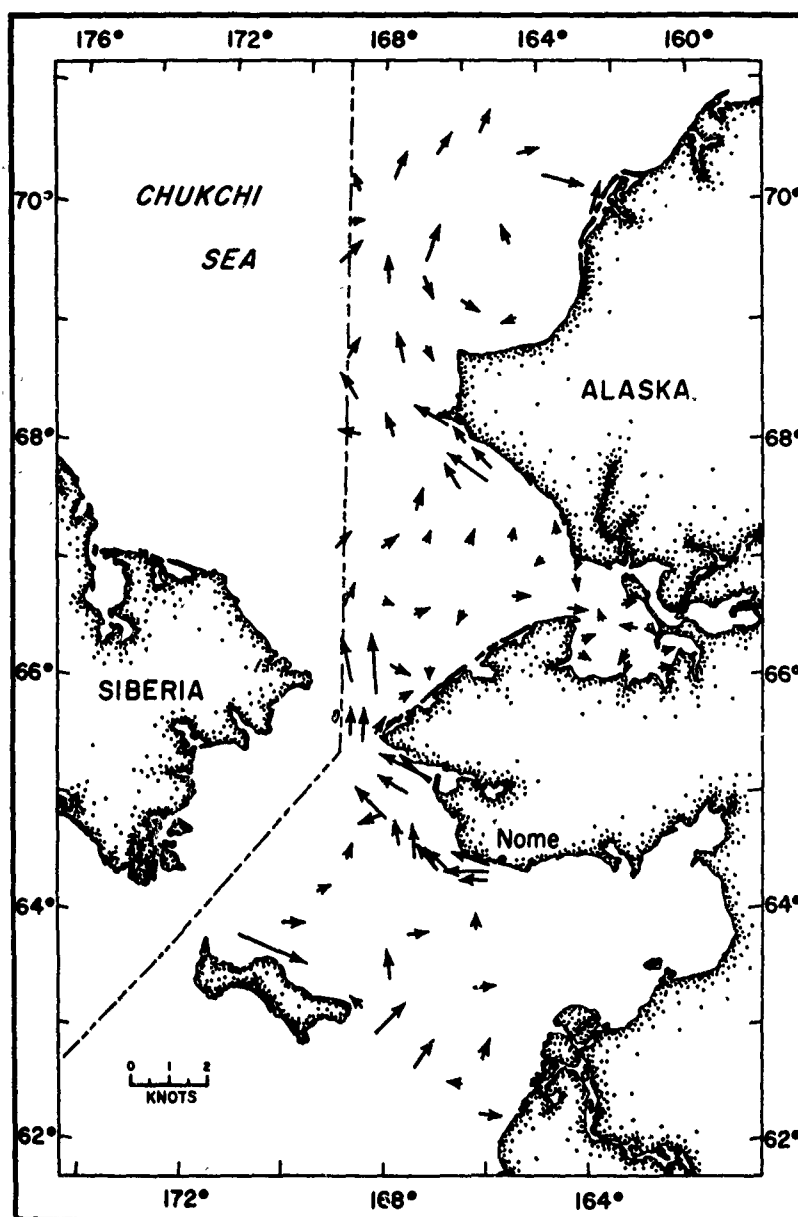


FIGURE 7 Current velocities at 5 meters, July-August 1960.

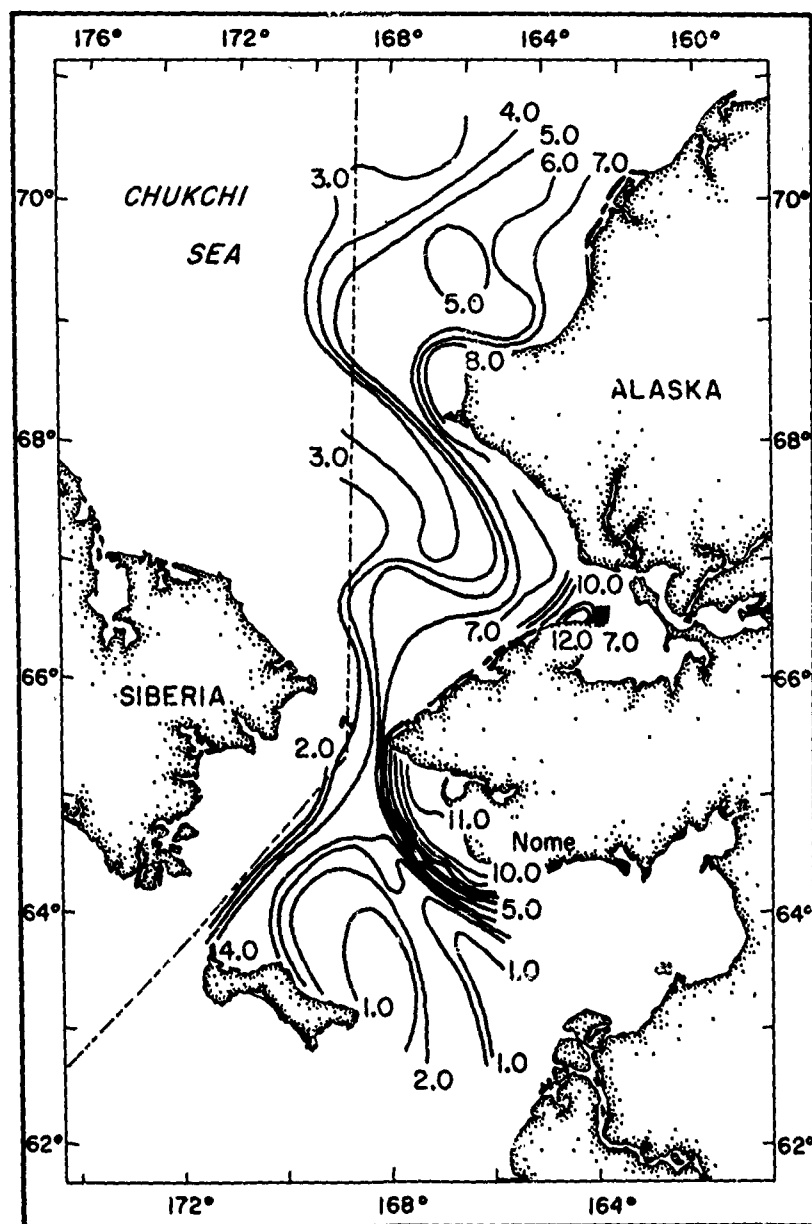
Hydrosphere

FIGURE 8 Isotherms (degrees Celsius) at 20 meters, July-August 1960.

Proceedings of the Arctic Basin Symposium

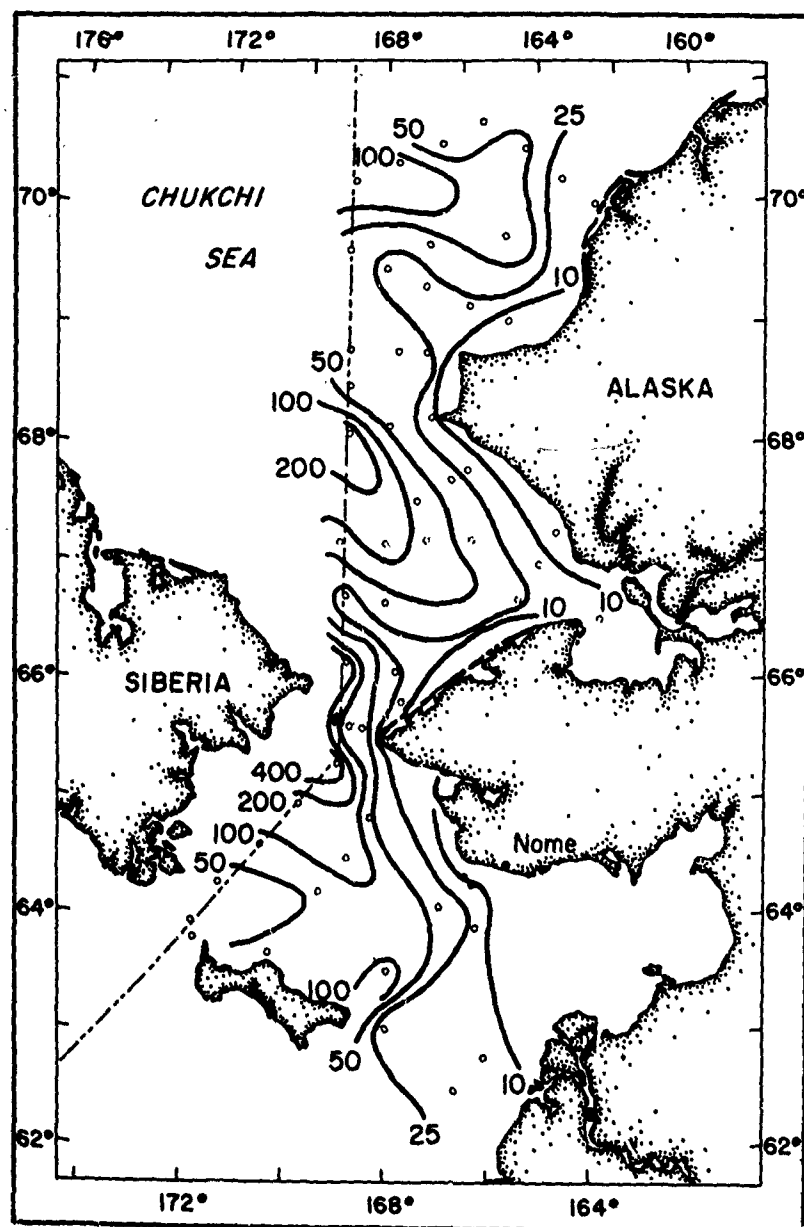


FIGURE 9 Chlorophyll *a* (milligrams/square meter) concentrations, July-August 1960.

Hydrosphere

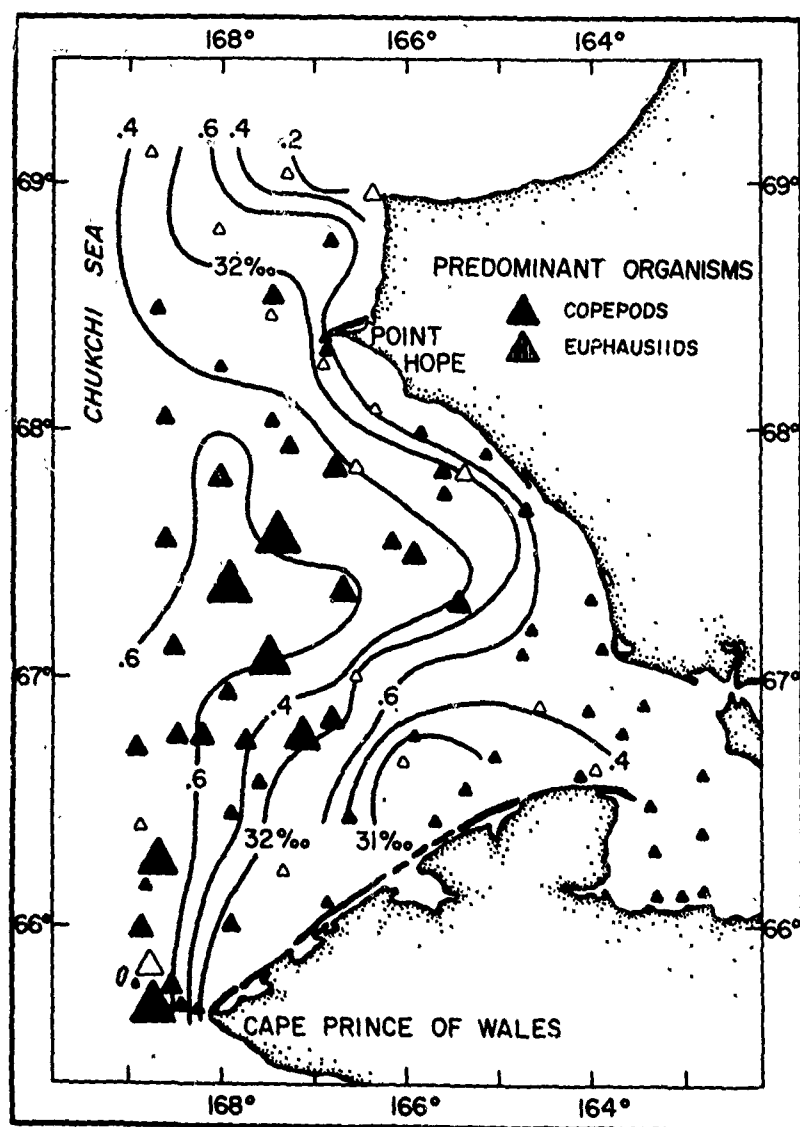


FIGURE 10 Relative settling volumes of zooplankton, July-August 1960; isohalines at 20 meters.

Proceedings of the Arctic Basin Symposium

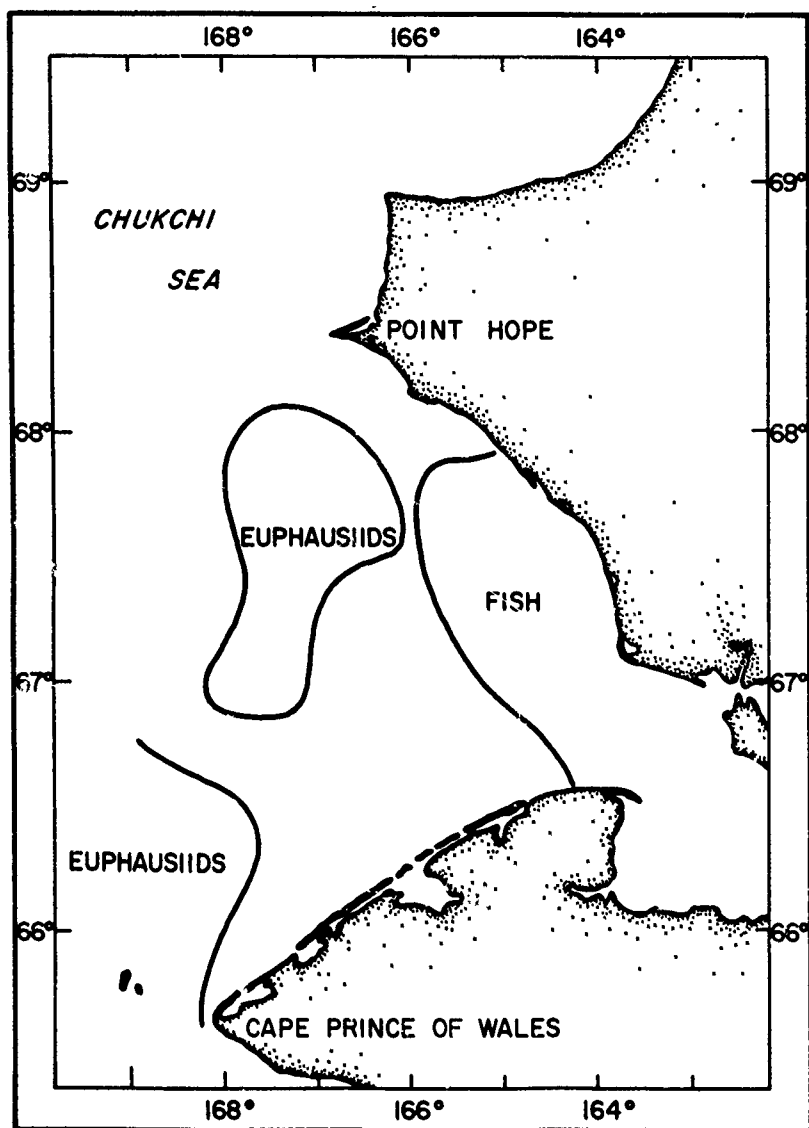


FIGURE 11 Euphausiids and small codfish, *Eleginus gracilis*, taken with a midwater trawl, July-August 1960.

**Arctic Archibenthal and Abyssal Mollusks
from Drifting Station Alpha**

A.H. Clarke, Jr.

Reprinted from the
BREVIORA, MUSEUM OF COMPARATIVE ZOOLOGY,
No. 119, 1960

B R E V I O R A

Museum of Comparative Zoology

CAMBRIDGE, MASS.

MARCH 8, 1960

NUMBER 119

ARCTIC ARCHIBENTHAL AND ABYSSAL MOLLUSKS FROM DRIFTING STATION ALPHA

By ARTHUR H. CLARKE, JR.

National Museum of Canada
Ottawa, Ontario, Canada

INTRODUCTION

During the summer of 1958 a floating Arctic ice station (Station Alpha) was manned by personnel from the Cambridge Air Force Research Center and the Lamont Geological Observatory. While the station drifted slowly northeasterly in the high Arctic region about 800 miles north of Point Barrow, Alaska and 300 miles from the North Pole, eight representative bottom samples were taken from deep archibenthal and abyssal depths.

All of these samples contained mollusks (see Tables 1 and 2), a total of seventeen species. Unfortunately, the samples were not placed in preservative and it is now impossible to ascertain which, if any, were taken alive. Notwithstanding this limitation, the collections are significant in that, (1) they come from a region that is very poorly known biologically; (2) they represent major extensions in the known geographic and bathymetric ranges of many of the species; (3) they contain three new species; and (4) they indicate the presence of large scale sediment transfer processes within the area studied.

There is only one other report on archibenthal and abyssal mollusks from this part of the Arctic Ocean. This is by O. A. Scarlato in a report by K. A. Brodskii and M. M. Nikitin of the hydrobiological work done at the Russian Scientific-Research Drifting Station of 1950-1951. Fourteen species of mollusks are listed from six stations scattered between points lying approximately 350 miles N.W. and 550 miles north of Point Barrow,

Alaska. For completeness, the station data and the mollusks obtained are listed below (see Tables 3 and 4).

Table 1. U. S. Station Alpha Bottom Samples Which Yielded Mollusks ¹

Sample No.	Depth (fms.)	Latitude ° N	Longitude ° W	Bottom	Instrument used	Quantity of material taken
2	1370	83° 59'	151° 44'	brown ooze	10 gal. can	3 gal.
3	1364	84° 09'	150° 23'	mud, and pebbles	1 M. trawl	1 gal.
4	907	84° 16'	149° 11'	pebbles	1 M. trawl	10 cc.
5	971	84° 23'	148° 51'	lt. brown sediment	Ekman grab	1½ qts.
6	924	84° 28'	148° 28'	mud & rocks	1 M. trawl	1 gal.
7	1208	84° 34'	146° 24'	brown mud	1 M. trawl	1 qt.
8	1257	84° 30'	145° 00'	brown clayey mud	1 M. trawl	1 gal.
10	1000	85° 01'	138° 00'	rocks & silt	1 M. trawl	1 pt. & rocks

Table 2. Mollusks in Bottom Samples Taken from U. S. Drifting Station Alpha ²

Sample No.	4	6	5	10	7	8	3	2
	924							
Depth (fathoms)	907	934	971	1000	1208	1257	1364	1370
<i>Colus hunkinsi</i> , n. sp.	—	1	—	1	4	—	—	—
<i>Siphonodentalium lobatum</i> Sby.	—	7	—	—	—	—	—	—
<i>Nucula zophos</i> , n. sp.	1	73	—	11	—	—	—	—
<i>Portlandia intermedia</i> Sars	—	3	—	—	14	—	11	—
<i>P. lenticula</i> Möller	—	1	—	—	—	—	—	—
<i>Malletia abyssopoli</i> is, n. sp.	—	30	—	12	31	4	5	6
<i>Bathyarca frielei</i> Priele	2	50	4	34	34	6	8	—
<i>Hyalopecten frigidus</i> Jensen	—	25	—	3	36	2	—	—
<i>Cyclopecten</i> (<i>Delectopecten</i>) <i>greenlandicus</i> Sowerby	—	5	—	3	13	6	10	4
<i>Astarte borealis</i> Schumacher	—	1	—	—	—	—	—	—
<i>A. montagui</i> Dillwyn	—	2	—	—	—	—	1	—
<i>Serripes groenlandicus</i> Bruguière	—	—	—	—	3	—	—	—
<i>Macoma</i> sp.	—	1	—	—	—	—	—	—
<i>Hiatella arctica</i> Linné	—	1	—	1	—	—	3	—
<i>Lyonsiella alaskana</i> Dall	—	—	—	—	1	—	—	—
<i>Poromya</i> sp. (fragment)	—	—	—	1	—	—	—	—
<i>Cuspidaria</i> sp. (fragments)	—	1	—	—	1	—	—	—
TOTALS	3	201	4	66	137	18	38	10

¹ One live brittle star and 4 live holothurians occurred in samples 7 and 10 respectively. No other living animals were specifically noted by the collector.

² Samples are arranged in order of increasing depth. Quantities refer to the number of specimens (gastropods and scaphopods) or valves (bivalves) obtained.

1960 ARCTIC ARCHIBENTHAL AND ABYSSAL MOLLUSKS

Table 3. Russian Bottom Samples Which Yielded Mollusks ³

SAMPLE No.	DEPTH (fms.)	LATITUDE °N	LONGITUDE °W
R 1	400	76° 25'	167° 14'
R 2	1400	76° 44'	170° 15'
R 4	550	78° 22'	167° 10'
R 6	1000	78° 52'	165° 00'
R 7	650	78° 54'	162° 00'
R 11	1800	80° 45'	161° 00'

Table 4. Mollusks Reported From Russian Bottom Samples ⁴

Sample No. Depth (fathoms)	R 1 400	R 4 550	R 7 650	R 6 1000	R 2 1400	R 11 1800
<i>Lora violacea</i> Mighels	—	—	2	—	—	—
<i>Lora</i> sp.	—	2	—	—	—	—
<i>Sipho</i> sp.	—	—	sev.	—	—	—
<i>Cylichna alba</i> (Brown)	—	—	2	—	—	—
<i>Siphonodentalium lobatum</i> Sby.	sev.	sev.	many	sev.	1	—
<i>Nucula tumidula</i> Malm	—	—	1	—	—	—
<i>Nucula</i> sp.	—	sev.	sev.	1	—	—
<i>Portlandia</i> sp.	—	1	1	—	—	sev.
<i>Arca pectunculoides</i> Scacchi	—	—	—	1	1 ⁵	—
<i>Arca frielei</i> Jeffries	—	—	sev.	—	—	—
<i>Dacrydium vitreum</i> (Möller)	—	—	—	sev.	—	—
<i>Propeamussium frigidus</i> (Jensen)	1	—	—	—	2	—
<i>Cuspidaria glacialis</i> (G. Sars)	frag.	—	2	—	—	—
<i>Cuspidaria</i> sp.	—	—	—	—	1	—

SYSTEMATICS

Family NEPTUNEIDAE

COLUS HUNKINSI, new species

Plate I, figure 9

Shell fusiform, approximately one inch long, white, rather thin, and with revolving carinae. Whorls 6½, convex, rather strongly shouldered, and with sutures deeply impressed. Sculpture consisting of about 18 well defined carinae on the body whorl (only the upper 5 or 6 of which are prominent), about 6 on the

³ Locations and depths are from a map showing the stations. The values are therefore only approximate.

⁴ The abbreviations "sev." and "frag." are for "several" and "fragments," respectively.

⁵ Taken alive. All other mollusks represented by empty shells only.

penultimate whorl, and 3 on the upper whorls. Fine, incremental lines are also present below the protoconch. Spire produced at an angle of about 42° . Parietal lip with a thin callus. Palatal lip thin or slightly thickened and convex. Columella broadly sigmoid. Aperture ovate, medium sized. Siphonal canal short and open. Umbilicus absent. Periostracum very thin, light brown. Nuclear whorls about $3\frac{1}{2}$, with no distinct demarcation between the nuclear whorls and the postnuclear whorls. First whorl small (0.8 mm. in diameter), planospiral, and unsculptured; second and later whorls turreted and rapidly increasing in size. On the second whorl the upper carina and numerous fine longitudinal riblets appear. On the third whorl the second and third carinae appear and the longitudinal riblets become stronger and evenly spaced, equaling the carinae in height and thickness. On the fourth whorl the carinae become stronger, the riblets gradually give way to fine, incremental lines, and the whorl assumes adult sculpture. Operculum not seen.

	Height	Width	Length of Aperture	Number of Whorls
Holotype (sample 6)	24.4 mm.	12.0 mm.	12.0 mm.	$6\frac{1}{2}$
Paratype (sample 10)	20.0 ⁶	12.2	11.2	—
Paratype (sample 7)	10.0	6.0	5.8	$4\frac{1}{2}$
Paratype (sample 7)	7.3	5.0	4.6	4

Types. The holotype, a dead specimen from Station Alpha sample 6 (924-934 fathoms, $84^\circ 28' N$, $148^\circ 28' W$), is No. 222066 in the Museum of Comparative Zoology. Paratypes from samples 7 and 10 are at the National Museum of Canada, the Museum of Comparative Zoology, and Lamont Geological Observatory.

Remarks. *C. hunkinsi* has the aspect of a typical archibenthal or abyssal neptuneid. It is similar to *C. parvus* (Verrill and Smith 1882) from off Martha's Vineyard in 312 to 506 fathoms, but that species is smaller (14 mm. in length, 7 whorls), much less strongly shouldered, and longitudinal riblets are not present on the nuclear whorls or at least they are not mentioned in the description. Another similar species is *C. krampi* (Thorson 1951) from 1028 fathoms between Disko Island, Greenland, and Baf-

⁶ Top of spire broken, only $2\frac{1}{2}$ whorls remaining.

1960 ARCTIC ARCHIBENTHAL AND ABYSSAL MOLLUSKS

finland, but that is significantly larger (36 to 39 mm., 5 to 6 whorls), the constriction between the aperture and siphonal canal is much less prominent, and the whorls are much less strongly shouldered.

The species is named for Mr. Kenneth Hunkins of the Lamont Geological Observatory who collected the Station Alpha material treated in this report.

Specimens examined. This species is known only from six dead specimens collected from Station Alpha in samples 6, 7, and 10, taken in 924 to 1208 fathoms about 800 miles north of Point Barrow, Alaska. The "*Sipho* sp." reported from Russian sample R 7 (650 fathoms, 470 miles N.N.W. of Point Barrow) may be *C. hunkinsi*, but this is uncertain.

Family SIPHONODONTALIIDAE
SIPHONODONTALIUM LOBATUM Sowerby 1860

The seven dead specimens from Station Alpha sample 6 (924-934 fms.) are all typical, measuring up to 13 mm. in length. *S. lobatum* occurs throughout the Arctic Ocean from shallow water to 2000 meters (approximately 1100 fathoms) on soft silty and silty-sandy bottoms with a bottom temperature of -1.8 to $+4^{\circ}\text{C}$ (Brodsii and Nikitin 1955). It is also recorded from the North Atlantic in 60 to 1813 fathoms (La Rocque 1953).

Family NUCULIDAE
NUCULA ZOPHOS, new species

Plate I, figures 15-18

Shell subtriangular, compressed, rather large for the genus (over $\frac{1}{2}$ inch long), finely sculptured, with medium sized, well developed taxodont hinge teeth and a brownish or blackish periostracum. Outline triangular, with prominent, elevated beaks located near the posterior third of the shell and with a flattened base which is usually nearly straight centrally. Surface sculptured with numerous, rather fine, closely spaced concentric ridges and grooves, and fine, closely spaced radial lines which cause the surface to appear cancellate when viewed under the microscope. Exterior stained with brown and black, but portions of what appears to be a thin brown periostracum remain. Inner

surface nacreous and exhibiting the radial lines which end at the strongly crenulated shell margin. Anterior and posterior muscle scars and simple pallial line present but not prominent. Hinge plate V-shaped, with an anterior and a posterior row of somewhat compressed, columnar, taxodont teeth. The two rows are separated by a prominent, narrow, anteriorly directed chondrophore. Taxodont teeth somewhat heavier anteriorly, and numbering about 15 to 17 in the anterior row and 7 to 10 in the posterior. Umbones deeply excavated.

	Length	Height	Width (1 valve)
Holotype (sample 6)	10.0 mm.	7.6 mm.	2.5 mm.
Paratype (sample 6)	14.6	9.9	2.8
Paratype (sample 6)	14.5	10.0	3.0
Paratype (sample 10)	9.7	7.3	2.2

Types. The holotype, a left valve from Station Alpha sample 6 (924-934 fathoms, 84° 28' N, 148° 28' W), is number 222067 in the Museum of Comparative Zoology. Paratypes from samples 4, 6, and 10 are at the National Museum of Canada, the Museum of Comparative Zoology, and Lamont Geological Observatory.

Remarks. Because of its peculiar elongate shape, flattened base, sub-central umbones, and reticular sculpturing, *N. zophos* does not closely resemble any other species. In sculpturing it is somewhat similar to *N. nucleus* Linné, but *nucleus* is smaller, more rounded, with the beaks far forward, and much different in general appearance. *N. iphigenia* Dall 1908 from 259 fathoms in the Bay of Panama is probably morphologically closer to *zophos* than is any other *Nucula*, but that is much larger and more ponderous, the base is more rounded, and the radial sculpturing is different and much more conspicuous.

Specimens examined. The only known specimens are the 85 single valves dredged from Station Alpha, about 800 miles north of Point Barrow, Alaska, in 907 to 1000 fathoms. It is possible that the "*Nucula* sp." collected from the Russian Drifting Station at localities R4, R6, and R7 (550 to 1000 fms.) also represent this species, but those specimens have not been examined by the writer.

1960 ARCTIC ARCHIBENTHAL AND ABYSSAL MOLLUSKS

Family MALLETIIDAE
MALLETIA ABYSSOPOLARIS, new species

Plate I, figures 19-22

Shell subovate, inflated, of medium size (length about $\frac{1}{2}$ inch) and thickness, weakly sculptured and with small, well developed taxodont hinge teeth and a brown (?) periostracum. Outline varying from nearly circular to ovate-rhomboid and with or without a postbasal swelling. Beaks rather prominent and inflated. Surface sculptured with narrow lines and rays. Ligament groove narrow and elongate, running from below the umbo to near the middle of the posterior row of teeth. Exterior stained brown or blackish, but portions of what appears to be a thin brown periostracum remain. Inner surface iridescent and showing the external sculpturing. Anterior muscle scar impressed, posterior scar and pallial line less prominent but usually clearly visible. Pallial sinus absent. Hinge plate concave anteriorly and convex posteriorly. Hinge teeth taxodont, V-shaped when viewed apically, continuous under the umbones, larger and higher anteriorly, smaller posteriorly, and numbering about 32 to 40 in adult specimens, of which 10 to 12 are anterior and 22 to 28 are posterior. Umbones excavated.

	Length	Height	Width (1 valve)
Holotype (sample 6)	12.6 mm.	11.0 mm.	3.6 mm.
Paratype (sample 6)	14.0	10.0	4.3
Paratype (sample 6)	12.9	9.6	3.7
Paratype (sample 7)	11.0	8.0	3.5

Types. The holotype, a left valve from Station Alpha bottom sample 6 (924-934 fathoms, $84^{\circ} 28' N$, $148^{\circ} 28' W$), is No. 222068 in the Museum of Comparative Zoology. Paratypes from samples 2, 3, 6, 7, 8, and 10 are at the National Museum of Canada, the Museum of Comparative Zoology and Lamont Geological Observatory.

Remarks. *M. abyssopolaris* resembles *M. abyssorum* Verrill and Bush 1898 taken off Chesapeake Bay in 2620 fathoms, but that species is only 5 mm. long, the teeth are not continuous under the beaks, and it is without radial lines. *M. dunkeri* Smith

1885 from off Japan in 1875 fathoms is also somewhat similar, but it too is only 5 mm. long, it is without radial lines, and the beaks are proportionately much smaller.

This species is apparently more closely related to *Malletia* than to other existing genera, notwithstanding the absence of the pallial sinus, which according to most authors is present in all species of *Malletia*. This is a case similar to that of *Tindaria erebus* Clarke, 1959, in which the pallial sinus is present, although it is supposedly absent in species of *Tindaria*. For reasons given there, this single character is not considered sufficient to disrupt an otherwise acceptable generic placement, and rather than place *M. abyssopolaris* in a new genus or subgenus, it is left in *Malletia*.

Specimens examined. Known only from 88 single valves collected from Station Alpha between 924 and 1370 fathoms about 800 miles north of Point Barrow, Alaska.

Family NUCULANIDAE

PORTLANDIA INTERMEDIA Sars 1865

Plate I, figures 6-8

Single valves of this species occurred in samples 3, 6, and 7 in depths ranging from 924 to 1364 fathoms. It is panarctic in distribution and has been recorded alive from depths ranging from 4 to 5 fathoms in the Siberian Ice Sea to 630 fathoms near the Shetland Islands. Dead shells have been recorded in the North Atlantic from depths as great as 1273 fathoms (Ockelmann, 1958). It usually occurs on clay or mud bottoms, sometimes with admixtures of sand and gravel.

PORTLANDIA LENTICULA Møller 1842

Plate I, figure 4

A single valve in sample 6 (924-934 fathoms) seems to belong to this species. It is another panarctic species and has been recorded from zero fathoms in eastern Greenland to about 765 fathoms north of the Shetland Islands. It is reported as usually occurring on clay or mud which may or may not contain additional sand or gravel, as in *Portlandia intermedia*.

1960 ARCTIC ARCHIBENTHAL AND ABYSSAL MOLLUSKS

Family ARCIDAE
BATHYARCA FRIELEI "Jeffreys" Friele

Plate I, figures 10-14

Arca frielei (Jeffreys m.s.) Friele 1877, *Nyt Magazin for Naturvidenskabene*, 23:2. Type locality: Norwegian Sea, Norwegian 1876 Expedition stations 40 (1180 fms.), 51 (1130 fms.), and 53 (1500 fms.); also Porcupine Expedition.

Arca imitata Smith 1885, *Challenger Reports, Lamellibranchiata*, p. 321 + text figs. Type locality: Challenger station 244, Mid-North Pacific in 2900 fathoms.

The specimens collected from Station Alpha are variable in shape, and since the extremes are all connected by intergrades it is impossible to separate them objectively. It is probable that the Russian report of both *Arca pectunculoides* Scacchi and *Arca frielei* is the result of such an attempt. The type figures of *pectunculoides* in Scacchi 1835 (pl. 1, figs. 12 a, 12 b) are poor but certainly do not represent this species. We are left with the choice of using *frielei* "Jeffreys" Friele 1877 or *imitata* Smith 1885, both of which represent forms which are very similar to each other and to the present species, but not identical to it. Smith's figures of the two forms of *imitata* resemble the most frequent variations seen in the present species, but since *frielei* is more frequently used and is the earlier name, it is used here. The problem should be studied further.

Dead specimens of this species were found in seven of the eight samples collected from Station Alpha, in depths ranging from 907 to 1364 fathoms. The Russian report of a living specimen of *A. pectunculoides* at 1400 fathoms probably represents this species. It is recorded from the North Atlantic and adjacent Arctic Ocean in depths ranging from 10 to 12 fathoms (north-east Greenland) down to 1540 fathoms (off western Norway), and as living only in regions having a temperature of -1° to $+1^{\circ}$ C. It is also reported from the Barents and Kara seas on brown, soft silt at depths of approximately 80 to 110 fathoms and deeper (Brodskii and Nikitin). According to Ockelmann (1958), on the coast of eastern Greenland it is much more common below 130 fathoms than in shallower depths.

Family PECTINIDAE
HYALOPecten FRIGIDUS Jensen

Plate I, figures 1-3

Pecten fragilis Jeffreys 1876, Annals and Magazine of Natural History, (4) 18, 424. Type locality: Valorous Expedition stations 9, 12, and 16, between Ireland and Greenland, 1450 to 1785 fathoms and Norwegian Expedition of 1876, 1000 to 1500 fathoms, Greenland and Norwegian Seas. Includes three species: *P. undatus* Verrill 1884, *P. greenlandicus* Sowerby 1845, and *P. frigidus* Jensen 1912. Figured by Jeffreys (Proceedings of the Zoological Society of London for 1879, pl. 45, figs. 1, 1). Not *Pecten fragilis* Montagu 1808.

Pecten frigidus Jensen 1912, The Danish Ingolf Expedition, 2, part 5 (Lamellibranchiata, part 1), p. 33, pl. 1, figs. 7 a-f. New name for *P. fragilis* Jeffreys, in part.

Jensen 1912 has clarified the previously confused taxonomic status of this species by pointing out the following facts: (1) Jeffreys' original description of *fragilis* was based on three species: *P. undatus* Verrill (= *P. biscayensis* Locard 1898), fragments of which were collected by the Valorous Expedition between Ireland and Greenland; *P. greenlandicus* Sowerby, from the same source, believed by Jeffreys to be the lower valve of *fragilis*; and a third species from the Norwegian Sea went to Jeffreys by Friele, and later named *frigidus* by Jensen. (2) Jeffreys' two figures of *fragilis* are of this third species but show a right valve in the right-hand figure and the mirror image of the right valve in the left-hand figure.

The right-hand figure (Jeffreys 1879, *loc. cit.*) is hereby selected as the type figure of *fragilis* Jeffreys 1876. It therefore becomes automatically also the type figure of *frigidus* Jensen 1912. Pending possible location of the specimen, with locality data, from which the figure was drawn, the type locality cannot be restricted within the region explored by the Norwegian North Atlantic Expedition of 1876 to 1878, viz., the Norwegian and Greenland seas.

Seventy-six specimens and fragments from Station Alpha samples 6, 7, 8, and 10 (924-1257 fathoms) appear to belong to this species. It has been reported alive from the Norwegian and Greenland seas in 579 to 1539 fathoms in localities where bottom temperature is between 0 and -1.1°C .

1960 ARCTIC ARCHIBENTHAL AND ABYSSAL MOLLUSKS

CYCLOPECTEN (DELECTOPECTEN) GREENLANDICUS Sowerby 1845

Forty-one single valves and fragments of this fragile species occurred in Alpha Station samples 2, 3, 6, 7, 8, and 10 (924 to 1370 fathoms). The species is recorded from the subarctic North Atlantic Ocean and from localities generally distributed over the entire Arctic coasts of North America, Europe, and Asia. It occurs alive from 2 fathoms in east Greenland (Ockelmann, 1958) to 1100 fathoms between Greenland and Jan Mayen (Hägg 1905), usually on clay containing stones, gravel, or shells.

Family ASTARTIDAE

ASTARTE BOREALIS Schumacher 1817

Only one small, damaged valve was collected from Station Alpha of what is assumed to be this species. This occurred in sample 6 (924-934 fathoms). It is a panarctic, circumpolar species, recorded also from the North Atlantic. Living specimens are known from 0 fathoms in east Finmark to 254 fathoms north of Spitzbergen. Dead shells have been recorded from 1482 fathoms in the North Atlantic.

ASTARTE MONTAGUI Dillwyn 1817

Plate I, figure 5

Jensen (1912) and Ockelmann (1958) have done much to clarify the status of this variable species. Three valves from Station Alpha samples 3 and 6 (924 to 1364 fathoms) appear to belong to it. *A. montagui* occurs in the North Atlantic and throughout the Arctic in depths ranging from the low tide line (western Baltic Sea) to 244 fathoms (western Greenland). Usually found on sand or clay, the species also occurs on rocky or muddy bottoms (Ockelmann, 1958).

Family CARDIIDAE

SERRIPES GROENLANDICUS Bruguière 1789

Three fragments from station 7 (1208 fathoms) belong to this species. *S. groenlandicus* is panarctic, extending south in the Pacific to Hokkaido, Japan, and Puget Sound, Washington, and

south in the Atlantic to Cape Cod, Massachusetts, and northern Norway.

In depth it ranges alive from just below the low tide line (Iceland) to 166 fathoms (western Greenland), and single valves have been found as deep as 1340 fathoms in the North Atlantic. Although it is most abundant on sand or mud bottoms, it occurs on other substrates also.

Family TELLINIDAE

MACOMA sp.

This genus is represented by a fragment collected in Station Alpha sample 6 (924 to 934 fathoms). It is a panarctic and circumboreal group and occurs alive from low tide to depths of only a few fathoms.

Family SAXICAVIDAE

HIATELLA ARCTICA Linné 1767

Five valves from Station Alpha samples 3, 6, and 10 (924 to 1364 fathoms) show the double row of spines on the posterior slope which is characteristic of *H. arctica* (see Abbott 1954, fig. 92, after Lebour, 1938). The species has an apparently enormous geographic range, being recorded as panarctic and south to western Panama, the West Indies, the Mediterranean, and even from the Cape of Good Hope. Probably several sibling species are involved however. In the Arctic it occurs principally at the low tide line or in shallow water, although a doubtful record for live specimens in 1200 fathoms off Ireland has been reported (Ockelmann, 1958). Single valves are reported from the North Atlantic in about 1300 fathoms. A common habitat is among the holdfasts of kelp although the species is also known to bore into soft rock.

Family VERTICORDIIDAE

LYONSIELLA (LAEVICORDIA) ALASKANA Dall 1895

One valve from sample 7 (1208 fathoms) apparently belongs to this species. It was described from a living specimen found in 1569 fathoms in the Gulf of Alaska south of Sitka, Alaska, in green ooze and later recorded also from off Catalina Island, California, in 600 fathoms.

1960 ARCTIC ARCHIBENTHAL AND ABYSSAL MOLLUSKS

Family POROMYIDAE

POROMYA sp.

A single unidentifiable fragment of *Poromya* occurred in sample 10 (1000 fathoms). *Poromya* is a cosmopolitan genus of archibenthal and abyssal bivalves.

Family CUSPIDARIIDAE

CUSPIDARIA sp.

An unidentifiable fragment of *Cuspidaria* occurred in samples 6 (924 to 934 fathoms) and 7 (1208 fathoms). Like *Poromya*, *Cuspidaria* is also a cosmopolitan archibenthal and abyssal genus.

CONCLUSIONS

Samples 3, 6, 7, and 10 (see Tables 2 and 5) contain shells which clearly were derived from shallow water. All of the samples contain species that might have come from shallow water and it is therefore probable that transport from shallow water has occurred at most, or possibly all, of the stations on which this study was based.

Table 5.

Species probably living where collected	Species probably transported from shallow water	Species which could be living where collected or could have been transported from shallow water
<i>Colus hunkiasi</i>	<i>Portlandia intermedia</i>	<i>Siphonodentalium lobatum</i>
<i>Nucula zophos</i>	<i>Portlandia lenticula</i>	<i>Bathyaena frielei</i>
<i>Malletia abyssopolaris</i>	<i>Astarte borealis</i>	<i>Cyclopeecten groenlandicus</i>
<i>Hyalopecten frigidus</i>	<i>Astarte montagui</i>	<i>Poromya</i> sp.
<i>Lyonsiella alaskana</i>	<i>Serripes groenlandicus</i>	<i>Cuspidaria</i> sp.
	<i>Macoma</i> sp.	
	<i>Hiatella arctica</i>	

Supporting evidence for the transport theory lies in the following observations. (1) Many of the specimens, especially those which are considered to have been transported and those in the questionable category, are predominantly fragmentary and give

evidence of having been subjected to much more friction and mechanical wear than is observed in specimens from stable environments. (2) Most of the species which are thought not to have been transported, because of agreement between observed depth and recorded depth range, including some which are very fragile (e.g. *Hyalopecten frigidus*), are noticeably less worn and fragmentary. (3) The character of the sediments in the samples from which the mollusks were removed shows them to be unsorted (see Table I) and composed of several kinds of rock.

Friele and Grieg (1901) and others report similar mixtures of shallow and deep water species from archibenthal and abyssal depths off northern Norway, south of Spitzbergen, and between Jan Mayen and Iceland. Large stones were also observed scattered over the bottom in the Greenland Sea and elsewhere. They also point out that ice masses are frequently seen to carry large quantities of mud and other sediment derived from shallow water areas, and postulate that it is the melting of such sediment-laden ice masses far from land that causes shallow water mollusks, stones, etc. to be deposited in these regions.

Similar mechanisms must have operated in the high Arctic and probably account for the presence of shallow water species in the archibenthal and abyssal samples dredged from Station Alpha. Most of the specimens were covered with a thin coating of magnesium oxide when collected, indicating that they had been exposed at the surface of the sediment for a protracted period. This observation, together with (1) data derived from gravity cores indicating a slow rate of sedimentation and (2) observations made at Station Alpha that the present Arctic Ocean ice cover contains little or no rock fragments or sand, has led Donn *et al.* (1959) to the conclusion that the rafting must have occurred during an interval of open water which predated the Recent Epoch.

In 1954 the author examined mollusk shells and other invertebrates taken along with stones and dirt from one of the floating ice islands (Arctic Ice Island T-3, see Crary, 1958 and Fletcher, 1953). Fifty-seven valves of *Astarte crenata* Gray and three of *Bathyrca frielei* Friele were present in the sediment as well as approximately 150 serpulid worm tubes and four colonies of an unidentified ectoproct bryozoan. The mollusks are common, panarctic, sub-tidal to archibenthal species. Clearly, some ice

1960 ARCTIC ARCHIBENTHAL AND ABYSSAL MOLLUSKS

transport of sediment, shells, etc. from shallow water is still going on and the process has not been confined to pre-Recent epochs.

BIBLIOGRAPHY

ABBOTT, R. T.

1954. American Seashells. D. Van Nostrand Company, Inc., New York, i-xiv + 1-541 pp., 40 pls.

BRODSKII, K. A. and M. M. NIKITIN

1955. Hydrobiological Work (English translation), Materialy nabliudeniia nauchno-issledovatel'skoi drefuiushchei stantsii 1950/51 gada, ed. M. M. Somov, 1 zd. 'Morskoi Transport'. Vol. 1, Sect. 4. Translated by American Meteorological Society. ASTIA document No. AD 117135.

CLARKE, A. H., JR.

1959. New Abyssal Mollusks from Off Bermuda Collected by the Lamont Geological Observatory. Proc. Malacological Soc. London, 33(5):231-238, pl. 1, fig. 1.

CRARY, A. P.

1958. Arctic Ice Island and Ice Shelf Studies. Arctic, 11 (1): 3-42.

DALL, W. H.

1895. Report on Mollusca and Brachiopoda Dredged in Deep Water, Chiefly Near the Hawaiian Islands, with Illustrations of Hitherto Unfigured Species from Northwest America. Proc. U. S. Nat. Mus., 17:675-733, pls. 23-32.

DONN, W. L., M. EWING, and R. J. MENZIES

1959. Characteristics of the Late Quaternary Arctic Ocean. International Oceanographic Congress, Preprints, pp. 19-20.

FLETCHER, J. O.

1953. Three Months on an Arctic Ice Island. The National Geographic Magazine, 103(4):489-504.

FRIELE, H.

1877. Preliminary Report on Mollusca from the Norwegian North Atlantic Expedition in 1876. Nyt Magazin for Naturvidenskaberne, 23(3):1-10.

FRIELE, H. and I. A. GRIEG

1901. Zoologi, Mollusca 3, Den Norske Nordhavs-Expedition 1876-1878, 28: 10-131, map.

- ILÄGG, R.
1905. Mollusca and Brachiopoda gesammelt von der schwedischen zoologischen Polarexpedition nach Spitzbergen, dem nordöstlichen Grönland und Jan Mayen i. J. 1900. Arkiv för Zoologi, 2(13):1-136, pl.
- HENDERSON, J. B.
1920. A Monograph of the East American Scaphopod Mollusks. Bull. U. S. Nat. Mus., 111: i-vi + 1-177, 20 pls.
- JENSEN, A. S.
1912. Lamellibranchiata, Part 1. The Danish Ingolf-Expedition, 2(5): 1-121, 4 pls.
- KNUDSEN, J.
1949. Scaphopoda. The Zoology of Iceland, 4(62):1-7.
- LA ROCQUE, A.
1953. Catalogue of the Recent Mollusca of Canada. Bull. Nat. Mus. Canada, 129: i-ix + 1-406.
- LECHE, W.
1883. Arktiska Hafsmollusker. 1. Lamellibranchiata. Vega Expeditionens. Velenshapliga Iakttagelser, 3: 433-529, 3 pls.
- OCKELMANN, W. K.
1958. Marine Lamellibranchiata. The Zoology of East Greenland. Meddelelser om Grønland, 122(4):1-256 + 3 pls.
- OLDROYD, I. S.
1924. Marine Shells of Puget Sound and Vicinity. Publications Puget Sound Biological Station, Univ. of Washington, 4:1-272.
- POSSELT, H. J. and A. S. JENSEN
1898. Grønlands Brachipoder og Bløddyr. Conspectus Faunae Groenlandicae. Meddelelser om Grønland, 23: i-xix + 1-298, map.
- SARS, G. O.
1878. I. Mollusca Regionae Arcticae Norvegiae. Bidrag til Kundaskaben om Norges Arktiske Fauna. Christiania, Norway. i-xiii + 1-467, 52 pls.
- SCACCHI, A.
1834-1835. Notizie Intorno Alle Conchiglie ed a' Zoofiti Fossili. Annali Civili (Sicilie) (Nov. + Dec. 1834) 6:75-84. *Ibid.*, 7:5-18, 2 pls. (Jan.-April 1835).

1960 ARCTIC ARCHIBENTHAL AND ABYSSAL MOLLUSKS

SMITH, E. A.

1885. Report on the Lamellibranchiata. Challenger Reports, Zoology, 13:1-341, 25 pls.

THORSON, G.

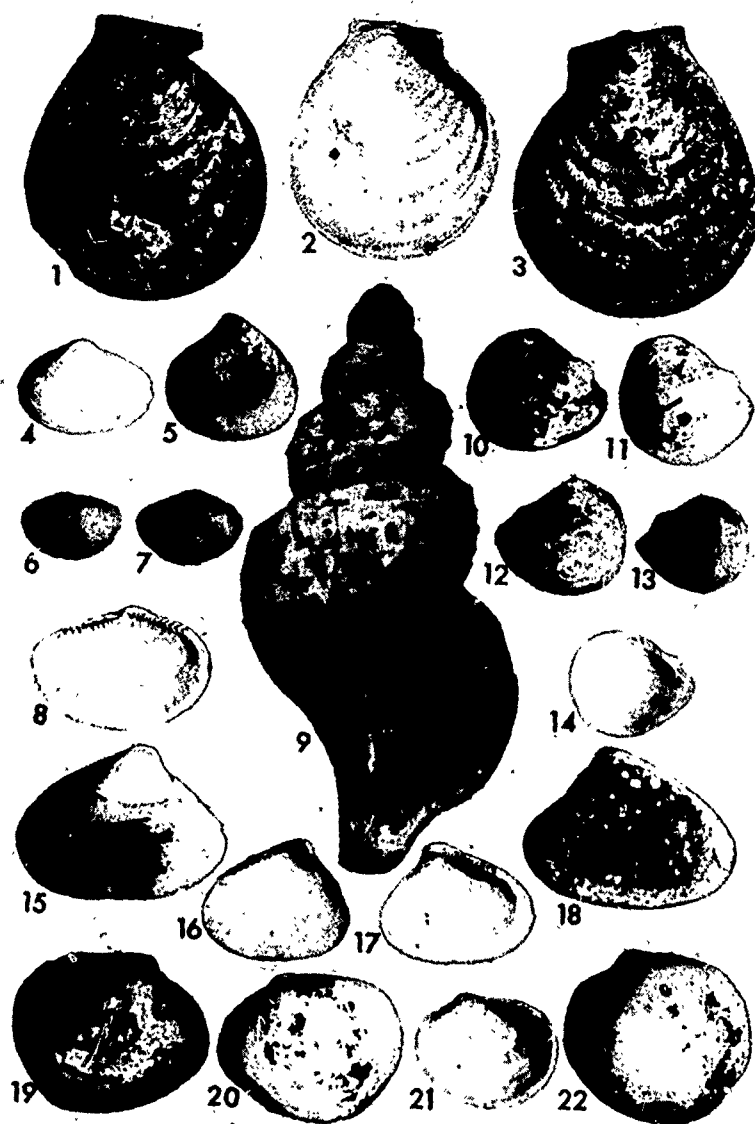
1941. Marine Gastropoda Prosobranchiata. The Zoology of Iceland, 4(60):1-150.
1944. Marine Gastropoda Prosobranchiata. The Zoology of East Greenland. Meddelelser om Grønland, 121(13):1-181.
1951. The Godthaab Expedition 1928. Meddelelser om Grønland, 81(2):1-118.

Plate

Arctic Archibenthal and Abyssal Mollusks collected from Station Alpha

- 1 - 3 *Hyalopecten frigidus* Jensen, sample 6;
- 4 *Portlandia lenticula* Møller, sample 6;
- 5 *Astarte montagui* Dillwyn, sample 6;
- 6 - 8 *Portlandia intermedia* Sars, sample 3;
- 9 *Colus hunkinsi* Clarke, holotype, sample 6;
- 10 - 14 *Bathyrca frielei* "Jeffreys" Friele, station 6;
- 15 - 18 *Nucula zophos* Clarke, holotype (16) and paratypes, all sample 6;
- 19 - 22 *Malletia abyssopolaris* Clarke, holotype (22) and paratypes from sample 6 (19, 20, 22) and sample 7 (21).

Figures 1 - 8 and 10 - 14 are 2.4 X, figure 9 is 3.2 X, and figures 15 - 22 are 2.1 X.



Plate

**Zooplankton Collections from the
High Polar Basin with Special
Reference to the Copepoda**

M.W. Johnson

Reprinted from
LIMNOLOGY AND OCEANOGRAPHY,
Vol. 5, No. 1, pp. 89-102, 1963

ZOOPLANKTON COLLECTIONS FROM THE HIGH POLAR BASIN WITH SPECIAL REFERENCE TO THE COPEPODA¹

Martin W. Johnson

Scripps Institution of Oceanography, University of California

ABSTRACT

Analysis was made of 57 plankton tows taken to depths of 2,000 m from 81°14' N, 85°16' N during a portion of the 1957-58 drift of the ice flow Drift Station Alpha in the high Polar Basin. Thirty-one species of calanoid and 3 species of cyclopoid copepods were identified. Some uncertain species are discussed and figured.

The most abundant species were *Calanus glacialis*, *Calanus hyperboreus*, and *Metridia longa*. These were most abundant above 100 to 200 m but were found sparsely distributed to depths of 1,000 to 2,000 m. There was an increased number of species with depth of sampling up to about 1,000 to 1,500 m. There appeared to be a rather wide period over which reproduction takes place in some species especially *Pareuchaeta glacialis*.

Although most copepods carried by water currents from the Bering Sea and Chukchi Sea areas succumb before reaching the high Arctic, still a few expatriates were taken, notably *Eucalanus bungii bungii* and possibly *Mimocalanus distinctocephalus*.

INTRODUCTION

Oceanographic observations in the Arctic Ocean have increased markedly over the last three decades, and the information gained has been considerable, despite the extreme difficulties encountered in an environment, a large portion of which is not accessible at any time to normal operation by surface ships. The development of air travel and the use of floating ice as station platforms drifting slowly in the Polar Basin, have proved a great boon to investigations which are, however, still largely in the exploratory stage. The zooplankton collections are still inadequate to provide a complete picture of the plankton community but the dominant constituents are now discernible.

It will be useful to record here the analysis of a series of net hauls, sampling various depths along the drift route of the ice floe "Drift Station Alpha," in latitude 81°14' N to 85°16' N, during 1957-58, within the large cyclonic gyral involving the northern part of the Beaufort Sea. This station was established by the U. S. Air Force in connection with the International Geophysical Year and is sometimes referred to as "Ice Skate Alpha" (Farlow 1958). A previous

study has been made of the plankton (mainly surface) of the southern portion of this gyral (Johnson 1956; Hand and Kan 1961). The analyses of the present samples will be concerned mainly with the copepods which constitute overwhelmingly the greater part of the plankton community in the area.

The samples from Drift Station Alpha were kindly provided by Dr T. Saunders English, University of Washington, formerly of the Arctic Aeromedical Laboratory, Ladd Air Force Base, Alaska. It is a pleasure to thank him and others who assisted in making the collections.

The earliest plankton collection from the high Polar Basin was made by the Norwegian North Pole Expedition during the famous drift of the *Fram* 1883-93 (Nansen 1902). The crustacea of that collection were reported upon by G. O. Sars (1900). More recently, Russian expeditions, including the *Sedov*, 1937-39, and the several subsequent floating ice stations in the Polar Basin, especially the NP-2, have contributed greatly to the overall knowledge of the pelagic crustacean fauna. (See especially Bogorov 1946; Brodsky and Nikitin 1955; Brodsky 1957.) Bernard (1959) has reported on the epipelagic amphipods associated with the Fletcher Ice Island T-3.

¹ Contribution from Scripps Institution of Oceanography, New Series.

MARTIN W. JOHNSON

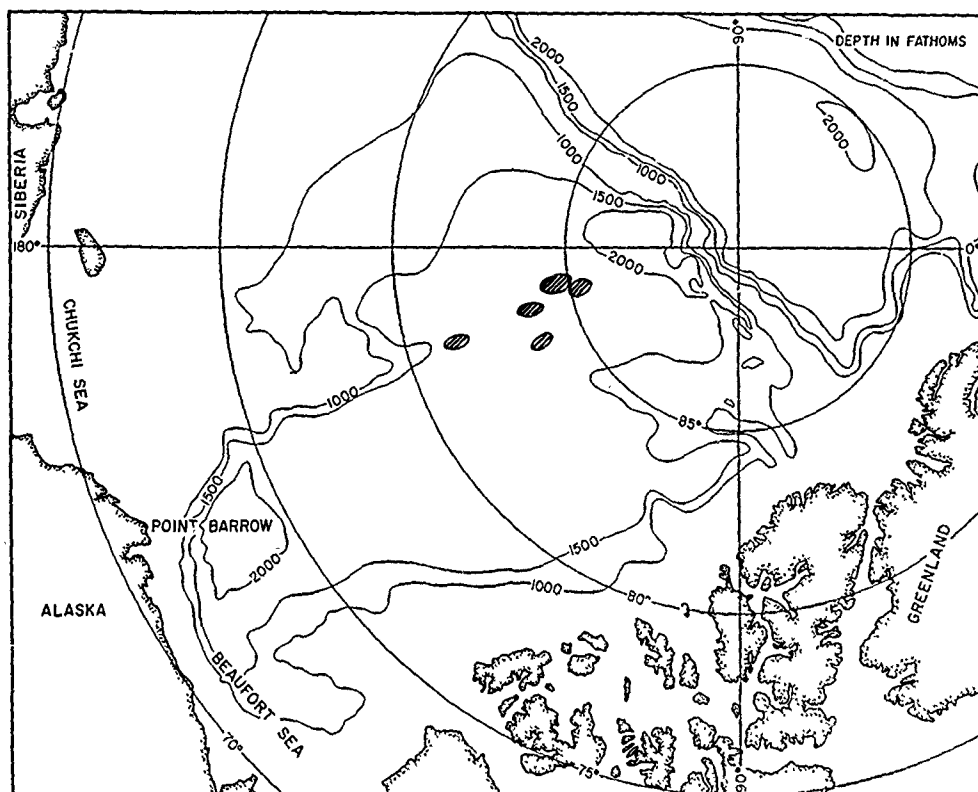


FIG. 1. Plankton sampling areas (encircled) along route of Drift Station Alpha, 18 July 1957 to 22 February 1958. (Chart based on Fig. 132, U.S.N. Hydrographic Office Publ. No. 705, 1958.)

MATERIAL AND METHODS

The present collection consists of a total of 57 tows, 48 of which were taken with a $\frac{1}{2}$ -m net of about 0.65–0.55 mm mesh and provided with a device to enable closing the net at subsurface levels. Nine tows were taken with a 1-m net. The front portion of this net was constructed of #30 XXX grit gauze having a mesh opening of 0.65 mm, while the minimum mesh opening at the cod end section was 0.306 mm. The mesh apertures when wet are approximately 0.55 and 0.23 mm respectively.

In operation, the nets were lowered with a weight through a hole cut in the ice and towed vertically through the specified depth of sampling. The sampling stations were made on 13 different dates, but some were taken on successive days, so the positions sampled fall roughly into 5 general localities along the first half of the drift route of

the ice floe, 18 July 1957–22 February 1958 (Fig. 1).

Previous plankton collections that have been analyzed for copepods in the high Polar Basin have for the most part been made in the eastern part of the Arctic Ocean, but the course of the Russian ice station NP-2 is near the southern route of Drift Station Alpha. The area of the drift is nearer the center of the Polar Basin than is the Geographic North Pole and is consequently further removed from coastal and shallow water influence and therefore probably more representative of the high Arctic.

RESULTS

The specific composition of the copepod fauna is shown in Table 1. Thirty-five species were identified, all but 3 of which are calanoids. By comparison, Sars (1900) recorded 23 calanoids and 5 cyclopoids, but

ZOOPLANKTON FROM THE HIGH POLAR BASIN

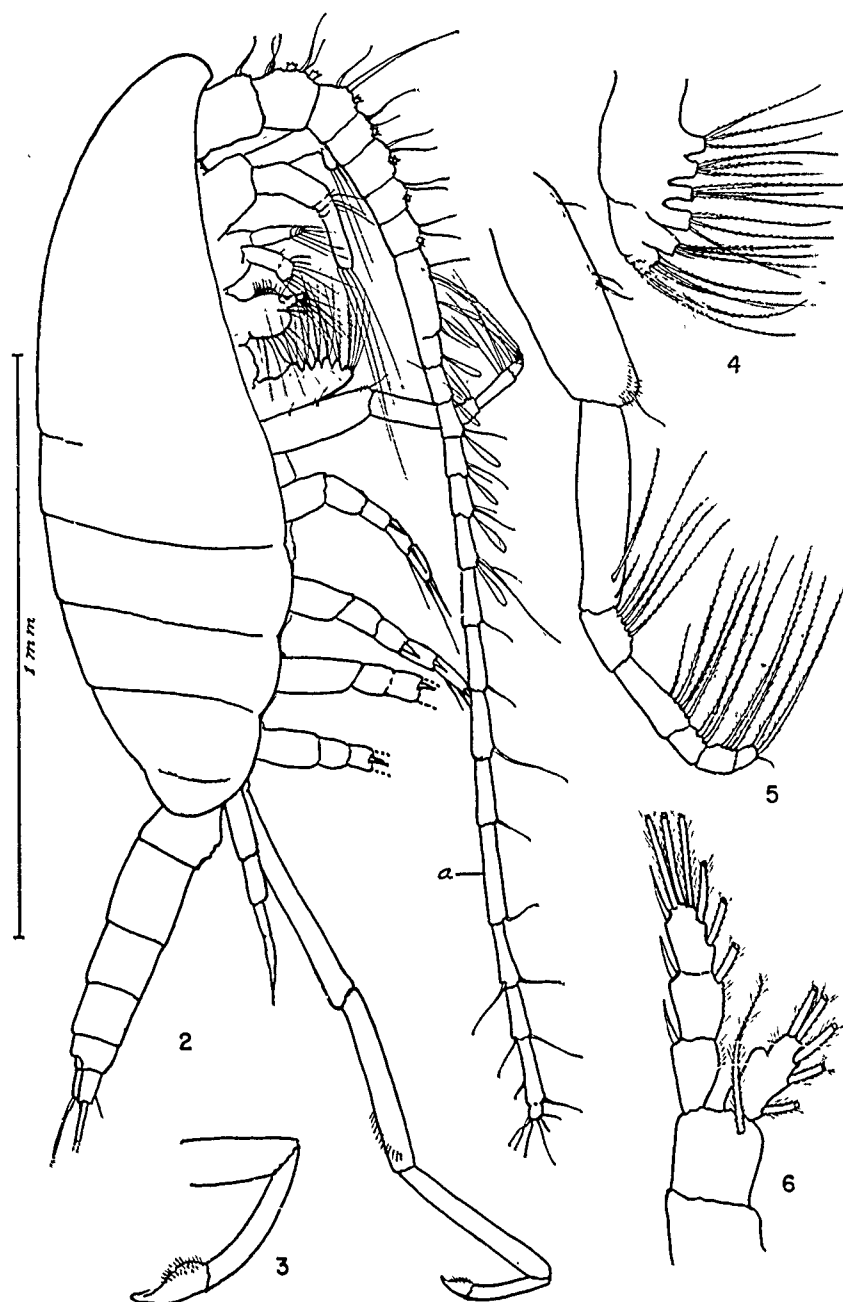


FIG. 2. *Spinocalanus*?: 2—male, lateral view; 3—tip of left foot, enlarged; 4—2nd maxilla; 5—maxilliped; 6—1st foot.

not all were taken in the more northern part of the drift, and the tows were rarely deeper than 300 m. Bogorov (1946) lists 19 calanoids and 6 cyclopoids. Brodsky (1957)

in summarizing north Polar species, lists 39 calanoids from depths ranging to 1,000 m. Cyclopoids were not listed, but in his earlier analysis there are included 4 or 5 cyclopoids

ZOOPLANKTON FROM THE HIGH POLAR BASIN

TABLE I. (Continued)

Date	29 Oct	30 Oct	31 Oct	1 Nov	4 Nov	9 Dec	22 Feb
Position	84°49' N, 167°59' W	84°43' N, 169°07' W	84°38' N, 169°42' W	84°35' N, 169°42' W	84°36' N, 170°38' W	83°47' N, 164°42' W	83°46' N, 155°13' W
Net used	1-m	1-m	1/2-m	1/2-m	1/2-m	1/2-m	1/2-m
Depth (m)	0-1000	0-1000	0-1000	0-1000	0-1000	0-1000	0-1000
<i>Aegaptius glacialis</i> Sars	3	1	1	1	1	1	1
<i>Aegaptius glacialis</i> (Gunnerus)	3	1	1	1	1	1	1
<i>Ceratius glacialis</i> Jägerskiöld	28	21	2	13	1	1	1
<i>Ceratius hyperboreus</i> Jägerskiöld	61	93	69	9	1	1	1
<i>Chiridius obtusifrons</i> Sars	1	3	4	1	1	1	1
<i>Derigania folii</i> (Linko)				4			
<i>Euaegaptius hyperboreus</i>							
Brotsky							
<i>Eucalanus bungii</i> Bungii							
Giesbrecht							
<i>Gaidius brevispinus</i> (Sars)	6	5	4	1	2	1	1
<i>Gaidius tenuispinus</i> (Sars)	1						
<i>Heterorhabdus compactus</i> (Sars)		3		1	1	1	1
<i>Heterorhabdus norvegicus</i> (Boeck)	2	1					
<i>Haloptilus acutifrons</i> (Giesbrecht)							
<i>Lucicutia glacialis</i> Sars	1						
<i>Lucicutia polaris</i> Brodsky							
<i>Metridia longa</i> (Lubbock)	33	55	24	8	4	7	30
<i>Microcalanus pygmaeus</i> (Sars)							
<i>Mimocalanus distinctocephalus</i> Brodsky							
<i>Mormonella minor</i> Giesbrecht							
<i>Oithona</i> sp.	18	20	6	2	1	4	4
<i>Paracuchaeta glacialis</i> (Hansen)							
<i>Paracuchaeta polaris</i> Brodsky							
<i>Paracuchaeta</i> ? nauplii	6	5	3	2	10	1	1
<i>Scaphocalanus brevicornis</i> Sars							
<i>Scaphocalanus magnus</i> (T. Scott)	15	9	7	4	3	16	8
<i>Scutellirhiza minor</i> (Brady)	1						
<i>Spinocalanus abyssalis</i> Giesbrecht							
<i>Spinocalanus magnus</i> Wolfenden							
<i>Spinocalanus spinosus</i> Farran							
<i>Spinocalanus</i> sp.							
<i>Spinocalanus</i> ? male	3	3	3	1	10	1	1
<i>Temorites brevis</i> Sars							
<i>Undinella oblonga</i> Sars							
<i>Xanthocalanus borealis</i> Sars							
Microcalanids, juveniles or damaged	10	2	6	2	2	4	10
Amphipods	14	7	14	2	6	2	1
Barnacle nauplii							
Chaetognaths	9	11	3	4	4	16	2
Larvaceans							
<i>Limacina</i>							
Ostracods (<i>Conchoecia</i>)	42	30	28	22	8	6	21
Shrimp juveniles	2	1	2	1	1	1	1

and some additional calanoids that are apparently not considered truly Arctic.

Notes on taxonomy

In the present study some doubt exists as to the identification of certain species, especially of *Spinocalanus*, since it has not been possible to reconcile them with published descriptions in taxonomic reports. It is not proposed here to present a taxonomic study, but it may be useful to indicate at this time some of the problems that were encountered with these and other species.

Two unidentified calanoid males were found in tows that reached depths of 2,000 m. With considerable uncertainty, they are included in Table 1 as *Spinocalanus*? males.

These males were 1.85 mm in length (Fig. 2). There is no trace of a rostrum. The urosome is a little more than half the length of the metasome. The exopods of the 1st feet consist of 3 segments, the endopod of only one segment. Each exopodal segment bears an external spine. The 2nd segment of the endopod of the maxilliped is elongated. These characteristics agree well with the genus *Spinocalanus* but no spinules whatever were present on the posterior surfaces of the swimming feet (only the basal and 1st segments of the rami were present on the 3rd and 4th feet) and the structure of the 5th pair of feet is strikingly different from that of known males of that genus. In the present males the 5th feet are uniramous, the left foot is exceedingly long and consists of 5 segments. The first 3 segments (i.e., the 2 basal and 1st exopodal) are much elongated and roughly of equal length, although the 1st basal is slightly longer than the others. The 4th segment is about one-third as long as the preceding segment and the 5th segment is short and somewhat claw-shaped with a pad covered with fine setae. The total length of the leg is about 1.75 times that of the urosome. The right foot is short, reaching about to the end of the 1st basal segment of the left foot, and consists of 2 broadened basal segments and 3 slender exopodal segments, which may be partly fused. The 1st anten-

nae reach a little beyond the end of the caudal rami. The 5th segment from the end (Fig. 2a) of the right antenna is elongated, while the corresponding segment is normal in the left antenna. The 2nd maxilla (Fig. 2: 4) is not provided with sensory structures as in *Xanthocalanus*, the males of which resemble somewhat the present specimens in the type of 5th feet.

Tanaka (1956) described the male of a new species which rather closely resemble the above males. He referred his species, apparently with some hesitation, to *Spinocalanus* naming it *S. longipes*. The presence of an external spine on the first segment of the 1st feet (Fig. 2: 6) is in keeping with *Spinocalanus*, but it is difficult to reconcile the strikingly different structure of the 5th feet with those of previously known *Spinocalanus* males. The 5th feet of Tanaka's males according to his drawings also differ considerably from the present specimens. In his species there is a rudimentary endopod on the left foot, and each of the first two segments of the exopod are about as long as the two basipodal segments combined.

Pending further evidence of the proper position of these males, the question may be considered whether they might be males of *Mimocalanus distinctocephalus*, established by Brodsky (1950) only on females. Some support of this view is found in the fact that one male was caught in the Polar Basin in the same tow as a female of that species. Tanaka's male assigned to *Spinocalanus* was taken in Sagami Bay in November where he also reports for the same month finding two females and a male of *Mimocalanus cultrifer* Farran. Males of that genus were not previously described, but his sketches of what he considers a male of that species suggest somewhat an immature specimen. Clarification of the position of these males and the whole complex of *Spinocalanus* species requires additional material and much more thorough study.

One female *Mimocalanus distinctocephalus* was found. It has not previously been reported from the Polar Basin. In size it agrees rather well with the original descrip-

ZOOPLANKTON FROM THE HIGH POLAR BASIN

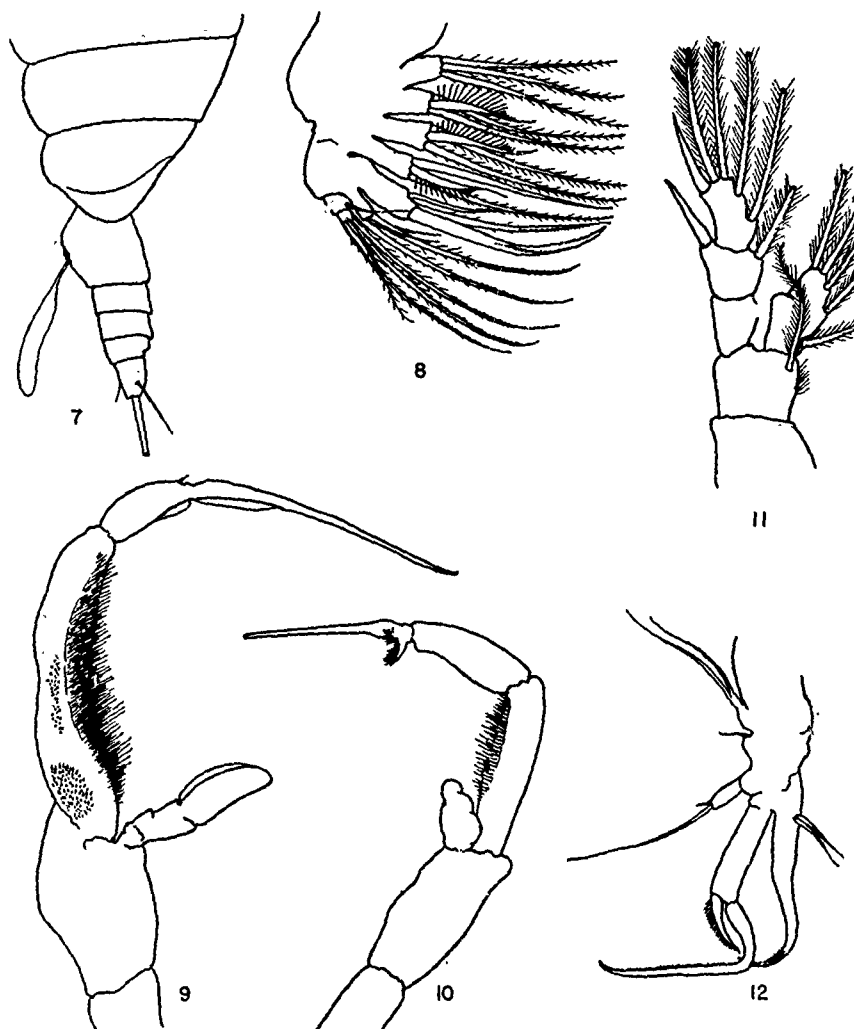


FIG. 3. *Derjuginia tolli*: 7—lateral view of portion of female showing 5th thoracic segment and urosome with attached spermatophore; 8—female, 2nd maxilla; 9—male, right 5th foot; 10—male, left 5th foot; 11—female, 1st foot. 12—*Chiridiella abyssalis*: female, 2nd maxilla.

tion and also in that the head is distinct from the thorax, but anteriorly the head is more vaulted in lateral view than indicated by Brodsky. His specimen was apparently damaged, part of the 1st antenna being lost. In the present specimen the 1st antennae consist of 25 segments and reach 3 long segments beyond the end of the caudal rami.

Eight specimens of *Derjuginia* were taken that appear to belong to the only known species *tollii* (Linko) although complete and adequate descriptions of that species are not known. The best available is that

by Brodsky (1950). The present specimens (Fig. 3) differ from his description in that the female genital segment is much longer and is swollen ventrally, and the 5th thoracic segment is smoothly rounded, not pointed. In the male the 5th thoracic segment is also smooth and bears no spines. The 2nd maxilla bears 3 setae with unusual comb-like processes (Fig. 3: 8). Other characters appear to agree well with *tollii* insofar as it has been described.

A species of *Chiridiella* measuring 2.1–2.3 mm was found in considerable numbers.

The 2nd maxilla (Fig. 3: 12) and the segmentation and spination of the swimming feet is most nearly that of *Chiridiella abyssalis* Brodsky which has been reported only from the North Pacific. The 1st pair of feet have one-segmented rami. The 2nd have three-segmented exopods (division between one and two incomplete) and one-segmented endopods. There is a normal external spine on the 1st exopod segment of each foot. The 3rd and 4th feet are similar to the 2nd pair but show slight marginal indentations on the endopod suggesting segmentation, and the 4th feet are somewhat elongated. The species might almost as readily be considered *Chiridiella reducta* described by Brodsky from the Polar Basin, but for the fact that that species is described as having no external spine on the 1st exopodal segments of the 2nd and 3rd pairs of feet. This might be a variable character. One specimen was found in which this spine on the 2nd foot was about $\frac{1}{4}$ normal size on one side and on the opposite foot it was either absent or lost. The 3rd feet had normal spines on all segments, but the terminal segment of the 4th feet had only two external spines on one foot whereas the opposite foot had the normal three.

In many Arctic and Subarctic waters there occurs a complex of two size-forms of *Calanus* that has been considered by authors as constituting one species, *Calanus finmarchicus*. By far the most abundant of these two forms encountered in the present survey is the larger one (4.29–4.95 mm) which was described by Jaschnov (1955) as *Calanus glacialis* a new species which he believed should be considered distinct from the closely related smaller Atlantic form *Calanus finmarchicus* (Gunnerus). Brodsky (1959) has accepted this distinction and recently Grainger (1961) comes to the same conclusion on a study of Arctic and Atlantic-Subarctic populations.

In the material from the Drift Station Alpha collection a distinction can be made between the larger *Calanus glacialis* and a few (12 adult females) of the small-sized forms that must be considered *Calanus fin-*

marchicus s.s. by direct comparison with specimens of that species from the Gulf of Maine and Bay of Fundy. These 12 specimens ranged from 3.3 mm to 3.8 mm in total length. The inner margin of the 1st basis of the 5th feet are only slightly concave and are fringed with 28 to 31 relatively fine teeth which, by direct comparison, are a little coarser in appearance than in specimens of about the same size from the Gulf of Maine, but finer than in the larger *C. glacialis*. (This is often difficult to assess because the number of teeth is not only variable but also overlaps in the two species such that when comparing adults of two sizes having about equal numbers of teeth those on the larger specimen must appear coarser if about equally spaced on the proportionally longer 1st basis.) The 1st antennae are relatively a little longer than observed for the larger form. Obviously these can be subtle morphological differences that do, however, together with size, serve to distinguish two groups in overlapping ranges. To what extent the differences are, as Jespersen (1934) believed, incidental to relative size may probably need further study through breeding experiments or culturing under different conditions. It is increasingly important at any rate to make such distinctions as are possible between the groups whether they be genotypic or phenotypic.

In order to clarify and add further to the record (Johnson 1956) of distribution of these *Calanus* species in the Arctic Ocean, a re-examination was made of selected plankton samples collected by the USS *Burton Island* in offshore waters at the following general areas: Point Barrow, Point Martin, Banks Island, and Amundsen Gulf, and by HMS *Cedarwood* in northern Bering Sea and southern Chukchi Sea. In each instance where examinations of adults were made, based mainly on size, only *Calanus glacialis* was observed.

In the natural economy of the area, the main biomass of zooplankton observed is made up of the three copepod species *Calanus glacialis*, *Calanus hyperboreus*, and *Metridia longa*. *Pareuchaeta glacialis* (er-

ZOOPLANKTON FROM THE HIGH POLAR BASIN

TABLE 2. Average number of individuals caught per haul in stratum indicated (not adjusted to uniform length of haul)

No. of hauls taken within the stratum	1/2-m net										1-m net									
	1	3	5	10	15	25	50	100	200	500	1000	2000	5000	10000	20000	50000	100000	200000	500000	1500000
Stratum	10-1	1-3	3-5	5-10	10-15	15-25	25-50	50-100	100-200	200-500	500-1000	1000-2000	2000-5000	5000-10000	10000-20000	20000-50000	50000-100000	100000-200000	200000-500000	500000-1500000
<i>Augetulus glacialis</i>																				
<i>Calanus glacialis</i>																				
<i>Calanus hyperboreus</i>																				
<i>Chydella abyssalis</i>																				
<i>Chydella obusifrons</i>																				
<i>Derjuginia toli</i>																				
<i>Euaugetulus hyperboreus</i>																				
<i>Eucalanus bungii bungii</i>																				
<i>Gaidius brevispinus</i>																				
<i>Gaidius brevispinus</i>																				
<i>Heterorhabdus compactus</i>																				
<i>Heterorhabdus norvegicus</i>																				
<i>Haloptilus acutifrons</i>																				
<i>Haloptilus glacialis</i>																				
<i>Lucicutia polaris</i>																				
<i>Merrilia longa</i>																				
<i>Microcalanus pygmaeus</i>																				
<i>Mimocalanus distinctocephalus</i>																				
<i>Mormonella minor</i>																				
<i>Oithona</i> spp.																				
<i>Pareuchaeta glacialis</i>																				
<i>Pareuchaeta polaris</i>																				
<i>Scaphocalanus brevicornis</i>																				
<i>Scaphocalanus magnus</i>																				
<i>Scotecthricea minor</i>																				
<i>Spinocalanus longicornis</i>																				
<i>Spinocalanus magnus</i>																				
<i>Spinocalanus spinosus</i>																				
<i>Spinocalanus</i> spp.																				
<i>Temorites brevis</i>																				
<i>Undinella oblonga</i>																				
<i>Xanthocalanus borealis</i>																				
No. of species caught in stratum	0	6	5	10	17	20	25	7	5	7	18	16	19	24	24	10	7	17	21	23

roniously listed as *P. norvegica* from the Beaufort Sea, Johnson 1956), although not so abundant numerically, must be an item of importance, because of its large size and fairly regular occurrence. The first three species are confined largely to the upper 200 m. In the deeper strata there is as previously observed an increased number of genera and species of copepods. These do not occur in numbers comparable to the above species, and some are found only very rarely. However, the regularity with which some of them occur, including especially *Scaphocalanus brevicornis*, *Scaphocalanus magnus*, *Spinocalanus magnus*, and *Temorites brevis*, would rank them comparatively high in an environment where the total mass is small.

Vertical distribution

The series of tows through isolated levels provides some information regarding the vertical range and principal habitat depths of individual species (Table 2). The upper 10 m appears to contain but little zooplankton. However, only one haul was taken in the 0-10 m level. No plankton whatever was caught by the net. With increasing depths to about 1,000 to 1,500 m there was an increase in the number of species caught, but there was a drop in numbers at levels below this. In the summary of Table 2 it will be seen that the $\frac{1}{2}$ -m net and the 1-m net tows show comparable increases in species as the greater depth is reached. Although this numerical difference is probably real for the water levels, still it must be noted that the data show a greater number of hauls through the 200 to 1,000-m horizon, and the hauls there were also relatively much longer than in the surface layers. Therefore, the likelihood of encountering the rarer species is enhanced.

The small copepods, such as *Pseudocalanus*, *Oithona*, and *Microcalanus* were strangely wanting or few in this collection. The NP-2 had considerable numbers of these, often in the upper 10 m. They were also numerically important elsewhere in the high Arctic (Bogorov 1946), and in the Chukchi and Beaufort seas (Johnson 1956).

TABLE 3. Average numbers caught per vertical haul adjusted to 100-m length tow through stratum indicated, $\frac{1}{2}$ -m net

Depth (m)	<i>Calanus glacialis</i>	<i>Calanus hyperboreus</i>	<i>Metridia longa</i>
0-10	0	0	0
0-25	8	0	28
25-50	4	0	60
50-100	30	14	36
100-200	6	13	27
200-500	<1	7	8
500-1,000	<1	2	<1
1,000-2,000	0	<1	<1
2,000-2,900	0	<1	2

The more abundant species *Calanus glacialis*, *Calanus hyperboreus*, and *Metridia longa* have a wide range of vertical distribution, but as shown in Table 3, when data for all hauls within the layers are averaged and put on a comparable basis for length of tow (100 m), the three species reach a maximum in numbers above 200 m. *Calanus glacialis* was present in greatest numbers within the 50 to 100-m stratum, but extended to much greater depths, at least below 500 m, for it was present in the 500 to 1,000-m tow.

Calanus hyperboreus was somewhat deeper, the maximum number being found between 50-200 m, but a somewhat reduced (about one-half) concentration occurred in the 200 to 500-m layer, and occasional specimens occurred below 2,000 m.

Metridia longa had its major vertical range near that of *Calanus glacialis*, but with the maximum number at 25-50 m, and continued as the major copepod numerically within the 100 to 200-m layer. Below 500 m, it dropped off to a few specimens, but was present in the 1,000 to 2,000-m layer. As a point of interest relative to bioluminescence in the high Arctic, it should be mentioned that some live copepods that were isolated at the time of collecting from 500-1,000 m were observed to be luminescent. These isolated specimens which were preserved in a separate bottle prove to be *Metridia longa*.

In comparing the divided hauls with the open net hauls from various depths, at different times and localities, there is in gen-

ZOOPLANKTON FROM THE HIGH POLAR BASIN

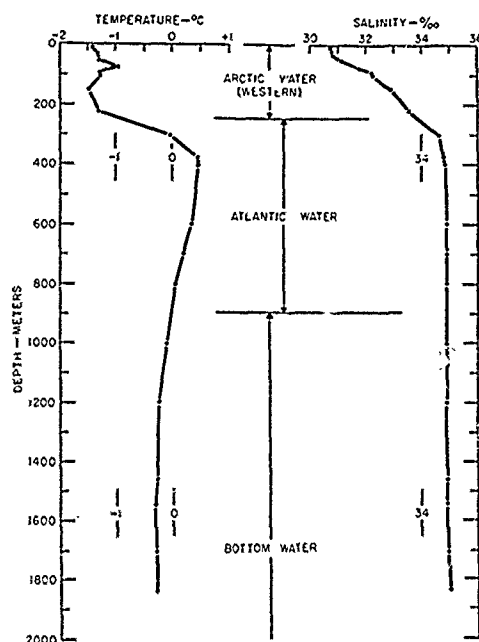


FIG. 4. Temperature-salinity profiles at 77°N, 160°W. (Based on Coachman and Barnes 1961.)

eral a good agreement as to the depth the net reached in catching several of the species. The analysis indicates a good deal of patchiness but the major population of the three numerically most abundant species

was found mainly in the upper part of the intermediate water layer, but from Table 2 it is clear that a number of the less frequent species inhabit the deeper part of this layer and also the cold subzero bottom water where they are probably endemic (Fig. 4).

Seasonal variations

Although the material available from Drift Station Alpha does not provide a continuous or complete series for interpretation of seasonal biological cycles, still there is sufficient spread in sampling to give some useful, if fragmentary, information. An analysis of the developmental stages was made only for the 4 most abundant large copepod species. The percentage composition of these species is given in Table 4, which indicates a considerable seasonal spread of early copepodid stages in at least three of these species. Copepodids I and II were not separated but to do so could not have yielded much additional information. Probably the most notable change in composition occurred in February when there was a conspicuously higher number of early and mid-stage copepodids of *Calanus hyperboreus*, *Metridia longa*, and *Pareuchaeta glacialis*. In the June and September sam-

TABLE 4. Percentage composition of developmental stages for three most abundant species

Net		½-m		1-m		½-m			
		18 June 1957	6 Sept 1957	8 Sept 1957	29/30 Oct 1957	31 Oct/4 Nov 1957	9/12 Dec 1957	22 Feb 1958	
<i>Calanus glacialis</i>	VI	31	59	64	63	54	67	45	
	V	49	33	32	33	42	33	52	
	IV	12	7	4	3	4	0	3	
	III	8	<1	0	0	0	0	0	
	I-II	0	0	0	0	0	0	0	
<i>Calanus hyperboreus</i>	VI	51	54	66	68	57	63	33	
	V	20	24	23	22	19	7	10	
	IV	23	15	9	9	14	7	1	
	III	6	6	2	1	9	23	48	
	I-II	0	1	0	0	1	0	8	
<i>Metridia longa</i>	VI	49	34	62	63	57	34	17	
	V	14	29	18	8	25	10	3	
	IV	19	27	16	5	11	52	18	
	III	15	7	4	23	3	4	43	
	I-II	3	2	0	0	3	0	19	
<i>Pareuchaeta glacialis</i>	VI	25	19	32	27	14	33	6	
	V	11	25	37	41	36	0	40	
	IV	20	27	21	21	21	67	42	
	III	28	19	8	11	29	0	10	
	I-II	16	10	2	0	0	0	2	

ples some females of the last species carried egg sacs and spermatophores and some males had spermatophores in the claw of the 5th foot. The only copepod nauplii observed in the collection were apparently of this species. These nauplii were especially conspicuous in the collection on 22 February 1958. On this date one male was observed holding a spermatophore, and one broken egg case, presumably of this species, had early nauplii within the eggs. No egg sacs or spermatophores were observed in the October, November, and December samples. The nauplii taken on 22 February occurred mainly in hauls that reached depths greater than 200 m. Smaller or early stage nauplii may have escaped through the meshes of the nets.

In *Calanus glacialis* no stage below copepodid IV was observed from September to near the end of February. In comparing these few findings with the seasonal faunal changes observed in the NP-2 collections in 1950-51 (Brodsky and Nikitin 1955), which were more complete and apparently taken with finer-mesh nets, they too record a rather wide spread of early copepodid stages, but in that survey, the greatest number of copepod nauplii were found in June and July and some reproduction indicated for following months but November, December, and January appear to have been low months for production of nauplii (no observation given for February). At least some calanoid nauplii were present in March. Thus it appears that some reproduction may take place over a wide season, and assuming some lag in copepodid growth for late-season larvae, the increased proportion of copepodids found in the present material in February may probably be accounted for.

The standing crop of zooplankton in the high Arctic is relatively low. This must follow from the low primary organic production by phytoplankton in this area. This is brought out especially in a study of organic production based on measurements of chlorophyll *a* and carbon fixation under the ice and in open leads at Drift Station Alpha by English (1961) who concludes that "the

annual primary production in the North Polar Sea is very low relatively to other ocean areas." The production occurred mainly in late July and early August.

The recruitment of zooplankton in relation to phytoplankton is poorly understood, but except for food that may be carried in on currents from more productive coastal areas or ice-free areas, this local Arctic production must suffice to carry the zooplankton population through several lean months. That some food is carried in from elsewhere is evidenced by the presence of certain copepod expatriates from the coast or areas of the Bering and Chukchi seas. But this addition must be very small and only slowly replenished in the high Arctic judging from the slow drift of ice floe stations. Despite this seemingly precarious existence, a population is maintained, in part by stored fat, through the winter and at least such carnivorous species as *Pareuchaeta glacialis* can produce eggs and larvae in the "off" season. The heavily yolked eggs can hatch and sustain nauplius larvae. Other species that are more dependent upon grazing in this stage would fare less well in February. Heinrich (1962) finds from his own work and a good review of the literature, that the initial reproduction of many herbivorous copepods such as *Calanus finmarchicus* s. lat. is closely associated with the vernal production of phytoplankton. Some other herbivores such as *Calanus plumchrus*, are not so closely bound to this trophic relationship. The predaceous copepods like *Pareuchaeta* breed over a wider period. Grainger (1959) concluded from Arctic studies at Igloolik, Canada, that nauplii of *Calanus hyperboreus* probably appear in late May and *Metridia longa* between March and July.

Expatriate species

There are a few copepod species that are of special interest as expatriates from the Bering Sea or from other areas of the Arctic. Earlier collections made in northern Chukchi Sea indicate that most Subarctic copepods that are carried northward by water currents from the Bering and Chukchi seas succumb before reaching

ZOOPLANKTON FROM THE HIGH POLAR BASIN

about latitude 75 to 80° N. Among these are especially such conspicuous species as *Calanus cristatus* Krøyer, *Calanus plumchus* Marukawa (shown by Tanaka 1956, to have previously been erroneously considered *Calanus tonsus* Brady), *Eucalanus bungii bungii* Giesbrecht, *Metridia lucens* Boeck (*pacifica*? Brodsky), *Acartia longiremis* (Lilljeborg) and others notably the more strongly neritic species. However, a few species do survive in numbers sufficiently large to be caught as stragglers well into the high Arctic Basin. One of these, *Eucalanus bungii bungii*, occurred at two different localities 85°6' N, 167°40' W, and 83°41' N, 155°13' W. One adult female was found at each locality. This species lives and reproduces in abundance in the Bering Sea, and south of the Aleutian Islands to the Asiatic Coast, and for some distance, in the California Current along the American Coast. At least some reproduction by this species occurs also as far north as the southern part of the Chukchi Sea (Johnson 1934), and occasionally adult or submature specimens have been caught in the region of Point Barrow. The present record is the farthest known penetration into the Polar Basin, and doubtless indicates a penetration of Bering Sea and Chukchi Sea water to this high latitude. Brodsky and Nikitin (1955) found it at latitudes 77°5' N and 80°51' N.

Figure 4 showing details of the upper water structure indicates a shallow temperature maximum at 75–100 m followed by a drop at 150 m. This temperature feature was best developed due north of the Chukchi Sea but was also in evidence far to the north in the Beaufort Sea gyral. Coachman and Barnes (1961) interpret this maximum as resulting from an intrusion of Bering Sea water. This intrusion then is apparently part of the water layer in which these and other expatriates from the Bering Sea are initially carried to the higher latitudes, where the remaining few may be dispersed into deeper strata and there survive for some time. The type of hauls in which these species occurred (*i.e.*, 0–500 m and 0–1,000 m) do not indicate their depth of cap-

ture. The two catches of *Eucalanus bungii bungii* by Brodsky and Nikitin (1955) were made above 265 and 310 m.

The expatriates caught in more southern parts of the Chukchi Sea or the Beaufort Sea in 1950–51 were with one exception taken in hauls reaching only 150 m but very few deep hauls were taken (Johnson 1956).

Another species, *Mimocalanus distinctocephalus* found at 83°46' N may also be transported into the area from the region of the Bering Sea. This is its first record for the Polar Basin, but Brodsky (1957) reports it as occurring at 50% of the stations in the oceanic collections from 500–1,000 m in the Bering Sea. Elsewhere it occurs in the North Pacific and Okhotsk Sea.

A third species *Derjuginia tolli* of which a total of 10 was found at three positions up to 85°15' N is probably also an expatriate from coastal waters. It has not been reported along the North American Coast, but Brodsky (1957) states that it is the characteristic species of the central-east Siberian Sea, where it lives in varying degrees of salinity.

Most of the other species encountered, even though rare, are probably at home in the high Arctic Ocean, although some have a wide Arctic distribution, and are to be found in deep water of other oceans. One of these, *Spinocalanus spinosus* which has not previously been reported from the Arctic, was found singly on three occasions. This extends considerably its already known wide distribution, having been reported from the northeastern Atlantic (Farran and Vervoort 1951); Indo-west Pacific (Vervoort 1946); Antarctic (Farran 1926); eastern North Pacific (A. Fleminger, *personal communication*). Except for somewhat larger size and relatively longer urosome the Arctic specimens agree well with specimens examined from the west coast of Ireland and from the coast of California. Further work is needed on the life histories of the rarer species found in the Arctic to determine the status of their presence there. The few *Calanus finmarchicus* s.s. found may have been expatriates. Sars (1900) was aware of the close relationship and continuous dis-

tribution of many high Arctic species with the Atlantic, and recognized this as being correlated with the inflow of North Atlantic water at subsurface levels into the Arctic as postulated by Nansen. Brodsky (1957) reiterates this but shows also an increased number of species (largely new) that appear to be truly endemic to the waters of the north Polar Basin, especially in the greater depths.

REFERENCES

- BARNARD, J. LAURENS. 1959. Epipelagic and under-ice amphipoda of the central Arctic Basin. In: Scientific Studies at Fletcher's Ice Island, T-3 (1952-1955). Geophys. Directorate; U.S.A.F. Camb. Res. Cent., Geophys. Res. Paper No. 63, 1: 115-152.
- BOGOROV, V. 1946. Zooplankton collected by the "Sedov" Expedition 1937-1939. Trudy, 3: 356-370.
- BRODSKY, K. A. 1950. Copepoda, Calanoida, of the far-eastern waters of the U.S.S.R. and the Polar Basin. Classification of the fauna of the U.S.S.R., Publ. Zool. Inst. (Acad. Sci.) U.S.S.R., 35: 441 pp.
- . 1957. The fauna of Copepoda (Calanoida) and zoogeographical division into districts in the northern part of the Pacific Ocean and of the adjacent waters. Zool. Inst. Acad. Sci. U.S.S.R., Moscow, 222 pp.
- . 1959. Concerning phylogenetic relationships of several species of *Calanus* (Copepoda) of the northern and southern hemisphere. Zool. J. Acad. Sci. U.S.S.R., 33(10): 1537-1552.
- , AND M. N. NIKITIN. 1955. Hydrobiological work. Observational Data of the Scientific Research Drifting Station of 1950-1951. Vol. 1, Sec. 4, Art. 7, 6 pp., 4 appendices. (Amer. Meteorol. Soc. translation.)
- COACHMAN, L. K., AND C. A. BARNES. 1961. The contribution of Bering Sea water to the Arctic Ocean. Arctic, 14(3): 147-161.
- ENGLISH, T. SAUNDERS. 1961. Some biological oceanographic observations in the central North Polar Sea, *Drift Station Alpha*, 1957-1958. Mimeo. Rept., Final Contract Rept., AF 19 (604) 3073, 59 pp.
- FARLOW, J. S. 1958. Project Ice Skate oceanographic data. Woods Hole Oceanographic Institution. Ref. No. 58-28, 18 pp.
- FARRAN, G. P. 1929. Copepoda. British Antarctic ("Terra Nova") Expedition, 1910. Nat. Hist. Report. Zool., 8(3): 203-306.
- , AND W. VERVOORT. 1951. Copepoda, Sub-order: Calanoida. Family: Spinocalanidae. Genus: *Spinocalanus*. Cons. Intern. Explor. Mer, Zooplankton Sheet 39, 4 pp.
- GRAINGER, E. H. 1959. The annual oceanographic cycle at Igloolik in the Canadian Arctic.
1. The zooplankton and physical and chemical observations. J. Fish. Res. Bd. Canada, 16: 453-501.
- . 1961. The copepods *Calanus glacialis* Jaschnov and *Calanus finmarchicus* (Gunnerus) in Canadian Arctic-Subarctic waters. J. Fish. Res. Bd. Canada, 18: 663-678.
- HAND, C., AND LAI BING KAN. 1961. The medusae of the Chukchi and Beaufort Seas of the Arctic Ocean including the description of a new species of *Eucodonium* (Hydrozoa: Anthomedusae). Tech. Paper 6, Arctic Inst. North Amer., 23 pp.
- HEINRICH, A. K. 1962. The life histories of plankton animals and seasonal cycles of plankton communities in the oceans. J. Cons. Intern. Explor. Mer, 27: 15-24.
- JASCHNOV, V. A. 1955. Morphology, distribution and systematics of *Calanus finmarchicus* S. L. Zool. J., Acad. Sci. U.S.S.R., 34(6): 1201-1223.
- JESPERSEN, P. 1934. The Godthaab Expedition 1928. Copepoda. Medd. om Grønland, 79(10): 1-166.
- JOHNSON, M. W. 1934. The production and distribution of zooplankton in the surface waters of Bering Sea and Bering Strait, Part II. In Report of oceanographic cruise U. S. Coast Guard Cutter *Chelan*—1934. Mimeo. Rept., pp. 45-82.
- . 1956. The plankton of the Beaufort and Chukchi Sea areas of the Arctic and its relation to the hydrography. Tech. Paper 1, Arctic Inst. North Amer., 32 pp.
- METCALF, W. G. 1960. A note on the water movement in the Greenland-Norwegian Sea. Deep-Sea Res., 7: 190-200.
- NANSEN, F. 1902. The oceanography of the North Polar Basin. Norwegian North Polar Exped. 1893-1896. Sci. Res., 3(9): 1-427.
- SARS, G. O. 1900. Crustacea. Norwegian North Polar Exped. 1893-1896. Sci. Res., 1(5): 1-137.
- SVERDRUP, H. U. 1956. Oceanography of the Arctic. In: The Dynamic North (U.S.N., Chief Nav. Oper. June 1956), Book I, Sec. V, 32 pp.
- TANAKA, O. 1956. The pelagic copepods of the Izu Region, middle Japan. Systematic account II. Families Paracalanidae and Pseudocalanidae. Publ. Seto Mar. Biol. Lab., 5: 367-406.
- TIMOFEEV, V. T. 1957a. Atlanticheskiye vodi v arkticheskoy basseine. Probl. Arkt., 2: 41-51.
- . 1957b. O formirovani donnikh vod tsentral'noi chasti arkticheskovo basseina. Probl. Arkt., 1: 29-33.
- VERVOORT, W. 1946. Biological results of the Snellius Expedition. XV. The bathypelagic Copepoda Calanoida of the Snellius Expedition. I. Families Calanidae, Eucalanidae, Paracalanidae, and Pseudocalanidae. Temminckia, 8: 1-181.

Ice Drift in the Arctic Ocean

I.M. Browne

Reprinted from the
TRANSACTIONS OF THE AMERICAN GEOPHYSICAL UNION,
Vol. 40, No. 2, pp. 195-200 (iGY Bulletin, 24), 1959

Ice Drift in the Arctic Ocean

The following report is based on a paper given by Irene M. Browne of the Geophysics Research Directorate, US Air Force Cambridge Research Center, at the IGY Symposium of the 125th Annual Meeting of the American Association for the Advancement of Science, held in Washington, D. C., December 29-30, 1958.

Study of Arctic Ocean ice movement provides information on the interaction of air and ocean not obtainable elsewhere, makes it possible to compare direct measurements of permanent ocean currents with concepts of these currents derived by analysis of hydrographic data, and may permit prediction of ice movement, thus aiding navigation in the Arctic Basin. The primary forces affecting ice drift are wind friction over the ice surface, friction between the ice bottom and the water, the Coriolis effect (the tendency of movement to be deflected to the right in the Northern Hemisphere and to the left in the Southern Hemisphere, owing to the earth's rotation), and internal stresses within the ice itself.

Prior to the IGY, most data on Arctic Ocean ice drift were obtained by isolated expeditions (on some of which ships were intentionally allowed to become frozen into the ice pack), by Soviet drifting stations, and by a US scientific station on ice island T-3 (Fletcher's Ice Island, later the site of IGY Drifting Station Bravo). During the IGY, drift data were obtained mostly from scientific stations established on the floating ice. US-IGY Drifting Station Alpha was on a ten-foot-thick ice floe and Station Bravo is on Fletcher's Ice Island. (*Bulletins*

1, 2, 6, 12, 16, 17, and 22 contain additional information about the US-IGY drifting stations and their scientific programs.)

This report is based primarily on a preliminary survey of drift information obtained during the first 12 months of the IGY. Basic data were supplied by scientists of the Lamont Geological Observatory and Woods Hole Oceanographic Institution, under contract to the Air Force Cambridge Research Center, and of the Fisheries Research Board of Canada, who conducted investigations at the drifting stations; the analyses were carried out by Irene M. Browne at the Cambridge Research Center.

General Character of Ice Drift

The general character of ice movement in the Arctic Ocean is evident from the drift patterns of US and USSR drifting stations and of ships accidentally or intentionally frozen into the ice. Figure 4 shows some of these drifts.

The *Fram* Expedition of 1893-96, led by the Norwegian explorer-scientist Fridtjof Nansen, was the first major scientific expedition to the Arctic Ocean. Nansen permitted his specially-designed ship to be frozen into the pack ice on the Siberian side of the Arctic. In the next three years, during which many scientific studies were made, the *Fram* drifted with the ice pack completely across the Arctic Basin and was finally freed from the ice in the Greenland Sea, near Svalbard.

The Soviet ship *Sedov*, in a similar venture, was frozen into the ice in the same region in 1937. Its course paralleled that of

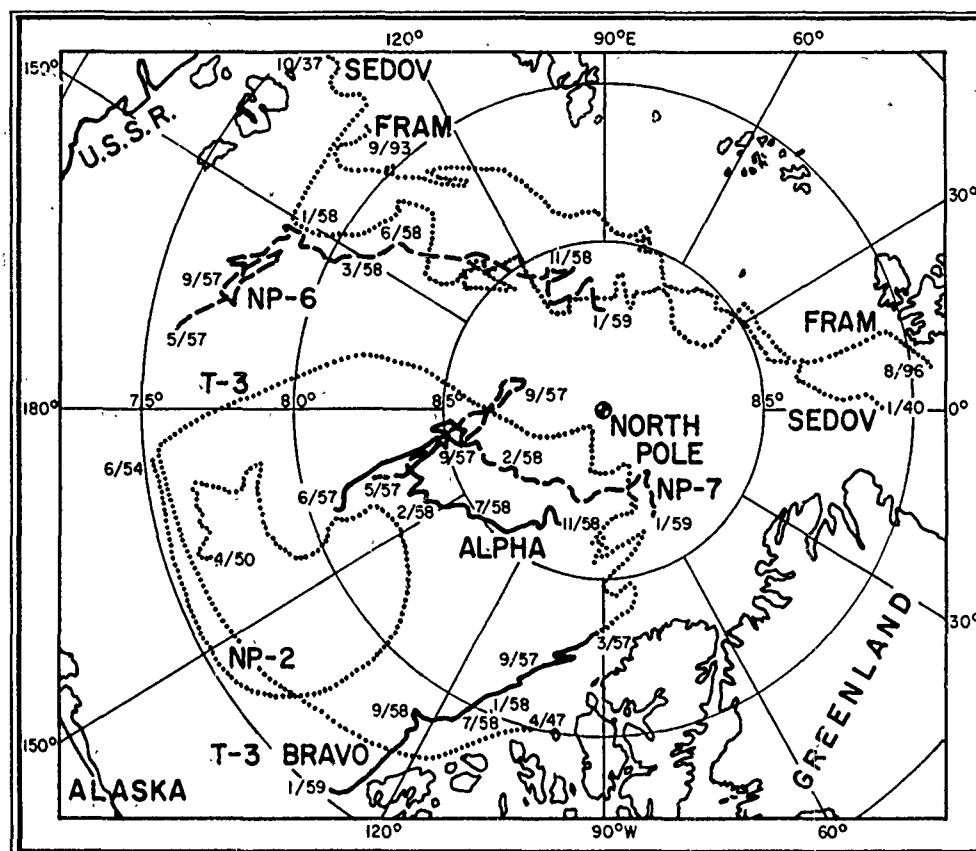


FIG. 4. Arctic Ocean Drift Patterns. Solid lines represent drift paths of US-IGY stations, dashed lines paths of USSR-IGY stations, and dotted lines paths of pre-IGY stations or ships locked in ice.

the *Fram*, thus confirming the drift pattern in that part of the Basin. Subsequent drifting-station studies by the Soviets further support the inference that the general movement on the Siberian side of the Pole is toward the Greenland Strait, with an accelerating speed. It takes about three years to complete the drift from the area of the Laptev Sea to Spitzbergen.

A clockwise pattern of drift on the North American side of the Pole was recognized by observations of the movement of ice islands T-1 and T-3 and confirmed later by the IGY drifting stations. In the vicinity of the Pole, movement is critical—either the ice may drift out with the Greenland current or back into another orbit. The time for circulation is about ten years.

If the ice moves into another orbit it is evidently subjected to intensive pressures, often resulting in breakup north of Canada and Greenland. Both North Pole 3 (one of the pre-IGY Soviet Drifting Stations) and US-IGY Drifting Station Alpha had to be abandoned in this region of ice convergence, and nearly half the drift cycles of ice islands T-1 and T-3 were spent in this area.

USSR-IGY Drifting Station North Pole 6, after an indecisive beginning is now drifting parallel to the *Fram* and *Sedov* courses. T-3 is moving southwest along the edge of the Canadian Archipelago.

The striking similarity of the drifts of Station Alpha and USSR-IGY Station North Pole 7 is immediately apparent (Fig. 4). Both stations were carried northward

IGY BULLETIN

until mid-September. The direction was reversed until mid-December and then the drift was in the general direction of Greenland. The distance between Station Alpha and North Pole 7 averaged 150 mi. The harmony of these drift patterns demonstrates quite distinctly the characteristic movement of the ice in this region.

Observations made thus far indicate that, in general, the ice drift follows closely the sea-level atmospheric pressure systems, that the clockwise orbit of ice movement on the North American side of the Arctic Ocean corresponds to the major motion of the surface currents, and that the rate of transport of surface waters and the rate of the observed ice drift in this region are on the same order of magnitude.

Wind Drift of the Ice

It appears certain from these IGY investigations that the main driving force for the drift of Stations Alpha and Bravo was the wind. When winds were strong and predominantly from one general direction, drift was relatively rapid and approximately before the wind (with some deviation to the right, as explained below). When winds were light and variable in direction, net movement was small.

Relationship to Atmospheric Pressure Systems: According to the Soviet theorist, Zubov, the Arctic Ocean ice pack moves parallel to the surface isobars (lines of equal atmospheric pressure); the higher pressures are to the right by about 1/100 of the geostrophic wind speed (wind deflection due to the earth's rotation). Figure 5 presents the mean sea-level pressure contours by quarters for the first twelve months of the IGY over the Arctic. Also shown are vectors representing the drift of the four stations during each period. Isobaric contouring in these high latitudes is subject to some error owing to the scarcity of meteorological stations, yet the conformity of the drift patterns to the pressure systems is evident.

In the first quarter, a low-pressure system situated north of the New Siberian Islands was responsible for the rapid northerly drift of Stations Alpha and North Pole 7. North Pole 6, located near the center of the low, and T-3, located between two pressure systems, were becalmed, as would be expected. The cyclonic system dissipated in the next quarter and was replaced by an intense high over the same general region. Correspondingly, the direction of ice movement was reversed, following the clockwise circulation of the anticyclone. This system persisted throughout the remainder of the 12-month period, during which North Pole 6 was in the region of strong trans-polar movement; Station Alpha and North Pole 7, after a period of southerly drift, were caught in a gradual movement toward the coasts of Canada and Greenland as the high moved across the Arctic Ocean; and T-3, first subjected to southeasterly flow, moved little during the rest of the period, when winds in general were shoreward.

Coriolis Effect and Drift Speeds: Beginning with the *Fram* expedition, it has been observed that the ice usually drifts to the right of the surface-wind direction in the Northern Hemisphere, owing to the Coriolis effect. Comparison of the predominant winds with the trend of Station Alpha's drift substantiates this observation. Over 90% of the drift angles (relative to wind direction) obtained for Station Alpha were oriented to the right of the surface-wind direction. The peak frequency is at drift angles between 30° and 50°, with a computed average of 33°.

Nansen first interpreted the deviation of the ice to the right of the wind as owing to the effect of earth's rotation. Later, V. W. Ekman provided a mathematical analysis which indicated that the angle of deviation of the surface current from the wind is 45°. The smaller value actually obtained for ice drift presents a problem. It has been attributed to internal ice resistance by some authors.

NATIONAL ACADEMY OF SCIENCES

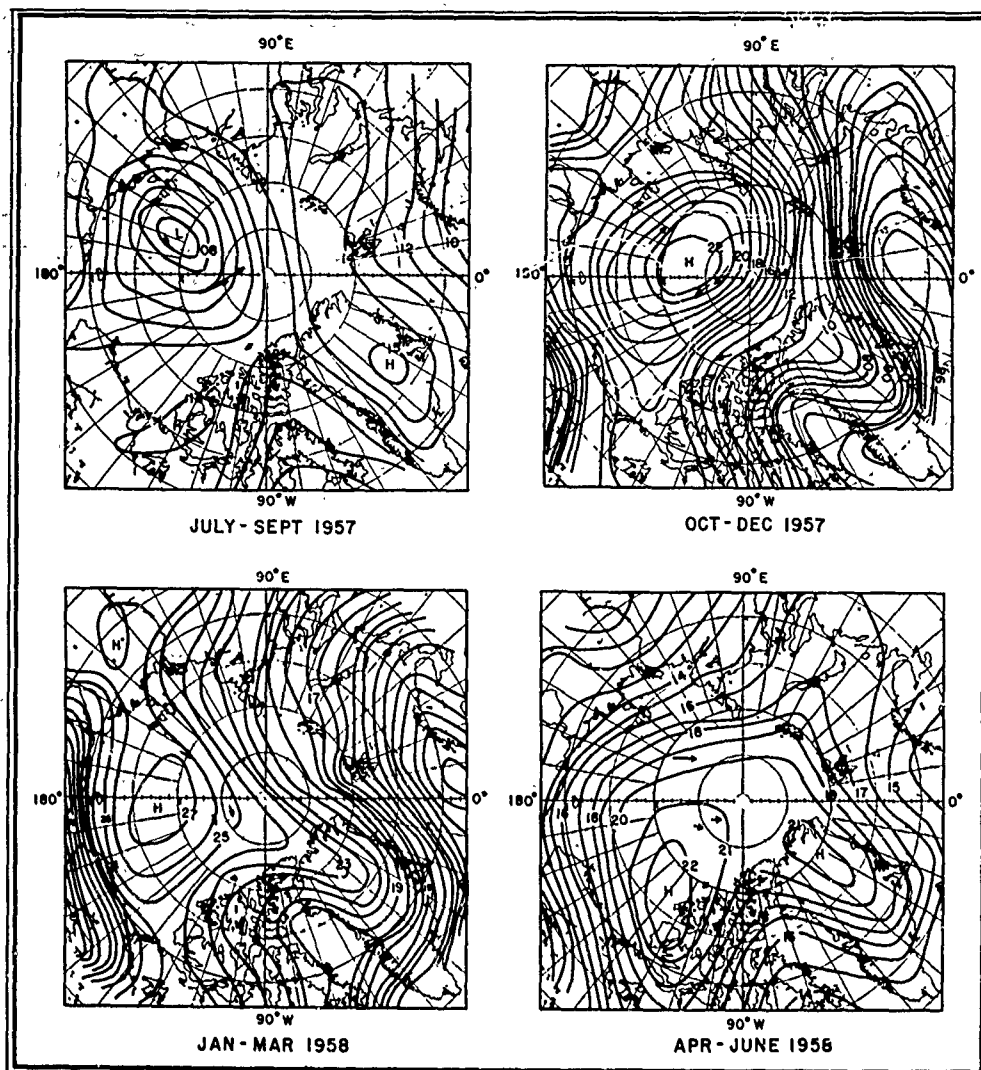


FIG. 5. Sea-level Pressure Contours over the Arctic, by Quarters from July 1957 through June 1958. Pressures in millibars (for actual values, add 1000 to numbers above 00 and 900 to numbers below); arrows are vectors showing direction and relative amounts of ice movement.

It was also found that over 60% of the time, the drift speed was 1/80th-1/40th of the surface wind speed. The average ratio was .0206, or about 1/50th.

The averages given above correlate well with the mean observations of angle deviation and drift-speed ratio found during the earlier expeditions, on which wind speeds were measured at heights of 6 or 8 m above the ice. A summary of these observations is given in Table 1.

TABLE 1

	Ratio of Ice Drift to Surface Wind Speed	Angle of Devia- tion of Ice Drift from Surface Wind Direction
<i>Fram</i>	.0182	28°
<i>Maud</i>	.0177	33°
<i>Sedov</i>	.0150	29°
T-3 (pre-IGY)	.0130	37°
Alpha	.0206	33°

The averages for the drift of T-3 are based on wind measurements at the higher

IGY BULLETIN

level of 10 m above the ice. Averages remained constant for both the pre-IGY and IGY movements of T-3, although there was a marked difference between the rate of movement in higher latitudes, where the ice is more closely packed, and in the regions of loosely packed ice nearer the coasts. In the higher latitudes, the island is locked tightly in the pack and is therefore strongly influenced by the rate of drift of the entire pack. Nearer the coasts, on the other hand, where the island is relatively free of the pack, its own large size probably has a greater effect on its movement.

Arctic Ocean Currents

Oceanic circulation must also be considered in analyzing the movement of the ice pack. The amount of hydrographic data for the Central Arctic is still limited but more is gradually being accumulated.

Hydrographic studies on Project *Skijump*, 1951-1952, indicated the existence of a giant eddy in the region north of Alaska (see *Bulletin No. 6*). The observed ice drifts conform to this circulation pattern. An analysis was made of the hydrographic data obtained from USSR drifting station North Pole 2, from ice island T-3 prior to the IGY, and from IGY Drifting Stations Alpha and Bravo. The results are given in Figure 6, which shows the dynamic height anomalies relative to the 600-decibar surface. (A decibar is the pressure exerted by a column of water one meter high. The dynamic height anomaly represents the deviation of the actual pressure surface from a level surface at the equivalent depth.)

If it is assumed that the 600-decibar surface is one of little or no motion, the surface-water movement will follow closely the contours of the sloping isobaric surfaces shown in Figure 6—the force of gravity moves the water down slope and the Coriolis force turns it to the right.

The addition of the IGY stations amplified knowledge of the circulation pattern and served to demonstrate that a closer

contouring interval in the Alpha region and a more complex contouring in the T-3 area existed than previously thought.

The average rates of circulation in kilometers per year between certain hydrographic stations have been computed and are also shown in Figure 6. These rates give an average time of ten years for circulation around the outer edge of the eddy, which compares favorably with the observed drifts of ice islands T-1 and T-3. The rate of surface movement between Alpha hydrographic station 4 and *Skijump* (the pre-IGY program on ice island T-3) station 3 is calculated as 895 km/yr; between *Skijump* station 7 and North Pole 2 station 12 it is 554 km/yr. Over this same general area, ice island T-1 in 1947 and 1948, and Station Alpha during the IGY, traveled in approximately the same direction at the average rate of 650 km/yr, which compares very

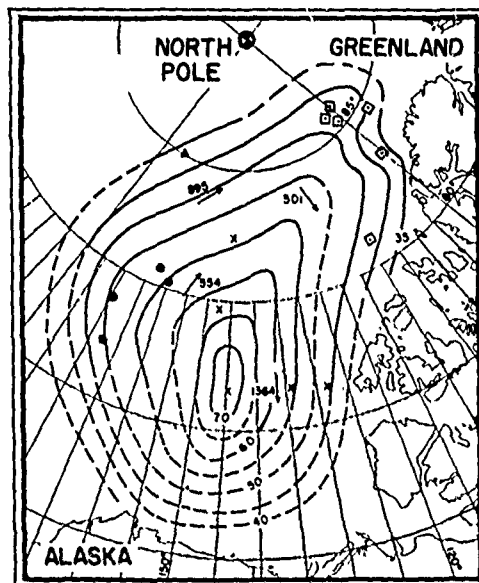


Fig. 6. Dynamic Height Anomaly in Arctic Ocean North of Alaska, Showing Circulation Pattern. Dots are NP-2 hydrographic stations; crosses are *Skijump* stations; small dots in squares are Bravo stations; and triangle is an Alpha Station. Arrows and associated numbers show drift direction and rate (in km/yr) between certain stations. Contour numbers are in dynamic millimeters.

well with the surface circulation computed from the available hydrographic data.

A small amount of current data was collected from Station Alpha. Analysis of these data shows that movement in the upper 16 m of the water corresponded to that of the ice in both speed and direction, with a small increase of speed with depth. Deeper current profiles and further information on daily ice movements were obtained during the summer of 1958. When analyzed, these data will help fill in the picture of water motion for this part of the Arctic Basin.

Statistical Investigations

In an effort to establish more clearly the nature of the forces affecting Arctic ice movement, certain statistical studies were made in addition to the direct measure-

ments and comparisons already described.

Both drift-speed/wind-speed ratios and angle deviations observed along the Station Alpha drift path were examined statistically for trends indicating permanent current effects. None were found. Instead, a general scattering of the data was evident for all wind speeds. This is not surprising in view of the complexity of some of the factors involved in the drift of the Arctic Ocean ice pack. Principal among these is the transmission, over distances as great as 100 mi or more in the closely-packed ice, of internal stresses originating in areas of convergence and divergence.

Data collected during the IGY occupation of the drifting stations may eventually lead to a fuller understanding of this and other factors influencing drift patterns.

**Preliminary Results of Thermal Budget
Studies on Arctic Pack Ice During
Summer and Autumn**

**N. Untersteiner
F.I. Badgley**

Reprinted from the
ARCTIC SEA ICE, NATIONAL ACADEMY OF SCIENCES - NATIONAL RESEARCH COUNCIL
Publication 598, pp. 85-95, 1958

PRELIMINARY RESULTS OF THERMAL BUDGET STUDIES ON ARCTIC PACK ICE DURING SUMMER AND AUTUMN

N. Untersteiner and Franklin I. Badgley*

INTRODUCTION

As part of the activity of the International Geophysical Year, the United States Air Force is maintaining an installation on the Arctic pack ice. The installation, Drifting Station A, provides facilities for scientists under the direction of the United States National Committee for the IGY. The station was first occupied on April 5, 1957, at a position 79°N , 159°W . It had drifted northward to 85.6°N , 171°W by September 25 and then retreated southward to 83.3°N , 188°W by January 16, 1958. (See figure 2.) The course Drifting Station A has taken is an approximate continuation of the drift of the Soviet Station North Pole II.

A major project on Drifting Station A is the study of the thermal budget for a period of at least 12 months. The program is being carried out by the Department of Meteorology and Climatology, University of Washington. This preliminary report covers some results of the initial phase of the work from June to December 1957 and is meant to serve as a basis for further discussion. The statements made are subject to review after final data reduction.

One object of our program is to obtain information on the relative importance of the radiative and latent heat transfer for the mass budget of sea ice, as well as the exchange of heat between atmosphere and ocean by conduction through the ice pack. Drifting stations as sites for thermal budget and other meteorological studies have great advantages. They are far from land masses and the surrounding surface is uniform. Both factors make the observations representative of a large area.

METHOD OF OBSERVATION

The equipment was installed during the first half of June, well before the melting began. The local ice topography and the location of the camp required that the micrometeorological observations be made northwest of the living area. During the first three months when east to southeast winds prevailed this put the observations in the lee of the

camp. The amount of pollution from the combustion of oil was very small, however, and little contamination of the snow could be observed at the measuring site, 170 meters from the nearest building. In the subsequent period, October through December, prevailing northerly winds and a new snow cover still further decreased any chance of local factors influencing the observations.

Records are kept of incoming and outgoing total and short-wave radiation. The total radiation incident on a horizontal surface from above is measured by one element of a Schultze radiometer and that from below by the other element. The instrument required frequent calibration checks since the delicate polyethylene hemispheres are dulled as a result of contact when removing frost. The operation has been satisfactory in other respects. Short-wave radiation, incoming and reflected, is measured with two Kipp Solarimeters of proved design.

Air temperatures at 25, 50, and 100 cm above the surface are measured with copper-constantan thermocouples. The number 28 thermocouple wire first used had appreciable temperature error from the absorption of radiation; number 38 thermocouple wire was found to have very little radiation bias, even during periods of slow air motion.

Additional thermocouples are installed at three sites, measuring the ice temperatures at four levels. The ocean temperature 3 meters below the bottom of the ice is followed from measurements by another set of thermocouples. It would undoubtedly be valuable to know details of the temperature distribution in the first few meters of water under the ice. Instruments to make these measurements will be installed in 1958.

For several periods of one to three hours each, an array of twelve thermocouples spaced very closely in the first 25 cm above the snow surface have been used to measure the details of the vertical temperature profile. A Speedomax recorder with 16 points is used to obtain continuous records of the above mentioned variables where required. A manually balanced potentiometer is used for making daily determinations of the more slowly changing variables.

The wind profile is obtained with a Thornthwaite wind register with recording levels at 20, 40,

* Department of Meteorology and Climatology, University of Washington, Seattle, Washington.

80, and 160 cm above the ice surface. Adequate sealing eliminated early difficulties caused by the penetration of moisture into the transmitters. Observations are taken whenever general weather or surface conditions are changing. A continuously recording anemometer is mounted 160 cm above the surface.

Observations are also made of ice thickness, density, chlorinity (salinity), surface temperature (thermocouples), and ablation (stakes). Evaporation or condensation is estimated by periodically weighing ice or snow in plexiglass pans which have been held buried level with the natural surface. This method is possible only in the absence of precipitation and drifting snow.

A major problem in the maintenance of radiation, air temperature, and wind equipment is the collection of hoar frost. During the fall season an ordinary electrical hand-held hair dryer was successfully used to remove frost from radiation instruments and thermocouples. Later this became inadequate and the instruments had to be returned occasionally to the laboratory for defrosting.

It has been difficult to obtain a direct evaluation of the change in the total mass of the ice pack. Ablation was measured at 16 locations and the amount of solid ice lost seems to be well established. However, the amount of melt under the snow and slush cover, as well as the initial amount of snow, could only be estimated. The problem was complicated by the irregular topography and the consequent formation of puddles, ponds and lakes. Natural and artificial drainage further obscured the situation. The number of observation sites needed to get a representative sample would have been impossible large.

During the accumulation period the problems are somewhat simpler, though still annoying. The first accumulation is in the form of snow at the surface. The total amount is not large but it drifts in irregular patterns. Beginning in late November, ice freezes at the bottom of the pack in a pattern which is partly determined by the pattern of insulating snow cover above. Added to this are the complications produced by the refreezing of the previous summer's melt trapped in crevices in the ice.

A water level recorder was installed in anticipation of the difficulties mentioned above. It records the relative changes between a fixed level in the ice and the water surface. The mechanism consists of a float in a pit communicating with the ocean through a vertical hole which was originally 10 cm in diameter. Attempts to prevent water in the pit from freezing involved a cover, addition of antifreeze, and a heating wire in the vertical hole. The records reflect the rise of the ice after natural and artificial drainage and depression under a blanket of snow. The continuity of the record has been disrupted by

blowing snow, freezing, thawing of supports, and the diffusion of antifreeze. Improvements in this technique should provide a convenient method of obtaining reliable information on melting and accumulation, representative of a large area. (See figure 1.) The extent of this area and its dependence on ice thickness could not be determined.

If we denote the total length of an ice column of unit area with H , and the portion below the water level with h ; then, assuming isostatic compensation, the respective changes are related by $\Delta h = \Delta H (\rho_{\text{ice}}/\rho_{\text{water}})$. For the present purpose, we assume the ice density to be a uniform 0.9g/cm^3 and that of the water, 1.0g/cm^3 . Since the water level recorder measures Δh , we have to increase its readings by 11 per cent in order to obtain the mass change that has taken place at the surface.

However, the water-level recorder readings do not permit distinction between mass changes taking place at the surface and the bottom of the ice, and they reflect bottom ablation or accretion with only $1/9$ of the sensitivity of those on the surface. In order to ascertain ablation or accretion taking place at the bottom, a separate instrument was installed. (See figure 1.) It consists of a No. 18 stainless wire put vertically through the ice, with a cross bar at each end. This wire will normally be frozen into the ice and is not movable. It can be released by putting a current through, using a second wire reaching ocean water, or by connecting the stainless wire to an ungrounded wire of the power circuit while the other wire is grounded. With the ground wire about 1 meter away from the measuring wire, the resistance of the circuit is of the order of 20 ohms, so that a 110 volt AC current can be applied. The measuring wire is released within a few seconds and can be pulled up until the cross bar touches the ice bottom. Readings are taken against a scale which is fixed with respect to a level within the ice. Changes in these readings indicate mass changes taking place at the ice bottom. These instruments can be made easily on the spot and installed in several places, making thickness determinations less laborious and more accurate than by drilling.

RESULTS OF OBSERVATIONS

General weather conditions. The weather at Drifting Station A is dominated by moving low pressure systems and, during the summer, advection of warm air from the surrounding continental areas. Due to the long distance the air has traveled over a uniform surface, fronts are poorly defined near the surface. The summer weather is characterized by a very high percentage of cloud cover. Table I gives preliminary monthly averages of some elements (compiled partly from observations by the U.S. Weather Bureau).

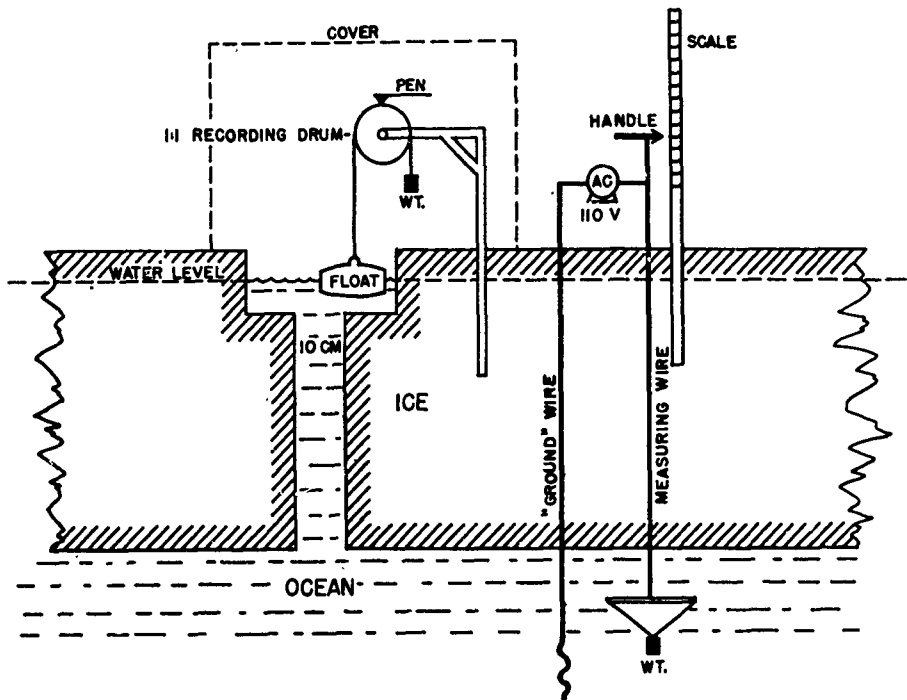


FIGURE 1.—Water level recorder.

High wind velocities are rare. The maximum hourly average observed between June and December at a height of 160 cm above the ground, was 50 km/h. The prevailing wind direction during the summer months was from the southeast sector and accounts for the relatively steady northward drift of the station, as shown in figure 2. During fall and early winter the winds were variable but prevailing northerly resulting in drift toward the south.

Surface ablation and accumulation. The snow

cover which accumulated during winter and spring, before the onset of melting, was estimated from numerous measurements to be 40 cm with a density of 0.3 to 0.4 g/cm³. Melting of the snow began in the middle of June and, once started, proceeded rapidly due to the low albedo of water-saturated snow. By July 8 most of the snow cover had disappeared and ablation stakes were set out to obtain measurements of ice ablation. The main ablation period lasted from July 9 to 24, with an ice ablation

TABLE 1
PRELIMINARY MONTHLY AVERAGES AT DRIFTING STATION A, 1957.

	Air Temp. (Screen)	Precipitation	Cloud Cover		Wind 160 cm above surface	
			Total	Low	Speed	Prevailing Direction
June 1957	- 1.6° C	19 mm	82	78	15.1 km/h	ESE
July	0.0	15	85	76	14.4	SSE
August	- 3.2	25	90	88	17.3	SE
September	-11.7	7	82	73	10.8	N/SW
October	-16.1	13	85	73	18.5	N
November	-27.8	3	48	39	9.6	NW
December	-36.8	—	41	35	—	S/NW

ARCTIC SEA ICE

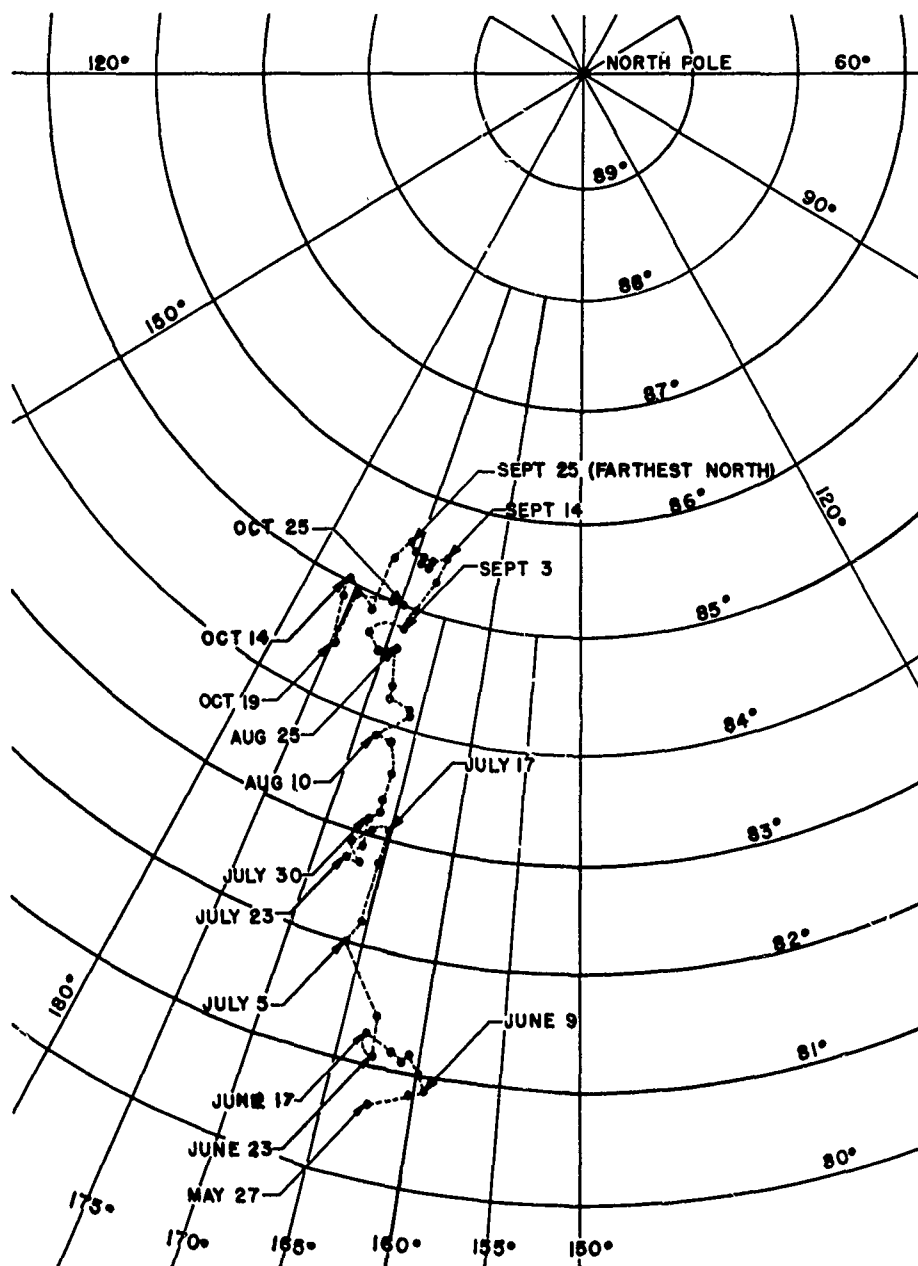


FIGURE 2.—Drift of station.

PRELIMINARY RESULTS OF THERMAL BUDGET STUDIES

of about 1 cm/day. After July 24 a new snow cover began to develop and refreezing began, but until August 8 this was occasionally interrupted by short periods of melting. In August and September the snow cover increased steadily and had reached a depth of about 20 cm by the end of September. From October on, the increase was very slow, and the total depth was only 28 cm at the end of December. The results of these observations during 1957 are given in figure 3. The water level recorder (dot-dashed line) indicates a total rise of the ice of 30 cm. From July 6 to 10 this rise was mainly due to artificial drainage.

In early July the ponded meltwater on the surface reached its maximum extent and was estimated to cover 30 per cent of the total area. When one especially large pond northeast of the camp began flooding the micrometeorological area, it had to be drained artificially. An area of about 0.5 km² was drained with a single hole with an initial diameter of 10 cm; the drainage hole (and two others in smaller ponds) was located within 50 m of the water level recorder site. Therefore, the hydrostatic rise of the ice and the ablation of "dry" ice (full line in figure 3) cannot be compared directly during this period.

The full line in figure 3 represents the average

readings of 7 stakes on ice between July 9 and 25, after the disappearance of the snow cover. After this date the stake readings are represented by the dotted line. The average density of this new snow cover was approximately 0.3 g/cm³. The full line after July 25 represents the snow accumulation, reduced to the density of ice.

When the water level recorder was installed on July 3, the central part of the ice (at 150 to 200 cm depth) had a temperature of -3.5°C and we assume that it was essentially impermeable to meltwater at that time. We further assume that the run-off over the edges of the floe (pressure ridges) was negligible. Thus by the beginning of July practically all the melt-water was still present at the surface of the floe.

The water level record indicates a total rise of the ice of 29.6 cm or a loss of 32.8 cm of ice. The total loss of ice was 26.5 cm including the spring snow cover as derived from ablation measurements. The remaining difference of 6.3 cm may be accounted for by a greater ablation in meltwater ponds, which during a period of 3 weeks covered 15 to 30 per cent of the surface area. By the middle of August practically all meltwater had drained off the surface. Ablation underneath 15 cm of water is shown by the dashed line in figure 3. It is approx-

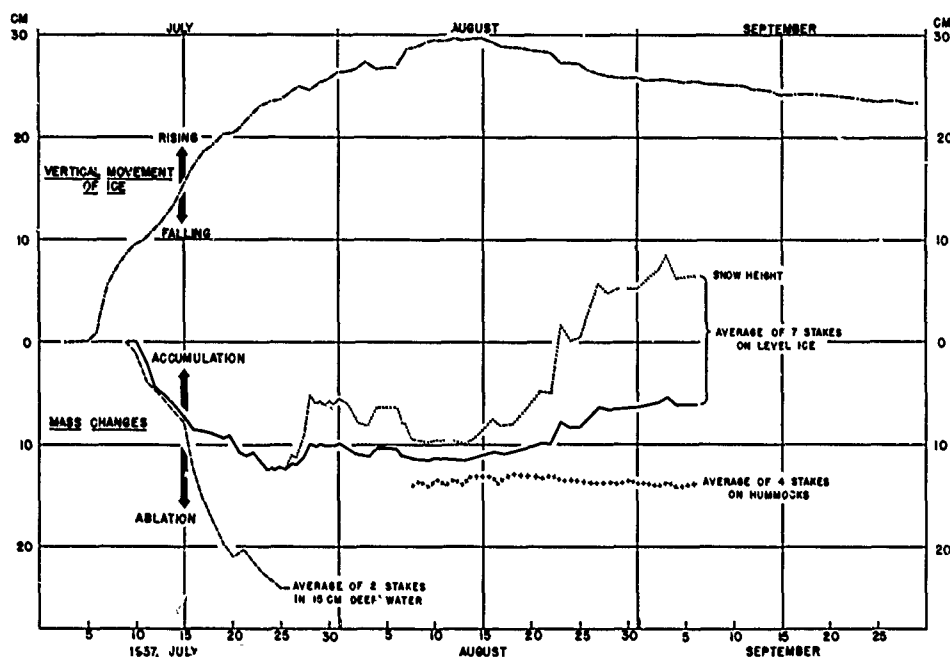


FIGURE 3.--Ice movements and mass changes, summer 1957.

imately twice as great as the ablation of bare ice, due to the low albedo of water.

Although the water level records cannot be used to determine ablation during short periods, they seem to give good total ablation values. An additional advantage for practical purposes is the fact that it does not show the melting but the runoff, i.e. the amount of water substance actually lost from the surface. The total accumulation between July 25 and September 6, according to stake readings, was 3.4 cm of ice. The accumulations shown by the water level recorder is 2.4 cm of ice. Here again the stake readings may be considered less reliable because they represent conditions of level ice and do not include hummocks or mounds. Four stakes set on hummocks (approximately 1 m high and 15 m in diameter) show no appreciable accumulation (line of crosses in fig. 3) during the same period.

Bottom accretion and ablation. On July 21 the formation of an ice layer 1 to 3 cm in thickness under the pack ice was first observed. It was separated from the previously existing ice bottom by a layer of fresh water or slushy ice of varying thickness and at a temperature of 0° C. Further drilling revealed that the fresh water was distributed following the bottom topography, forming pools under thin (250 cm) ice and being absent under hummocks and under thick (more than 300 cm) ice. During the early stages of its development, a specimen of this ice layer secured with a coring auger was found to be practically free of salt.

In one place, this layer of new ice had attained a thickness of 20 cm by July 25, and was separated by the original ice bottom by 12 cm of water. The ocean water below the new layer had a constant temperature of -1.6° C.

The formation of this layer can be visualized as follows: fresh meltwater from the surface penetrates the pack ice through drain holes and pores and accumulates at the bottom, floating on top of the cold ocean water. At the interface between fresh (0° C) and salty (-1.6° C) water, fine ice crystals (needles and plates) are formed. The crystals are loose and float upward, gradually filling the fresh water layer with a loose fabric of delicate crystals (they cannot be felt when going through with the drill). When the crystals continually forming at the boundary can no longer rise, the formation of a solid layer begins. Due to the irregular distribution of this fresh ice, and the inefficient method of thickness measurements by drilling, it proved to be very difficult to follow further development or to determine the mass increase.

Furthermore, it was noted that during August the sub-layer, once formed, appeared to move upward while its thickness showed little increase. However, an actual rise of the sub-layer due to buoyancy seems unlikely. When trying to explain its forma-

tion, one had to assume that the whole fresh water body had to be filled with a network of crystals which could withstand the buoyant force of ice forming at its lower boundary. It seems more likely that the rise of the upper surface of the sub-layer represents freezing of the fresh water layer. The rise of the bottom of the sub-layer is due to action of salty water on the fresh ice; this assumption is made more probable by the observation that the ice kept thinning even after the intermediate water layer was completely frozen. At the location of both thickness gauges (fig. 1) which had thin sublayers when they were installed there was a continuing rise of the bottom after the water layer had disappeared. This bottom ablation was terminated when cooling from the surface reached the bottom of the pack in November. The ice began to thicken from the bottom late in November, but not until late December did it proceed rapidly. How much, if any, of the fresh bottom ice of the preceding summer was still present could not be determined. Crystallographic examination planned for the summer of 1958 may be able to clear this point.

The schematic graph, figure 4, may demonstrate qualitatively the previous discussion. The first appearance of the new layer should coincide with the beginning of substantial drainage, according to the water level recorder.

The observation of a layer of 20 cm of fresh ice on July 25 indicates a surprisingly rapid freezing. Let us assume that a layer of 1 cm of ice has already formed, separating fresh water of 0° C and salt water of -1.6° C. In view of the turbulence in the salt water due to ice drift we may further assume that the temperature at the lower boundary of the ice layer is always at -1.6° C while the opposite boundary remains at 0° C for the duration of the freezing of fresh water. If s , T , and t denote ice thickness, temperature, and time, then the amount of heat conducted through the ice is $dq = k \frac{dT}{ds} dt$ (k = thermal conductivity of ice = 0.005 cal/cm, sec, °C). Introducing the heat of fusion of water we can convert dq into a thickness change; $dq = 80 ds$, where 80 is the latent heat of fusion of water in calorie per gm, hence

$$\frac{ds}{dt} = \frac{k}{80} \frac{dT}{ds} \quad (1)$$

Under the assumption of constant temperatures at the boundaries we can say that

$$\frac{dT}{ds} = \frac{T_2 - T_1}{s + s_0} \quad (2)$$

s_0 being an initial thickness of, say, 1 cm ($T_1 = -1.6° C$, $T_2 = 0° C$)

After introducing (2) in (1) we can write

$$\frac{k}{80} [T_2 - T_1] \int_0^t dt = \int_{s_0}^s s ds$$

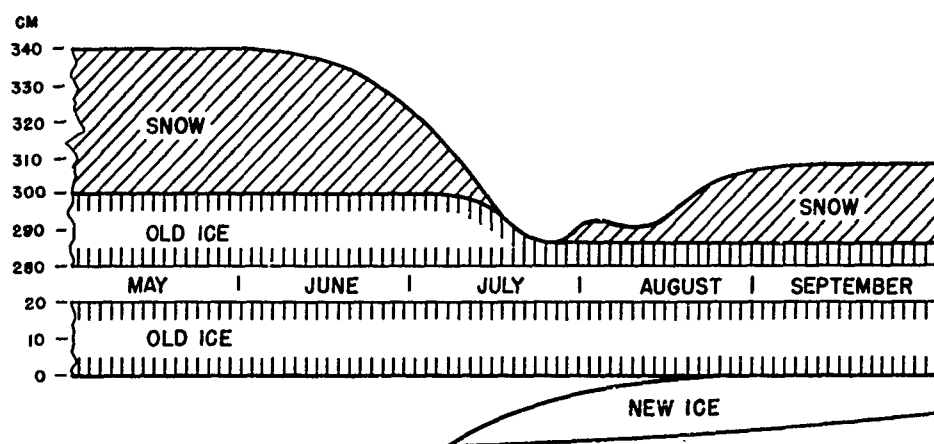


FIGURE 4.—Schematic graph of changes during summer.

By integrating and solving for s we obtain

$$s = (1 + 17.3t)^{1/2}, \quad (s \text{ in cm, } t \text{ in days})$$

This equation describes the growth of the sub-layer with time. Under the ideal conditions implied in this formula the ice layer would increase in thickness from 1 cm to about 19 cm within 20 days, which seems to be in good agreement with the observation mentioned before. Because the possible ablation by the action of salt water has been neglected, this formula would tend to give maximum thicknesses for the sub-layer. If the first accumulation of fresh water under the pack ice occurs during a period of rapid ice drift and strong turbulent mixing, this fresh ice layer may not form at all. The floe drifted an average of about 8 km per day from June 17 to July 17.

The reason for going into such detail about this feature is that it may be of basic importance in the mass budget of pack ice. The growth of a sheet of sea ice by the removal of heat from the surface, upward conduction of heat through the ice, and freezing of salt water at the bottom is limited, i.e. decreases with increasing thickness. From all observations it can reasonably be assumed that everywhere in the Arctic Basin the total heat supply during a part of the summer is sufficient to melt the recent snow cover and a certain amount of solid ("old") ice. When the annual amount of bottom accretion equals the summer ablation, then the pack ice has reached its stationary thickness. Bottom accretion continues even after the establishment of a stationary thickness. A considerable part of this accretion may be the fresh water ice. This possibility will have to be considered when investigating problems of the salinity of pack ice.

The continuing bottom accretion on ice of stationary thickness also necessitates the assumption of an upward transport of mass within the ice pack. Thus, on a very old, unbroken floe one should expect to find the oldest ice immediately beneath the new "superimposed" ice formed by the refreezing of thaw water at the top of the pack.

Thermal budget. Before further data evaluation, only a few cursory statements can be made with regard to the thermal budget.

The great importance of long-wave radiation in surface melting has been an outstanding feature. During the summer melting occurred mostly when there was overcast and strong atmospheric radiation. Radiosonde observations reveal frequent inversions, with comparatively high cloud temperatures. Temporary breaks in the overcast were frequently accompanied by freezing at the surface even though direct solar radiation was relatively larger in such periods.

The corollary is true in the accretion period. Cooling of the pack is almost entirely by long-wave radiation from its surface. Turbulent conduction from the air and condensation of water vapor onto the snow surface contribute relatively small amounts of heat to the pack. Long-wave radiation from air and clouds is only occasionally large enough during the accretion period to balance the outgoing radiation.

During melting conditions, the surface of pack ice disintegrates into a loose layer of granular ice, the grains being somewhat larger than the largest firm grains. Therefore, the albedo of the pack, except where it is water covered, always remains relatively high, higher than that of clean glacier ice. The reason for this may lie in a different crystal

structure, and the penetration of radiation into the ice.

According to temperature measurements 25, 50, and 100 cm above the ice, the temperature gradients in this air layer are usually very small, often unmeasurable during the melt season. In the winter an inversion is characteristic of this layer but its magnitude varies from almost nothing to 8° C per meter.

Similar conditions seem to prevail in the humidity regime in this layer. From the direct measurements (weighing snow-filled pans) maximum evaporation occurred on June 29; on this date a heat loss due to evaporation of 30 cal/cm² for 12 hours was calculated from the evaporation measurements. Maximum condensation was observed on September 14; this amounted to a heat gain of 16 cal/cm² in 12 hours. Normally the averages are only of the order of several calories per cm² per day.

During the fall and winter months, measurements of condensation were complicated by the almost constant presence of tiny ice crystals in the air. These crystals, colloquially called "diamond dust," evidently form by direct condensation from vapor in the lowest few hundred meters of the atmosphere. It is possible that they form at higher levels than this and fall very slowly, growing as they fall. In any case they are so small, 0.1 mm or less in their longest dimension, that they usually escape observation except when illuminated strongly as by a searchlight. Just how much they contributed to the increase of weight measured for the evaporation-condensation pans was impossible to determine. From visual inspection of frost on exposed surfaces it would seem that the deposit of crystals was of the same order of magnitude as the deposit of frost by direct condensation of vapor. The aggregate deposit seemed to be made of many tiny crystals bonded together by condensed vapor.

Even by the most generous estimate condensation cannot contribute significantly to the heat budget of the pack ice. It would be well to know more about the process, however, in order to understand the dehydration of the troposphere during the arctic winter.

It may be anticipated that the data will show radiative heat to be the most prominent factor in the thermal budget, whereas the transfer of both perceptible and latent heat are of less importance.

The distribution of wind velocities with height was usually close to logarithmic but there was often a tendency to depart from a logarithmic curve in a characteristic manner. The actual wind for periods of several hours would tend to be greater than the logarithmic profile would predict close to the surface and to be less than the logarithmic at a little higher level (80 cm). The effect of the anemometer

mounts, as well as random fluctuations are unlikely to be the causes. No further comment can be offered at the present time. Similar conditions were previously found over water by other observers (Dr. R. G. Fleagle, personal communication).

Surface roughness, determined by graphical extrapolation of the wind profiles, shows scattering of at least three orders of magnitude, the smallest values being but a fraction of a millimeter over a new snow cover.

SOME PRACTICAL APPLICATIONS AND FURTHER PROBLEMS

In view of the great importance of radiation for summer melting, more information about the albedo of pack ice is required. Large scale surveys of the albedo and its changes with the amount of ponded meltwater are desirable. Small, low-flying aircraft may be most efficient for these surveys.

Measurements on the penetration of short-wave radiation into solid ice and snow are planned for the summer of 1958. Little is known about the respective efficiencies of direct and diffuse solar radiation in penetrating pack ice.

For practical purposes of camp and runway preservation it is often desirable to artificially reduce ablation. A simple and efficient method to do this is to drain away meltwater from the surface thus preventing accumulation and consequent albedo decrease. Methods other than mechanical drilling would greatly facilitate this task (electrical hot-point or heat from chemical reactions, thermite). Artificial ponds of water for camp use can be made conveniently by spreading aluminum chips on the ice (about 2 kg per square meter).

Another problem of practical importance for construction on pack ice is the hydrostatic adjustment of individual pieces of ice. If every part of the ice were in perfect hydrostatic equilibrium then the bottom topography should be an image of the surface topography, multiplied by a factor of 9. Of course, this ideal state is unlikely. Hydrostatic maladjustment results in shear stresses in the ice and possibly vertical movements. In the course of landing strip construction in May a large hummock of about 200 cm height was levelled; by early August the landing strip showed a gentle bulge at the same place, about 60 cm high, which apparently was due to hydrostatic adjustment of the ice. During the cold season the ice under the scraped and packed runway lost heat more rapidly than the rest of the floe beneath the undisturbed snow cover. This may lead to greater thickening and slight elevation of the runway ice by hydrostatic adjustment, but whether this will prove to be of practical importance is questionable and must be determined by observations in the summer of 1958.

**The Trachymedusa, Botrynema Ellinorae,
an Indicator Plankton of Arctic Water**

J.L. Mohr
T.S. English

Reprinted from the
INTERNATIONAL OCEANOGRAPHIC CONGRESS (PREPRINTS),
1961

THE TRACHYMEDUSA, BOTRYNEMA ELLINORAE,
AN INDICATOR PLANKTON OF ARCTIC WATER

J. L. Mohr

University of Southern California, Los Angeles

T. S. English

University of Alaska, College

Distribution of most planktonic coelenterates and ctenophores of the North Polar Basin taken from Ice Island T3 by C. Horvath and from IGY Station A by T. S. English, is cosmopolitan or at least boreo-arctic. Wide-ranging forms such as the Hydromedusa, Sarsia sp., the siphonophore, Lensia subtilis, and the ctenophore, Beroe cucumis, are represented. Similarly Brodskii and Nikitin (in Somov, 1955, Research Drifting Sta. I. appendix 3) report for the Russian North Polar collections Hydromedusae, Aglantha digitale and Aeginopsis laurentii, and the siphonophore, Dimophyes arctica, which despite its trivial name occurs in the southern hemisphere.

In comparison, distribution of the trachymedusan genus Botrynema appears anomalous. Kramp (1942; 1947) studying several hundred individuals of Botrynema found striking discontinuous distribution between Norway and North America with B. ellinorae (Hartlaub) always north and B. brucei Browne always south. Occurrence is striking in Baffin Bay-Davis Strait where all B. ellinorae are north of the 67th and B. brucei south of the 63rd parallel. B. ellinorae taken at T3 Biological Stations 60 (83° 11' N 89° 20' W) and 53 (83° 15' N 90° 15' W) extend the range considerably north and west, confirming Kramp's characterization as northern.

Whether Botrynema brucei may be considered an indicator of southern, that is Pacific Ocean, water in the polar region is a complementary problem. Brodskii and Nikitin (Somov, loc. cit.) reported B. brucei from three NP stations, the northernmost at 81° 31' N. Previously Bigelow (1913) reported B. brucei (recognizable as such from the excellent photograph, though reported as B. ellinorae) in the Pacific Ocean at 53° 57' N, that is, south of Alaska. Though first questioning Brodskii and Nikitin's records without illustration, the writers subsequently found B. brucei in IGY Station A collections from the same

region. These records raise several questions. Northernmost B. brucei occurred within two degrees of latitude of northernmost B. ellinorae, far north of most B. ellinorae so far collected. However, closest stations of the two species are still those in Davis Strait. NP and IGY Station A localities are north of Bering Strait; thus B. brucei may indicate intrusion of Pacific Ocean water in the Polar Basin.

The two species of Botrynema are very much alike, differing mainly in a prominent apical knob on B. brucei and not B. ellinorae and in color in life. Possibility that the two might be conspecific, being phenotypes of cold and less cold water, was considered; however, the recent records of B. brucei are so far north as to cast doubt on the hypothesis. It is difficult to explain why B. ellinorae should be confined to its far northern range although moved in the same way as the other medusae.

**Primary Production in the Central North Polar
Sea; Drifting Station Alpha, 1957 - 1958**

T.S. English

Reprinted from the
INTERNATIONAL OCEANOGRAPHIC CONGRESS (PREPRINTS),
1959

PRIMARY PRODUCTION IN THE CENTRAL NORTH POLAR SEA;
DRIFTING STATION ALPHA, 1957 - 1958

T. Saunders English
University of Alaska, College

Drifting Station Alpha, an IGY camp, was located on a large ice floe of the Arctic pack in the North Polar Sea. The track of the drift was on the American side, near the center of the North Polar Basin. Studies on primary productivity were carried out from the station during 1957 and 1958.

The seasonal change in the abundance of chlorophyll a was followed by filtering several liters of sea water through an HA millipore filter and extracting the pigments with acetone. Light absorption of the acetone extract was measured at selected wavelengths in a Beckman Model DU spectrophotometer and the chlorophyll a calculated from nomographs.

The concentration of chlorophyll a increased steadily from late June to reach a single peak in early August. The concentrations decreased steadily to almost undetectable levels in February.

The amount of solar radiation penetrating the ice pack appeared to be the factor controlling the abundance of chlorophyll a. There was continuous daylight on the snow-covered ice pack for several months before the chlorophyll a values began to increase. The snow cover decreased through the spring, and ponds of melt water appeared on the floes in early July. When the snow cover vanished completely, the surface of the floe was covered with melt ponds (20-35%), decaying, or firn, ice (65-80%), and old ridges and hummocks (1-5%).

The submarine daylight under the ice varied considerably with the cover of the floe surface. The light was not detectable by a submarine photometer under areas covered with deep snow, while enough light was available under ponds and thin firn cover to force the meter off scale (70 foot-candles). Observations were made to determine the change in intensity and spectral composition of solar radiation reaching the ocean through the ice with changes in snow cover, ice thickness, and surface conditions. The extinction coefficients of sea water

were determined for several spectral regions, both under the ice floes and in open water.

Nutrient analyses for nitrate- and nitrite-nitrogen, phosphate-phosphorus, and silicate-silicon clarified the contribution of the melting floes to the supply of inorganic nutrients. It is clear that the melting ice does not release enough inorganic nutrients to lead to an increase in primary production. The melt water ponds on the floes appeared to be devoid of living phytoplankton organisms.

The Ice Floes of Station Alpha

A. Hansen

The Ice Floes of Station Alpha

The following set of sketches was prepared by A. HANSON from aerial photographs taken in 1957 and from local ground surveys. The original setting shown in Figure 1 persisted for a whole year (see Introduction). Many of the surface features entered in this figure, such as hummocks, persisted throughout the period described but are not shown on the subsequent figures to avoid undue clutter. Figures 2 to 7 represent stages of the destruction of the station floes. The figures are arranged such that the orientation of Runway No. 1 is maintained throughout, regardless of the continuous rotation during the drift. The north arrows are approximate.

SUMMER, 1957

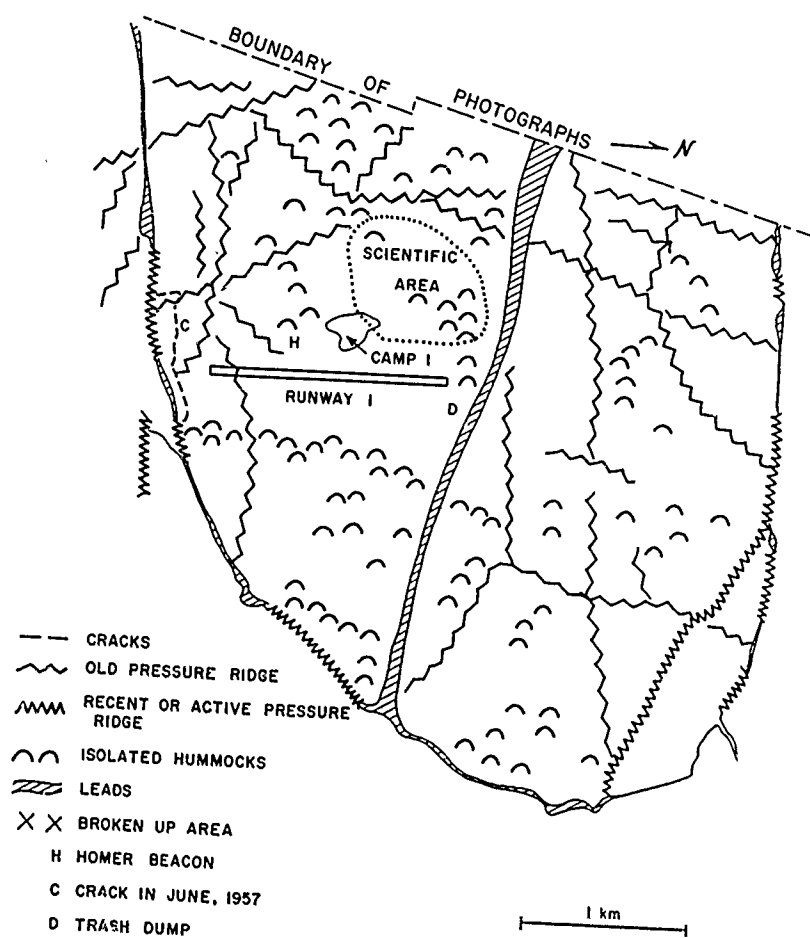


Figure 1. Drifting Station Alpha, April 1957 to March 1958

31 MARCH 1958

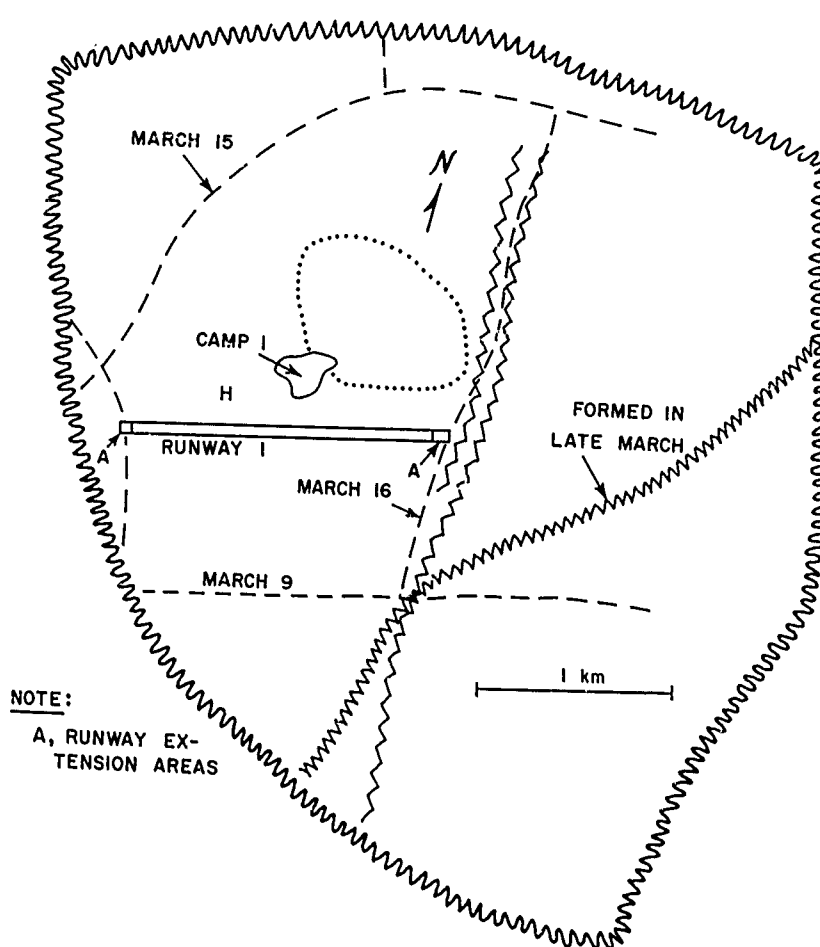


Figure 2. Heavy ridging occurred near one end of the runway and along the scientific area. The size of the floe was reduced to about one-half.

END OF MAY, 1958

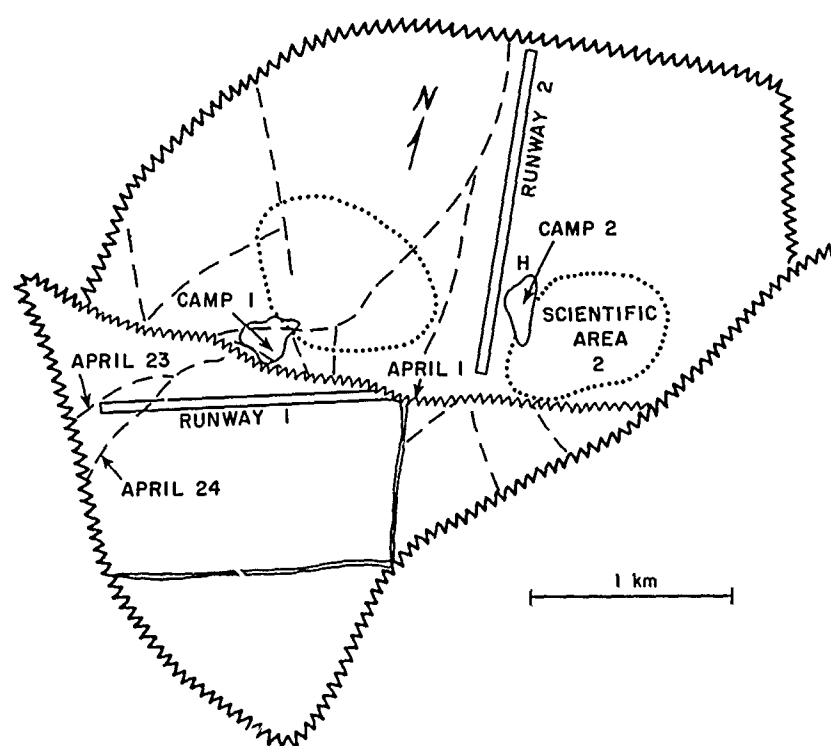


Figure 3. Cracks shortened the runway and split the camp and scientific area. Camp 2 and a new runway have been completed. The two runways are separated by an active pressure ridge.

15 JUNE 1958

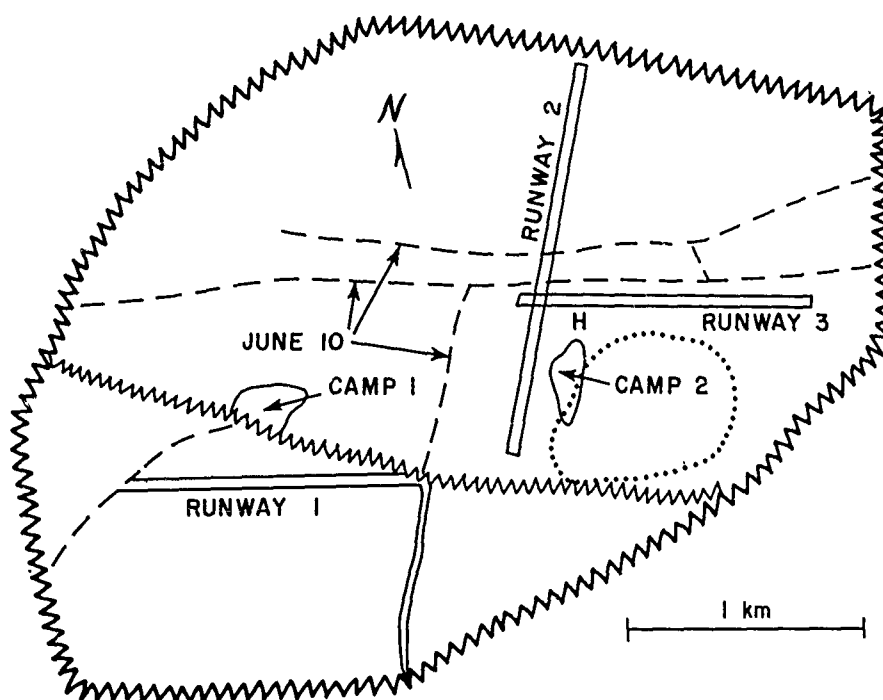


Figure 4. Runway 2 was split by two cracks shortly after completion and was never used. A third runway was constructed and used once for landing the summer crew.

21 JUNE 1958

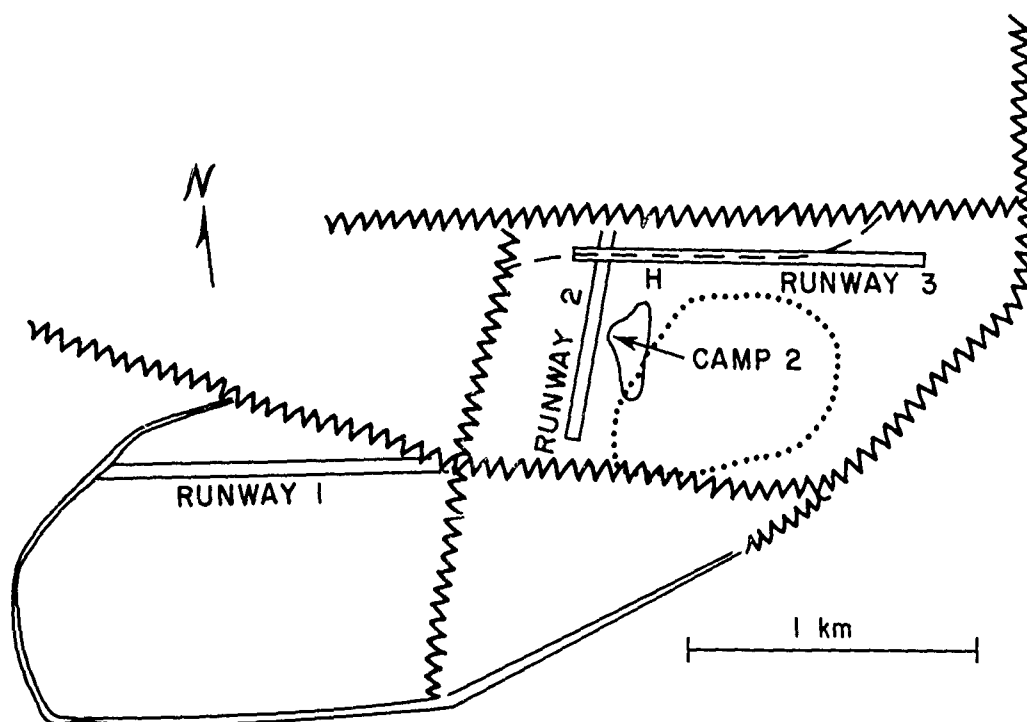
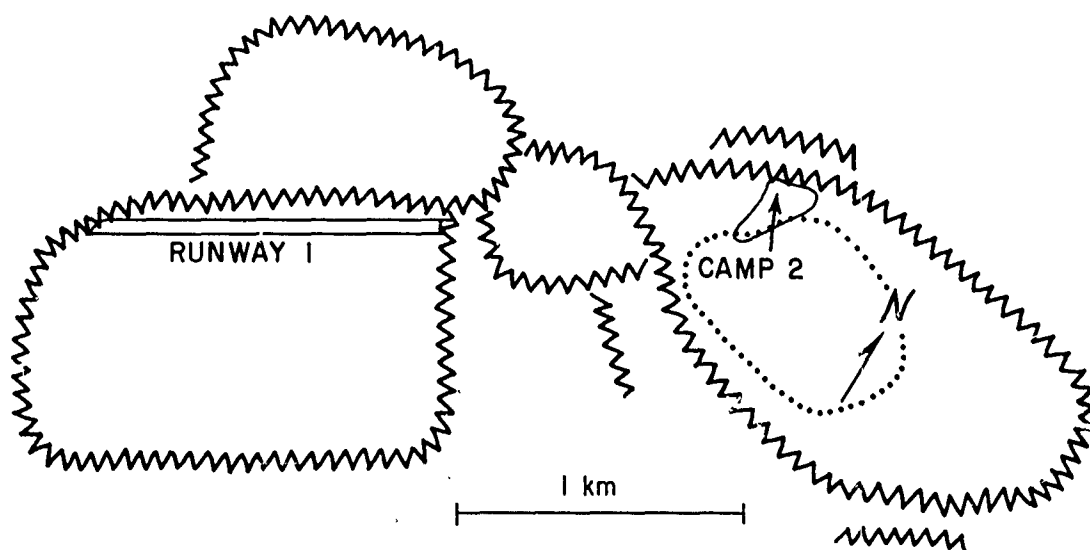


Figure 5. The advancing melt season made it necessary to construct Runway 3 as quickly as possible, leaving no time to spread out the large amounts of wet snow bulldozed from the ice. The excessive weight of the snowbanks alongside the runway caused a lengthwise split. Runway 1, though difficult to reach, remained unbroken.

23 SEPTEMBER 1958



NOTE: FLOE ARRANGEMENT VARIED DURING
SUMMER AND AUTUMN

Figure 6. Ice movement continued throughout the summer. Again a pressure ridge has approached the camp area.

NOVEMBER, 1958 (EVACUATION)

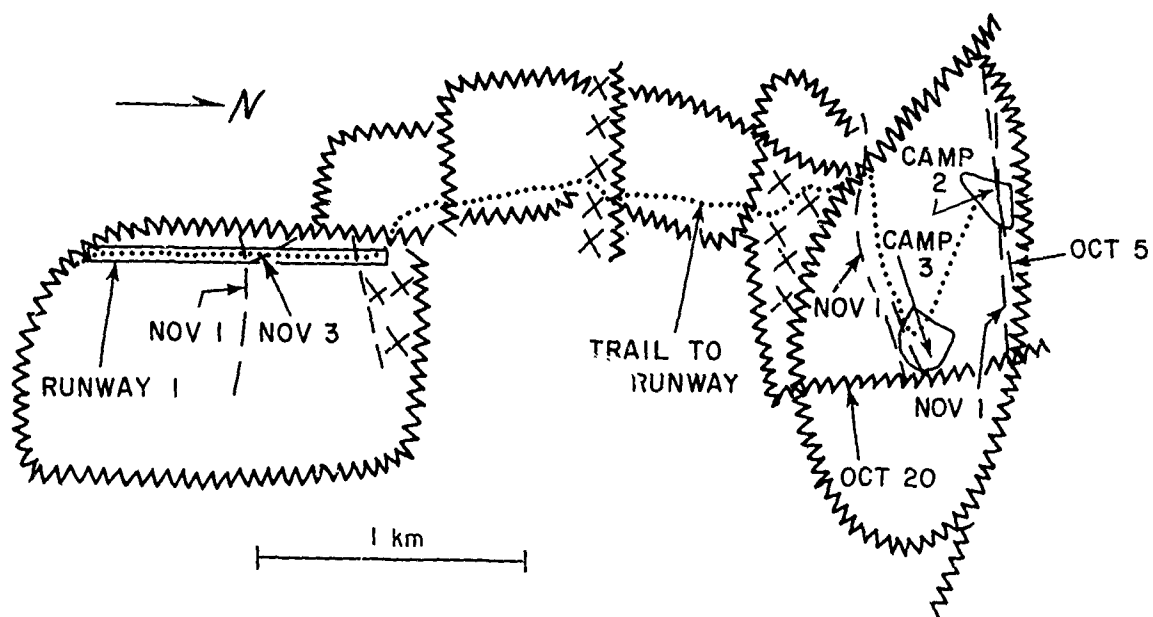


Figure 7. Camp and Runway 1 are separated by 2 km of broken ice. A grader kept on the runway floe made it possible to keep the landing strip in usable condition. On 1 November further cracking occurred in Camp 3 and on the runway, leading to final abandonment of the station on 7 November. The crew was evacuated by a C-123J which landed on the remaining 650 m of runway.

SPECIAL REPORTS

- No. 1. Today's Meteorological Rocket Network and Atmospheric Problems of Aerospace Vehicles, *Norman Sissenwine, May 1964 (REPRINT).*
- No. 2. Ferrimagnetic Resonance Relations for Magnetocrystalline Anisotropy in Cubic Crystals, *Hans Roland Zapp, April 1964.*
- No. 3. Worldwide Collection and Evaluation of Earthquake Data, Final Report on Evaluation of 1960 Seismicity, *R.L. Fisher, R.G. Baker, and R.R. Guidroz, June 1964.*
- No. 4. Visual Observations Beneath a Developing Tornado, *Ralph J. Donaldson, Jr., and William E. Lamkin, August 1964 (REPRINT).*
- No. 5. Bibliography of Rock Deformation, *R.E. Riecker, 1/Lt, USAF, September 1964.*
- No. 6. The Modification of Electromagnetic Scattering Cross Sections in the Resonant Region, A Symposium Record, Volume I, *J.K. Schindler, 1/Lt, USAF, R.B. Mack, Editors, September 1964.*
- No. 6. The Modification of Electromagnetic Scattering Cross Sections in the Resonant Region (U), A Symposium Record, Volume II, *J.K. Schindler, 1/Lt, USAF, R.B. Mack, Editors, September 1964 (SECRET).*
- No. 7. The Natural Environment for the Manned Orbiting Laboratory System Program (MOL), *25 October 1964.*
- No. 8. The Vertical Transfer of Momentum and Heat At and Near the Earth's Surface, *Morton L. Barad, October 1964 (REPRINT).*
- No. 9. Bibliography of Lunar and Planetary Research—1963, *J.W. Salisbury, R.A. VanTassel, J.E.M. Adler, R.T. Dodd, Jr., and V.C. Smalley, November 1964.*
- No. 10. Hourly Rawinsondes for a Week (Part II), *Arnold A. Barnes, Jr., and Henry A. Salmela, November 1964.*
- No. 11. An Appraisal of Rayleigh, *John Howard, Editor, November 1964 (REPRINT).*
- No. 12. Communication by Electroencephalography, *E.M. Dewan, November 1964.*
- No. 13. Proceedings of AFCRL Workshop on 20 July 1963 Solar Eclipse, *J.A. Klobuchar and R.S. Allen, Editors, December 1964.*
- No. 14. Continuous Zone Refining, *John K. Kennedy and N. Grier Parke, III, December 1964.*
- No. 15. Applications of Lasers, *C. Martin Stickley, November 1964.*
- No. 16. On the Physical Necessity for General Covariance in Electromagnetic Theory, *E.J. Post, December 1964.*
- No. 17. A Compendium of Papers in the Fields of Wave Propagation and Geotechnics Prepared at AFCRL During 1963, *Owen W. Williams, December 1964.*
- No. 18. A Compendium of Papers in the Fields of Geodesy and Planetary Geometry Prepared at AFCRL During 1963, *Owen W. Williams, Editor, January 1965.*
- No. 19. Study of Ferrimagnetic Crystals by Parallel Pumping, *James C. Sethares and Frank A. Olson, January 1965.*
- No. 20. Studies of the Characteristics of Probable Lunar Surface Materials, *John W. Salisbury and Peter E. Glaser, Editors, January 1964.*
- No. 21. Research in Computer Sciences, *Hans H. Zschirnt, February 1965 (REPRINT).*
- No. 22. Airglow Calibrations Symposium, *C.J. Hernandez and A.L. Carrigan, December 1964.*
- No. 23. An Introduction to the Geology of the Moon, *Luciano B. Ronca, May 1965.*
- No. 24. Ultrapurification, Its Attainment and Analysis, *A.F. Armington, B. Rubin, and J. Paul Cali, June 1965 (REPRINT).*
- No. 25. A Bibliography of the Electrically Exploded Conductor Phenomenon, Supplement No. 1, *William G. Chace and Eleanor M. Watson, June 1965.*
- No. 26. Observations on Solar Flares, *John T. Jefferies, Frank Q. Orrall, Josip Kleczek, Hermann U. Schmidt, and Anton Bruzek, June 1965 (REPRINT).*
- No. 27. Geophysical Implications of Shear Deformation in Rocks, *Robert E. Riecker, June 1965.*
- No. 28. Atmospheric Water Vapor Divergence: Measurements and Applications, *Arnold A. Barnes, Jr., July 1965 (REPRINT).*
- No. 29. Direct Observation of Dislocations and Plasticity in Mineral Crystals With Special Reference to Plagioclase, *K.E. Seifert, July 1965.*
- No. 30. A Survey of Radio Observations of Solar Eclipses, *John P. Castelli, and Jules Aarons, August 1965.*
- No. 31. AFCRL Participation in Project BANSHEE, *Francis X. Doherty, August 1965.*
- No. 32. A Family Outbreak of Severe Local Storms—A Comprehensive Study of the Storms in Oklahoma on 26 May 1963, Part I, *Keith A. Browning and T. Fujita, September 1965.*
- No. 33. Tables Related to Light Scattering in a Turbid Atmosphere, Volume I, *E. deBary, B. Braun, and K. Bullrich, September 1965.*
- No. 33. Tables Related to Light Scattering in a Turbid Atmosphere, Volume II, *E. deBary, B. Braun, and K. Bullrich, September 1965.*
- No. 33. Tables Related to Light Scattering in a Turbid Atmosphere, Volume III, *E. deBary, B. Braun, and K. Bullrich, September 1965.*
- No. 34. The AFCRL 29-ft Millimeter-Wave Antenna, *L.M. Keane, October 1965.*

SPECIAL REPORTS (Continued)

- No. 35. Bibliography of Experimental Rock Deformation, Second Edition, *R.E. Riecker, H.L. Cook, and D.L. Pendleton, October 1965.*
- No. 36. A Look Into the Future of Radar Scattering Research and Development, *W.F. Bahret and C.J. Sletten, November 1965 (REPRINT).*
- No. 37. Introduction to Radar Cross-Section Measurements, *P. Blacksmith, Jr., R.E. Hiatt, and R.B. Mack, November 1965 (REPRINT).*
- No. 38. US-IGY Drifting Station Alpha Arctic Ocean 1957-1958, *G.H. Cabaniss, K.L. Hunkins, and N. Untersteiner, November 1965 (REPRINT).*

Unclassified

Security Classification

DOCUMENT CONTROL DATA - R&D		
(Security classification of title, body of abstract and indexing annotation must be entered when the overall report is classified)		
1. ORIGINATING ACTIVITY (Corporate author) Hq. AFCRL, OAR (CRJ) United States Air Force Bedford, Massachusetts		2a. REPORT SECURITY CLASSIFICATION Unclassified
		2b. GROUP
3. REPORT TITLE US-IGY Drifting Station Alpha, Arctic Ocean 1957-1958		
4. DESCRIPTIVE NOTES (Type of report and inclusive dates) Scientific Report. Interim.		
5. AUTHOR(S) (Last name, first name, initial) CABANISS, G.H., HUNKINS, K.L., and UNTERSTEINER N., Compilers		
6. REPORT DATE November 1965	7a. TOTAL NO. OF PAGES 336	7b. NO. OF REFS
8a. CONTRACT OR GRANT NO.	9a. ORIGINATOR'S REPORT NUMBER(S) AFCRL-65-848	
b. PROJECT AND TASK NO. 8623-03		
c. DOD ELEMENT 61445014		
d. DOD SUBELEMENT 681309	9b. OTHER REPORT NO(S) (Any other numbers that may be assigned this report) AFCRL-65-848	
10. AVAILABILITY/LIMITATION NOTICES Requests for additional copies by Agencies of the Department of Defense, their contractors, and other government agencies should be directed to DDC. Limitation: Reproduction in whole or in part is permitted for any purpose of the U.S. Government.		
11. SUPPLEMENTARY NOTES	12. SPONSORING MILITARY ACTIVITY Hq AFCRL, OAR (CRJ) United States Air Force Bedford, Massachusetts	
13. ABSTRACT During the International Geophysical Year a drifting ice floe, ALPHA, served as a platform for scientific studies of the Arctic Ocean environment from June 1957 to November 1958. Disciplines represented were meteorology, ice physics, oceanography, geophysics, geology, and marine biology. The scientific papers that presented the results of the various investigations are reproduced in this volume.		

DD FORM 1473
1 JAN 64

Unclassified
Security Classification

Unclassified
Security Classification

14. KEY WORDS	LINK A		LINK B		LINK C	
	ROLE	WT	ROLE	WT	ROLE	WT
Arctic Ocean Drifting Station (US, IGY) Drifting Station Alpha (1957-1958) Meteorology and Climatology Mass and Heat Budget Geophysics Seismic Studies Marine Geophysics Crustal Structure Sea Ice Oceanography Oceanographic Data Ice Drift Ocean Currents Submarine Geology Marine Biology						

INSTRUCTIONS

1. **ORIGINATING ACTIVITY:** Enter the name and address of the contractor, subcontractor, grantee, Department of Defense activity or other organization (*corporate author*) issuing the report.

2a. **REPORT SECURITY CLASSIFICATION:** Enter the overall security classification of the report. Indicate whether "Restricted Data" is included. Marking is to be in accordance with appropriate security regulations.

2b. **GROUP:** Automatic downgrading is specified in DoD Directive 5200.10 and Armed Forces Industrial Manual. Enter the group number. Also, when applicable, show that optional markings have been used for Group 3 and Group 4 as authorized.

3. **REPORT TITLE:** Enter the complete report title in all capital letters. Titles in all cases should be unclassified. If a meaningful title cannot be selected without classification, show title classification in all capitals in parenthesis immediately following the title.

4. **DESCRIPTIVE NOTES:** If appropriate, enter the type of report, e.g., interim, progress, summary, annual, or final. Give the inclusive dates when a specific reporting period is covered.

5. **AUTHOR(S):** Enter the name(s) of author(s) as shown on or in the report. Enter last name, first name, middle initial. If military, show rank and branch of service. The name of the principal author is an absolute minimum requirement.

6. **REPORT DATE:** Enter the date of the report as day, month, year, or month, year. If more than one date appears on the report, use date of publication.

7a. **TOTAL NUMBER OF PAGES:** The total page count should follow normal pagination procedures, i.e., enter the number of pages containing information.

7b. **NUMBER OF REFERENCES:** Enter the total number of references cited in the report.

8a. **CONTRACT OR GRANT NUMBER:** If appropriate, enter the applicable number of the contract or grant under which the report was written.

8b, 8c, & 8d. **PROJECT NUMBER:** Enter the appropriate military department identification, such as project number, subproject number, system numbers, task number, etc.

9a. **ORIGINATOR'S REPORT NUMBER(S):** Enter the official report number by which the document will be identified and controlled by the originating activity. This number must be unique to this report.

9b. **OTHER REPORT NUMBER(S):** If the report has been assigned any other report numbers (*either by the originator or by the sponsor*), also enter this number(s).

10. **AVAILABILITY/LIMITATION NOTICES:** Enter any limitations on further dissemination of the report, other than those imposed by security classification, using standard statements such as:

- (1) "Qualified requesters may obtain copies of this report from DDC."
- (2) "Foreign announcement and dissemination of this report by DDC is not authorized."
- (3) "U. S. Government agencies may obtain copies of this report directly from DDC. Other qualified DDC users shall request through _____."
- (4) "U. S. military agencies may obtain copies of this report directly from DDC. Other qualified users shall request through _____."
- (5) "All distribution of this report is controlled. Qualified DDC users shall request through _____."

If the report has been furnished to the Office of Technical Services, Department of Commerce, for sale to the public, indicate this fact and enter the price, if known.

11. **SUPPLEMENTARY NOTES:** Use for additional explanatory notes.

12. **SPONSORING MILITARY ACTIVITY:** Enter the name of the departmental project office or laboratory sponsoring (*paying for*) the research and development. Include address.

13. **ABSTRACT:** Enter an abstract giving a brief and factual summary of the document indicative of the report, even though it may also appear elsewhere in the body of the technical report. If additional space is required, a continuation sheet shall be attached.

It is highly desirable that the abstract of classified reports be unclassified. Each paragraph of the abstract shall end with an indication of the military security classification of the information in the paragraph, represented as (TS), (S), (C), or (U).

There is no limitation on the length of the abstract. However, the suggested length is from 150 to 225 words.

14. **KEY WORDS:** Key words are technically meaningful terms or short phrases that characterize a report and may be used as index entries for cataloging the report. Key words must be selected so that no security classification is required. Identifiers, such as equipment model designation, trade name, military project code name, geographic location, may be used as key words but will be followed by an indication of technical context. The assignment of links, rules, and weights is optional.

Unclassified
Security Classification